Biofilm growth in a homogeneous porous medium
by Sunil Kumar Tiwari

A thesis submitted in partial fulfillment of the requirements for the degree of Doctor of Philosophy in Mathematics
Montana State University

Abstract:
As biofilms intervene in a porous medium, they affect the porosity and permeability, which in turn alters the hydrodynamics. A biofilm growth model is presented which is suitable for microscale simulations of biofilm activity in a porous medium. The model is then used to predict the changing porosity and permeability. The predictions are compared to experimental data and finally these calculated properties are used to simulate flow in a biofilm infested porous medium.

BIOFILM GROWTH IN A HOMOGENEOUS POROUS MEDIUM

by

Sunil Kumar Tiwari

A thesis submitted in partial fulfillment
of the requirements for the degree

of

Doctor of Philosophy

in

Mathematics

MONTANA STATE UNIVERSITY
Bozeman, Montana

January 1997

APPROVAL

of a thesis submitted by

Sunil Kumar Tiwari

This thesis has been read by each member of the thesis committee and has been found to be satisfactory regarding content, English usage, format, citations, bibliographic style, and consistency, and is ready for submission to the College of Graduate Studies.

1/17/97
Date

Kenneth L. Bowers
Kenneth L. Bowers
Chairperson, Graduate Committee

Approved for the Major Department

1/17/97
Date

John Lund
John Lund
Head, Mathematics

Approved for the College of Graduate Studies

1/23/97
Date

R L Brown
Robert Brown
Graduate Dean

STATEMENT OF PERMISSION TO USE

In presenting this thesis in partial fulfillment for a doctoral degree at Montana State University, I agree that the Library shall make it available to borrowers under rules of the Library. I further agree that copying of this thesis is allowable only for scholarly purposes, consistent with "fair use" as prescribed in the U. S. Copyright Law. Requests for extensive copying or reproduction of this thesis should be referred to University Microfilms International, 300 North Zeeb Road, Ann Arbor, Michigan 48106, to whom I have granted "the exclusive right to reproduce and distribute copies of the dissertation for sale in and from microform or electronic format, along with the right to reproduce and distribute my abstract in any format in whole or in part."

Signature Sunil K Tiwari

Date Jan 17' 1997

ACKNOWLEDGEMENTS

I am indebted to my advisor, Dr. Kenneth L. Bowers, for his guidance, support and encouragement throughout my association with him. In particular, his criticisms and suggestions during the writing of this thesis have been invaluable. My appreciation is also extended to professors Jack Dockery and Gary Bogar for their careful reading of this manuscript and their technical guidance.

I am grateful to Dr. Ken Tiahrt and Dr. John Lund for giving me the opportunity to continue my graduate studies at Montana State University. Thanks are also due to the rest of the faculty and my fellow graduate students who made my stay here such an enjoyable and intellectually rewarding experience. Special appreciation is due to the office staff of the Department of Mathematical Sciences who were very helpful.

Finally, I wish to thank my wife, Kala, for her patience, encouragement and support during these past years.

TABLE OF CONTENTS

LIST OF TABLES

LIST OF FIGURES

ABSTRACT

As biofilms intervene in a porous medium, they affect the porosity and permeability, which in turn alters the hydrodynamics. A biofilm growth model is presented which is suitable for microscale simulations of biofilm activity in a porous medium. The model is then used to predict the changing porosity and permeability. The predictions are compared to experimental data and finally these calculated properties are used to simulate flow in a biofilm infested porous medium.

CHAPTER 1

Introduction

The goal of this dissertation is to develop a mathematical model to describe the change in the hydrodynamic properties of a porous medium due to biofilm growth. A one-dimensional mathematical model called the Biofilm Growth Model (BGM) has been developed which describes the growth of biofilm on a surface. The results of the one-dimensional BGM and its zero-dimensional version have been compared. Also the results of the zero-dimensional BGM and the zero-dimensional versions of two existing models called the Biofilm Accumulation Model (BAM) and Rittman's model have been compared. Different model equations relating the porosity and the permeability of a porous medium have been discussed and some of the relations have been compared with the experimental data from [5], [6]. A complete porous media model describing the effect of biofilm growth on porosity, permeability, and hence the flow, has been presented. Finally, the numerical results of the one-dimensional porous media flow model simulations have been presented and these numerical results are compared with the experimental data from [5], [6].

Controlled, artificially grown biofilm in porous media provides significant opportunities for improving the performance of industrial and environmental processes. The petroleum industry, for example, uses biofilm for deliberate plugging of parts of the oil reservoir to enhance oil recovery. A controlled biofilm accumulation in high permeability zones can be used to prevent injection water from reaching the production well. This can be accomplished by injecting cells and nutrients into the oil-bearing formation, [16], [19]. Also, controlling biofilm accumulation is important

to both injection and production well operation in order to avoid unwanted formation plugging near the well bore. The environmental industry likewise uses deliberate plugging of pore channels between spilled contaminants and lakes or rivers to prevent the contamination of these water resources. Subsurface biofilms also offer the potential for biotransformation of organic compounds providing an in situ method (Figure 1) for treating contaminated groundwater supplies, [4], [26]. The mining industry is developing methods for microbially enhanced leaching of metals from ores and recovery of metals from solutions, [11]. An efficient use of biofilm by engineers

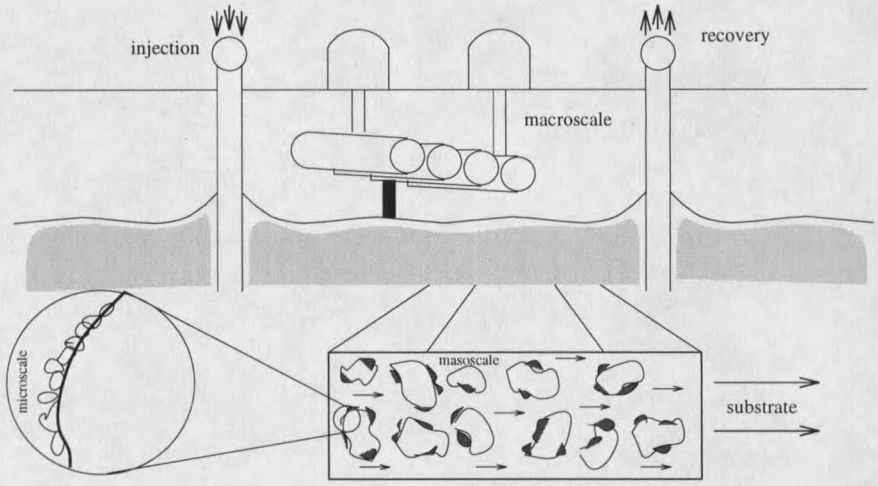

Figure 1: Injection/recovery scheme for enhancing in situ bioremediation of contaminated aquifer. Inset shows the growing biofilm in porous media.

requires an improved understanding of the interrelationship between porous media hydrodynamic properties and the accumulation rate and spatial distribution of the biofilm.

The pressure driven flow between two points in an isotropic homogeneous porous medium depends on the pressure gradient between the two points and the viscosity of the liquid flowing through it as well as the porosity and the permeability of the medium, [2], [7], [20]. If the pressure gradient between the two points and the viscosity of the liquid are assumed to be constant then the porosity and the

permeability dictate the flow rate. If one assumes the presence of an initial thin layer of biofilm on the pore surface and a high concentration of substrate (food for the bacteria) in the liquid flowing through the porous medium then it is reasonable to expect a decrease in the porosity and the permeability of the medium due to the biofilm growth in it. How fast does the biofilm grow? How does the flow rate change? In this work, a mathematical model has been developed that should help in the understanding of these issues.

In order to derive a mathematical model to study the effect of biofilm growth on porous media flow, one must combine the system of flow equations with a system of biofilm growth equations. A one-dimensional mathematical model called the Biofilm Growth Model (BGM) has been developed in Chapter 2 which describes the growth of a biofilm on a surface. The one-dimensional Biofilm Accumulation Model (BAM, [14], originally developed in [25]) and Rittman's model (originally developed in [12]) have also been described in Chapter 2. Based on Rittman's zero-dimensional model, the zero-dimensional versions of BAM and BGM have also been derived. A zero-dimensional model ignores the spatial dependence of the variables, namely the substrate concentration in the biofilm and the volume fraction of the active and inactive bacteria in the biofilm and describes the change in the spatial average value of these variables with respect to time.

A comparison, undertaken in Chapter 3, of the numerical solutions of one-dimensional BGM and zero-dimensional BGM show that (*i*) the qualitative behavior of the solutions from both the models are very similar and they are also quantitatively close, and (*ii*) the zero-dimensional model equations are comparatively easy to solve and the computation time is much less than the computation time for the one-dimensional model. The zero-dimensional model lacks some of the features which the one-dimensional model possesses. For example, the substrate concentration or the

active biomass volume fraction at a certain point in the biofilm can not be computed with a zero-dimensional model. However, since we intend to use the biofilm growth model in a porous medium setting, the zero-dimensional BGM is chosen over the one-dimensional BGM. This is because the zero-dimensional model efficiently describes the average change in the substrate concentration and the biofilm thickness which suffices our need. After a comparison of the three zero-dimensional models (BGM, BAM, and Rittman's model), also completed in Chapter 3, the zero-dimensional BGM has been chosen over the other two models primarily because BGM assumes the bulk volume (in the case of a porous medium it is the pore volume) to be a variable as opposed to the other two models (BAM and Rittman's model) in which the bulk volume is assumed to be a constant. This is necessary in order to study the effect of biofilm growth on porosity and hence permeability.

The relation between porosity and permeability of a porous medium has been investigated by many researchers in the past. A collection of experiment-based algebraic relations between porosity and permeability and a list of references can be found in the Chapter 3 of [9]. Some of the relations which are relevant for the models developed in this dissertation are described here in Chapter 4 and the validity of two of such formulas has been checked against the experimental data given in [5], [6]. Finally in Chapter 4, the complete model describing biofilm growth in a porous medium and its effect on porosity and the permeability of the medium is formulated.

The complete model describing the biofilm growth in a homogeneous porous medium and its effect on the one-dimensional incompressible fluid flow through the medium is numerically solved in Chapter 5 and numerical solutions are presented. The model equations are solved for a short bed (5 cm long) of spherical balls and a long bed (60 cm long) of spherical balls. The numerical results for a short bed experiment have been compared with the experimental data from [5], [6]. Lastly, the

change in the variables over time is predicted for a long bed experiment.

CHAPTER 2

Biofilm Models

Introduction

What follows is the discussion of biofilm growth on a surface. In addition, the derivation of one-dimensional and zero-dimensional mathematical models which describe these physical phenomena is given.

Consider a water filled tank with an initial biofilm thickness on one of its walls. Assume that the substrate (food or nutrient) for the bacteria is dissolved in the water and diffuses into the biofilm. The bacteria in the biofilm will consume the substrate and will multiply. The growth of the biofilm (increase in thickness) depends on the volume fraction of the active biomass, the substrate concentration in the biofilm, the substrate concentration in the bulk liquid in the tank, the rate of the consumption of the substrate by the bacteria, the diffusion rate of the substrate in the biofilm, and possibly other factors. In fact, the growth of the biofilm is a very complicated phenomenon and to produce an accurate mathematical model is not easy. This physical system is shown in Figure 2, where $L(t)$ is the biofilm thickness at time t, $u(L,t)$ is the biomass velocity at the film-water interface and Q is the volumetric flow rate of the influent fluid.

A similar problem has been discussed in [12] and [25] and one-dimensional models have been derived that describe the growth of the thickness of a biofilm with respect to time and space. The model developed in [12] is also called **Rittman's**

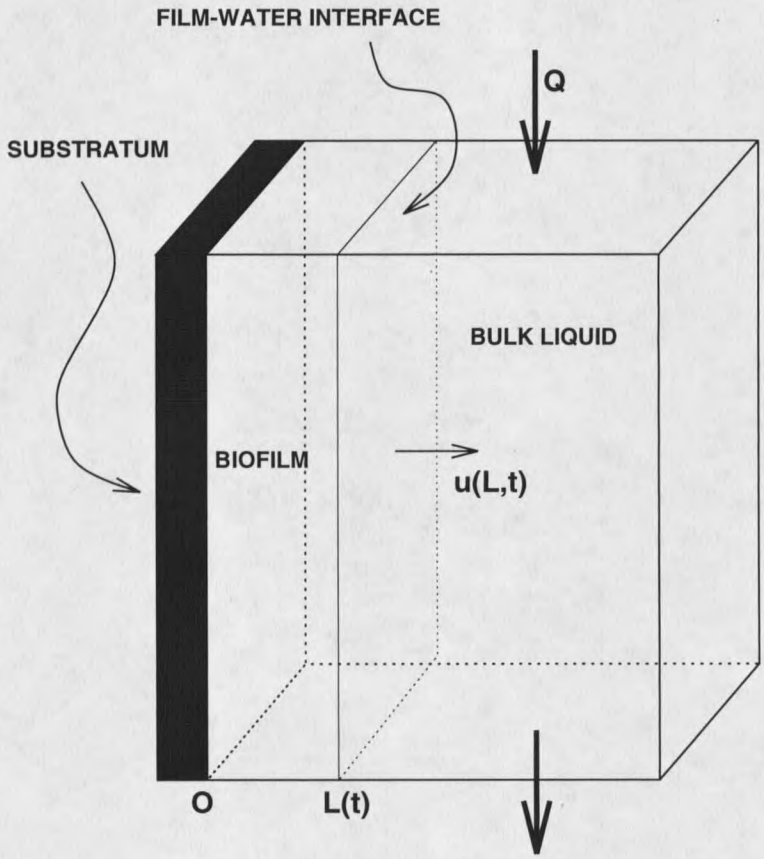

Figure 2: Biofilm on a surface

Model. The Center for Biofilm Engineering at Montana State University, has developed a computer simulator called the **Biofilm Accumulation Model, (BAM)**, [14] which studies the growth of biofilm on a flat surface. The model equations are based on [25]. Both of these models assume the volume of the bulk liquid is constant. Also some of the terms in the model equations are not consistent with the underlying assumptions. Hence a new model called the **Biofilm Growth Model (BGM)** is developed here which considers the volume of the bulk liquid to be a time-dependent function instead of a constant. The equations described in these models cannot be used directly in a problem where biofilm grows in a porous media because of the simplified assumptions of these models and the complicated geometry of the pore surface, however the idea of the zero-dimensional model discussed in [12] is very useful here. In both Rittman's model and BAM, different types of bacteria are consuming different types of substrates and are growing simultaneously. But, for now, in order to keep the notation clean and the problem simple and explainable, we shall restrict ourselves to only one bacteria consuming only one substrate.

Rittman's Model

One-dimensional Model

In this model, originally proposed in [12], the microbial interactions and diffusion phenomena are described by two sets of mathematical equations. The first set is called diffusional equations, the other one transport equations. They are derived from basic mass balances. The following a *priori* assumptions have been made to develop this model:

- The biofilm is homogeneous and can be treated as a continuum.
- Changes occur only in the direction normal to the biofilm surface.

- There is a laminar diffusional sublayer of constant thickness in the bulk liquid.
- The biofilm is composed entirely of active or inactive biomass.

This model predicts four time-dependent functions, two of which depend on the spatial variable y as well. These functions and their fundamental units of length (L) and substrate mass (M_s) are given in Table 1.

Variables	Physical quantity	Units
$L(t)$	biofilm thickness	L
$S_b(t)$	bulk substrate concentration	$M_s L^{-3}$
$S(y,t)$	substrate concentration in the biofilm	$M_s L^{-3}$
$f(y,t)$	volume fraction of active biomass in the biofilm	dimensionless

Table 1: Unknown dependent variables and their fundamental units in Rittman's one-dimensional model

Other variables and the parameters used in the development of this model and their fundamental units of length (L), time (T), substrate mass (M_s), and biomass (M_x), are given in Table 2.

A visualization of the physical system to be modeled is given in Figure 3 where σ is the surface area of the film-water interface.

Diffusional Equations The mass balance equation for the total substrate in the bulk liquid, $V_L S_b$, has the form

$$V_L \frac{d}{dt}(S_b(t)) = Q(S_0 - S_b(t)) - \sigma J(t), \tag{2.1}$$

where V_L is the volume (L^3), Q represents the bulk liquid flow rate ($L^3 T^{-1}$), σ is the surface area of the film-water interface (L^2), S_0 refers to the influent substrate concentration ($M_s L^{-3}$) and $J(t)$ refers to the substrate flux through the laminar diffusional sublayer ($M_s L^{-2} T^{-1}$). V_L, Q, σ and S_0 are assumed constant. According

Parameters	Physical quantity	Units
V_L	volume of the bulk liquid	L^3
Q	volumetric flow rate of the bulk liquid	L^3T^{-1}
S_0	substrate concentration in the influent fluid	M_sL^{-3}
σ	area of the film-water interface	L^2
D	diffusivity coefficient of the substrate through the laminar diffusional sublayer	L^2T^{-1}
L_l	thickness of laminar diffusional sublayer	L
d	diffusivity coefficient of the substrate inside the biofilm	L^2T^{-1}
V_r	maximum specific growth rate	$M_sM_x^{-1}T^{-1}$
K	Monod constant	M_sL^{-3}
ρ	biomass density	M_xL^{-3}
b	inactivation coefficient of bacteria	T^{-1}
Y	yield coefficient	$M_xM_s^{-1}$
G_s	global shear stress coefficient	T
B'	average shear stress coefficient	T^{-1}
f_d	biodegradable fraction of the biomass	dimensionless
Variables	**Physical quantity**	**Units**
$J(t)$	influx rate of the substrate into the biofilm	$M_sL^{-2}T^{-1}$
$u(y,t)$	velocity of the biomass particle at (y,t)	LT^{-1}
$G(y,t)$	active biomass quantity in the interval $[0,y]$	M_xL^{-2}
$c(y,t)$	net growth of active biomass	$M_xL^{-3}T^{-1}$
$R(y,t)$	reaction rate	$M_sL^{-3}T^{-1}$
$b'(y)$	shear function along y-axis	T^{-1}
$f_0(t)$	volume fraction at the substratum	dimensionless
$\bar{G}(y,t)$	inactive biomass quantity in the interval $[0,y]$	M_xL^{-2}
$\bar{f}(y,t)$	volume fraction of inactive biomass in the biofilm	dimensionless
$\bar{c}(y,t)$	net growth of inactive biomass	$M_xL^{-3}T^{-1}$
$B(y,t)$	total biomass amount	M_xL^{-2}

Table 2: Parameters and the variables used in Rittman's model and their fundamental units

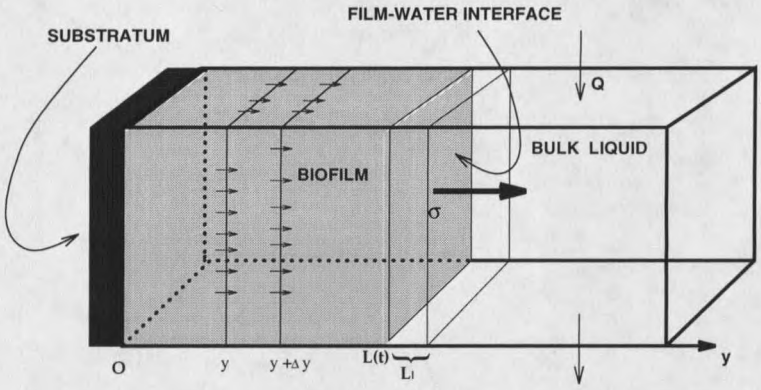

Figure 3: Biofilm on a surface

to Fick's first law, $J(t)$ is expressed by

$$J(t) = \frac{D}{L_l}\left(S_b(t) - S(L(t),t)\right), \tag{2.2}$$

where D is the diffusivity coefficient of the substrate through the laminar diffusional sublayer (L^2T^{-1}) and L_l is the thickness of the laminar diffusional sublayer (L). Both D and L_l are constants. Combining (2.1) and (2.2) yields

$$\frac{d}{dt}(S_b(t)) = \frac{1}{V_L}\left(QS_0 - \left(Q + \frac{\sigma D}{L_l}\right)S_b(t) + \frac{\sigma D}{L_l}S(L(t),t)\right). \tag{2.3}$$

The mass balance on the substrate in the biofilm ($0 \leq y \leq L(t)$) is expressed by

$$\frac{\partial S(y,t)}{\partial t} = d\frac{\partial^2 S(y,t)}{\partial y^2} - R(y,t), \tag{2.4}$$

where d is the constant diffusivity coefficient of the substrate inside the biofilm (L^2T^{-1}). The reactional term, $R(y,t)$, which is based on Monod kinetics [10] and is given as

$$R(y,t) = R(S(y,t), f(y,t)) = \frac{V_r S(y,t)}{K + S(y,t)} f(y,t)\rho. \tag{2.5}$$

Here V_r represents the maximum specific growth rate ($M_s M_x^{-1} T^{-1}$), K represents the Monod coefficient ($M_s L^{-3}$), and ρ is the biomass density ($M_x L^{-3}$) where M_x is the

fundamental unit of biofilm mass. V_r, ρ, and K are all assumed constant. Combining (2.4) and (2.5) gives

$$\frac{\partial S(y,t)}{\partial t} = d\frac{\partial^2 S(y,t)}{\partial y^2} - \frac{V_r S(y,t)}{K + S(y,t)} f(y,t)\rho. \tag{2.6}$$

The boundary conditions state that there is no substrate flux through the substratum ($y = 0$), and at the film-water interface ($y = L(t)$) the flux through the biofilm is equal to the flux through the laminar diffusional sublayer. Hence,

$$-d\,\frac{\partial S}{\partial y}(0,t) = 0, \tag{2.7}$$

and

$$-d\,\frac{\partial S}{\partial y}(L(t),t) = -J(t). \tag{2.8}$$

The differential equations (2.3) and (2.6) and the boundary conditions (2.7) and (2.8) are the diffusional set of equations for Rittman's model.

Transport Equations To describe biomass growth we define a control volume which has surface area σ and extends from $y = 0$ to $y = y(t)$ with $y(t) \leq L(t)$. At time $t + dt$ this volume has grown and the control volume extends from $y = 0$ to $y = y(t + dt)$.

The biomass particle speed $u(y,t)$, (LT^{-1}), is described by $u(t) = \frac{dy}{dt}$. The active biomass quantity $G(y,t)$, $(M_x L^{-2})$, on the interval $[0, y]$ is expressed by

$$G(y,t) = \int_0^y \rho f(\xi,t) d\xi. \tag{2.9}$$

Since the interval $[0, y(t)]$ at time t grows to the interval $[0, y(t + dt)]$ at time $t + dt$ we can let $dt \to 0$ and obtain the time derivative of $G(y,t)$, which is a particle time derivative, given by

$$\lim_{dt\to 0} \frac{G(y(t+dt), t+dt) - G(y(t),t)}{dt} = \frac{d}{dt}(G(y(t),t)) = u\frac{\partial G}{\partial y} + \frac{\partial G}{\partial t}. \tag{2.10}$$

Then an active biomass balance may be written. The time rate of change of $G(y,t)$ is equal to the sum of the growth of active biomass minus the biomass lost by shear stress. Thus

$$u(y,t)\frac{\partial G}{\partial y}+\frac{\partial G}{\partial t}=\int_0^y\left(c(\xi,t)-b'(\xi)f(\xi,t)\rho\right)\,d\xi, \tag{2.11}$$

where $c(y,t)$ is the net growth of active biomass $(M_xL^{-3}T^{-1})$, which results from a production term minus a decay term. The net growth $c(y,t)$ is expressed as

$$c(y,t)=YR(S(y,t),f(y,t))-bf(y,t)\rho \tag{2.12}$$

where Y is the yield coefficient $(M_xM_s^{-1})$, b represents the inactivation coefficient of bacteria (T^{-1}) and $b'(y)$ is a shear function along the y-axis (T^{-1}). Both Y and b are assumed constant. Shear stress is expressed as a function of spatial and temporal variables y and t rather than as a constant applied only at the biofilm surface, avoiding the Dirac effect of discontinuity. That is why this term appears inside the integral and is not simply added at the biofilm surface. The shear function $b'(y)$ used for this work is

$$b'(y)=\frac{1+\arctan(30(y-.9))}{.2G_s}, \tag{2.13}$$

where the detachment layer thickness is fixed at 20% of the biofilm thickness. G_s is an experimental constant which represents a fraction of biomass detached from total biomass (T). The shear function $b'(y)$ describes biomass loss distributed throughout the biofilm and a detachment layer is defined everywhere $b'(y)>0$. Taking the partial derivative of (2.11) with respect to y, using the definition of $G(y,t)$ from (2.9) and dividing by ρ, which is a constant, yields

$$\frac{\partial f(y,t)}{\partial t}+u(y,t)\frac{\partial f(y,t)}{\partial y}=\frac{c(y,t)}{\rho}-b'(y)f(y,t)-f(y,t)\frac{\partial u}{\partial y}. \tag{2.14}$$

As biomass growth does not occur at the substratum we introduce the following boundary conditions

$$f(0,t) \;=\; f_0(t) \tag{2.15}$$

$$\frac{df_0}{dt} = \left(Y\frac{V_r S(0,t)}{K+S(0,t)} - b\right) f_0(t) - f_0(t)\frac{\partial u}{\partial y}(0,t) \tag{2.16}$$

where $f_0(t)$ is the dimensionless volume fraction at the substratum ($y = 0$). Similar to the above treatment of the active biomass quantities, $G(y,t)$, we can introduce the inert biomass amount $\bar{G}(y,t)$, $(M_x L^{-2})$, on the interval $[0,y]$. It can be expressed by

$$\bar{G}(y,t) = \int_0^y \rho \bar{f}(\xi,t) d\xi, \tag{2.17}$$

where $\bar{f}(y,t)$ is the volume fraction of the inert biomass. The inert biomass balance is then given as

$$u(y,t)\frac{\partial \bar{G}}{\partial y} + \frac{\partial \bar{G}}{\partial t} = \int_0^y \left(\bar{c}(\xi,t) - b'(\xi)\rho\bar{f}(\xi,t)\right)\, d\xi, \tag{2.18}$$

where $\bar{c}(y,t)$ is the net inert biomass increase $(M_x L^{-3} T^{-1})$. This function is given as

$$\bar{c}(y,t) = b(1-f_d) f(y,t)\rho \tag{2.19}$$

where f_d is the dimensionless biodegradable fraction of biomass, which is a constant between 0 and 1. We can now express the total biomass amount $B(y,t)$ on interval $[0,y]$ as

$$B(y,t) = G(y,t) + \bar{G}(y,t) = \int_0^y \rho\left(\bar{f}(\xi,t) + f(\xi,t)\right) d\xi = y\rho \tag{2.20}$$

because $\bar{f}(y,t) + f(y,t) = 1$. Hence $B(y,t)$ is independent of t. Adding (2.11) and (2.18) we can express the particle derivative of $B(y,t)$ as

$$u(y,t)\frac{\partial B}{\partial y} + \frac{\partial B}{\partial t} = \int_0^y \Big(\left(\bar{c}(\xi,t) + c(\xi,t)\right) - b'(\xi)\rho\left(\bar{f}(\xi,t) + f(\xi,t)\right)\Big) d\xi. \tag{2.21}$$

Using (2.20) this reduces to

$$u(y,t)\rho = \int_0^y \Big(\left(\bar{c}(\xi,t) + c(\xi,t)\right) - b'(\xi)\rho\left(\bar{f}(\xi,t) + f(\xi,t)\right)\Big) d\xi \tag{2.22}$$

which simplifies to

$$u(y,t) = \int_0^y \left(\frac{Y}{\rho} R(S(\xi,t), f(\xi,t)) - b f_d f(\xi,t) - b'(\xi) \right) d\xi. \tag{2.23}$$

Hence, the velocity of the film-water interface will be given by,

$$\begin{aligned} u(L(t),t) = \frac{dL(t)}{dt} &= \int_0^{L(t)} \left(\frac{Y}{\rho} R(S(\xi,t), f(\xi,t)) \right. \\ &\quad \left. - b f_d f(\xi,t) - b'(\xi) \right) d\xi. \end{aligned} \tag{2.24}$$

Equations (2.14), (2.23), and (2.24) and the boundary conditions (2.15), (2.16) are referred to as the transport equations.

One-dimensional Rittman's Model

Diffusional Equations $0 \le y \le L(t)$

$$\frac{d}{dt}(S_b(t)) = \frac{1}{V_L} \left(Q S_0 - \left(Q + \frac{\sigma D}{L_l} \right) S_b(t) + \frac{\sigma D}{L_l} S(L(t),t) \right) \tag{2.25}$$

$$\frac{\partial S(y,t)}{\partial t} = d \frac{\partial^2 S(y,t)}{\partial y^2} - \frac{V_r S(y,t)}{K + S(y,t)} f(y,t) \rho \tag{2.26}$$

Boundary Conditions

$$-d \frac{\partial S}{\partial y}(0,t) = 0 \tag{2.27}$$

$$-d \frac{\partial S}{\partial y}(L(t),t) = -\frac{D}{L_l} \left(S_b(t) - S(L(t),t) \right) \tag{2.28}$$

Transport Equations $0 \le y \le L(t)$

$$\begin{aligned} \frac{\partial f(y,t)}{\partial t} + u(y,t) \frac{\partial f(y,t)}{\partial y} &= \left(Y \frac{V_r S(y,t)}{K + S(y,t)} - b \right. \\ &\quad \left. - b'(y) \right) f(y,t) - f(y,t) \frac{\partial u(y,t)}{\partial y} \end{aligned} \tag{2.29}$$

$$u(y,t) = \int_0^y \left(\left(Y \frac{V_r S(\xi,t)}{K + S(\xi,t)} - b f_d \right) f(\xi,t) - b'(\xi) \right) d\xi \tag{2.30}$$

Boundary Conditions

$$f(0,t) = f_0(t) \tag{2.31}$$

$$\frac{df_0}{dt} = \left(Y \frac{V_r S(0,t)}{K + S(0,t)} - b \right) f_0(t) - f_0(t) \frac{\partial u}{\partial y}(0,t) \tag{2.32}$$

$$\frac{dL(t)}{dt} = u(L(t),t) \tag{2.33}$$

Zero-dimensional Model

In the model described above, the functions $S(y,t)$ and $f(y,t)$ depend on time as well as space. The zero-dimensional model ignores the dependence of these functions on the spatial variable y and considers the average growth and decay of the functions S and f on the interval $0 \leq y \leq L(t)$, which depend on time only. The four dependent variables and their fundamental units are given in Table 1. A detailed description and derivation of the zero-dimensional equations follows.

Variables	Physical quantity	Units
$L(t)$	biofilm thickness	L
$S_b(t)$	bulk substrate concentration	$M_s L^{-3}$
$S(t)$	average substrate concentration in the biofilm	$M_s L^{-3}$
$f(t)$	average volume fraction of active biomass in the biofilm	dimensionless

Table 3: Unknown dependent variables and their fundamental units in Rittman's zero-dimensional model

The derivation follows along the same lines as that for the one-dimensional model. Let $S(t)$ be the average value of $S(y,t)$ for $y \in [0, L(t)]$ and let $f(t)$ be the average value of $f(y,t)$ for $y \in [0, L(t)]$. A substrate balance in the bulk fluid gives

(see (2.1)),

$$V_L \frac{d}{dt}(S_b(t)) = Q(S_0 - S_b(t)) - \sigma J(t) \tag{2.34}$$

where

$$J(t) = \frac{D}{L_l}(S_b(t) - S(t)).$$

Hence (2.34) simplifies to the zero-dimensional version of (2.3)

$$\frac{d}{dt}(S_b(t)) = \frac{1}{V_L}\left(QS_0 - \left(Q + \frac{\sigma D}{L_l}\right) S_b(t) + \frac{\sigma D}{L_l} S(t)\right). \tag{2.35}$$

The mass balance of the substrate in the biofilm is given by (see (2.6))

$$\frac{d}{dt}(L(t)S(t)) = \frac{D}{L_l}(S_b(t) - S(t)) - \frac{V_r S(t)}{K + S(t)} L(t) f(t) \rho, \tag{2.36}$$

where the first term on the right-hand side is the rate of diffusion of the substrate from the bulk fluid to the laminar diffusional sublayer of thickness L_l of the biofilm and the second term is the average consumption rate of the substrate by the species based on Monod kinetics. This is the zero-dimensional version of (2.6). The mass balance of the active biomass in the biofilm is

rate of increase of the active biomass = growth rate due to
substrate consumption
−rate of cell decay
−detachment rate

which translates into (see (2.14))

$$\frac{d}{dt}(L(t)f(t)\rho) = \left(Y \frac{V_r S(t)}{K + S(t)} - (b + B')\right) L(t) f(t) \rho$$

where B' is the average shear stress coefficient (average value of b' for $y \in [0, L(t)]$). Dividing by ρ yields the zero-dimensional version of (2.14)

$$\frac{d}{dt}(L(t)f(t)) = \left(Y \frac{V_r S(t)}{K + S(t)} - (b + B')\right) L(t) f(t). \tag{2.37}$$

Similarly, the mass balance of the inactive biomass in the biofilm is

rate of increase of the inactive biomass = inactivation rate of active bacteria −bio-degradation rate −detachment rate

which translates into

$$\frac{d}{dt}(L(t)\bar{f}(t)\rho) = bL(t)f(t)\rho - bf_dL(t)f(t)\rho - B'L(t)\bar{f}(t)\rho.$$

Dividing by ρ, adding with (2.37), and using the assumption $f(t) + \bar{f}(t) = 1$ yields

$$\frac{d}{dt}(L(t)) = \left(Y\frac{V_rS(t)}{K+S(t)} - bf_d\right)L(t)f(t) - B'L(t), \tag{2.38}$$

which is the zero-dimensional version of (2.30). Again B' is the average shear stress coefficient (T^{-1}).

Zero-dimensional Rittman's Model

$$\frac{d}{dt}(S_b(t)) = \frac{1}{V_L}\left(QS_0 - \left(Q + \frac{\sigma D}{L_l}\right)S_b(t) + \frac{\sigma D}{L_l}S(t)\right) \tag{2.39}$$

$$\frac{d}{dt}(L(t)S(t)) = \frac{D}{L_l}(S_b(t) - S(t)) - \frac{V_rS(t)}{K+S(t)}L(t)f(t)\rho \tag{2.40}$$

$$\frac{d}{dt}(L(t)f(t)) = \left(Y\frac{V_rS(t)}{K+S(t)} - (b+B')\right)L(t)f(t) \tag{2.41}$$

$$\frac{d}{dt}(L(t)) = \left(Y\frac{V_rS(t)}{K+S(t)} - bf_d\right)L(t)f(t) - B'L(t) \tag{2.42}$$

Biofilm Accumulation Model

One-dimensional Model

In this model, originally described in [25], the mathematical description of microbial interaction in a fixed biofilm is based on conservation principles. This model has the same underlying assumptions as that of Rittman's model hence the mathematical model equations are similar. But when it comes to modeling the detachment of the biofilm into the bulk liquid, these two models differ. Since detachment occurs only at the film-water interface, BAM assumes the effect of detachment close to the interface only whereas Rittman's model assumes that the detachment effects all the variables at each spatial point.

It is assumed that

- The biofilm is homogeneous and may be treated as a continuum.
- The changes occur only in the direction perpendicular to the biofilm surface.
- There is a laminar diffusional sublayer of constant thickness in the bulk liquid.
- The biofilm is made of active and inactive cells of bacteria and water.

This model will predict the same four functions as in Table 1. The other variables and different parameters used to develop this model along with their fundamental units are given in Table 4. A visualization of the physical system to be modeled is given in Figure 4

This model also consists of two sets of differential equations. One is the diffusional equations and the other is the transport equations.

Diffusional Equations The mass balance of substrate is given by,

$$\frac{\partial}{\partial t}(S(y,t)) = \left(- R(y,t) - \frac{\partial J(y,t)}{\partial y} \right) \tag{2.43}$$

Parameters	Physical quantity	Units
V_L	volume of the bulk liquid	L^3
ϵ_l	volume fraction of water in the biofilm	dimensionless
Q	volumetric flow rate of the bulk liquid	L^3T^{-1}
S_0	substrate concentration in the influent fluid	M_sL^{-3}
σ	area of the film-water interface	L^2
D	diffusivity coefficient of the substrate through the laminar diffusional sublayer	L^2T^{-1}
L_l	thickness of laminar diffusional sublayer	L
d	diffusivity coefficient of the substrate inside the biofilm	L^2T^{-1}
ρ	biomass density	M_xL^{-3}
b	inactivation coefficient	T^{-1}
Y	yield coefficient	$M_xM_s^{-1}$
λ	detachment coefficient	$L^{-1}T^{-1}$

Variables	Physical quantity	Units
$J(y,t)$	influx rate of the substrate into the biofilm	$M_sL^{-2}T^{-1}$
$u(y,t)$	velocity of the biomass particle at (y,t)	LT^{-1}
$u_L(t)$	velocity of the film-water interface	LT^{-1}
$g(y,t)$	flux of active biomass	$M_xL^{-2}T^{-1}$
$R(y,t)$	reaction rate	$M_sL^{-3}T^{-1}$
$\delta(t)$	detachment rate of the biofilm	LT^{-1}
$\bar{f}(y,t)$	volume fraction of inactive biomass in the biofilm	dimensionless

Table 4: Parameters and the variables used in BAM and their fundamental units

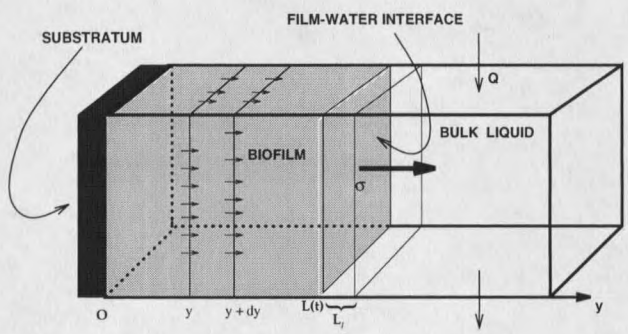

Figure 4: Biofilm on a surface

where $S(y,t)$ is the concentration of the substrate in the biofilm ($M_s L^{-3}$), $J(y,t)$ is the flux of substrate into the biofilm, ($M_s L^{-2} T^{-1}$), and $R(y,t)$ is the reaction rate of substrate, ($M_s L^{-3} T^{-1}$).

According to Fick's first law, the flux of substrate within the film is proportional to the diffusivity d ($L^2 T^{-1}$) and may be expressed as

$$J(y,t) = -d\frac{\partial S(y,t)}{\partial y}. \tag{2.44}$$

Substitution of equation (2.44) into equation (2.43) leads to

$$\frac{\partial S(y,t)}{\partial t} = \left(-R(y,t) + \frac{\partial}{\partial y}\left(d\frac{\partial S(y,t)}{\partial y} \right) \right). \tag{2.45}$$

At the substratum there is no flux which gives

$$\frac{\partial S}{\partial y}(0,t) = 0. \tag{2.46}$$

If an external mass transfer limitation is included, then the other boundary condition at the film-water interface is

$$d\frac{\partial S}{\partial y}(L(t),t) = \frac{D}{L_l}\left(S_b(t) - S(L(t),t) \right) \tag{2.47}$$

and if it is neglected then,

$$S_b(t) = S(L(t),t), \tag{2.48}$$

where D is the diffusivity of the substrate in the laminar diffusional sublayer ($L^2 T^{-1}$), L_l is the thickness of the laminar sublayer (L), and $S_b(t)$ is the concentration of the substrate in the bulk liquid. D and L_l are assumed to be constants.

Finally the model equation for the substrate in the bulk liquid is

$$\begin{aligned} \frac{dS_b(t)}{dt} &= \frac{1}{V_L}\Big(Q\ \left(S_0 - S_b(t) \right) - \\ &\quad \sigma\left(\frac{D}{L_l} - u(L(t),t) \right)\left(S_b(t) - S(L(t),t) \right) \Big). \end{aligned} \tag{2.49}$$

The differential equations (2.45) and (2.49) and the boundary conditions (2.46) and (2.47) are the diffusional equations for BAM.

Transport Equations A mass balance of active microbial species for a differential volume σdy, as shown in Figure 4, has the form

$$\frac{\partial}{\partial t}\Big(\sigma\ dy\ \rho\ f(y,t)\Big) = \sigma\ dy\ Y\ R(y,t) - b\sigma\ dy\ \rho\ f(y,t) + \sigma\ g(y,t) - \sigma\ g(y+dy,t), \tag{2.50}$$

where σ is the area of the film-water interface (L^2), σdy is the differential volume element (L^3), ρ is the constant density of the biomass $(M_x L^{-3})$, $R(y,t)$ is the reaction rate of the active biomass $(M_s L^{-3} T^{-1})$, $f(y,t)$ is the dimensionless volume fraction of the active biomass, b is the inactivation coefficient (T^{-1}), and $g(y,t)$ is the mass flux $(M_x L^{-2} T^{-1})$. Approximating $g(y+dy,t)$ by its first-order Taylor's expansion, (2.50) reduces to

$$\frac{\partial}{\partial t}\Big(\sigma\ dy\ \rho\ f(y,t)\Big) = \sigma\ dy\ Y\ R(y,t) - b\sigma\ dy\ \rho\ f(y,t) - \sigma\ \frac{\partial g(y,t)}{\partial y}\ dy. \tag{2.51}$$

Dividing by $\sigma\ dy\ \rho$ we get,

$$\frac{\partial f(y,t)}{\partial t} = \frac{Y}{\rho}\ R(y,t) - b\ f(y,t) - \frac{1}{\rho}\frac{\partial g(y,t)}{\partial y}. \tag{2.52}$$

The flux $g(y,t)$ of active biomass may be expressed in terms of the velocity $u(y,t)$ at which the microbial mass is displaced with respect to the substratum and the concentration of the microorganisms $\rho f(y,t)$, as

$$g(y,t) = u(y,t)\ \rho\ f(y,t). \tag{2.53}$$

Now (2.52) implies,

$$\frac{\partial f(y,t)}{\partial t} = \frac{Y}{\rho} R(y,t) - b\ f(y,t) - \frac{\partial u(y,t)}{\partial y} f(y,t) - u(y,t)\frac{\partial f(y,t)}{\partial y}. \tag{2.54}$$

Similarly the mass balance of the inactive biomass simplifies to

$$\frac{\partial \bar{f}(y,t)}{\partial t} = b\ f(y,t) - \frac{\partial u(y,t)}{\partial y}\bar{f}(y,t) - u(y,t)\frac{\partial \bar{f}(y,t)}{\partial y} \tag{2.55}$$

where $\bar{f}(y,t)$ is the dimensionless volume fraction of inactive biomass. Adding (2.54) and (2.55) and assuming that $f(y,t) + \bar{f}(y,t) = 1 - \epsilon_l$, where ϵ_l is the constant dimensionless volume fraction of water in the biofilm, we get

$$0 = \frac{Y\ R(y,t)}{\rho} - (1-\epsilon_l)\frac{\partial u(y,t)}{\partial y} \tag{2.56}$$

which simplifies to

$$\frac{\partial u(y,t)}{\partial y} = \frac{1}{(1-\epsilon_l)}\frac{Y\ R(y,t)}{\rho}. \tag{2.57}$$

Integrating both sides and using the assumption that $u(0,t) = 0$ we get

$$u(y,t) = \frac{1}{(1-\epsilon_l)}\int_0^y \frac{Y\ R(\xi,t)}{\rho} d\xi. \tag{2.58}$$

If the biofilm grows or shrinks, the thickness $L(t)$ of the biofilm changes and the film-water interface moves at a velocity

$$u_L(t) \equiv u(L(t),t) = \frac{dL(t)}{dt} \tag{2.59}$$

with respect to the substratum. If $\delta(t)$ is defined to be the velocity (LT^{-1}), at which biomass is exchanged between biofilm and the bulk liquid (detachment rate), then using equation (2.58) the velocity of the film-water interface may be expressed as

$$u_L(t) = \frac{1}{(1-\epsilon_l)}\int_0^{L(t)} \frac{Y\ R(\xi,t)}{\rho} d\xi + \delta(t). \tag{2.60}$$

The detachment function, $\delta(t)$, is given by $\delta(t) = -\lambda L^2(t)$, [25]. The constant λ is called the coefficient of detachment $(L^{-1}T^{-1})$. Substitution of (2.57) into (2.54) yields,

$$\begin{aligned}\frac{\partial f(y,t)}{\partial t} &= \frac{Y\ R(y,t)}{\rho} - b\ f(y,t) - \frac{f(y,t)}{(1-\epsilon_l)}\frac{Y\ R(y,t)}{\rho} \\ &\quad -u(y,t)\frac{\partial f(y,t)}{\partial y}.\end{aligned} \tag{2.61}$$

At $y = 0$, (2.61) reduces to

$$\frac{\partial f(0,t)}{\partial t} = \frac{Y\ R(0,t)}{\rho} - b\ f(0,t) - \frac{f(0,t)}{(1-\epsilon_l)}\frac{Y\ R(0,t)}{\rho} \tag{2.62}$$

because $u(y,t) = 0$ at the substratum. The equations (2.58) and (2.61) and the boundary conditions (2.60) (which uses $u(0,t) = 0$) and (2.62) are the transport equations for BAM.

One-dimensional BAM

Diffusional Equations

$$\frac{\partial S(y,t)}{\partial t} = \left(- R(y,t) + \frac{\partial}{\partial y}\left(d\frac{\partial S(y,t)}{\partial y}\right)\right) \tag{2.63}$$

$$\begin{aligned}\frac{dS_b(t)}{dt} &= \frac{1}{V_L}\Big(Q \left(S_0 - S_b(t)\right) - \\ &\quad \sigma\left(\frac{D}{L_l} - u(L(t),t)\right)\left(S_b(t) - S(L(t),t)\right)\Big)\end{aligned} \tag{2.64}$$

Boundary conditions

$$\frac{\partial S}{\partial y}(0,t) = 0 \tag{2.65}$$

$$d\frac{\partial S}{\partial y}(L(t),t) = \frac{D}{L_l}\left(S_b(t) - S(L(t),t)\right) \tag{2.66}$$

Transport Equations

$$u(y,t) = \frac{1}{(1-\epsilon_l)}\int_0^y \frac{Y\ R(\xi,t)}{\rho} d\xi \tag{2.67}$$

$$\begin{aligned}\frac{\partial f(y,t)}{\partial t} &= \frac{Y\ R(y,t)}{\rho} - b\ f(y,t) - \frac{f(y,t)}{(1-\epsilon_l)}\frac{Y\ R(y,t)}{\rho} \\ &\quad -u(y,t)\frac{\partial f(y,t)}{\partial y}\end{aligned} \tag{2.68}$$

Boundary conditions

$$u_L(t) \equiv u(L(t),t) = \frac{1}{(1-\epsilon_l)}\int_0^{L(t)} \frac{Y\ R(\xi,t)}{\rho} d\xi + \delta(t) \tag{2.69}$$

$$u(0,t) = 0 \tag{2.70}$$

$$\frac{\partial f(0,t)}{\partial t} = \frac{Y\ R(0,t)}{\rho} - b\ f(0,t) - \frac{f(0,t)}{(1-\epsilon_l)}\frac{Y\ R(0,t)}{\rho} \tag{2.71}$$

Zero-dimensional Model

The derivation of the zero-dimensional model equations is based on the approach described in Rittman's model. The four dependent variables and their fundamental units are given in Table 5.

Variables	Physical quantity	Units
$L(t)$	biofilm thickness	L
$S_b(t)$	bulk substrate concentration	$M_s L^{-3}$
$S(t)$	average substrate concentration in the biofilm	$M_s L^{-3}$
$f(t)$	average volume fraction of active biomass	dimensionless

Table 5: Unknown dependent variables and their fundamental units in BAM zero-dimensional model

The velocity of the film-water interface comes from (2.60),

$$u_L(t) = \frac{1}{(1-\epsilon_l)} \frac{Y\ R(t)\ L(t)}{\rho} + \delta(t). \tag{2.72}$$

The mass balance for the active biomass in the biofilm is modeled by,

$$\frac{d}{dt}(\sigma L(t) \rho f(t)) = \text{Average growth rate - inactivation rate + detachment rate}$$

which is

$$\frac{d}{dt}\Big(\sigma L(t)\rho f(t)\Big) = Y\ R(t)\ L(t) - b\sigma L(t)\rho f(t) + \delta(t)\sigma\rho f(t).$$

Dividing by $\sigma\rho$ gives

$$\frac{d}{dt}\Big(L(t)f(t)\Big) = \frac{Y\ R(t)\ L(t)}{\rho} - bL(t)f(t) + \delta(t)f(t) \tag{2.73}$$

where $\delta(t)$ is the detachment rate and $R(t)$ is the average growth rate of active biomass (average value of $R(y,t)$ for $y \in [0, L(t)]$). The increase in the concentration of the substrate in the biofilm depends on the rate with which the substrate diffuses into the

biofilm and the rate the substrate is consumed by the active bacteria in the biofilm. The model equation governing the mass balance of the substrate in the biofilm is (see(2.45))

$$\frac{d}{dt}\Big(L(t)S(t)\Big) = \frac{D}{L_l}\Big(S_b(t) - S(t)\Big) - R(t)L(t), \tag{2.74}$$

where the first term on right-hand side is due to diffusion of the substrate in the biofilm and $R(t)$ may be given by Monod kinetics. Assume that the film-water interface is moving with a velocity u_L perpendicular to the interface. The mass of the substrate in the laminar diffusional sublayer at any time, t, is $\sigma L_l(S_b(t) - S(t))$. The mass balance of the substrate will be given by,

$$\begin{aligned} V_L\frac{dS_b(t)}{dt} &= Q\Big(S_0 - S_b(t)\Big) - \frac{\sigma D}{L_l}\Big(S_b(t) - S(t)\Big) \\ &\quad + \sigma u_L(t)\Big(S_b(t) - S(t)\Big), \end{aligned}$$

which reduces to (see(2.49)),

$$\begin{aligned} \frac{dS_b(t)}{dt} &= \frac{1}{V_L}\Big(\, Q\Big(S_0 - S_b(t)\Big) - \sigma\Big(\,\frac{D}{L_l} - u_L(t)\,\Big) \\ &\quad \Big(S_b(t) - S(t)\Big)\Big). \end{aligned} \tag{2.75}$$

Zero-dimensional BAM

$$u_L(t) = \frac{1}{(1-\epsilon_l)}\frac{Y\ R(t)\ L(t)}{\rho} + \delta(t) \tag{2.76}$$

$$\frac{d}{dt}\Big(L(t)f(t)\Big) = \frac{Y\ R(t)L(t)}{\rho} - bL(t)f(t) + \delta(t)f(t) \tag{2.77}$$

$$\frac{d}{dt}\Big(L(t)S(t)\Big) = \frac{D}{L_l}\Big(S_b(t) - S(t)\Big) - R(t)L(t) \tag{2.78}$$

$$\begin{aligned} \frac{dS_b(t)}{dt} &= \frac{1}{V_L}\Big(\, Q\Big(S_0 - S_b(t)\Big) - \sigma\Big(\,\frac{D}{L_l} - u_L(t)\,\Big) \\ &\quad \Big(S_b(t) - S(t)\Big)\Big) \end{aligned} \tag{2.79}$$

Biofilm Growth Model

One-dimensional Model

Like BAM and Rittman's model, the model developed here is also based on conservation principles. BAM and Rittman's model assume that the volume of the biofilm is negligible compared to the volume of the bulk liquid and hence they treat the volume of the bulk liquid as a constant. If the biofilm grows on the inner surface of a capillary tube or the pore channels of a porous media then the volume of the biofilm and the volume of the bulk liquid will have the same order of magnitude. In this case the volume of the bulk liquid cannot be assumed constant. In the Biofilm Growth Model (BGM), a new set of model equations have been derived which assumes that the volume of the bulk liquid is a function of time. It is assumed that

- The biomass is homogeneous and it may be treated as a continuum.
- The growth of the biofilm is perpendicular to the surface of the film-water interface.
- There is a laminar diffusional sublayer of constant thickness in the bulk liquid.
- The biofilm is made of active and inactive cells of the bacteria and water.

Consider a rectangular box of thickness $2\Delta y$, called a control volume, centered at point y inside the biofilm as shown in Figure 5. If we assume that the box is fixed then, in the box, the volume fraction of the active and inactive biomass and the concentration of the substrate changes with time. The mathematical equations governing the change in the volume fraction of the active and inactive biomass and the substrate concentration are derived from the mass balance equations. The unknown dependent variables determined in this model are shown in Table 6 and the other variables and the parameters used to develop this model are given in Table 7.

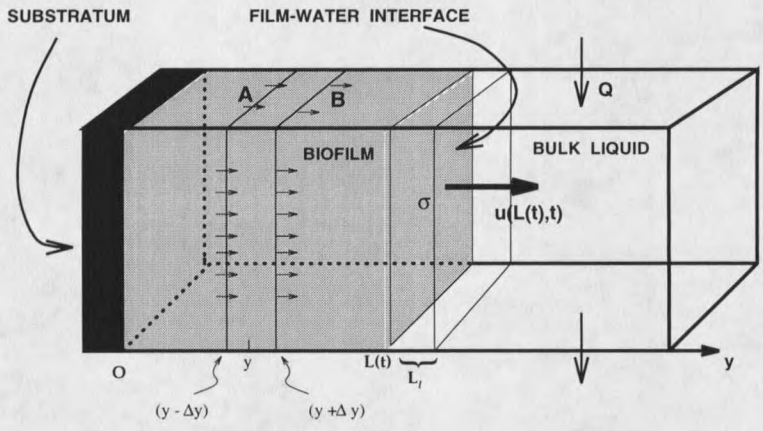

Figure 5: Biofilm on a surface

Variables	Physical quantity	Units
$L(t)$	biofilm thickness	L
$V_L(t)$	volume of the bulk liquid	L^3
$S_b(t)$	bulk substrate concentration	$M_s L^{-3}$
$S(y,t)$	substrate concentration in the biofilm	$M_s L^{-3}$
$f(y,t)$	volume fraction of active biomass in the biofilm	dimensionless

Table 6: Unknown dependent variables and their fundamental units in the Biofilm Growth Model

Parameters	Physical quantity	Units
S_0	substrate concentration in the influent fluid	$M_s L^{-3}$
σ	area of the film-water interface	L^2
D	diffusivity coefficient of the substrate through the laminar diffusional sublayer	$L^2 T^{-1}$
L_l	thickness of laminar diffusional sublayer	L
d	diffusivity coefficient of the substrate inside the biofilm	$L^2 T^{-1}$
V_r	maximum specific growth rate	$M_s M_x^{-1} T^{-1}$
K	Monod constant	$M_s L^{-3}$
ρ	biomass density	$M_x L^{-3}$
b	inactivation coefficient	T^{-1}
Y	yield coefficient	$M_x M_s^{-1}$
λ	detachment coefficient	$L^{-1} T^{-1}$

Variables	Physical quantity	Units
$Q(t)$	volumetric flow rate of the bulk liquid	$L^3 T^{-1}$
$m_f(t)$	mass of the active biofilm at time t	M_x
$m_s(t)$	mass of the substrate in the film at time t	M_s
$2\Delta y$	thickness of the rectangular control volume	L
$\delta(t)$	detachment rate of the biofilm	LT^{-1}
$u(y,t)$	velocity of the biomass particle at (y,t)	LT^{-1}
$u_L(t)$	velocity of the film-water interface	LT^{-1}
$\bar{f}(y,t)$	volume fraction of inactive biomass in the biofilm	dimensionless
$m_{\bar{f}}(t)$	mass of the inactive biofilm at time t	M_x

Table 7: Parameters and the variables used in Biofilm Growth Model and their fundamental units

Mass Balance of the Active Biomass Let $m_f(t)$ be the mass (M_x) of the biofilm inside the box at any time, t. Then

$$m_f(t) = \sigma \cdot 2\Delta y \cdot \rho \cdot f(y,t) \tag{2.80}$$

where σ is the area (L^2) of side A or side B of the box, $2\Delta y$ is the thickness (L) of the rectangular control volume, ρ is the constant density of the biomass $(M_x L^{-3})$, and $f(y,t)$ is the dimensionless volume fraction of the active biomass.

As the biofilm grows in the box, the biomass enters the box through side A and leaves the box through side B. Also the active biomass growth in the biofilm is caused by the substrate consumption and the cell division. We further assume that a certain fraction of the active biomass becomes inactive and it never consumes substrate. The time rate of change of the biomass in the box is

$$\begin{aligned}
\frac{\partial m_f(t)}{\partial t} &= \text{influx rate of the biomass through side A} \\
&\quad - \text{outflux rate of the biomass through side B} \\
&\quad + \text{growth rate of the active biomass} \\
&\quad - \text{inactivation rate of the active biomass} \\
&= I_r - O_r + G_r - D_r.
\end{aligned} \tag{2.81}$$

Now we will write the mathematical expression for each term in the right-hand side of (2.81) separately.

The influx rate of the biomass through side A, I_r $(M_x T^{-1})$ is given by

$$\begin{aligned}
I_r &= \sigma\, u(y-\Delta y,t)\, \rho\, f(y-\Delta y,t) \\
&= \sigma\, \rho \left(u(y,t) - u_y(y,t)\Delta y + u_{yy}(\eta_1,t)\frac{(\Delta y)^2}{2} \right) \\
&\qquad \left(f(y,t) - f_y(y,t)\Delta y + f_{yy}(\zeta_1,t)\frac{(\Delta y)^2}{2} \right)
\end{aligned}$$

where η_1 and ζ_1 are points between $y - \Delta y$ and y. Ignoring the higher order terms in Δy, the above equation simplifies to

$$I_r = \sigma\rho \left(u(y,t)\ f(y,t) - u(y,t) f_y(y,t)\Delta y - u_y(y,t) f(y,t)\Delta y \right). \tag{2.82}$$

The outflux rate of the biomass through side B, O_r $(M_x T^{-1})$ is given by

$$\begin{aligned} O_r &= \sigma\ u(y+\Delta y,t)\ \rho\ f(y+\Delta y,t) \\ &= \sigma\ \rho \left(u(y,t) + u_y(y,t)\Delta y + u_{yy}(\eta_2,t)\frac{(\Delta y)^2}{2} \right) \\ &\qquad \left(f(y,t) + f_y(y,t)\Delta y + f_{yy}(\zeta_2,t)\frac{(\Delta y)^2}{2} \right) \end{aligned}$$

where η_2 and ζ_2 are points between y and $y + \Delta y$. Ignoring the higher order terms in Δy, the above equation simplifies to

$$O_r = \sigma\rho \left(u(y,t)\ f(y,t) + u(y,t) f_y(y,t)\Delta y + u_y(y,t) f(y,t)\Delta y \right). \tag{2.83}$$

If we assume that the growth of the active biomass is governed by Monod kinetics then G_r $(M_x T^{-1})$, will be given by,

$$G_r = \frac{Y V_r S(y,t)}{K + S(y,t)}\ 2\Delta y\ \sigma\ \rho\ f(y,t), \tag{2.84}$$

where Y is the yield coefficient $(M_x M_s^{-1})$, V_r is the maximum growth rate $(M_s M_x^{-1} T^{-1})$, and K is the Monod constant $(M_s L^{-3})$. Assuming that the inactivation rate of the active biomass is proportional to the mass of the active cells in the box D_r $(M_x T^{-1})$, will be given by

$$D_r = b\ 2\Delta y\ \sigma\rho\ f(y,t). \tag{2.85}$$

Using (2.80), (2.82), (2.83), (2.84), and (2.85), (2.81) simplifies to,

$$\begin{aligned} \frac{\partial f(y,t)}{\partial t} &= -u(y,t) f_y(y,t) - u_y(y,t) f(y,t) \\ &\quad + \frac{Y V_r S(y,t) f(y,t)}{K + S(y,t)} - b f(y,t) \end{aligned} \tag{2.86}$$

We have also assumed here that ρ and σ are constants.

Mass Balance of the Inactive Biomass If $\bar{f}(y,t)$ denotes the volume fraction of the inactive biomass at any instant, t, then the inactive biomass, $m_{\bar{f}}(t)$ (M_x), is given by

$$m_{\bar{f}}(t) = \sigma \cdot 2\Delta y \cdot \rho \cdot \bar{f}(y,t). \tag{2.87}$$

Also,

$$\begin{aligned}\frac{\partial m_{\bar{f}}(t)}{\partial t} &= \text{influx rate of the inactive biomass through side A} \\ &\quad - \text{outflux rate of the inactive biomass through side B} \\ &\quad + \text{inactivation rate of the active biomass} \\ &= \bar{I}_r - \bar{O}_r + D_r. \end{aligned} \tag{2.88}$$

The influx rate of the inactive biomass through side A, $\bar{I}_r$ $(M_x T^{-1})$, is given by,

$$\begin{aligned}\bar{I}_r &= \sigma\, u(y-\Delta y,t)\, \rho\, \bar{f}(y-\Delta y,t) \\ &= \sigma\, \rho \left(u(y,t) - u_y(y,t)\Delta y + u_{yy}(\eta_3,t)\frac{(\Delta y)^2}{2}\right) \\ &\qquad \left(\bar{f}(y,t) - \bar{f}_y(y,t)\Delta y + \bar{f}_{yy}(\zeta_3,t)\frac{(\Delta y)^2}{2}\right)\end{aligned}$$

where η_3 and ζ_3 are numbers between $y-\Delta y$ and y. Ignoring the higher order terms in Δy, the above equation simplifies to

$$\bar{I}_r = \sigma\rho \left(u(y,t)\, \bar{f}(y,t) - u(y,t)\bar{f}_y(y,t)\Delta y - u_y(y,t)\bar{f}(y,t)\Delta y\right). \tag{2.89}$$

The outflux rate of the inactive biomass through side B, $\bar{O}_r$ $(M_x T^{-1})$, is given by

$$\begin{aligned}\bar{O}_r &= \sigma\, u(y+\Delta y,t)\, \rho\, \bar{f}(y+\Delta y,t) \\ &= \sigma\, \rho \left(u(y,t) + u_y(y,t)\Delta y + u_{yy}(\eta_4,t)\frac{(\Delta y)^2}{2}\right) \\ &\qquad \left(\bar{f}(y,t) + \bar{f}_y(y,t)\Delta y + \bar{f}_{yy}(\zeta_4,t)\frac{(\Delta y)^2}{2}\right)\end{aligned}$$

where η_4 and ζ_4 are points between y and $y+\Delta y$. Ignoring the higher order terms in Δy, the above equation simplifies to

$$\bar{O}_r = \sigma\rho \left(u(y,t)\ \bar{f}(y,t) + u(y,t)\bar{f}_y(y,t)\Delta y + u_y(y,t)\bar{f}(y,t)\Delta y \right). \tag{2.90}$$

Using (2.87),(2.89),(2.90), and (2.85), (2.88) simplifies to,

$$\frac{\partial \bar{f}(y,t)}{\partial t} = -u(y,t)\bar{f}_y(y,t) - u_y(y,t)\bar{f}(y,t) + bf(y,t). \tag{2.91}$$

Adding (2.86) and (2.91) and using the assumption $f(y,t) + \bar{f}(y,t) = 1 - \epsilon_l$, we get

$$-(1-\epsilon_l)u_y(y,t) + \frac{YV_rS(y,t)f(y,t)}{K+S(y,t)} = 0$$

which gives

$$u_y(y,t) = \frac{1}{(1-\epsilon_l)} \frac{YV_rS(y,t)f(y,t)}{K+S(y,t)}. \tag{2.92}$$

Integrating both sides and using $u(0,t) = 0$, we get,

$$u(y,t) = \frac{1}{(1-\epsilon_l)} \int_0^y \frac{YV_rS(\xi,t)f(\xi,t)}{K+S(\xi,t)}\ d\xi. \tag{2.93}$$

If we assume that the rate with which the biofilm detaches into the bulk liquid is $\delta(t)$, (LT^{-1}), then the velocity of the interface will be given by,

$$u_L(t) \equiv u(L(t),t) = \frac{1}{(1-\epsilon_l)} \int_0^{L(t)} \frac{YV_rS(\xi,t)f(\xi,t)}{K+S(\xi,t)}\ d\xi\ + \delta(t). \tag{2.94}$$

The detachment rate, $\delta(t)$, is given by $\delta(t) = -\lambda L^2(t)$, [25]. The constant λ is called the coefficient of detachment $(L^{-1}T^{-1})$. Using (2.92), (2.86) becomes

$$\begin{aligned}
\frac{\partial f(y,t)}{\partial t} &= -u(y,t)f_y(y,t) - \frac{1}{(1-\epsilon_l)} \frac{YV_rS(y,t)f^2(y,t)}{K+S(y,t)} \\
&\quad + \frac{YV_rS(y,t)f(y,t)}{K+S(y,t)} - bf(y,t) \\
&= -u(y,t)f_y(y,t) + \frac{YV_rS(y,t)f(y,t)}{K+S(y,t)} \left(1 - \frac{f(y,t)}{1-\epsilon_l}\right) \\
&\quad - bf(y,t) \\
&= -u(y,t)f_y(y,t) + \frac{YV_rS(y,t)f(y,t)\bar{f}(y,t)}{(K+S(y,t))(1-\epsilon_l)} - bf(y,t).
\end{aligned} \tag{2.95}$$

Similarly using (2.92), (2.91) becomes

$$\frac{\partial \bar{f}(y,t)}{\partial t} = -u(y,t)\bar{f}_y(y,t) - \frac{YV_rS(y,t)f(y,t)\bar{f}(y,t)}{(K+S(y,t))(1-\epsilon_l)} + bf(y,t). \tag{2.96}$$

Mass Balance of the Substrate in the Biofilm If we denote the substrate concentration in the film by $S(y,t)$ then the mass of the substrate in the box, $m_S(t)$, (M_s), will be given by,

$$m_S(t) = \sigma\ 2\Delta y\ S(y,t). \tag{2.97}$$

Also,

$$\begin{aligned}
\frac{\partial m_S(t)}{\partial t} &= \text{influx rate of the substrate through side A} \\
&\quad - \text{outflux rate of the substrate through side B} \\
&\quad - \text{consumption rate of the substrate} \\
&\quad + \text{diffusion rate of the substrate into the box.} \\
&= \sigma u(y-\Delta y,t)S(y-\Delta y,t) \\
&\quad - \sigma u(y+\Delta y,t)S(y+\Delta y,t) \\
&\quad - \frac{V_rS(y,t)}{K+S(y,t)}\,(\sigma 2\Delta y)\rho f(y,t) \\
&\quad + d\,\frac{\partial^2 S(y,t)}{\partial y^2}(\sigma 2\Delta y)
\end{aligned} \tag{2.98}$$

where d is the diffusivity coefficient of the substrate into the biofilm (L^2T^{-1}). Ignoring the higher order terms (2.98) reduces to,

$$\begin{aligned}
\frac{\partial m_S(t)}{\partial t} &= \sigma(u(y,t)-u_y(y,t)\Delta y)(S(y,t)-S_y(y,t)\Delta y) \\
&\quad - \sigma(u(y,t)+u_y(y,t)\Delta y)(S(y,t)+S_y(y,t)\Delta y) \\
&\quad - \frac{V_rS(y,t)}{K+S(y,t)}\,(\sigma 2\Delta y)\rho f(y,t) \;+\; d\,\frac{\partial^2 S(y,t)}{\partial y^2}(\sigma 2\Delta y) \\
&= -(\sigma\ 2\Delta y)(u(y,t)S_y(y,t)+u_y(y,t)S(y,t)) \\
&\quad - \frac{V_rS(y,t)}{K+S(y,t)}\,(\sigma 2\Delta y)\rho f(y,t) \;+\; d\,\frac{\partial^2 S(y,t)}{\partial y^2}(\sigma 2\Delta y).
\end{aligned} \tag{2.99}$$

Using (2.97), (2.99) reduces to

$$\begin{aligned}\frac{\partial S(y,t)}{\partial t} &= -u(y,t)S_y(y,t) - u_y(y,t)S(y,t) \\ &\quad - \frac{V_r S(y,t)}{K + S(y,t)}\,\rho\, f(y,t) + d\,\frac{\partial^2 S(y,t)}{\partial y^2}. \end{aligned} \tag{2.100}$$

Using (2.92), (2.100) becomes

$$\begin{aligned}\frac{\partial S(y,t)}{\partial t} &= -u(y,t)\frac{\partial S(y,t)}{\partial y} \\ &\quad -\frac{V_r S(y,t) f(y,t)}{K + S(y,t)}\left(\frac{Y S(y,t)}{1-\epsilon_l} + \rho\right) + d\,\frac{\partial^2 S(y,t)}{\partial y^2}. \end{aligned} \tag{2.101}$$

Change in the Bulk Liquid Volume Let us denote the volume of the bulk liquid by $V_L(t)$ (L^3). Then at time $t + \Delta t$ the volume of the bulk liquid will be given by,

$$V_L(t + \Delta t) = V_L(t) - \sigma u_L(t)\Delta t.$$

As $\Delta t \to 0$, this equation reduces to,

$$\frac{dV_L(t)}{dt} = -\sigma\, u_L(t). \tag{2.102}$$

Substrate Concentration in the Bulk Liquid Let $S_b(t)$ be the concentration of the substrate in the bulk liquid $(M_s L^{-3})$, S_0 be the concentration of the substrate in the influent fluid $(M_s L^{-3})$, and $Q(t)$ be the volumetric flow rate of the influent fluid $(L^3 T^{-1})$. Then the rate of change of the total mass of the substrate in the bulk liquid is

$$\begin{aligned}\frac{d}{dt}\Big(S_b(t)V_L(t)\Big) &= \text{rate of mass increase due to influent fluid} \\ &\quad - \text{rate of mass loss due to fluid flowing out} \\ &\quad - \text{rate of mass loss due to biofilm growth}\end{aligned}$$

$$
\begin{aligned}
& -\text{rate of mass loss due to substrate} \\
& \text{diffusion into the film} \\
= \; & Q(t)S_0 - Q(t)S_b(t) - u_L(t)\sigma S_b(t) \\
& -\frac{\sigma D}{L_l}\Big(S_b(t) - S(L(t),t)\Big) \qquad (2.103)
\end{aligned}
$$

which gives,

$$
\begin{aligned}
S_b(t)\frac{dV_L(t)}{dt} + V_L(t)\frac{dS_b(t)}{dt} &= Q(t)S_0 - Q(t)S_b(t) - u_L(t)\sigma S_b(t) \\
& -\frac{\sigma D}{L_l}\Big(S_b(t) - S(L(t),t)\Big). \qquad (2.104)
\end{aligned}
$$

Using (2.102) this simplifies to,

$$
\frac{dS_b(t)}{dt} = \frac{1}{V_L(t)}\Big(Q(t)(S_0 - S_b(t)) - \frac{\sigma D}{L_l}(S_b(t) - S(L(t),t))\Big). \qquad (2.105)
$$

One-dimensional BGM

$$
\begin{aligned}
\frac{\partial f(y,t)}{\partial t} &= -u(y,t)f_y(y,t) + \frac{YV_rS(y,t)f(y,t)\bar{f}(y,t)}{(K+S(y,t))(1-\epsilon_l)} \\
& \quad -bf(y,t) \qquad (2.106) \\
\frac{\partial S(y,t)}{\partial t} &= -u(y,t)\frac{\partial S(y,t)}{\partial y} \\
& \quad -\frac{V_rS(y,t)f(y,t)}{K+S(y,t)}\left(\frac{YS(y,t)}{1-\epsilon_l} + \rho\right) + d\,\frac{\partial^2 S(y,t)}{\partial y^2} \qquad (2.107) \\
\bar{f}(y,t) &= 1 - \epsilon_l - f(y,t) \qquad (2.108) \\
u(y,t) &= \frac{1}{(1-\epsilon_l)}\int_0^y \frac{YV_rS(\xi,t)f(\xi,t)}{K+S(\xi,t)}\,d\xi \qquad (2.109) \\
\frac{dV_L(t)}{dt} &= -\sigma\, u_L(t) \qquad (2.110) \\
\frac{dS_b(t)}{dt} &= \frac{1}{V_L(t)}\Big(Q(t)(S_0 - S_b(t)) \\
& \quad -\frac{\sigma D}{L_l}(S_b(t) - S(L(t),t))\Big) \qquad (2.111)
\end{aligned}
$$

Boundary conditions

$$
\frac{\partial S}{\partial y}(0,t) = 0 \qquad (2.112)
$$

$$d\,\frac{\partial S}{\partial y}(L(t),t) = \frac{D}{L_l}\Big(S_b(t) - S(L(t),t)\Big) \tag{2.113}$$

$$u(0,t) = 0 \tag{2.114}$$

$$u_L(t) \equiv u(L(t),t) = \frac{1}{(1-\epsilon_l)}\int_0^{L(t)} \frac{YV_rS(\xi,t)f(\xi,t)}{K+S(\xi,t)}\;d\xi + \delta(t) \tag{2.115}$$

and

$$\frac{\partial f}{\partial t}(0,t) = \frac{YV_rS(0,t)f(0,t)\bar{f}(0,t)}{(K+S(0,t))(1-\epsilon_l)} - bf(0,t). \tag{2.116}$$

Zero-dimensional Model

The derivation of zero-dimensional BGM is also based on the idea described in Rittman's model. The unknown dependent variables determined by this model are given in Table 8. The rate of change of the active biomass depends on the growth

Variables	Physical quantity	Units
$L(t)$	biofilm thickness	L
$V_L(t)$	volume of the bulk liquid	L^3
$S_b(t)$	bulk substrate concentration	M_sL^{-3}
$S(t)$	average substrate concentration in the biofilm	M_sL^{-3}
$f(t)$	average volume fraction of active biomass in the biofilm	dimensionless

Table 8: Unknown dependent variables and their fundamental units in the zero-dimensional Biofilm Growth Model

rate of active biomass, inactivation rate of active biomass and the detachment rate. A mathematical expression for the rate of change of active biomass may be given by (see (2.95))

$$\frac{d}{dt}\Big(\sigma\rho f(t)L(t)\Big) = \left(\frac{YV_rS(t)}{(K+S(t))} - b\right)\sigma\rho L(t)f(t) + \delta(t)\sigma\rho f(t).$$

Using the chain rule and the assumption that ρ and σ are constants, the above equation reduces to

$$\frac{df(t)}{dt} = -\frac{f(t)}{L(t)}\frac{dL(t)}{dt} + \left(\frac{YV_rS(t)}{(K+S(t))} - b + \frac{\delta(t)}{L(t)}\right)f(t). \tag{2.117}$$

The inactive biomass increases as the active biomass becomes inactive and it decreases as the biofilm detaches at the interface between the film and the liquid. The rate of change of inactive biomass can be given by,

$$\frac{d}{dt}\left(\sigma\rho\bar{f}(t)L(t)\right) = b\sigma\rho L(t)f(t) + \delta(t)\sigma\rho\bar{f}(t),$$

which simplifies to,

$$\frac{d\bar{f}(t)}{dt} = -\frac{\bar{f}(t)}{L(t)}\frac{dL(t)}{dt} + bf(t) + \frac{\delta(t)}{L(t)}\bar{f}(t).$$

Adding this to (2.117) and using the assumption that $f(t) + \bar{f}(t) + \epsilon_l = 1$ we get,

$$\frac{dL(t)}{dt} = \frac{1}{1-\epsilon_l}\frac{YV_rL(t)S(t)f(t)}{K+S(t)} + \delta(t). \tag{2.118}$$

The average rate of change of the substrate in the biofilm depends on the consumption rate of the substrate and the diffusion rate of the substrate into the film. A mathematical expression for the rate of change of the substrate in the film may be given by,

$$\frac{d}{dt}\left(\sigma S(t)L(t)\right) = \frac{\sigma D}{L_l}\left(S_b(t) - S(t)\right) - \frac{V_rS(t)}{K+S(t)}\rho\sigma L(t)f(t)$$

which reduces to

$$\frac{dS(t)}{dt} = -\frac{S(t)}{L(t)}\frac{dL(t)}{dt} + \frac{D}{L_lL(t)}\left(S_b(t) - S(t)\right) - \frac{V_rS(t)\ \rho\ f(t)}{K+S(t)}. \tag{2.119}$$

The substrate concentration in the bulk liquid from (2.105) is

$$\frac{dS_b(t)}{dt} = \frac{1}{V_L(t)}\left(Q(t)(S_0 - S_b(t)) - \frac{\sigma D'}{L_l}(S_b(t) - S(t))\right) \tag{2.120}$$

and the volume of the bulk liquid from (2.102) is,

$$\frac{dV_L(t)}{dt} = -\sigma\ \frac{dL(t)}{dt}. \tag{2.121}$$

Zero-dimensional BGM

$$\frac{df(t)}{dt} = -\frac{f(t)}{L(t)}\frac{dL(t)}{dt} + \left(\frac{YV_rS(t)}{(K+S(t))} - b + \frac{\delta(t)}{L(t)}\right)f(t) \tag{2.122}$$

$$\frac{dL(t)}{dt} = \frac{1}{1-\epsilon_l}\frac{YV_r L(t)S(t)f(t)}{K+S(t)} + \delta(t) \tag{2.123}$$

$$\frac{dS(t)}{dt} = -\frac{S(t)}{L(t)}\frac{dL(t)}{dt} + \frac{D}{L_l L(t)}\Big(S_b(t) - S(t)\Big) - \frac{V_r S(t)\ \rho\ f(t)}{K+S(t)} \tag{2.124}$$

$$\frac{dS_b(t)}{dt} = \frac{1}{V_L(t)}\left(Q(t)(S_0 - S_b(t)) - \frac{\sigma D}{L_l}(S_b(t) - S(t))\right) \tag{2.125}$$

$$\frac{dV_L(t)}{dt} = -\sigma\ \frac{dL(t)}{dt} \tag{2.126}$$

CHAPTER 3

Comparison of the Biofilm Models

Introduction

When the biofilm grows on the pore surface of the porous media, the pore volume decreases which effects the porosity and the permeability of the porous media [2], [5], [9], [18], [23]. The physical properties, porosity and permeability, of the porous media are defined in Chapter 4. Experimentally it has been shown that the change in the porosity and the permeability affects the flow rate of the bulk fluid through the pore channels [5], [18]. How fast do the pore channels clog? How does the biofilm growth affect the flow rate through the porous media? To answer these questions we must have an efficient model which describes the biofilm growth on a surface and can be combined easily with porous media flow models [2], [9], [23]. In this chapter the numerical results of the three models (BGM, BAM, and Rittman's model) developed in Chapter 2 are compared. We seek the most efficient mathematical model which describes the biofilm growth on a surface. The Biofilm Growth Model (BGM) assumes that the volume of the bulk liquid is a function of time rather than a constant. In the next two sections the numerical solutions of one-dimensional and zero-dimensional BGM are discussed and compared. Then the solutions of the zero-dimensional Rittman's model, BAM, and BGM (restricted so that is comparable to BAM and Rittman's model) are discussed in the fourth, fifth, and sixth sections, respectively. The last section provides a comparison of all three zero dimensional models (where again BGM is restricted to be like BAM and Rittman's model).

Both the one-dimensional Rittman's model and the one-dimensional BAM are accepted models for biofilm growth and the zero-dimensional Rittman's model has been compared to the one-dimensional version [12]. This comparison of the three different zero-dimensional models validates the use of the zero-dimensional BGM for the porous media applications considered in this dissertation.

Solution of One-dimensional BGM

The system of equations (2.106)-(2.116) from the one-dimensional BGM are solved numerically for the dependent variables given in Table 6 and then the results are discussed. The spatial derivatives in (2.106) and (2.107) are replaced by their finite difference approximations

$$\frac{\partial}{\partial y}\Big(f(y,t)\Big) = \frac{f(y+\Delta y,t) - f(y-\Delta y,t)}{2\Delta y}, \tag{3.1}$$

$$\frac{\partial}{\partial y}\Big(S(y,t)\Big) = \frac{S(y+\Delta y,t) - S(y-\Delta y,t)}{2\Delta y}, \tag{3.2}$$

and

$$\frac{\partial^2}{\partial y^2}\Big(S(y,t)\Big) = \frac{S(y+\Delta y,t) - 2S(y,t) + S(y-\Delta y,t)}{(\Delta y)^2}. \tag{3.3}$$

Also the velocity, $u(y,t)$, which is an integral given in (2.109), has been approximated using the trapezoidal rule [3], [15] and $u(y,t)$ has been replaced with its approximation in (2.106), (2.107), and (2.110). The trapezoidal rule is explained briefly below.

Trapezoidal Rule Let $F(y)$ be a continuous function over $[a,b]$ as shown in Figure 6. Divide $[a,b]$ into n equal subintervals of length $\Delta y = \frac{b-a}{n}$ and define $y_i = a + i\Delta y, \;\; i = 0, \cdots, n$. Then the approximation of the integral of $F(y)$ over the interval $[y_{i-1}, y_i]$ is given by

$$\int_{y_{i-1}}^{y_i} F(y)dy = \frac{F(y_i) + F(y_{i-1})}{2}\Delta y \tag{3.4}$$

and the integral of $F(y)$ over the interval $[a, b]$ is given by

$$\int_a^b F(y)dy = \sum_{i=1}^{n} \frac{F(y_i) + F(y_{i-1})}{2} \Delta y. \tag{3.5}$$

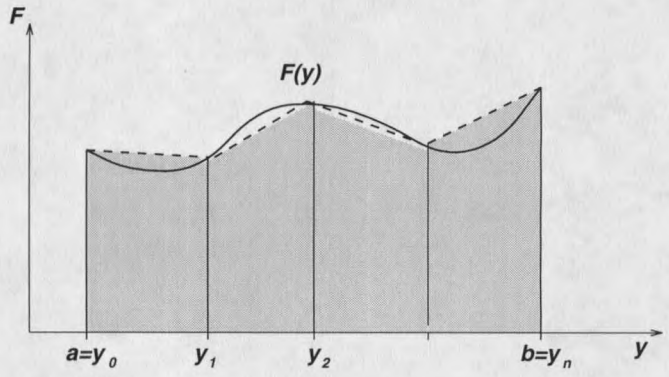

Figure 6: Function $F(y)$ and the approximation of its integral over $[a, b]$

After replacing all the spatial derivatives and the velocity, $u(y, t)$, in (2.106), (2.107), (2.110), and (2.111) with their approximations, a system of ordinary differential equations results. The system of ordinary differential equations is then solved using the MATLAB (version 4.2a) package 'ODE23s'. The software 'ODE23s' solves systems of stiff ordinary differential equations using the modified Rosenbrock method. A computer code for the subroutine 'ODE23s' is given in Appendix A. More information on 'ODE23s' can be found in [24] and the Rosenbrock method is explained in [13]. The modified Rosenbrock method can be found in [27]. The values of the parameters and the initial values of the dependent variables used to run the simulation are based on [12], [25] and are displayed in Table 9. All codes are developed in MATLAB and run on a DECstation 5000/240. The computer code which approximates the solution of the one-dimensional BGM equations is given in Appendix B.

Parameters	Values	Units
K	0.0001	mg/cm^3
V_r	4.3	mg/(mg day)
Y	.5	mg/mg
b	.35	day^{-1}
D	1.3	cm^2/day
$Q(t) \quad \forall t$	1100	cm^3/day
σ	1	cm^2
L_l	.8	cm
ϵ_l	.8	dimensionless
d	1.04	cm^2/ day
ρ	12.2	mg/cm^3
S_0	.02	mg/cm^3
λ	500	$cm^{-1}day^{-1}$
Variables	**Initial Values**	**Units**
$S_b(0)$	.04	mg/cm^3
$L(0)$	.00005	cm
$S(y,0) \quad \forall y$	.00004	mg/cm^3
$f(y,0) \quad \forall y$	.15	dimensionless
$V_L(0)$	.03	cm^3

Table 9: Parameter values and initial values for one-dimensional BGM

Change in the Biofilm Thickness

The biofilm thickness is governed by growth and detachment. The bacteria in the biofilm consume the substrate and multiply. Bacteria near the substratum get less food than the bacteria near the film-water interface, hence the bacteria near the interface grow faster than the bacteria near the substratum. The cumulative growth of each mass particle determines the growth rate of the biofilm thickness, $L(t)$. Figure 7 shows that the biofilm thickness initially (for the first .5 days) grows slowly then the growth rate increases and the biofilm thickness grows rapidly over the next 1.5 days. The growth after 2 days is very slow (see Figure 7 and Table 11). The biofilm thickness reaches a steady state at .008202 cm after 4 days.

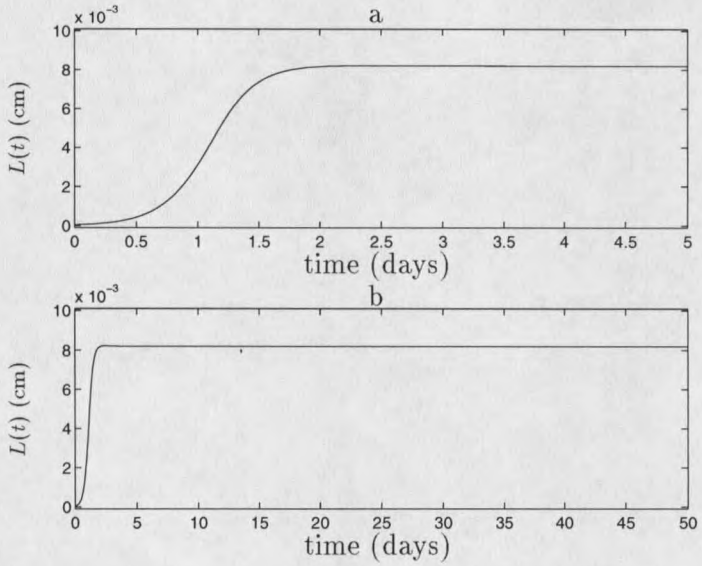

Figure 7: The thickness of the biofilm, $L(t)$, over 5 days (a) and 50 days (b) for the one-dimensional BGM

Change in the Volume of the Bulk Liquid

As the biofilm thickness grows, the volume of the bulk liquid, $V_L(t)$, decreases. It is clear from Figures 7 and 8 that when biofilm thickness reaches its steady state, the

volume of the bulk liquid also reaches its steady state. We observe a 27% decrease in the volume over the first 2 days of bacterial growth. The bulk liquid volume then reaches its steady state of .02185 cm^3 after 4 days (see Table 12).

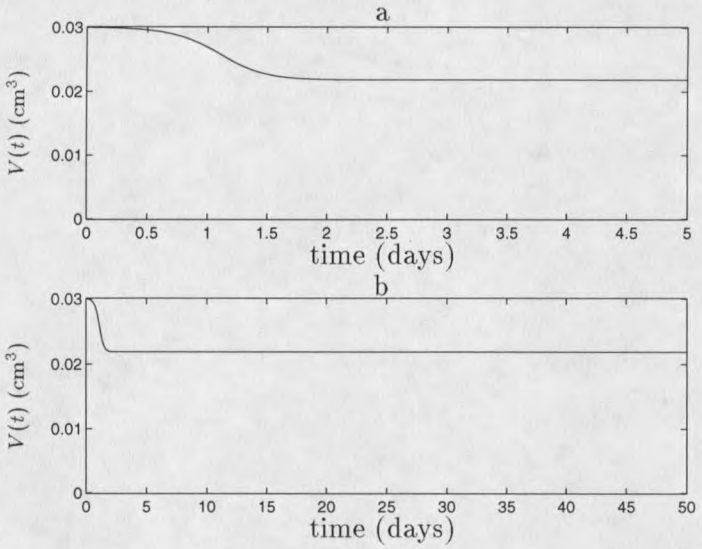

Figure 8: The volume of the bulk liquid, $V_L(t)$, over 5 days (a) and 50 days (b) for the one-dimensional BGM

Change in the Substrate Concentration in the Biofilm

The substrate concentration, $S(y,t)$, at a fixed point in the biofilm depends on the distance of the point from the film-water interface. A point near the film-water interface has a much higher substrate concentration than a point near the substratum. This is due to the fact that a significant fraction of the substrate molecules, which diffuse into the biofilm, are consumed by the bacteria before they get close to the substratum. When we fix a point in the biofilm and calculate the substrate concentration at that point, we observe that as biofilm grows, the substrate concentration at that point decreases because as biofilm grows, the distance between the point and the film-water interface increases. The graphs of substrate concentration at two

points y_1 and y_2 are shown in Figures 9 and 10. y_1 is a point which is at 20% of the biofilm thickness, $L(t)$, from the substratum and y_2 is a point which is at 80% of the biofilm thickness from the substratum. Thus y_1 and y_2 move as the biofilm thickness increases. Since the biofilm is initially very thin, the substrate from the bulk liquid diffuses very quickly into the film and the substrate concentration rises from its initial value, .00004 mg/cm^3, to .04 mg/cm^3, which is the initial bulk substrate concentration, $S_b(0)$. Then the substrate concentration in the biofilm very rapidly decreases to .02 mg/cm^3 which is the substrate concentration of the influent fluid (see Figure 9). Figure 9 and Table 13 show that between .5 days and 1.5 days the substrate concentration at y_1 decreases faster than the substrate concentration at y_2. The substrate concentrations $S(y_1, t)$ and $S(y_2, t)$ both attain their steady states after 4 days. The steady state value of $S(y_2, t)$ is .01566 mg/cm^3 which is significantly higher than the steady state value of $S(y_1, t)$ (.000066 mg/cm^3) because y_2 is closer to the interface than y_1.

Change in the Volume Fraction of the Active and Inactive Bacteria

It has been assumed in this model that a constant fraction, $\epsilon_l = .8$, of the biofilm is water. The volume fractions of active and inactive bacteria change between 0 and $(1 - \epsilon_l) = .2$ and their sum remains a constant, $(1 - \epsilon_l) = .2$. In the case of high substrate concentration in the biofilm, the active bacteria multiply faster than they inactivate (die). Hence in any arbitrary volume of the biofilm the relative fraction of the active bacteria, $f(y, t)$, increases and the volume fraction of the inactive bacteria, $\bar{f}(y, t)$, decreases. The volume fractions of the active bacteria at points y_1 (which is at 20% of the biofilm thickness from the substratum) and y_2 (which is at 80% of the biofilm thickness from the substratum) are displayed in Figure 11 (over 2.5 days) and Figure 12 (over 50 days). Initially, when the biofilm is thin, the volume fraction

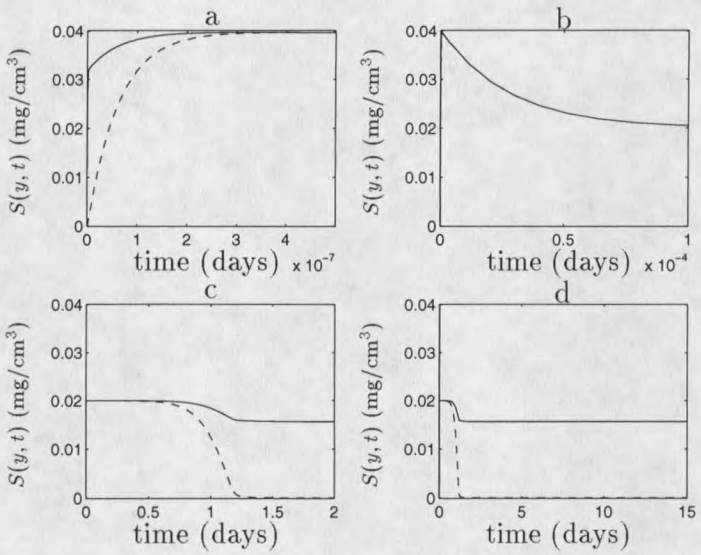

Figure 9: The substrate concentration, $S(y,t)$, in the biofilm at points y_1 (dashed line) and y_2 (solid line) in the biofilm over 10^{-7} days (a), .0001 days (b), 2 days (c), and 15 days (d), for the one-dimensional BGM

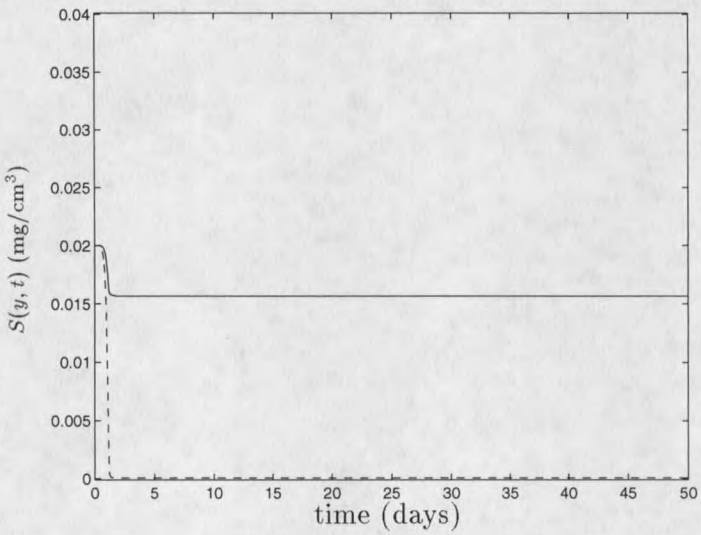

Figure 10: The substrate concentration, $S(y,t)$, at points y_1 (dashed line) and y_2 (solid line) in the biofilm over 50 days for the one-dimensional BGM

of the active bacteria at y_1, $f(y_1, t)$, and the volume fraction of the active bacteria at y_2, $f(y_2, t)$, increase with almost the same rate. After 1.2 days, when the biofilm thickness is significantly large, the bacteria at y_1 do not get enough substrate hence $f(y_1, t)$ begins to decrease, however $f(y_2, t)$ continues to increase. Figure 12 and Table 15 show that $f(y_1, t)$ and $f(y_2, t)$, after 5 days, attain their steady states at .173465 and .189406, respectively.

The volume fraction of inactive biomass, $\bar{f}(y, t)$, changes with the change in the volume fraction of active biomass, $f(y, t)$, such that at any point y^* and time t^* the sum of $f(y^*, t^*)$ and $\bar{f}(y^*, t^*)$ remains 0.2. Figure 12 and Table 16 show that $\bar{f}(y_1, t)$ and $\bar{f}(y_2, t)$, after 5 days, attain their steady states at .026534 and .010594, respectively.

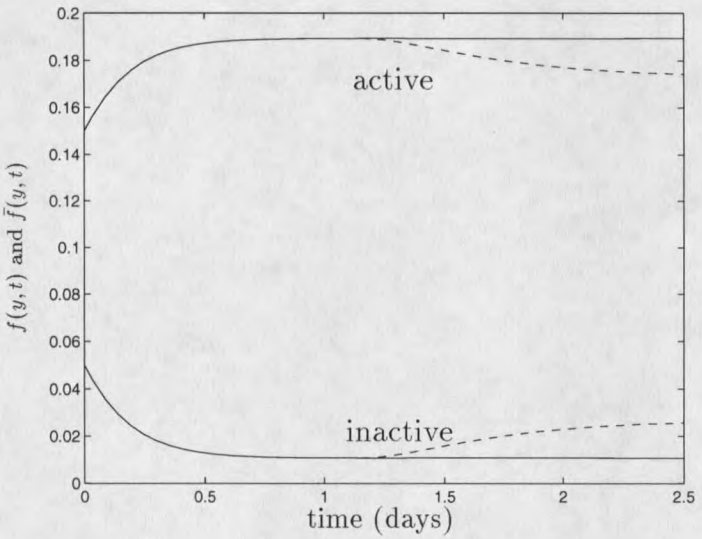

Figure 11: The active biomass volume fraction, $f(y, t)$, and the inactive biomass volume fraction, $\bar{f}(y, t)$, at points y_1 (dashed line) and y_2 (solid line) over 2.5 days for the one-dimensional BGM

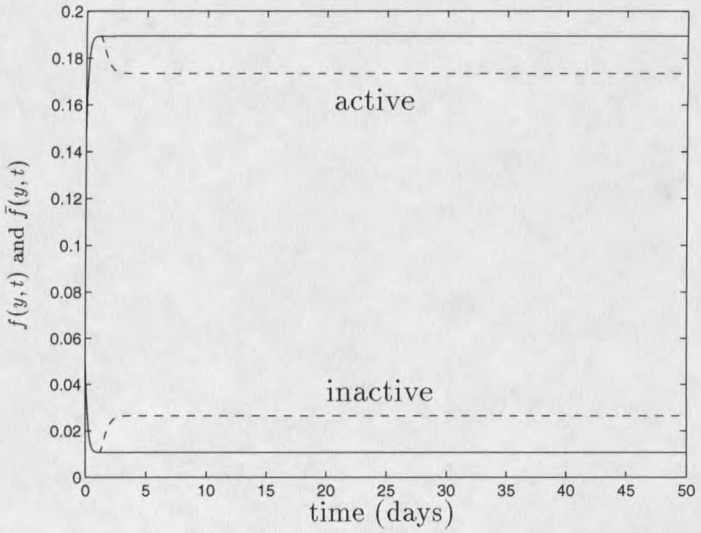

Figure 12: The active biomass volume fraction, $f(y,t)$, and the inactive biomass volume fraction, $\bar{f}(y,t)$, at points y_1 (dashed line) and y_2 (solid line) over 50 days for the one-dimensional BGM

Change in the Substrate Concentration in the Bulk Liquid

Figure 13 shows that the substrate concentration, $S_b(t)$, in the bulk liquid very rapidly (in .0004 days) approaches its steady state value which is the constant value $S_0 =$ .02 mg/cm^3. This is the concentration of the substrate in the influent fluid. Since the volumetric flow rate is very high, the substrate solution is continuously being replaced with new solution of constant concentration, $S_0 =$ .02 mg/cm^3. This is shown in Figure 13 and the numerical values of $S_b(t)$ are displayed in Table 17.

Comparison of Zero- and One-dimensional BGM

The system of equations (2.122) - (2.126) from the zero-dimensional BGM are solved numerically for the dependent variables given in Table 8 and then the results are discussed. The solution is determined using 'ODE23s' from MATLAB (version 4.2a). The computer code which approximates the solution of the zero-dimensional

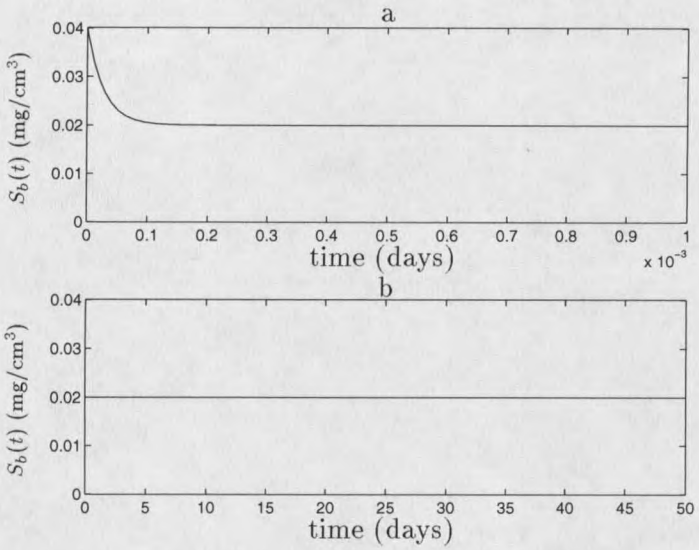

Figure 13: The substrate concentration, $S_b(t)$, in the bulk liquid over .001 days (a) and 50 days (b) for the one-dimensional BGM

BGM equations is given in Appendix C.

Replacing $\frac{dL(t)}{dt}$ in equations (2.122), (2.124) and (2.126) with the right-hand side of (2.123) yields the following system of differential equations:

$$\frac{df(t)}{dt} = \frac{YV_rS(t)f(t)}{K+S(t)}\left(1-\frac{f(t)}{1-\epsilon_1}\right) - bf(t) \tag{3.6}$$

$$\frac{dL(t)}{dt} = \frac{1}{1-\epsilon_l}\frac{YV_rL(t)S(t)f(t)}{K+S(t)} + \delta(t) \tag{3.7}$$

$$\frac{dS(t)}{dt} = -\frac{V_rS(t)f(t)}{K+S(t)}\left(\rho+\frac{S(t)Y}{1-\epsilon_l}\right) - \frac{\delta(t)S(t)}{L(t)} + \frac{D}{L_lL(t)}\Big(S_b(t)-S(t)\Big) \tag{3.8}$$

$$\frac{dS_b(t)}{dt} = \frac{1}{V_L(t)}\left(Q(t)(S_0-S_b(t)) - \frac{\sigma D}{L_l}(S_b(t)-S(t))\right) \tag{3.9}$$

$$\frac{dV_L(t)}{dt} = -\sigma\left(\frac{1}{1-\epsilon_l}\frac{YV_rL(t)S(t)f(t)}{K+S(t)} + \delta(t)\right) \tag{3.10}$$

The model equation for the detachment function, $\delta(t)$, that we have used here, is, [25]

$$\delta(t) = -\lambda(L(t))^2 \tag{3.11}$$

where λ $(L^{-1}T^{-1})$ is the detachment coefficient.

This system is solved for five unknown variables; substrate in the bulk fluid, $S_b(t)$, thickness of the biofilm, $L(t)$, average substrate concentration in the biofilm, $S(t)$, average volume fraction of the biomass in the biofilm, $f(t)$, and the volume of the bulk liquid, $V_L(t)$. The parameter values and the initial values of the variables are given in Table 10 and are the same as those used for the one-dimensional BGM (see Table 9). The numerical approximation of these functions is displayed in Figures 14 through 27 and in Tables 11 through 17. A comparison of the values of the variables from the one-dimensional and zero-dimensional models is also given.

Parameters	Values	Units
K	0.0001	mg/cm^3
V_r	4.3	mg/(mg day)
Y	.5	mg/mg
b	.35	day^{-1}
D	1.3	cm^2/day
$Q(t)$ $\forall t$	1100	cm^3/day
σ	1	cm^2
L_l	.8	cm
ϵ_l	.8	dimensionless
ρ	12.2	mg/cm^3
S_0	.02	mg/cm^3
λ	500	$cm^{-1}day^{-1}$
Variables	**Values**	**Units**
$S_b(0)$	.04	mg/cm^3
$L(0)$	.00005	cm
$S(0)$	.00004	mg/cm^3
$f(0)$	.15	dimensionless
$V_L(0)$	.03	cm^3

Table 10: Parameter values and initial values for the zero-dimensional BGM

Change in the Biofilm Thickness

Figure 14 shows that the biofilm thickness, $L(t)$, increases slowly over the first .5 days and over the next 1.5 days it grows rapidly. The growth rate of the biofilm thickness is very slow after 2.5 days and a steady state is reached after 8 days of .008152 cm. A comparison of $L(t)$ computed from one-dimensional BGM and zero-dimensional BGM is shown in Figure 15 and the numerical values are displayed in Table 11. The steady state in the zero-dimensional BGM is attained after a longer time at a smaller value than in the one-dimensional BGM but qualitatively both graphs are very similar.

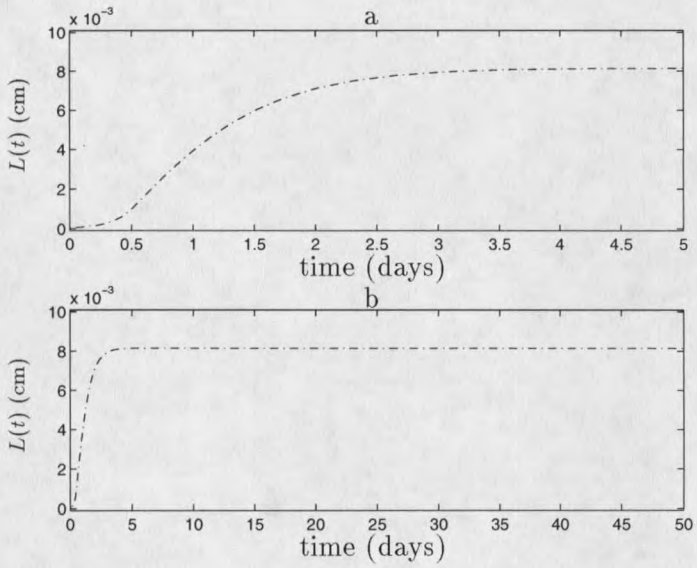

Figure 14: Biofilm thickness, $L(t)$, over 5 days (a) and 50 days (b) for the zero-dimensional BGM

Change in the Volume of the Bulk Liquid

Figure 16 and Table 12 show that initially (over the first .5 days) the volume, $V_L(t)$, of the bulk liquid decreases slowly. But over the next 1.5 days, $V_L(t)$ decreases rapidly because between .5 days and 2 days the biofilm thickness, $L(t)$, increases very fast

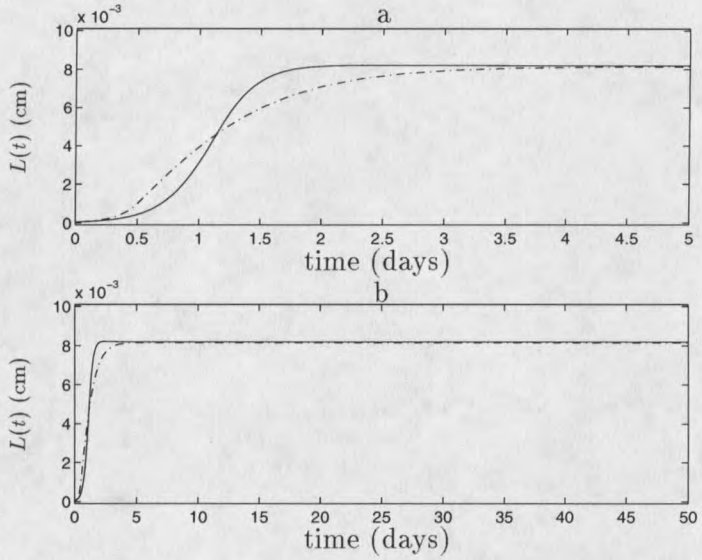

Figure 15: Biofilm thickness, $L(t)$, over 5 days (a) and 50 days (b) for the zero-dimensional (dash-dot line) and one-dimensional (solid line) BGM

(leaving less room for the bulk liquid). Notice that $V_L(t)$ reaches a steady state of .021898 cm^3 after 9 days. Table 12 also shows that $V_L(t)$ in the zero-dimensional model attains its steady state at a slightly higher value than it does in the one-dimensional model because the steady biofilm thickness in the zero-dimensional model is smaller than it is in the one-dimensional model.

Change in Substrate Concentration in the Biofilm

Initially, because of the high substrate concentration difference across the film-water interface (.00004 mg/cm^3 in the biofilm and .04 mg/cm^3 in the bulk liquid), the substrate diffuses rapidly from high to low concentration. This causes the substrate concentration, $S(t)$, in the biofilm to increase rapidly. Simultaneously the substrate concentration in the bulk liquid, $S_b(t)$, decreases rapidly because it is replaced with the influent liquid of constant substrate concentration, $S_0 = .02$ mg/cm^3. After about .00006 days (or 5.2 seconds) $S(t)$ increases to .0222 mg/cm^3 (see Figure 18) and $S_b(t)$

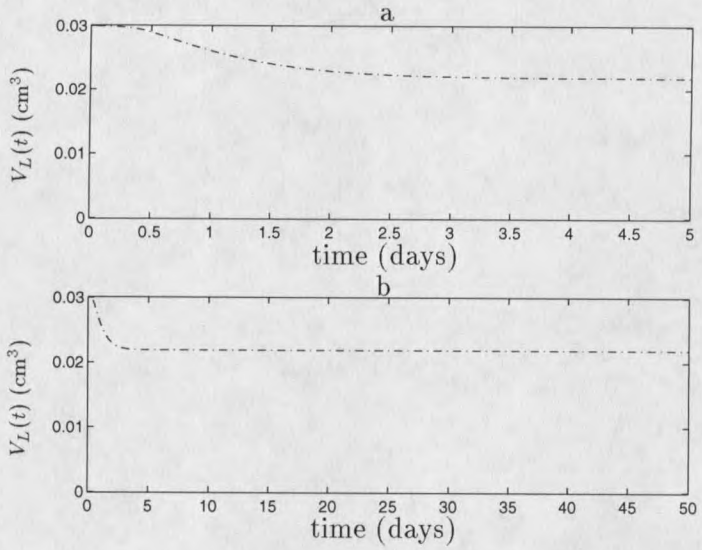

Figure 16: The bulk fluid volume, $V_L(t)$, over 5 days (a) and 50 days (b) for the zero-dimensional BGM

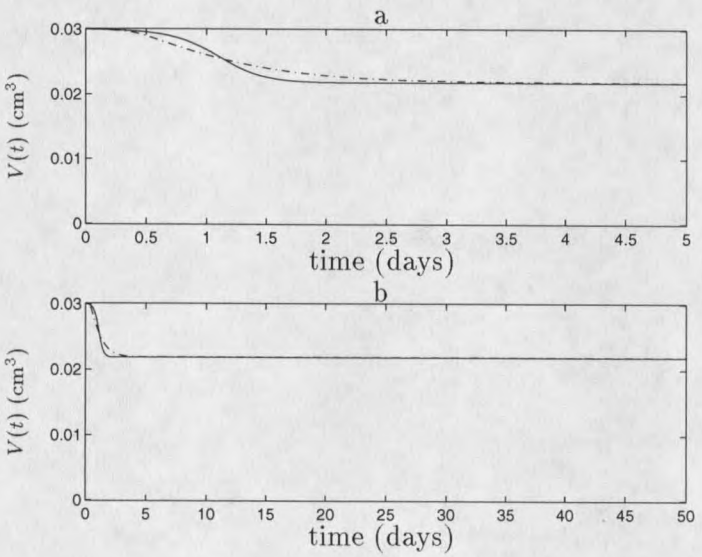

Figure 17: The bulk fluid volume, $V(t)$, over 5 (a) days and 50 days (b) for the zero-dimensional (dash-dot line) and one-dimensional (solid line) BGM

decreases to .0222 mg/cm^3 (see Figure 27). Since the concentration difference across the film-water interface is zero there (at $t = .00006$ days), $S(t)$ stops increasing, which can be visualized in Figure 18 as the slope of $S(t)$ is zero at $t = .00006$ days. Figure 27 shows that after .00006 days, $S_b(t)$ continues to decrease which causes a concentration difference across the film water interface (high in the biofilm and low in the bulk fluid). Therefore the substrate from the biofilm diffuses into the bulk liquid and decreases to a value close to $S_0 = .02$ mg/cm^3. As biofilm grows, the substrate in the biofilm get consumed faster causing a slow decrease in $S(t)$ which can be seen in Figure 19. After 1.5 days, when the biofilm thickness becomes significantly large, the substrate consumption rate increases which causes relatively faster decrease in the substrate concentration. A comparison of the substrate concentration, $S(t)$, from the zero-dimensional BGM and the substrate concentrations $S(y_1, t)$ and $S(y_2, t)$ from one-dimensional BGM is shown in Figure 20 (over 2.5 days) and Figure 22 (over 50 days). The numerical values of $S(t)$, $S(y_1, t)$, and $S(y_2, t)$ are given in Table 13 and Table 14. Figure 22 and Table 14 show that $S(t)$ reaches its steady state after 4 days at .003965 mg/cm^3 which is between the steady state values of $S(y_1, t)$ (.000066 mg/cm^3) and $S(y_2, t)$ (.01566 mg/cm^3) .

Change in the Volume Fraction of Active and Inactive Bacteria

The graphs of the volume fraction of active biomass, $f(t)$, and the volume fraction of inactive biomass, $\bar{f}(t)$, are shown in Figure 23 (over 2.5 days) and Figure 24 (over 50 days). The numerical values of $f(t)$ are displayed in Table 15 and the numerical values of $\bar{f}(t)$ are displayed in Table 16. The volume fraction of active biomass increases from its initial value .15 to its steady state value .1821 and the volume fraction of the inactive biomass decreases from its initial value .05 to its steady state value .0179. Also notice that the steady state value of $f(t)$ (which is the average volume fraction

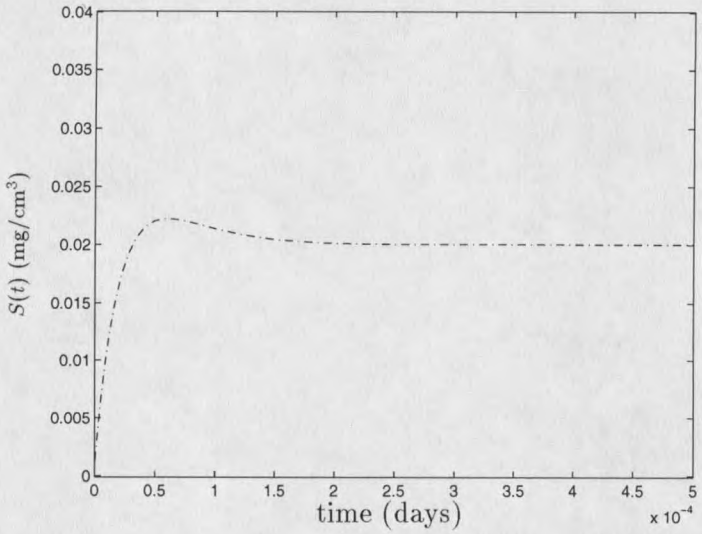

Figure 18: The substrate concentration, $S(t)$, over .0005 days for the zero-dimensional BGM

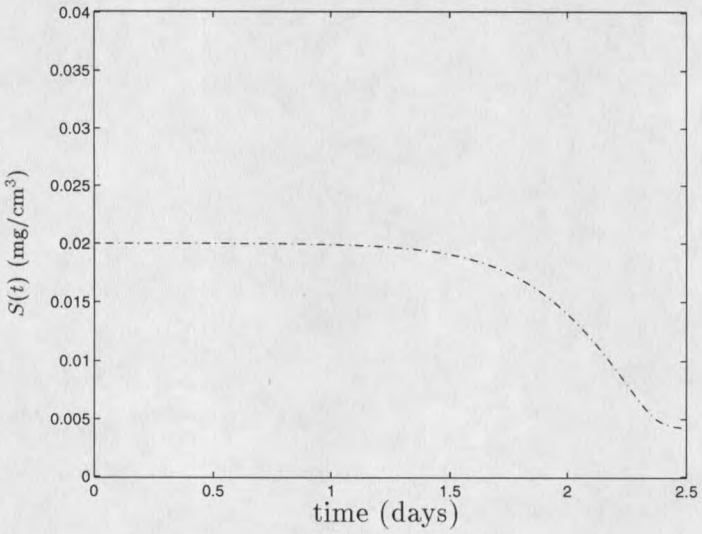

Figure 19: The substrate concentration, $S(t)$, over 2.5 days for the zero-dimensional BGM

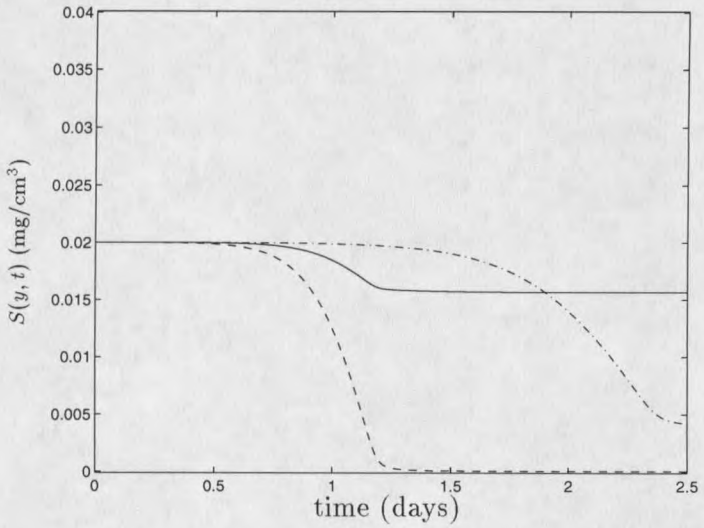

Figure 20: The substrate concentration, $S(y,t)$, at points y_1 (dashed line) and y_2 (solid line) in the biofilm over 2.5 days for the one-dimensional BGM and the substrate concentration, $S(t)$, (dash-dot line) over 2.5 days for the zero-dimensional BGM

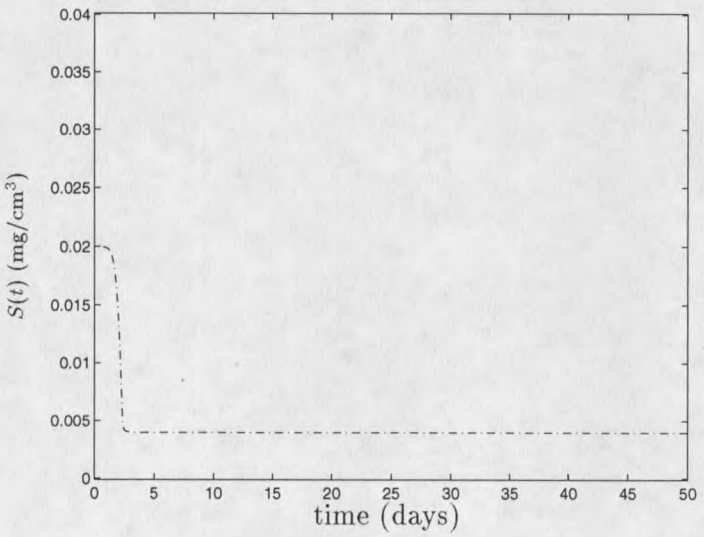

Figure 21: The substrate concentration, $S(t)$, over 50 days for the zero-dimensional BGM

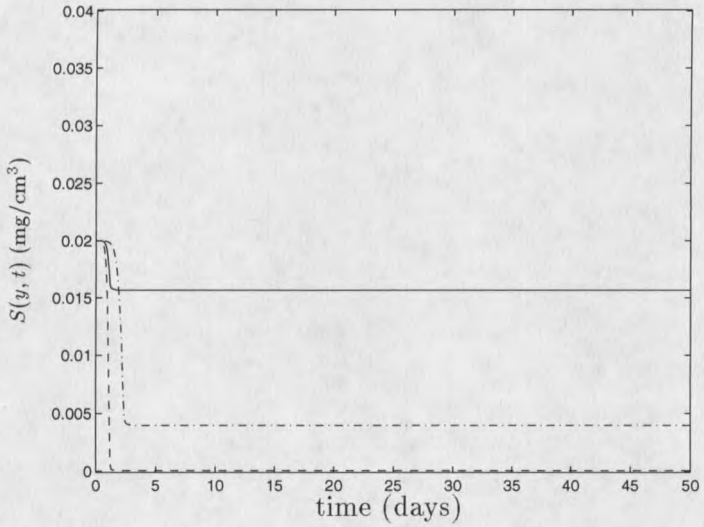

Figure 22: The substrate concentration, $S(y,t)$, at points y_1 (dashed line) and y_2 (solid line) in the biofilm over 50 days for the one-dimensional BGM and the substrate concentration, $S(t)$, (dash-dot line) over 50 days for the zero-dimensional BGM

of active biomass) remains between the steady state values of $f(y_1,t)$ and $f(y_2,t)$ calculated from the one-dimensional BGM and the steady state value of $\bar{f}(t)$ (which is the average volume fraction of inactive biomass) remains between the steady state values of $\bar{f}(y_1,t)$ and $\bar{f}(y_2,t)$ (see Figures 25 and 26). This shows a good agreement between the results of the zero-dimensional BGM and the one-dimensional BGM.

Change in the Substrate Concentration in the Bulk Liquid

Figure 27 shows that the substrate concentration in the bulk liquid very quickly decreases from its initial value .04 mg/cm^3 to the influent substrate concentration, S_0 = .02 mg/cm^3, and remains almost constant. A quantitative comparison of the numerical values of S_b from the one-dimensional and zero-dimensional models is given in Table 17. In this model we have assumed that the bulk liquid is constantly replaced by the substrate solution with constant substrate concentration, S_0 = .02 mg/cm^3.

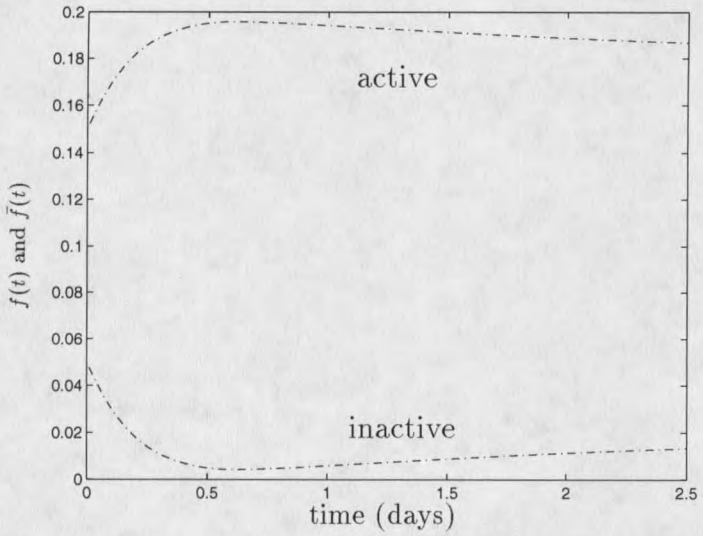

Figure 23: The active biomass volume fraction, $f(t)$, and inactive biomass volume fraction, $\bar{f}(t)$, over 2.5 days for the zero-dimensional BGM

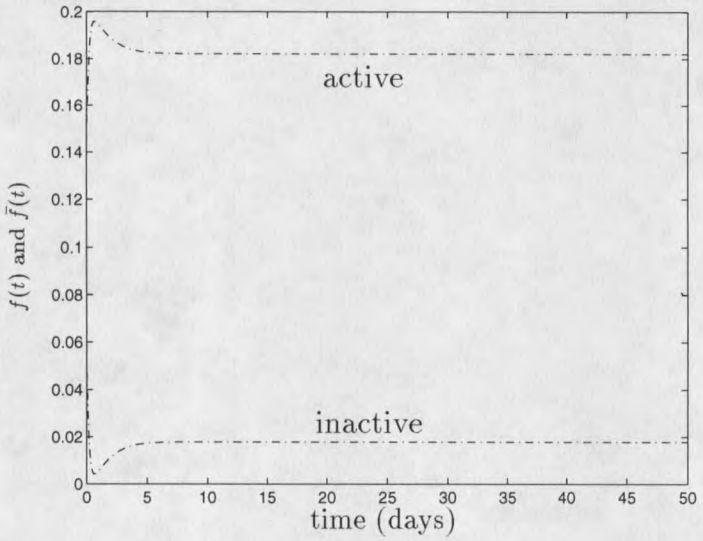

Figure 24: The active biomass volume fraction, $f(t)$, and inactive biomass volume fraction, $\bar{f}(t)$, over 50 days for the zero-dimensional BGM

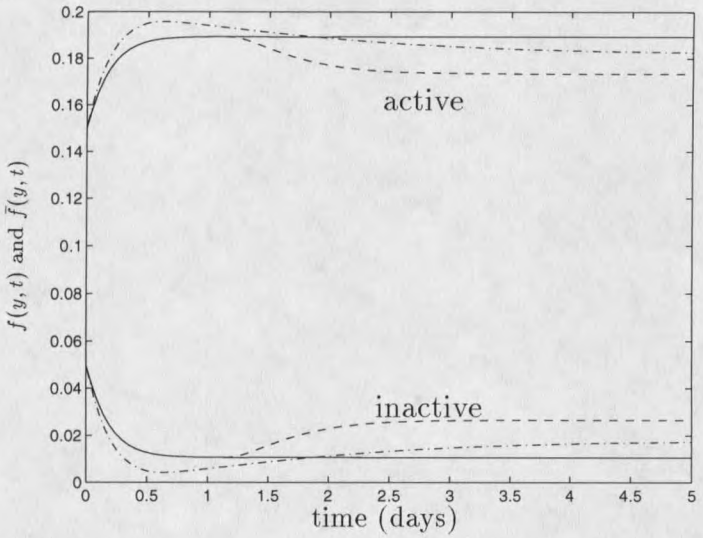

Figure 25: The active biomass volume fraction, $f(t)$, and inactive biomass volume fraction, $\bar{f}(t)$, over 5 days for the zero-dimensional BGM (dash-dot line) and the active biomass volume fraction, $f(y,t)$, and the inactive biomass volume fraction, $\bar{f}(y,t)$, at points y_1 (dashed line) and y_2 (solid line) over 5 days for the one-dimensional BGM

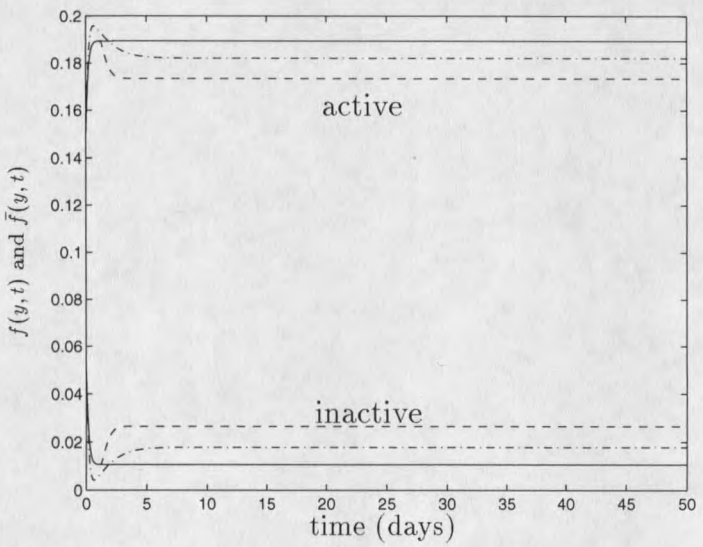

Figure 26: The active biomass volume fraction, $f(t)$, and inactive biomass volume fraction, $\bar{f}(t)$, over 50 days for the zero-dimensional BGM (dash-dot line) and the active biomass volume fraction, $f(y,t)$, and the inactive biomass volume fraction, $\bar{f}(y,t)$, at points y_1 (dashed line) and y_2 (solid line) over 50 days for the one-dimensional BGM

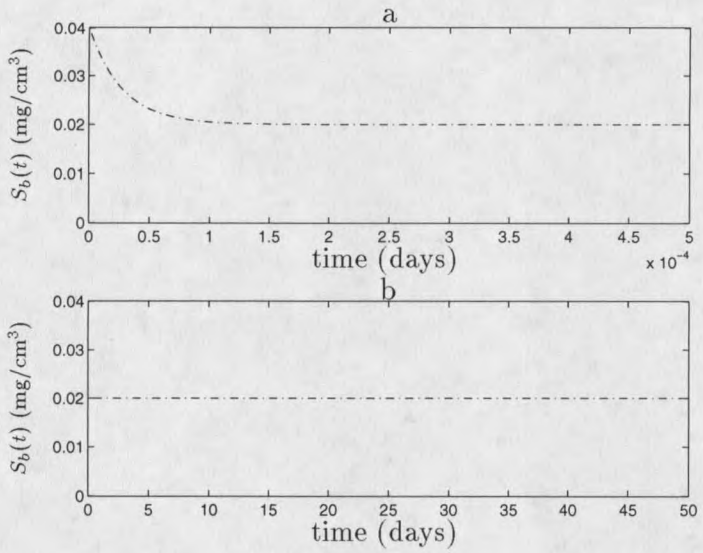

Figure 27: The substrate concentration, $S_b(t)$, in the bulk liquid, over .0005 days (a) and 50 days (b) for the zero-dimensional BGM

t(days)	0-D $L(t)$ (cm)	1-D $L(t)$ (cm)
0.0	0.00005000	0.00005000
1.0	0.00393395	0.00308647
2.0	0.00712767	0.00819558
3.0	0.00796676	0.00820523
4.0	0.00812581	0.00820161
5.0	0.00814681	0.00820157
6.0	0.00814919	0.00820155
7.0	0.00815038	0.00820155
8.0	0.00815157	0.00820155
9.0	0.00815159	0.00820156
10.0	0.00815159	0.00820156
50.0	0.00815159	0.00820156

Table 11: Biofilm thickness, $L(t)$, over 50 days for the zero-dimensional and one-dimensional BGM

t (days)	0-D $V_L(t)$ (cm^3)	1-D $V_L(t)$ (cm^3)
0.0	0.03000000	0.03000000
1.0	0.02611604	0.02696352
2.0	0.02292232	0.02185441
3.0	0.02208323	0.02184476
4.0	0.02192418	0.02184838
5.0	0.02190318	0.02184842
6.0	0.02190139	0.02184844
7.0	0.02189961	0.02184844
8.0	0.02189959	0.02184844
9.0	0.02189840	0.02184843
10.0	0.02189840	0.02184843
50.0	0.02189841	0.02184843

Table 12: Volume, $V_L(t)$, of the bulk liquid over 50 days for zero-dimensional and one-dimensional BGM

t (days)	0-D $S(t)$ (mg/cm^3)	1-D $S(y_1,t)$ (mg/cm^3)	1-D $S(y_2,t)$ (mg/cm^3)
0.00	0.00004000	0.00004000	0.00004000
0.20	0.01999329	0.01999163	0.01999826
0.40	0.01995124	0.01993918	0.01998741
0.60	0.01970063	0.01962661	0.01992272
0.80	0.01834961	0.01794149	0.01957394
1.00	0.01357709	0.01198887	0.01834175
1.20	0.00465585	0.00086576	0.01602612
1.40	0.00402774	0.00011370	0.01576986
1.60	0.00398152	0.00007518	0.01570053
1.80	0.00396847	0.00006677	0.01567356
2.00	0.00396329	0.00006412	0.01566080

Table 13: Substrate concentration, $S(t)$, in the biofilm for the zero-dimensional BGM and the substrate concentration, $S(y,t)$, at points y_1 and y_2 in the biofilm for the one-dimensional BGM over 2 days

t (days)	0-D $S(t)$ (mg/cm^3)	1-D $S(y_1,t)$ (mg/cm^3)	1-D $S(y_2,t)$ (mg/cm^3)
0.00	0.00004000	0.00004000	0.00004000
1.00	0.01357709	0.01198887	0.01834175
2.00	0.00396329	0.00006412	0.01566080
3.00	0.00396450	0.00006557	0.01566129
4.00	0.00396471	0.00006573	0.01566164
5.00	0.00396473	0.00006575	0.01566169
6.00	0.00396474	0.00006575	0.01566169
7.00	0.00396474	0.00006575	0.01566169
8.00	0.00396474	0.00006575	0.01566169
9.00	0.00396474	0.00006575	0.01566169
10.00	0.00396474	0.00006575	0.01566169
50.00	0.00396474	0.00006575	0.01566169

Table 14: Substrate concentration, $S(t)$, in the biofilm for the zero-dimensional BGM and the substrate concentration, $S(y,t)$, at points y_1 and y_2 in the biofilm for the one-dimensional BGM over 50 days

Solution of Zero-dimensional Rittman's Model

The system of ordinary differential equations (2.39)-(2.42) is first simplified and then is solved using the code 'ODE23s' from MATLAB (version 4.2a). The computer code which approximates the solution of the zero-dimensional Rittman's model equations is given in Appendix D. Starting with (2.39)

$$\frac{dS_b(t)}{dt} = \frac{1}{V_L}\left(QS_0 - \left(Q + \frac{\sigma D}{L_l}\right)S_b(t) + \frac{\sigma D}{L_l}S(t)\right),$$

we write this as

$$\frac{dS_b(t)}{dt} = \frac{1}{V_L}\left(QS_0 - QS_b(t) - \frac{\sigma D}{L_l}S_b(t) + \frac{\sigma D}{L_l}S(t)\right). \tag{3.12}$$

Similarly (2.42) is written

$$\frac{dL(t)}{dt} = \left(\left(Y\frac{V_r S(t)}{K + S(t)} - bf_d\right)f(t) - B'\right)L(t). \tag{3.13}$$

t (days)	0-D $f(t)$	1-D $f(y_1, t)$	1-D $f(y_2, t)$
0.00	0.15000000	0.15000000	0.15000000
0.50	0.19520130	0.18733056	0.18733068
1.00	0.19424553	0.18932086	0.18933049
1.50	0.19115583	0.18401590	0.18931887
2.00	0.18869909	0.17633567	0.18933877
2.50	0.18688385	0.17421025	0.18940333
3.10	0.18506860	0.17357378	0.18940975
3.50	0.18406933	0.17348751	0.18940770
4.00	0.18357616	0.17347671	0.18940714
4.50	0.18308299	0.17346572	0.18940654
5.00	0.18261836	0.17346543	0.18940649
10.30	0.18212676	0.17346527	0.18940646
15.30	0.18212592	0.17346525	0.18940646
20.30	0.18212610	0.17346525	0.18940646
25.30	0.18212607	0.17346525	0.18940646
30.30	0.18212607	0.17346525	0.18940646
35.30	0.18212607	0.17346525	0.18940646

Table 15: Active biomass volume fraction, $f(t)$, for the zero-dimensional BGM and active biomass volume fraction, $f(y, t)$, at points y_1 and y_2 in the biofilm for the one-dimensional BGM over 35 days

t (days)	0-D $\bar{f}(t)$	1-D $\bar{f}(y_1, t)$	1-D $\bar{f}(y_2, t)$
0.00	0.05000000	0.05000000	0.05000000
0.50	0.00479869	0.01266943	0.01266931
1.00	0.00575446	0.01067913	0.01066950
1.50	0.00884416	0.01598409	0.01068112
2.00	0.01130090	0.02366432	0.01066122
2.50	0.01311614	0.02578974	0.01059666
3.00	0.01493139	0.02642621	0.01059024
3.50	0.01593066	0.02651248	0.01059229
4.00	0.01642383	0.02652328	0.01059285
4.50	0.01691700	0.02653427	0.01059345
5.00	0.01738163	0.02653456	0.01059350
10.00	0.01787323	0.02653472	0.01059353
15.00	0.01787407	0.02653474	0.01059353
20.00	0.01787389	0.02653474	0.01059353
25.00	0.01787392	0.02653474	0.01059353
30.00	0.01787392	0.02653474	0.01059353
35.30	0.01787392	0.02653474	0.01059353

Table 16: Inactive biomass volume fraction, $\bar{f}(t)$, for the zero-dimensional BGM and inactive biomass volume fraction, $\bar{f}(y, t)$, at points y_1 and y_2 in the biofilm for the one-dimensional BGM over 35 days

t (days)	0-D $S_b(t)$ (mg/cm^3)	1-D $S_b(t)$ (mg/cm^3)
0.000000	0.04000000	0.04000000
0.000020	0.02980148	0.02942642
0.000040	0.02433157	0.02451977
0.000060	0.02224666	0.02213547
0.000080	0.02090228	0.02108512
0.000100	0.02047238	0.02057680
0.000120	0.02020717	0.02026683
0.000140	0.02010431	0.02009900
0.000160	0.02005596	0.02006178
0.000180	0.02001375	0.02002456
0.000200	0.02001274	0.02001333
0.000400	0.01999888	0.01999984
0.000600	0.01999889	0.02000004
0.000800	0.01999889	0.02000003
0.001000	0.01999888	0.02000002

Table 17: The bulk substrate concentration, $S_b(t)$, for the zero-dimensional and one-dimensional BGM over .001 days

Next (2.40)

$$\frac{d}{dt}\Big(L(t)S(t)\Big) = \frac{D}{L_l}\Big(S_b(t) - S(t)\Big) - \frac{V_r S(t)}{K + S(t)} L(t) f(t) \rho$$

is written as

$$\frac{dS(t)}{dt} = \left(-\frac{S(t)}{L(t)}\frac{dL(t)}{dt} + \frac{D}{L(t)L_l}\left(S_b(t) - S(t)\right) - \frac{V_r S(t)}{K + S(t)} f(t)\rho\right).$$

Using (3.13) this becomes

$$\begin{aligned}\frac{dS(t)}{dt} &= \left(-\left(Y\frac{V_r S(t)}{K + S(t)} - b f_d\right) f(t) + B'\right) S(t) \\ &\quad + \frac{D}{L(t)L_l}\left(S_b(t) - S(t)\right) - \frac{V_r S(t)}{K + S(t)} f(t)\rho\end{aligned}$$

which reduces to

$$\frac{dS(t)}{dt} = -\frac{V_r f(t) S(t)}{K + S(t)}\Big(Y S(t) + \rho\Big) + b f_d f(t) S(t) + B' S(t)$$

$$+\frac{D}{L(t)L_l}\Big(S_b(t)-S(t)\Big). \tag{3.14}$$

Finally, (2.41)

$$\frac{d}{dt}\Big(L(t)f(t)\Big)=\left(Y\frac{V_rS(t)}{K+S(t)}-(b+B')\right)L(t)f(t)$$

becomes

$$\frac{df(t)}{dt}=-\frac{f(t)}{L(t)}\frac{dL(t)}{dt}+Y\frac{V_rS(t)f(t)}{K+S(t)}-(b+B')f(t).$$

Again using (3.13) this reduces to

$$\begin{aligned}\frac{df(t)}{dt} &= -\left(Y\frac{V_rS(t)}{K+S(t)}-bf_d\right)f^2(t)+B'f(t)\\ &+ \frac{YV_rS(t)f(t)}{K+S(t)}-(b+B')f(t)\end{aligned}$$

which simplifies to

$$\frac{df(t)}{dt}=\left(\frac{YV_rS(t)}{K+S(t)}(1-f(t))-b(1-f_df(t))\right)f(t). \tag{3.15}$$

The system of equations (3.12)-(3.15) is solved using the parameter values and the initial values given in Table 18. The system is solved for four unknown variables; substrate concentration in the bulk liquid, $S_b(t)$, thickness of the biofilm, $L(t)$, the average substrate concentration in the biofilm, $S(t)$, and the average volume fraction of the biomass in the biofilm, $f(t)$.

A qualitative analysis of the numerical results is given in Figures 28 through 31. Figure 28 contains the graphs of $S_b(t)$ and $S(t)$ as functions of time, t. Each of the figures (Figures 29-31) contains the graphs of $S_b(t)$, $L(t)$, $S(t)$, and $f(t)$ as functions of time, t.

Since the volumetric flow rate is relatively high, the substrate concentration in the bulk liquid very quickly (within .01 days) decreases to the influent substrate concentration, $S_0 = .02$ mg/cm^3, as seen in Figure 28. The substrate concentration in

Parameters	Values	Units
K	0.0001	mg/cm^3
V_r	4.3	mg/(mg day)
Y	.2	mg/mg
b	.35	day^{-1}
D	1.3	cm^2 /day
V_L	2.0	cm^3
Q	1100	cm^3/day
σ	1	cm^2
L_l	.8	cm
ρ	12.2	mg/cm^3
B'	.31	day^{-1}
S_0	.02	mg/cm^3
f_d	0	dimensionless
Variables	Initial Values	Units
$S_b(0)$	.04	mg/cm^3
$L(0)$	.00005	cm
$S(0)$	.00004	mg/cm^3
$f(0)$	.2	dimensionless

Table 18: Parameter values and initial values for the zero-dimensional Rittman's model

the biofilm, $S(t)$, rises initially (for the first .0002 days) because of the high concentration difference across the interface. After .0002 days (17.3 sec) $S_b(t)$ and $S(t)$ have the same value (around .038 mg/cm^3). Since the substrate concentration difference across the film-water interface is zero there (at $t = .0002$ days), $S(t)$ stops increasing which can be visualized in Figure 28 as the slope of $S(t)$ is zero at $t = .0002$ days. The two substrate concentrations $S_b(t)$ and $S(t)$ decrease to the influent substrate concentration, $S_0 = .02$ mg/cm^3 within .01 days. As the consumption of the substrate becomes significant, $S(t)$ begins to decrease (see Figure 30c). The active bacteria in the biofilm consume the substrate and multiply which causes a rapid increase in the volume fraction of the active biomass, f(t) which can be seen in Figure 30d. As long as $S(t)$ is sufficiently high (close to .02 mg/cm^3), $f(t)$ increases rapidly. Between the sixth and the twelfth days, the biofilm thickness increases rapidly causing a rapid decrease in $S(t)$. The decay in $S(t)$ controls the growth of $L(t)$ and $f(t)$. All the variables reach their steady states after 30 days (see Figure 31).

Solution of Zero-dimensional BAM

The system of ordinary differential equations (2.76) - (2.79) is first simplified and then is solved using the code 'ODE23s' from MATLAB (version 4.2a). The computer code which approximates the solution of the zero-dimensional BAM equations is given in Appendix E. Beginning with (2.76)

$$\frac{dL(t)}{dt} = \frac{1}{1-\epsilon_l}\frac{YR(t)L(t)}{\rho} + \delta(t). \tag{3.16}$$

Next is (2.77)

$$\frac{d}{dt}\Big(L(t)f(t)\Big) = \frac{Y\ R(t)L(t)}{\rho} - bL(t)f(t) + \delta(t)f(t).$$

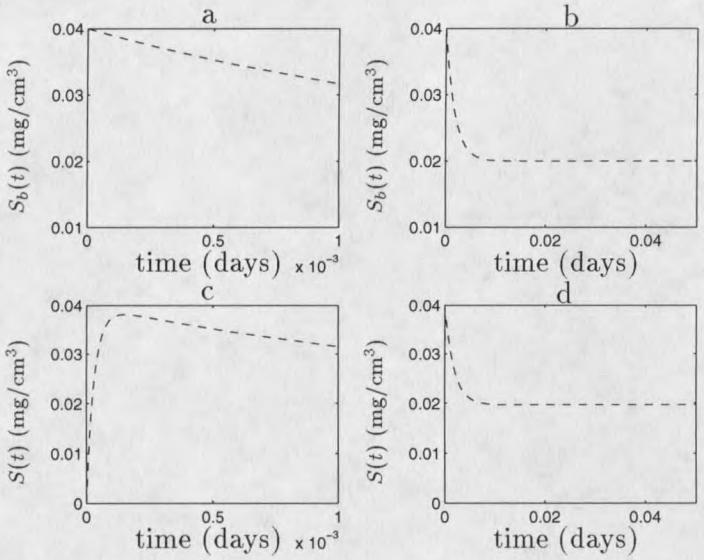

Figure 28: Bulk substrate concentration, $S_b(t)$ over .001 days, (a), and .05 days, (b) and substrate concentration in the biofilm, $S(t)$, over .001 days, (c), and .05 days, (d) for the zero-dimensional Rittman's model

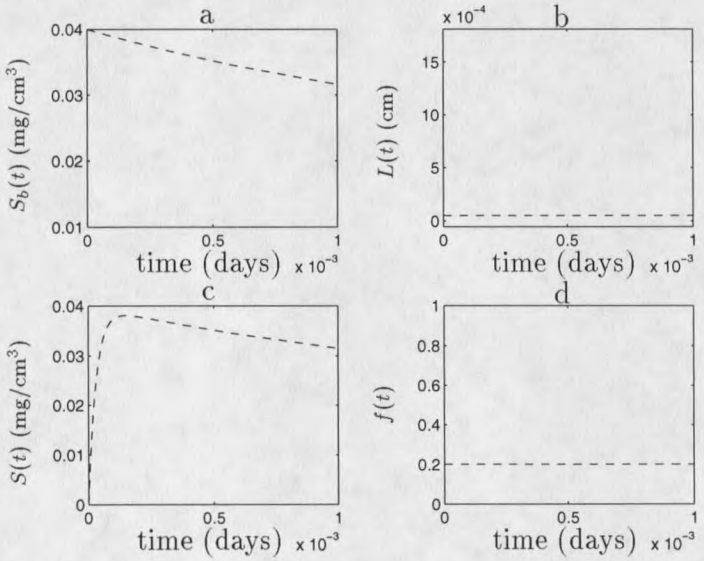

Figure 29: Bulk substrate concentration, $S_b(t)$, (a), biofilm thickness, $L(t)$, (b), substrate concentration in the biofilm, $S(t)$, (c), and active biomass volume fraction, $f(t)$, (d), over .001 days for the zero-dimensional Rittman's model

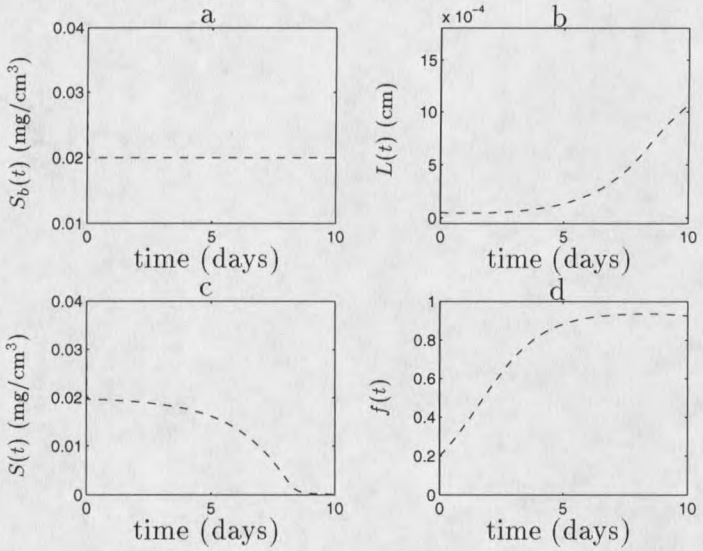

Figure 30: Bulk substrate concentration, $S_b(t)$, (a), biofilm thickness, $L(t)$, (b), substrate concentration in the biofilm, $S(t)$, (c), and active biomass volume fraction, $f(t)$, (d), over 10 days for the zero-dimensional Rittman's model

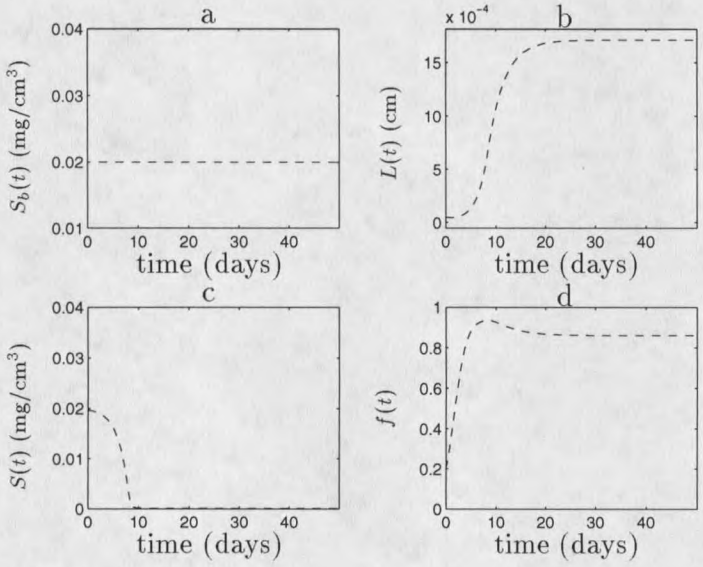

Figure 31: Bulk substrate concentration, $S_b(t)$, (a), biofilm thickness, $L(t)$, (b), substrate concentration in the biofilm, $S(t)$, (c), and active biomass volume fraction, $f(t)$, (d), over 50 days for the zero-dimensional Rittman's model

Using the chain rule and (3.16) this reduces to

$$\frac{df(t)}{dt} = -\frac{f(t)}{L(t)}\left(\frac{1}{1-\epsilon_l}\frac{YR(t)L(t)}{\rho} + \delta(t)\right) + \frac{YR(t)}{\rho} - bf(t) + \frac{\delta(t)f(t)}{L(t)}$$

which simplifies to

$$\frac{df(t)}{dt} = \frac{YR(t)}{\rho}\left(1 - \frac{f(t)}{1-\epsilon_l}\right) - bf(t). \tag{3.17}$$

Similarly (2.78)

$$\frac{d}{dt}\Big(L(t)S(t)\Big) = \frac{D}{L_l}\Big(S_b(t) - S(t)\Big) - R(t)L(t)$$

reduces to

$$\frac{dS(t)}{dt} = -\frac{S(t)}{L(t)}\left(\frac{1}{1-\epsilon_l}\frac{YR(t)L(t)}{\rho} + \delta(t)\right) + \frac{D}{L_l L(t)}\Big(S_b(t) - S(t)\Big) - R(t)$$

which further simplifies to

$$\begin{aligned}\frac{dS(t)}{dt} &= -\frac{R(t)}{\rho}\left(\rho + \frac{YS(t)}{1-\epsilon_l}\right) - \frac{\delta(t)S(t)}{L(t)} \\ &\quad + \frac{D}{L_l L(t)}(S_b(t) - S(t)).\end{aligned} \tag{3.18}$$

Lastly (2.79)

$$\begin{aligned}\frac{dS_b(t)}{dt} &= \frac{1}{V_L}\Big[\, Q\Big(S_0 - S_b(t)\Big) - \sigma\left(\frac{D}{L_l} - u_L(t)\right) \\ &\quad \Big(S_b(t) - S(t)\Big)\,\Big]\end{aligned}$$

becomes

$$\begin{aligned}\frac{dS_b(t)}{dt} &= \frac{1}{V_L}\Big[\, Q\Big(S_0 - S_b(t)\Big) - \sigma\Big\{\, \frac{D}{L_l} - \left(\frac{1}{1-\epsilon_l}\frac{YR(t)L(t)}{\rho} + \delta(t)\right)\Big\} \\ &\quad \Big(S_b(t) - S(t)\Big)\,\Big].\end{aligned} \tag{3.19}$$

By [25], appropriate choices for $R(t)$ and $\delta(t)$ are

$$R(t) = \frac{V_r S(t)\rho f(t)}{K + S(t)} \tag{3.20}$$

and

$$\delta(t) = -\lambda(L(t))^2. \tag{3.21}$$

This system is solved for four unknown variables; substrate in the bulk liquid, $S_b(t)$, thickness of the biofilm, $L(t)$, the average substrate concentration in the biofilm, $S(t)$, and the average volume fraction of the biomass in the biofilm, $f(t)$. The values of the parameters and the initial values of the variables are given in Table 19.

A qualitative analysis of the numerical results is given in Figures 32 through 35. Figure 32 contains the graphs of $S_b(t)$ and $S(t)$ as functions of time, t. Each of the figures (Figures 33-35) contains the graphs of $S_b(t)$, $L(t)$, $S(t)$, and $f(t)$ as functions of time, t.

Parameters	Values	Units
K	0.0001	mg/cm^3
V_r	4.3	mg/(mg day)
Y	.2	mg/mg
b	.35	day^{-1}
D	1.3	cm^2 /day
V_L	2.0	cm^3
ϵ_l	0.0	dimensionless
Q	1100	cm^3/day
σ	1	cm^2
L_l	.8	cm
ρ	12.2	mg/cm^3
S_0	.02	mg/cm^3
λ	500	$cm^{-1}day^{-1}$
Variables	Initial Values	Units
$S_b(0)$	.04	mg/cm^3
$L(0)$	.00005	cm
$S(0)$	.00004	mg/cm^3
$f(0)$	.2	dimensionless

Table 19: Parameters values and the initial values for the zero-dimensional BAM

We begin the qualitative analysis of the change in dependents variables with the substrate concentration, $S_b(t)$. Figure 32 shows that $S_b(t)$ very quickly (within

.01 days) decreases from its initial value $S_b(0) = .04$ mg/cm^3 to the constant substrate concentration $S_0 = .02$ mg/cm^3 which is the substrate concentration of the influent fluid. Figure 34a and Figure 35a show that the substrate concentration does not change with time because the influent fluid of constant substrate concentration continuously keeps replacing the old fluid. The substrate concentration in the biofilm, $S(t)$, rises initially (for the first .0002 days) because of the high concentration difference across the interface. After .0002 days (17.3 sec) $S_b(t)$ and $S(t)$ have the same value (around .038 mg/cm^3). Since the substrate concentration difference across the film-water interface is zero there (at $t = .0002$ days), $S(t)$ stops increasing which can be visualized in Figure 32 as the slope of $S(t)$ is zero at $t = .0002$ days. The two substrate concentrations $S_b(t)$ and $S(t)$ decrease to the influent substrate concentration, $S_0 = .02$ mg/cm^3 within .01 days. As the consumption of the substrate becomes significant, $S(t)$ begins to decrease (see Figure 34c). The active bacteria in the biofilm consume the substrate and multiply which causes a rapid increase in the volume fraction of the active biomass, f(t) which can be seen in Figure 34d. As long as $S(t)$ is sufficiently high (close to .02 mg/cm^3), $f(t)$ increases rapidly. Between day 6 and day 12, the biofilm thickness increases rapidly causing a rapid decrease in $S(t)$. The decay in $S(t)$ controls the growth of $L(t)$ and $f(t)$. All the variables reach their steady states after 30 days (see Figure 35).

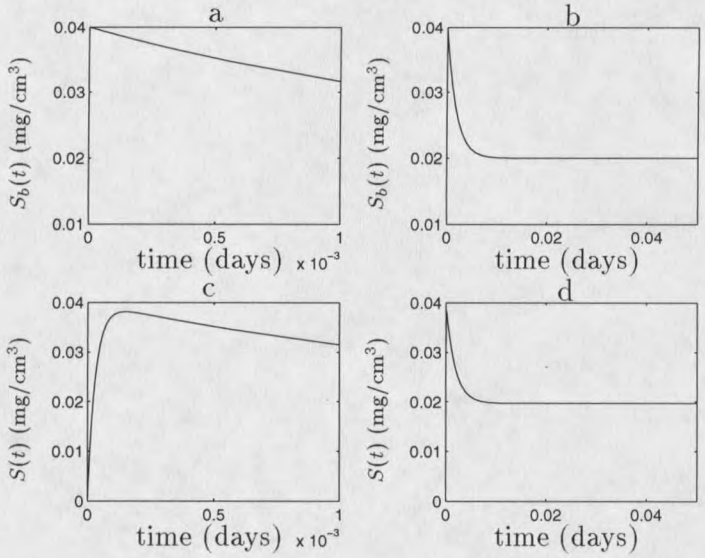

Figure 32: Bulk substrate concentration, $S_b(t)$ over .001 days, (a), and .05 days, (b) and substrate concentration in the biofilm, $S(t)$, over .001 days, (c), and .05 days, (d) for the zero-dimensional Rittman's model

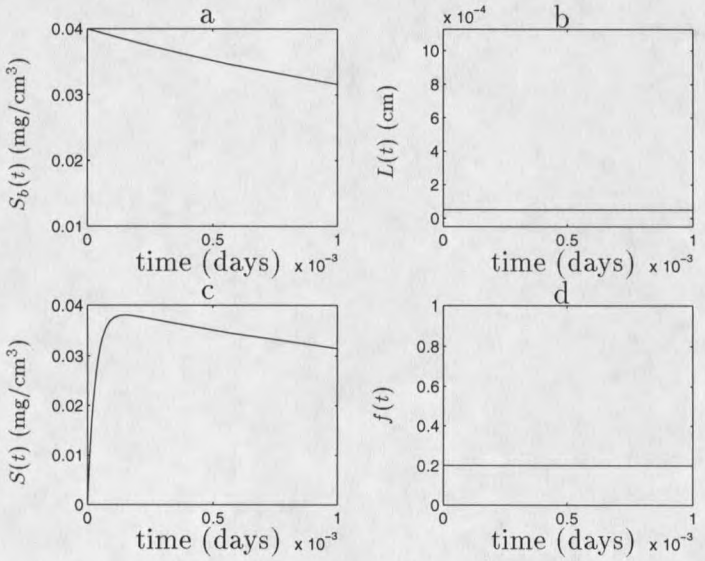

Figure 33: Bulk substrate concentration, $S_b(t)$, (a), biofilm thickness, $L(t)$, (b), substrate concentration in the biofilm, $S(t)$, (c), and active biomass volume fraction, $f(t)$, (d), over .001 days for the zero-dimensional BAM

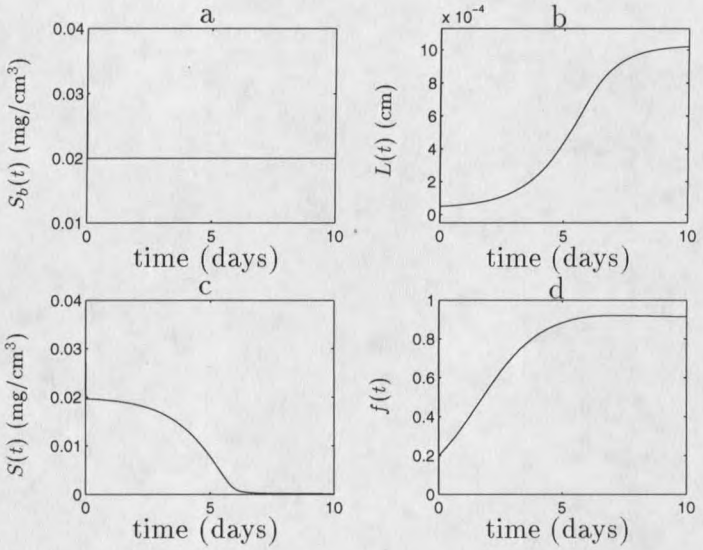

Figure 34: Bulk substrate concentration, $S_b(t)$, (a), biofilm thickness, $L(t)$, (b), substrate concentration in the biofilm, $S(t)$, (c), and active biomass volume fraction, $f(t)$, (d), over 10 days for the zero-dimensional BAM

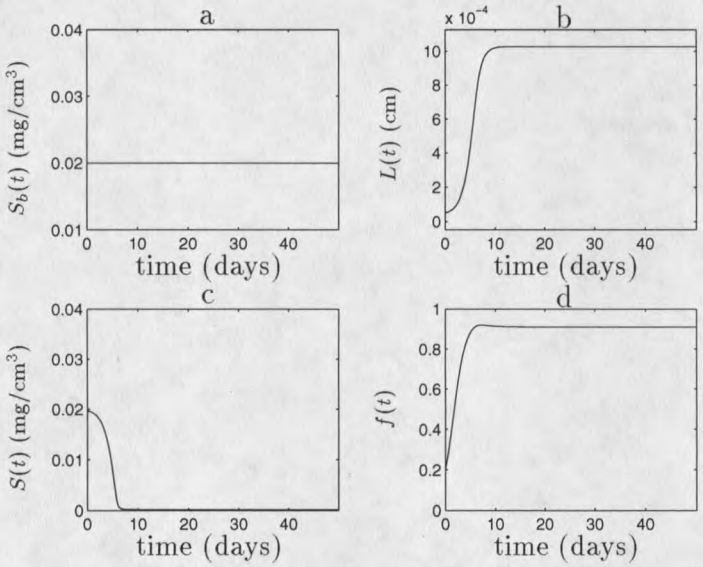

Figure 35: Bulk substrate concentration, $S_b(t)$, (a), biofilm thickness, $L(t)$, (b), substrate concentration in the biofilm, $S(t)$, (c), and active biomass volume fraction, $f(t)$, (d), over 50 days for the zero-dimensional BAM

Solution of Zero-dimensional BGM

The zero-dimensional BGM equations from (3.6)-(3.11) are solved for five unknown variables; substrate in the bulk liquid, $S_b(t)$, thickness of the biofilm, $L(t)$, average substrate concentration in the biofilm, $S(t)$, average volume fraction of the biomass in the biofilm, $f(t)$ and the volume of the bulk liquid, $V_L(t)$. In this section the model has been restricted so that valid comparisons can be made with BAM and Rittman's model. The parameters' values and the initial values of the variables are given in Table 20. The computer code which approximates the solution of zero-dimensional BGM equations is given in Appendix F. This code is virtually identical to that in Appendix C.

A qualitative analysis of the numerical results is given in Figures 36 through 39. Figure 36 contains the graphs of $S_b(t)$ and $S(t)$ as functions of time, t. Each of the figures (Figures 37-39) contains the graphs of $S_b(t)$, $L(t)$, $S(t)$, and $f(t)$ as functions of time, t. Again since the volumetric flow rate is relatively high, the substrate concentration in the bulk liquid very quickly (within .01 days) decreases to the influent substrate concentration, $S_0 = .02$ mg/cm^3, as seen in Figure 36. The substrate concentration in the biofilm, $S(t)$, rises initially (for the first .0002 days) because of the high concentration difference across the interface. After .0002 days (17.3 sec) $S_b(t)$ and $S(t)$ have the same value (around .038 mg/cm^3). Since the substrate concentration difference across the film-water interface is zero there (at $t =$ .0002 days), $S(t)$ stops increasing which can be visualized in Figure 36 as the slope of $S(t)$ is zero at $t = .0002$ days. The two substrate concentrations $S_b(t)$ and $S(t)$ decrease to the influent substrate concentration, $S_0 = .02$ mg/cm^3 within .01 days. As the consumption of the substrate becomes significant, $S(t)$ begins to decrease (see Figure 38c). The active bacteria in the biofilm consume the substrate and multiply which causes a rapid increase in the volume fraction of the active biomass, f(t) which

Parameters		Values
K	0.0001	mg/cm^3
V_r	4.3	mg/(mg day)
Y	.2	mg/mg
b	.35	day^{-1}
D	1.3	cm^2/day
$Q(t)$ $\forall t$	1100	cm^3/day
σ	1	cm^2
L_l	.8	cm
ϵ_l	0.0	dimensionless
ρ	12.2	mg/cm^3
S_0	.02	mg/cm^3
λ	500	cm^{-1}day^{-1}
Variables	Initial Values	
$S_b(0)$	.04	mg/cm^3
$L(0)$	.00005	cm
$S(0)$	.00004	mg/cm^3
$f(0)$	.2	dimensionless
$V_L(0)$	2.0	cm^3

Table 20: Parameter values and initial values for zero-dimensional BGM

can be seen in Figure 38d. As long as $S(t)$ is sufficiently high (close to .02 mg/cm^3), $f(t)$ increases rapidly. Between the sixth and twelfth days, the biofilm thickness increases rapidly causing a rapid decrease in $S(t)$. The decay in $S(t)$ controls the growth of $L(t)$ and $f(t)$. All the variables reach their steady states after 30 days (see Figure 39). The volume of the bulk liquid, V_L, in the BAM and the Rittman's model is assumed to be a constant however in the BGM it is assumed to be a function of time, t. $V_L(t)$ in BGM decreases as the biofilm thickness, $L(t)$, increases (qualitatively very similar to the change in the bulk volume for one-dimensional and zero-dimensional BGM discussed earlier in this chapter). Since BGM and Rittman's model assume $V_L(t)$ to be a constant, the quantitative comparison of $V_L(t)$ from these three different models is not interesting.

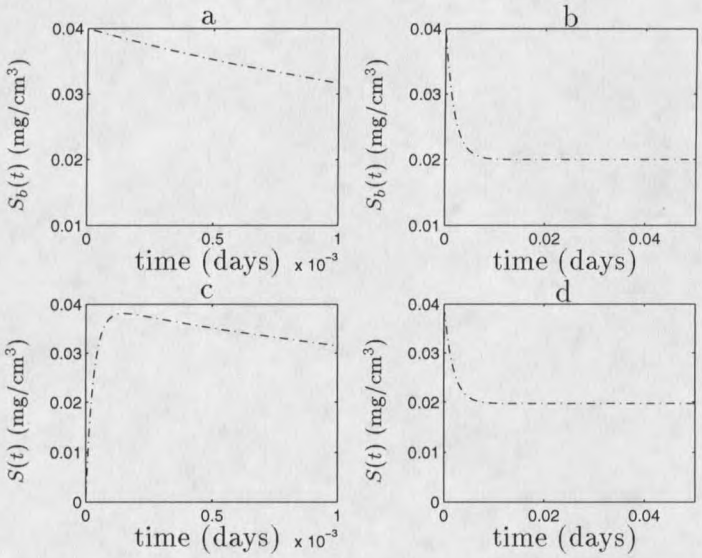

Figure 36: Bulk substrate concentration, $S_b(t)$ over .001 days, (a), and .05 days, (b) and substrate concentration in the biofilm, $S(t)$, over .001 days, (c), and .05 days, (d) for the zero-dimensional BGM

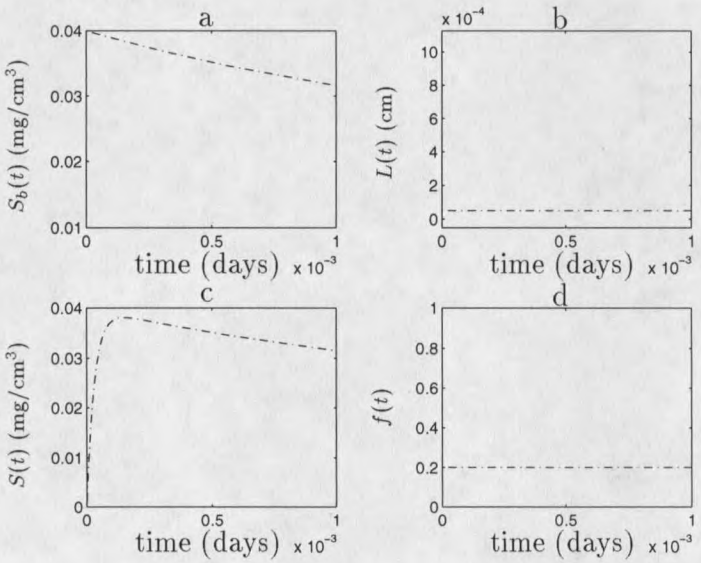

Figure 37: Bulk substrate concentration, $S_b(t)$, (a), biofilm thickness, $L(t)$, (b), substrate concentration in the biofilm, $S(t)$, (c), and active biomass volume fraction, $f(t)$, (d), over .001 days for the zero-dimensional BGM

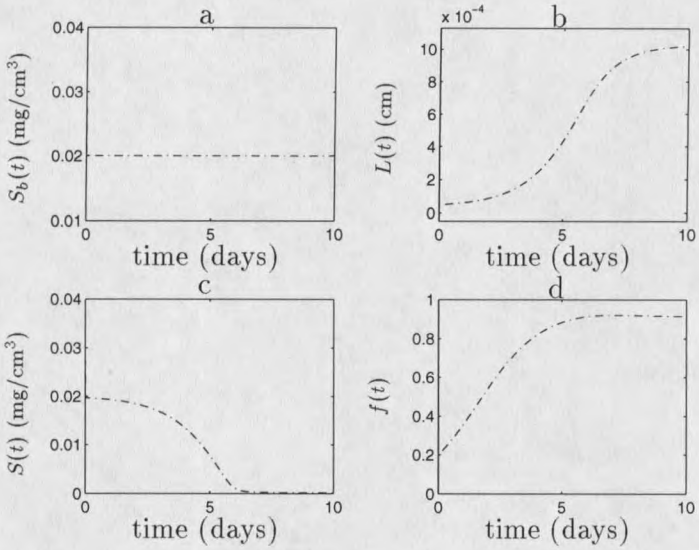

Figure 38: Bulk substrate concentration, $S_b(t)$, (a), biofilm thickness, $L(t)$, (b), substrate concentration in the biofilm, $S(t)$, (c), and active biomass volume fraction, $f(t)$, (d), over 10 days for the zero-dimensional BGM

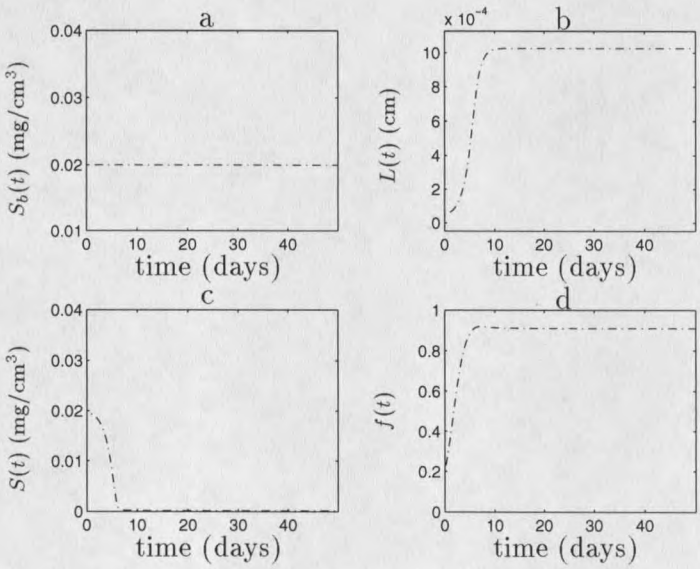

Figure 39: Bulk substrate concentration, $S_b(t)$, (a), biofilm thickness, $L(t)$, (b), substrate concentration in the biofilm, $S(t)$, (c), and active biomass volume fraction, $f(t)$, (d), over 50 days for the zero-dimensional BGM

t (days)	$S_b(t)$(RIT) (mg/cm^3)	$S_b(t)$ (BAM) (mg/cm^3)	$S_b(t)$ (BGM) (mg/cm^3)
0.0000	0.04000000	0.04000000	0.04000000
0.0001	0.03885991	0.03885990	0.03885990
0.0002	0.03798990	0.03798986	0.03798986
0.0003	0.03704396	0.03704388	0.03704388
0.0004	0.03612413	0.03612403	0.03612403
0.0005	0.03513771	0.03513758	0.03513758
0.0006	0.03436042	0.03464436	0.03464436
0.0007	0.03379226	0.03370611	0.03370611
0.0008	0.03285420	0.03276785	0.03276785
0.0009	0.03220021	0.03229872	0.03229872
0.0010	0.03089224	0.03089134	0.03089134

Table 21: Bulk substrate concentration, $S_b(t)$, over .001 days for the zero-dimensional Rittman's model (RIT), BAM, and BGM

t (days)	$S_b(t)$ (RIT) (mg/cm^3)	$S_b(t)$ (BAM) (mg/cm^3)	$S_b(t)$ (BGM) (mg/cm^3)
0.0	0.04000000	0.04000000	0.04000000
1.0	0.01999919	0.01999892	0.01999892
2.0	0.01999878	0.01999740	0.01999740
3.0	0.01999801	0.01999510	0.01999510
4.0	0.01999601	0.01998955	0.01999086
5.0	0.01999386	0.01998098	0.01998097
6.0	0.01999037	0.01997215	0.01997215
7.0	0.01998293	0.01997092	0.01997092
8.0	0.01997553	0.01997082	0.01997082
9.0	0.01997098	0.01997078	0.01997078
10.0	0.01997074	0.01997077	0.01997077

Table 22: Bulk substrate concentration, $S_b(t)$, over 10 days for the zero-dimensional Rittman's model (RIT), BAM, and BGM

t (days)	$S_b(t)$(RIT) (mg/cm^3)	$S_b(t)$ (BAM) (mg/cm^3)	$S_b(t)$ (BGM) (mg/cm^3)
0.0	0.04000000	0.04000000	0.04000000
5.0	0.01999386	0.01998098	0.01998097
10.0	0.01997074	0.01997077	0.01997077
15.0	0.01997061	0.01997077	0.01997077
20.0	0.01997060	0.01997077	0.01997077
25.0	0.01997060	0.01997077	0.01997077
30.0	0.01997060	0.01997077	0.01997077
35.0	0.01997060	0.01997077	0.01997077
40.0	0.01997060	0.01997077	0.01997077
45.0	0.01997060	0.01997077	0.01997077
50.0	0.01997060	0.01997077	0.01997077

Table 23: Bulk substrate concentration, $S_b(t)$, over 50 days for the zero-dimensional Rittman's model (RIT), BAM, and BGM

t (days)	$S(t)$(RIT) (mg/cm^3)	$S(t)$ (BAM) (mg/cm^3)	$S(t)$ (BGM) (mg/cm^3)
0.00000	0.00004000	0.00004000	0.00004000
0.00010	0.03764128	0.03764094	0.03764094
0.00020	0.03791233	0.03791196	0.03791196
0.00030	0.03701169	0.03701128	0.03701128
0.00040	0.03608020	0.03607978	0.03607978
0.00050	0.03513922	0.03507604	0.03507604
0.00060	0.03457462	0.03457417	0.03457417
0.00070	0.03362044	0.03361980	0.03361980
0.00080	0.03266626	0.03266542	0.03266542
0.00090	0.03218917	0.03171105	0.03171105
0.00100	0.03171208	0.03075668	0.03075668

Table 24: Substrate concentrations, $S(t)$, in the film over .001 days for the zero-dimensional Rittman's model (RIT), BAM, and BGM

t (days)	$S(t)$(RIT) (mg/cm^3)	$S(t)$ (BAM) (mg/cm^3)	$S(t)$ (BGM) (mg/cm^3)
0.0	0.00004000	0.00004000	0.00004000
1.0	0.01945582	0.01926840	0.01926840
2.0	0.01917354	0.01823809	0.01844482
3.0	0.01847047	0.01667685	0.01667684
4.0	0.01756596	0.01380202	0.01380218
5.0	0.01583675	0.00709441	0.00708876
6.0	0.01346803	0.00111523	0.00111841
7.0	0.00842338	0.00028539	0.00028659
8.0	0.00339949	0.00021831	0.00021908
9.0	0.00033132	0.00019696	0.00019743
10.0	0.00016384	0.00019144	0.00019167

Table 25: Substrate concentrations, $S(t)$, in the film over 10 days for the zero-dimensional Rittman's model (RIT), BAM, and BGM

t (days)	$S(t)$(RIT) (mg/cm^3)	$S(t)$ (BAM) (mg/cm^3)	$S(t)$ (BGM) (mg/cm^3)
0.0	0.00004000	0.00004000	0.00004000
5.0	0.01583675	0.00709441	0.00708876
10.0	0.00016384	0.00019144	0.00019167
15.0	0.00007781	0.00018970	0.00018967
20.0	0.00007319	0.00018986	0.00018986
25.0	0.00007220	0.00018985	0.00018985
30.0	0.00007203	0.00018985	0.00018985
35.0	0.00007200	0.00018985	0.00018985
40.0	0.00007200	0.00018985	0.00018985
45.0	0.00007200	0.00018985	0.00018985
50.0	0.00007200	0.00018985	0.00018985

Table 26: Substrate concentrations, $S(t)$, in the film over 50 days for the zero-dimensional Rittman's model (RIT), BAM, and BGM

t (days)	$L(t)$(RIT) (cm)	$L(t)$ (BAM) (cm)	$L(t)$ (BGM) (cm)
0.00000	0.00005000	0.00005000	0.00005000
0.00010	0.00004999	0.00005000	0.00005000
0.00020	0.00004999	0.00005000	0.00005000
0.00030	0.00004999	0.00005000	0.00005000
0.00040	0.00004999	0.00005000	0.00005000
0.00050	0.00004999	0.00005000	0.00005000
0.00060	0.00004999	0.00005000	0.00005000
0.00070	0.00004999	0.00005000	0.00005000
0.00080	0.00004999	0.00005000	0.00005000
0.00090	0.00004999	0.00005000	0.00005000
0.00100	0.00004999	0.00005000	0.00005000

Table 27: Biofilm thickness, $L(t)$, over .001 days for the zero-dimensional Rittman's model (RIT), BAM, and BGM

t (days)	$L(t)$(RIT) (cm)	$L(t)$ (BAM) (cm)	$L(t)$ (BGM) (cm)
0.0	0.00005000	0.00005000	0.00005000
1.0	0.00004632	0.00006246	0.00006246
2.0	0.00004914	0.00009490	0.00008836
3.0	0.00006553	0.00014468	0.00014468
4.0	0.00009161	0.00023717	0.00023716
5.0	0.00014555	0.00045633	0.00045652
6.0	0.00022214	0.00069699	0.00069672
7.0	0.00038885	0.00089462	0.00089360
8.0	0.00056484	0.00097035	0.00096920
9.0	0.00084740	0.00100734	0.00100638
10.0	0.00106647	0.00101981	0.00101921

Table 28: Biofilm thickness, $L(t)$, over 10 days for the zero-dimensional Rittman's model (RIT), BAM, and BGM

t (days)	$L(t)$(RIT) (cm)	$L(t)$ (BAM) (cm)	$L(t)$ (BGM) (cm)
0.0	0.00005000	0.00005000	0.00005000
5.0	0.00014555	0.00045633	0.00045652
10.0	0.00106647	0.00101981	0.00101921
15.0	0.00159722	0.00102663	0.00102662
20.0	0.00167967	0.00102659	0.00102659
25.0	0.00170327	0.00102659	0.00102659
30.0	0.00170849	0.00102659	0.00102659
35.0	0.00170970	0.00102659	0.00102659
40.0	0.00170991	0.00102659	0.00102659
45.0	0.00170994	0.00102659	0.00102659
50.0	0.00170995	0.00102659	0.00102659

Table 29: Biofilm thickness, $L(t)$, over 50 days for the zero-dimensional Rittman's model (RIT), BAM, and BGM

t (days)	$f(t)$(RIT)	$f(t)$ (BAM)	$f(t)$ (BGM)
0.00000	0.20000000	0.20000000	0.20000000
0.00010	0.20001351	0.20001351	0.20001351
0.00020	0.20002443	0.20002443	0.20002443
0.00030	0.20003700	0.20003700	0.20003700
0.00040	0.20005010	0.20005010	0.20005010
0.00050	0.20006379	0.20006471	0.20006471
0.00060	0.20007201	0.20007201	0.20007201
0.00070	0.20008907	0.20008908	0.20008908
0.00080	0.20010613	0.20010614	0.20010614
0.00090	0.20011465	0.20012320	0.20012320
0.00100	0.20012318	0.20014026	0.20014026

Table 30: Active biomass volume fraction, $f(t)$, over .001 days for the zero-dimensional Rittman's model (RIT), BAM, and BGM

t (days)	$f(t)$(RIT)	$f(t)$ (BAM)	$f(t)$ (BGM)
0.0	0.20000000	0.20000000	0.20000000
1.0	0.36534027	0.36542105	0.36542104
2.0	0.52385856	0.57893662	0.54663155
3.0	0.72503597	0.71534553	0.71534636
4.0	0.82587087	0.81441488	0.81441135
5.0	0.89069616	0.88712948	0.88716122
6.0	0.91646572	0.91321466	0.91319726
7.0	0.93149813	0.92038965	0.92038410
8.0	0.93576451	0.91934995	0.91939570
9.0	0.93452756	0.91677990	0.91689023
10.0	0.92629745	0.91464041	0.91478118

Table 31: Active biomass volume fraction, $f(t)$, over 10 days for the zero-dimensional Rittman's model (RIT), BAM, and BGM

t (days)	$f(t)$(RIT)	$f(t)$ (BAM)	$f(t)$ (BGM)
0.0	0.20000000	0.20000000	0.20000000
5.0	0.89069616	0.88712948	0.88716122
10.0	0.92629745	0.91464041	0.91478118
15.0	0.88164443	0.91145000	0.91150708
20.0	0.86836681	0.91122610	0.91122335
25.0	0.86306177	0.91123774	0.91123786
30.0	0.86161585	0.91123708	0.91123708
35.0	0.86121020	0.91123713	0.91123713
40.0	0.86112942	0.91123712	0.91123712
45.0	0.86111438	0.91123712	0.91123712
50.0	0.86111152	0.91123712	0.91123712

Table 32: Active biomass volume fraction, $f(t)$, over 50 days for the zero-dimensional Rittman's model (RIT), BAM, and BGM

Comparison of the Zero-dimensional Models

The zero-dimensional version of Rittman's model, BAM, and BGM are solved and qualitative and quantitative comparison are made for the following variables; biofilm thickness, $L(t)$, substrate concentration in the biofilm, $S(t)$, substrate concentration of the bulk liquid, $S_b(t)$, and the volume fraction of the active biomass in the biofilm, $f(t)$. For a qualitative comparison, the graphs of each variable computed from the three different models have been superimposed. Frames (a) and (b) of Figure 40 compare $S_b(t)$ over .001 and .05 days, respectively. Frame (c) of Figure 40 compares $S(t)$ over .001 days and frame (d) compares $S(t)$ over .05 days. The graphs are indistinguishable. Frame (a) of Figures 41 - 43 compares $S_b(t)$ over three time intervals (.001 days, 10 days, and 50 days) computed from these three models. Likewise frame (b), frame (c), and frame (d) of Figures 41-43 compare $L(t)$, $S(t)$, and $f(t)$, respectively. Also, a quantitative comparison of numerical values of these variables are displayed in Tables 21 through 32. Each variable calculated from the three models is analyzed and compared separately.

Substrate Concentration in the Bulk Liquid

The graphs of the bulk substrate concentration, $S_b(t)$, computed from the three zero-dimensional models (zero-dimensional Rittman's model (dashed line), zero-dimensional BAM (solid line), and zero-dimensional BGM (dash-dot line)) over times .001 days, 10 days, and 50 days are given in Figure 41a, Figure 42a and Figure 43a, respectively. Initially (over .01 days), $S_b(t)$ decreases from its initial value, $S_b(0) = .04$ mg/cm^3, to a constant value .02 mg/cm^3 which is the substrate concentration of the influent liquid. This is caused by the relatively high volumetric flow rate of the influent liquid into the tank. Figure 40b shows that $S_b(t)$ in all three models (Rittman's model, BAM and BGM) decreases with the same rate.

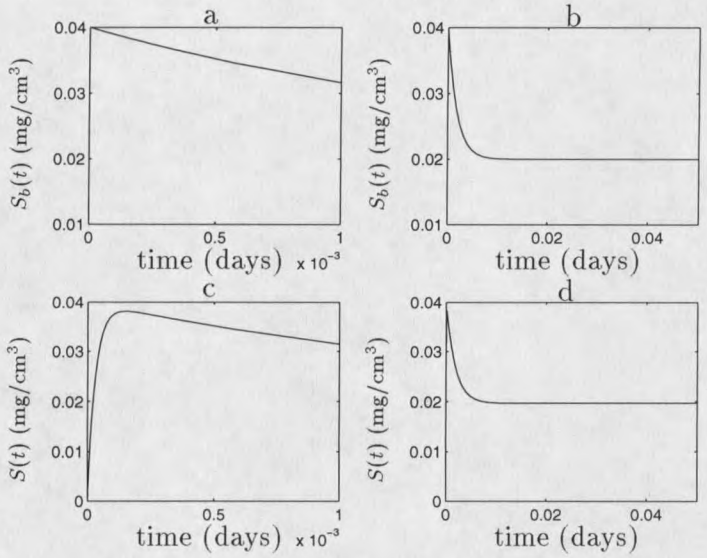

Figure 40: Bulk substrate concentration, $S_b(t)$ over .001 days, (a), and .05 days, (b) and substrate concentration in the biofilm, $S(t)$, over .001 days, (c), and .05 days, (d) for the zero-dimensional Rittman's model (dashed line), BAM (solid line), and BGM (dash-dot line)

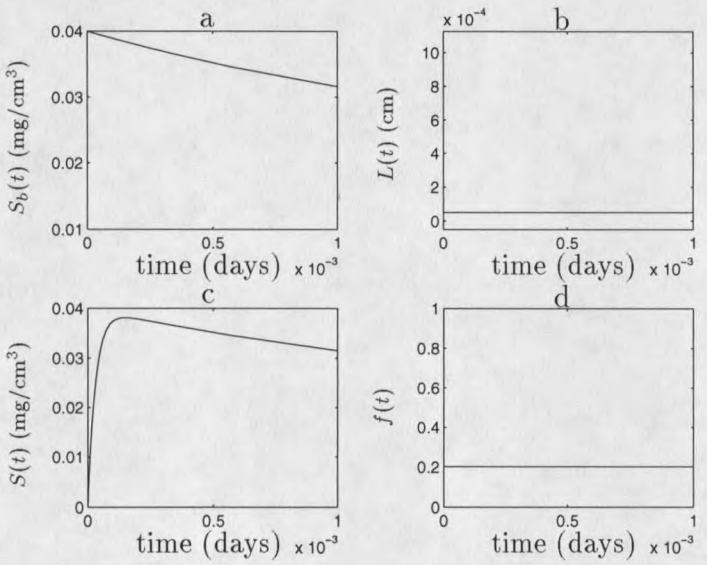

Figure 41: Bulk substrate concentration, $S_b(t)$, (a), biofilm thickness, $L(t)$, (b), substrate concentration in the biofilm, $S(t)$, (c), and active biomass volume fraction, $f(t)$, (d), over .001 days for the zero-dimensional Rittman's model (dashed line), BAM (solid line), and BGM (dash-dot line)

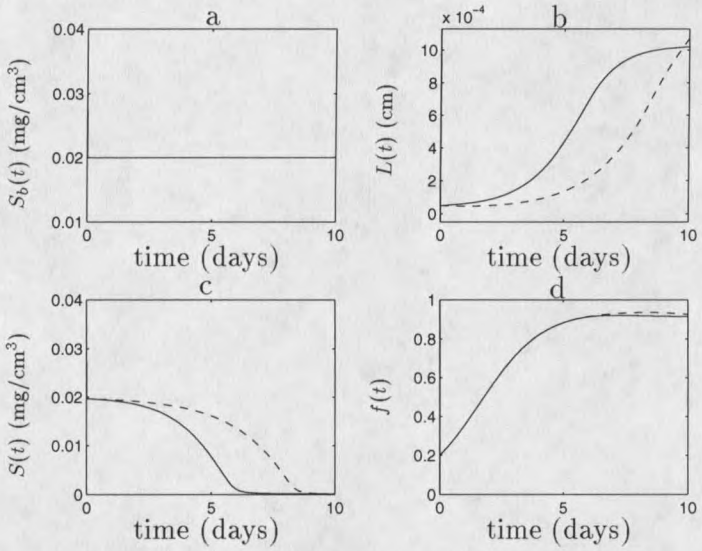

Figure 42: Bulk substrate concentration, $S_b(t)$, (a), biofilm thickness, $L(t)$, (b), substrate concentration in the biofilm, $S(t)$, (c), and active biomass volume fraction, $f(t)$, (d), over 10 days for the zero-dimensional Rittman's model (dashed line), BAM (solid line), and BGM (dash-dot line)

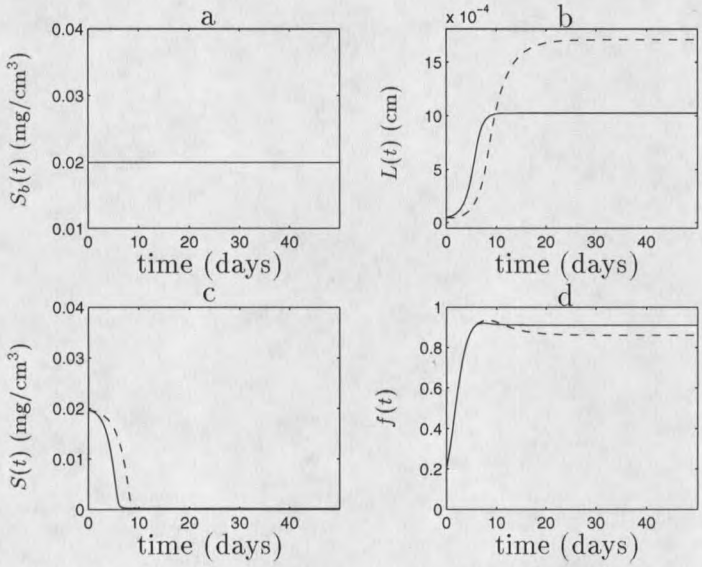

Figure 43: Bulk substrate concentration, $S_b(t)$, (a), biofilm thickness, $L(t)$, (b), substrate concentration in the biofilm, $S(t)$, (c), and active biomass volume fraction, $f(t)$, (d), over 50 days for the zero-dimensional Rittman's model (dash line), BAM (solid line), and BGM (dash-dot line)

Substrate Concentration in the Biofilm

Because of a high concentration difference across the interface, the substrate diffuses from high concentration to low concentration. Since initially the substrate concentration, $S(t)$, in the biofilm is less than the bulk substrate concentration, Figure 40 shows a rapid increase in the substrate concentration in the biofilm. The substrate concentration in the biofilm, $S(t)$, rises initially (for the first .0002 days) because of the high concentration difference across the interface. Figure 40 and Tables 21 and 24 show that after .0002 days (17.3 sec) $S_b(t)$ and $S(t)$ have the same value (around .038 mg/cm^3). Since the substrate concentration difference across the film-water interface is zero there (at $t = .0002$ days), $S(t)$ stops increasing which can be visualized in Figure 40 as the slope of $S(t)$ is zero at $t = .0002$ days. The two substrate concentrations $S_b(t)$ and $S(t)$ decrease to the influent substrate concentration, $S_0 = .02$ mg/cm^3 within .01 days. As the consumption of the substrate becomes significant, $S(t)$ begins to decrease (see Figure 42c). Figure 42c shows that the decrease in $S(t)$ in the Rittman's model is slower than it is in BGM or BAM. Also, $S(t)$ in Rittman's model reaches a steady state after 25 days and in BAM and BGM reaches a steady state after 15 days (see Table 26). Also notice that the steady state value of $S(t)$ in Rittman's model (.000072 mg/cm^3) is significantly smaller than it is in BGM or BAM (.000190 mg/cm^3) because the steady state biofilm thickness in Rittman's model (.001710 cm) is significantly higher than that of BAM or BGM (.001027 cm)(see Figure 43, Table 26 and Table 29).

Biofilm Thickness

Figures 41b, 42b and 43b and Tables 27, 28 and 29 compare the biofilm thickness, $L(t)$, computed from the three models. Since biofilm growth is a much slower process than diffusion, even though the substrate concentration in the biofilm is high we

do not notice any change in the biofilm thickness until after .5 days. The biofilm growth in Rittman's model is slow which causes a slow decrease in the substrate consumption whereas the biofilm growth in BAM and BGM is more rapid hence the substrate consumption is higher. The growth of biofilm thickness is controlled by the detachment of biofilm occurring at the interface and the lack of substrate near the substratum. Table 29 shows that the biofilm thickness in all the models reaches a steady state. The steady state value of the thickness in Rittman's model (.001710 cm) is greater than the steady state value of the thickness in BAM or BGM (.001027 cm) because Rittman's model considers a different function for detachment than BAM or BGM. The detachment in Rittman's model is smaller than the detachment in BAM or BGM.

Volume Fraction of Active Biomass

In all three models the volume fraction of active biomass, $f(t)$, increases with the same rate over the first 6 days, slowly in the beginning (over the first .2 days) and then the growth rate becomes faster which causes decay in the substrate concentration and an increase in the biofilm thickness. When the substrate concentrate becomes low, the volume fraction slowly approaches a steady state. Figure 43d and Table 32 show that between the tenth and fifteenth days the volume fraction in Rittman's model becomes smaller than the volume fraction in BAM and BGM. This is because the substrate concentration in the biofilm, $S(t)$, in Rittman's model is less than the substrate concentration in the biofilm, $S(t)$, in BAM and BGM. The graphs of the volume fraction, $f(t)$, are displayed in Figures 41d, 42d, and 43d and the comparison between the numerical values of $f(t)$ is given in Tables 30, 31, and 32.

CHAPTER 4

Biofilm Accumulation in Porous Media

Introduction

Fluid flow through a porous medium has been well studied since a series of experiments done by Darcy in 1856. The experimental results and the mathematical models describing the flow phenomena was discussed in [7]. The historic and current experimental and mathematical models describing porous media flow can be found in [1], [2], [9], [20], [22], [23], as well as many other references. The study of biofilm accumulation is comparatively new. A description of scientific studies of biofilm growth and related problems can be found in [4].

In the next section, mathematical models describing the velocity and pressure distribution in porous media are presented. Bundles of capillary tubes and beds of spherical balls are often used as idealized representations of porous media characteristics and this is described in the third section. An overview of the problem concerning biofilm growth in a porous media is then given in the fourth section. A combination of flow models and the biofilm accumulation models, described in previous chapters, give the models which allow one to study the effect of biofilm growth on porosity and permeability of the porous medium. Models describing effects of biofilm growth on incompressible fluid flow in a porous medium are then presented in the fifth section.

Flow of a Single Fluid Through Porous Media

Mass Balance and Momentum Balance

Assume that a fluid of density $\rho_f(\mathbf{z},t)$ (ML^{-3}), is flowing through a porous medium whose porosity is $\phi(\mathbf{z},t)$ (dimensionless). If $\boldsymbol{\omega}(\mathbf{z},t)$ is the fluid velocity (LT^{-1}) at a point whose position vector is $\mathbf{z}$ at time t, then the mass balance equation [1], [2] is given by

$$\frac{D}{Dt}\Big(\phi(\mathbf{z},t)\rho_f(\mathbf{z},t)\Big) + \phi(\mathbf{z},t)\rho_f(\mathbf{z},t)\nabla\cdot\boldsymbol{\omega}(\mathbf{z},t) = 0, \tag{4.1}$$

where $\boldsymbol{\omega}(\mathbf{z},t) = (u(\mathbf{z},t), v(\mathbf{z},t), w(\mathbf{z},t))$ and $\mathbf{z} = (x,y,z)$. The notation $\frac{D}{Dt}$ represents the material derivative. This equation is called the continuity equation.

Also assume that at a point $(\mathbf{z},t)$, $P(\mathbf{z},t)$ is the pressure (ML^{-1}), $\mu(\mathbf{z},t)$ is the viscosity $(ML^{-1}T^{-1})$ of the fluid, $k(\mathbf{z},t)$ is the permeability (L^2) of the medium, and h is the constant height (L) of the fluid surface from the datum plane. Then the momentum balance equation [1], [2] is given by

$$\begin{aligned}\frac{D}{Dt}\Big(\phi(\mathbf{z},t)\rho_f(\mathbf{z},t)\boldsymbol{\omega}(\mathbf{z},t)\Big) &+ \phi(\mathbf{z},t)\rho_f(\mathbf{z},t)\boldsymbol{\omega}(\mathbf{z},t)\nabla\cdot\boldsymbol{\omega}(\mathbf{z},t) + \nabla P(\mathbf{z},t)\\ -\rho_f(\mathbf{z},t)g\nabla(h-z) &= -\frac{\phi(\mathbf{z},t)\mu(\mathbf{z},t)}{k(\mathbf{z},t)}\boldsymbol{\omega}(\mathbf{z},t).\end{aligned} \tag{4.2}$$

The unknown dependent variables in this model are typically the pressure $P(\mathbf{z},t)$ and the velocity $\boldsymbol{\omega}(\mathbf{z},t)$, which are tabulated in Table 33 along with their fundamental units in terms of mass (M), length (L) and time (T). The other variables and constants in this model are given in Table 34.

Using the chain rule (4.2) becomes

$$\begin{aligned}&\phi(\mathbf{z},t)\rho_f(\mathbf{z},t)\frac{D}{Dt}\Big(\boldsymbol{\omega}(\mathbf{z},t)\Big) + \boldsymbol{\omega}(\mathbf{z},t)\frac{D}{Dt}\Big(\phi(\mathbf{z},t)\rho_f(\mathbf{z},t)\Big)\\ &+\phi(\mathbf{z},t)\rho_f(\mathbf{z},t)\boldsymbol{\omega}(\mathbf{z},t)\nabla\cdot\boldsymbol{\omega}(\mathbf{z},t) + \nabla P(\mathbf{z},t)\\ &-\rho_f(\mathbf{z},t)g\nabla(h-z) = -\frac{\phi(\mathbf{z},t)\mu(\mathbf{z},t)}{k(\mathbf{z},t)}\boldsymbol{\omega}(\mathbf{z},t)\end{aligned}$$

Variables	Physical quantity	Units
$\boldsymbol{\omega}(\mathbf{z},t) = (u(\mathbf{z},t), v(\mathbf{z},t), w(\mathbf{z},t))$	fluid velocity	LT^{-1}
$u(\mathbf{z},t)$	velocity component along x-axis	LT^{-1}
$v(\mathbf{z},t)$	velocity component along y-axis	LT^{-1}
$w(\mathbf{z},t)$	velocity component along z-axis	LT^{-1}
$P(\mathbf{z},t)$	pressure	$ML^{-1}T^{-2}$

Table 33: Unknown dependent variables in a porous media flow model and their fundamental units

Variables	Physical quantity	Units
$\mathbf{z} = (x,y,z)$	position vector	L
$\rho_f(\mathbf{z},t)$	density of the fluid	ML^{-3}
$\mu(\mathbf{z},t)$	viscosity of the fluid	$ML^{-1}T^{-1}$
$\phi(\mathbf{z},t)$	porosity of the media	dimensionless
$k(\mathbf{z},t)$	permeability of the media	L^2
g	gravitational acceleration	LT^{-2}

Table 34: Variables and constants used in the porous media flow model with their fundamental units

which simplifies to

$$\phi(\mathbf{z},t)\rho_f(\mathbf{z},t)\frac{D}{Dt}\Big(\boldsymbol{\omega}(\mathbf{z},t)\Big)+\boldsymbol{\omega}(\mathbf{z},t)\Big[\frac{D}{Dt}\Big(\phi(\mathbf{z},t)\rho_f(\mathbf{z},t)\Big)+\phi(\mathbf{z},t)\rho_f(\mathbf{z},t)\nabla\cdot\boldsymbol{\omega}(\mathbf{z},t)\Big]$$
$$+\nabla P(\mathbf{z},t)-\rho_f(\mathbf{z},t)g\nabla(h-z)=-\frac{\phi(\mathbf{z},t)\mu(\mathbf{z},t)}{k(\mathbf{z},t)}\boldsymbol{\omega}(\mathbf{z},t).$$

The second term of this equation is zero due to (4.1). This leaves

$$\phi(\mathbf{z},t)\rho_f(\mathbf{z},t)\frac{D}{Dt}\Big(\boldsymbol{\omega}(\mathbf{z},t)\Big)+\nabla P(\mathbf{z},t)+\rho_f(\mathbf{z},t)\mathbf{G}=-\frac{\phi(\mathbf{z},t)\mu(\mathbf{z},t)}{k(\mathbf{z},t)}\boldsymbol{\omega}(\mathbf{z},t) \quad (4.3)$$

where $\mathbf{G}=(0,0,g)$ and g is the gravitational acceleration (LT^{-2}).

If $\mu(\mathbf{z},t)$, $k(\mathbf{z},t)$ and $\phi(\mathbf{z},t)$ are known, the model given by (4.1) and (4.3) can be solved for the velocity, $\boldsymbol{\omega}(\mathbf{z},t)$, and the pressure, $P(\mathbf{z},t)$, as a function of time and space provided we have a constitutive relation between $\rho_f(\mathbf{z},t)$ and $P(\mathbf{z},t)$. We now look at various simplifications of this model.

Incompressible Flow

Using the chain rule (4.1) can be written in the form

$$\phi(\mathbf{z},t)\frac{D}{Dt}\Big(\rho_f(\mathbf{z},t)\Big)+\rho_f(\mathbf{z},t)\frac{D}{Dt}\Big(\phi(\mathbf{z},t)\Big)+\phi(\mathbf{z},t)\rho_f(\mathbf{z},t)\nabla\cdot\boldsymbol{\omega}(\mathbf{z},t)=0. \quad (4.4)$$

If one assumes that the fluid is incompressible, which means that $\frac{D}{Dt}(\rho_f(\mathbf{z},t))=0$, then (4.4) reduces to

$$\rho_f(\mathbf{z},t)\frac{D}{Dt}\Big(\phi(\mathbf{z},t)\Big)+\phi(\mathbf{z},t)\rho_f(\mathbf{z},t)\nabla\cdot\boldsymbol{\omega}(\mathbf{z},t)=0.$$

This continuity equation further simplifies to

$$\frac{D}{Dt}\Big(\phi(\mathbf{z},t)\Big)+\phi(\mathbf{z},t)\nabla\cdot\boldsymbol{\omega}(\mathbf{z},t)=0. \quad (4.5)$$

In one dimension (replace $\mathbf{z}$ with z and $\boldsymbol{\omega}(\mathbf{z},t)$ with $w(z,t)$), (4.3) becomes

$$\phi(z,t)\rho_f(z,t)\frac{D}{Dt}\Big(w(z,t)\Big)+\frac{\partial}{\partial z}\Big(P(z,t)\Big)+\rho_f(z,t)g=-\frac{\phi(z,t)\mu(z,t)}{k(z,t)}w(z,t)$$

which simplifies to

$$\begin{aligned}\frac{\partial}{\partial t}\Big(w(z,t)\Big) \;+\; & w(z,t)\frac{\partial}{\partial z}\Big(w(z,t)\Big)+\frac{1}{\rho_f(z,t)\phi(z,t)}\frac{\partial}{\partial z}\Big(P(z,t)\Big)\\ +\; & \frac{g}{\phi(z,t)}=-\frac{\mu(z,t)}{k(z,t)\rho_f(z,t)}w(z,t).\end{aligned}\tag{4.6}$$

Also in one dimension, the continuity equation (4.5) becomes

$$\frac{D}{Dt}\Big(\phi(z,t)\Big)+\phi(z,t)\frac{\partial}{\partial z}\Big(w(z,t)\Big)=0$$

which simplifies to

$$\frac{\partial}{\partial t}\Big(\phi(z,t)\Big)+w(z,t)\frac{\partial}{\partial z}\Big(\phi(z,t)\Big)+\phi(z,t)\frac{\partial}{\partial z}\Big(w(z,t)\Big)=0.\tag{4.7}$$

In two dimensions, (4.3) can be written in the form

$$\begin{aligned}&\frac{\partial}{\partial t}\Big(\boldsymbol{\omega}(x,z,t)\Big)+\Big(\boldsymbol{\omega}(x,z,t)\cdot\nabla\Big)\boldsymbol{\omega}(x,z,t)+\frac{\nabla P(x,z,t)}{\rho_f(x,z,t)\phi(x,z,t)}\\ &+\frac{\mathbf{G}}{\phi(x,z,t)}=-\frac{\mu(x,z,t)}{k(x,z,t)\rho_f(x,z,t)}\boldsymbol{\omega}(x,z,t)\end{aligned}$$

where $\boldsymbol{\omega}(x,z,t)=\Big(u(x,z,t),w(x,z,t)\Big)$. The two components of this momentum balance equation may be written as

$$\begin{aligned}&\frac{\partial}{\partial t}\Big(u(x,z,t)\Big)+u(x,z,t)\frac{\partial}{\partial x}\Big(u(x,z,t)\Big)+w(x,z,t)\frac{\partial}{\partial z}\Big(u(x,z,t)\Big)\\ &+\frac{1}{\rho_f(x,z,t)\phi(x,z,t)}\frac{\partial}{\partial x}\Big(P(x,z,t)\Big)=-\frac{\mu(x,z,t)}{k(x,z,t)\rho_f(x,z,t)}u(x,z,t)\end{aligned}\tag{4.8}$$

and

$$\begin{aligned}&\frac{\partial}{\partial t}\Big(w(x,z,t)\Big)+u(x,z,t)\frac{\partial}{\partial x}\Big(w(x,z,t)\Big)+w(x,z,t)\frac{\partial}{\partial z}\Big(w(x,z,t)\Big)\\ &+\frac{1}{\rho_f(x,z,t)\phi(x,z,t)}\frac{\partial}{\partial z}\Big(P(x,z,t)\Big)+\frac{g}{\phi(x,z,t)}\\ &=-\frac{\mu(x,z,t)}{k(x,z,t)\rho_f(x,z,t)}w(x,z,t).\end{aligned}\tag{4.9}$$

Further the continuity equation (4.5) can be expanded to

$$\frac{\partial}{\partial t}\Big(\phi(\mathbf{z},t)\Big)+\Big(\boldsymbol{\omega}(\mathbf{z},t)\cdot\nabla\Big)\,\phi(\mathbf{z},t)+\phi(\mathbf{z},t)\nabla\cdot\boldsymbol{\omega}(\mathbf{z},t)=0.$$

In two dimensions this can be written in the form

$$\begin{aligned}&\frac{\partial}{\partial t}\Big(\phi(x,z,t)\Big)+u(x,z,t)\frac{\partial}{\partial x}\Big(\phi(x,z,t)\Big)+w(x,z,t)\frac{\partial}{\partial z}\Big(\phi(x,z,t)\Big)\\&+\phi(x,z,t)\frac{\partial}{\partial x}\Big(u(x,z,t)\Big)+\phi(x,z,t)\frac{\partial}{\partial z}\Big(w(x,z,t)\Big)=0.\end{aligned}\tag{4.10}$$

Further Simplifications If it is assumed that the inertia of the fluid has negligible effect on the flow, then $\frac{D\boldsymbol{\omega}(\mathbf{z},t)}{Dt}=0$. Hence (4.3) reduces to,

$$\boldsymbol{\omega}(\mathbf{z},t)=-\frac{k(\mathbf{z},t)}{\mu(\mathbf{z},t)\phi(\mathbf{z},t)}\Big(\nabla P(\mathbf{z},t)+\rho_f(\mathbf{z},t)\mathbf{G}\Big).\tag{4.11}$$

This is called *Darcy's equation.* We can rewrite (4.11) in the form

$$\mu(\mathbf{z},t)\phi(\mathbf{z},t)\boldsymbol{\omega}(\mathbf{z},t)=-k(\mathbf{z},t)\Big(\nabla P(\mathbf{z},t)+\rho_f(\mathbf{z},t)\mathbf{G}\Big).\tag{4.12}$$

Taking the divergence of both sides and using the chain rule, (4.12) becomes

$$\begin{aligned}&\nabla\Big(\mu(\mathbf{z},t)\Big)\cdot\Big(\phi(\mathbf{z},t)\boldsymbol{\omega}(\mathbf{z},t)\Big)+\mu(\mathbf{z},t)\nabla\cdot\Big(\phi(\mathbf{z},t)\boldsymbol{\omega}(\mathbf{z},t)\Big)\\&=-\nabla\Big(k(\mathbf{z},t)\Big)\cdot\Big(\nabla P(\mathbf{z},t)+\rho_f(\mathbf{z},t)\mathbf{G}\Big)\\&\quad-k(\mathbf{z},t)\nabla\cdot\Big(\nabla P(\mathbf{z},t)+\rho_f(\mathbf{z},t)\mathbf{G}\Big)\end{aligned}\tag{4.13}$$

which can be rewritten in the form

$$\begin{aligned}&\nabla^2P(\mathbf{z},t)+\frac{\nabla\Big(k(\mathbf{z},t)\Big)}{k(\mathbf{z},t)}\cdot\nabla P(\mathbf{z},t)=-\frac{1}{k(\mathbf{z},t)}\Big[\nabla\Big(\mu(\mathbf{z},t)\Big)\cdot\Big(\phi(\mathbf{z},t)\boldsymbol{\omega}(\mathbf{z},t)\Big)\\&+\mu(\mathbf{z},t)\nabla\cdot\Big(\phi(\mathbf{z},t)\boldsymbol{\omega}(\mathbf{z},t)\Big)\Big]-\frac{\nabla\Big(k(\mathbf{z},t)\Big)}{k(\mathbf{z},t)}\cdot\Big(\rho_f(\mathbf{z},t)\mathbf{G}\Big)\\&-\nabla\cdot\Big(\rho_f(\mathbf{z},t)\mathbf{G}\Big).\end{aligned}\tag{4.14}$$

If the density, $\rho_f(\mathbf{z},t)$, and the viscosity, $\mu(\mathbf{z},t)$, of the fluid are assumed to be constants, namely ρ_f and μ, then (4.14) reduces to,

$$\nabla^2 P(\mathbf{z},t)+\frac{\nabla\Big(k(\mathbf{z},t)\Big)}{k(\mathbf{z},t)}\cdot\nabla P(\mathbf{z},t)=-\frac{\mu}{k(\mathbf{z},t)}\nabla\cdot\Big(\phi(\mathbf{z},t)\boldsymbol{\omega}(\mathbf{z},t)\Big)-\frac{\nabla\Big(k(\mathbf{z},t)\Big)}{k(\mathbf{z},t)}\cdot\Big(\rho_f\mathbf{G}\Big). \tag{4.15}$$

Expanding the material derivative, (4.5) becomes

$$\frac{\partial}{\partial t}\Big(\phi(\mathbf{z},t)\Big)+\Big(\boldsymbol{\omega}(\mathbf{z},t)\cdot\nabla\Big)\Big(\phi(\mathbf{z},t)\Big)+\phi(\mathbf{z},t)\nabla\cdot\boldsymbol{\omega}(\mathbf{z},t)=0 \tag{4.16}$$

which can be written in the form

$$\nabla\cdot\Big(\phi(\mathbf{z},t)\boldsymbol{\omega}(\mathbf{z},t)\Big)=-\frac{\partial}{\partial t}\Big(\phi(\mathbf{z},t)\Big). \tag{4.17}$$

Using (4.17), (4.15) becomes

$$\nabla^2 P(\mathbf{z},t)+\frac{\nabla\Big(k(\mathbf{z},t)\Big)}{k(\mathbf{z},t)}\cdot\nabla P(\mathbf{z},t)=\frac{\mu}{k(\mathbf{z},t)}\frac{\partial}{\partial t}\Big(\phi(\mathbf{z},t)\Big)-\frac{\nabla\Big(k(\mathbf{z},t)\Big)}{k(\mathbf{z},t)}\cdot\Big(\rho_f\mathbf{G}\Big). \tag{4.18}$$

Notice that if the porous media is isotropic and homogeneous (i.e. $k(\mathbf{z},t)$ and $\phi(\mathbf{z},t)$ are constants, namely k and ϕ) and the fluid flowing through it is incompressible (i.e. the continuity equation reduces to $\nabla\cdot\boldsymbol{\omega}(\mathbf{z},t)=0$) then (4.18) reduces to *Laplace's equation*

$$\nabla^2 P(\mathbf{z},t)=0 \tag{4.19}$$

which, together with the simplified (4.11)

$$\boldsymbol{\omega}(\mathbf{z},t)=-\frac{k}{\mu\phi}\Big(\nabla P(\mathbf{z},t)+\rho_f\mathbf{G}\Big) \tag{4.20}$$

models the pressure and velocity distribution throughout the porous media [1],[2].

Permeability and Porosity in Different Porous Media Models

The flow of a fluid in many porous media settings can be imagined with equal justification to occur either in a network of closed capillaries or around solid spherical particles forming a spatial array. Both of these approaches have been pursued

extensively by various researchers. The relation between permeability and porosity in both type of models (bundles of capillaries and bed of spherical balls) is discussed in the following two subsections.

Permeability in Bundles of Capillary Tubes Models

The models described here consist of systems of parallel capillary tubes of well defined geometry. The tubes can be uniform and identical, uniform but with distributed diameters, periodically constricted and identical, or periodically constricted and different. In all these models a relation between porosity and the permeability has been described. The variables and constants used in these models are given in Table 35.

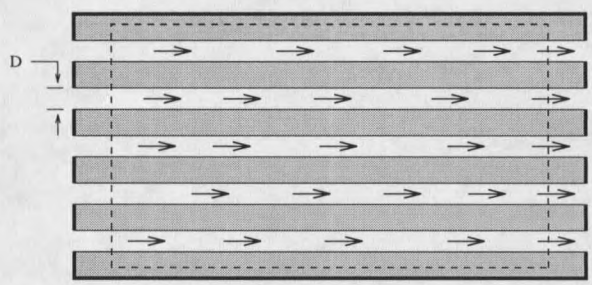

Figure 44: Bundle of identical capillaries in parallel representing a porous medium

Bundle of Identical Capillaries Consider a cube shaped sample of edge length H (L) with n (dimensionless) parallel capillaries of length H and diameter D (L), see Figure 44. Then the porosity ϕ (dimensionless) of the sample satisfies

$$\phi = \frac{n\pi(\frac{D}{2})^2 H}{H^3} = \frac{n\pi D^2}{4H^2}. \tag{4.21}$$

If a fluid of viscosity μ $(ML^{-1}T^{-1})$ is flowing through the sample porous media then the volumetric flow rate Q (L^3T^{-1}) under the influence of the pressure gradient ΔP $(ML^{-1}T^{-2})$ satisfies [2], [9]

$$Q = \frac{nD^4\pi}{128\mu}\frac{\Delta P}{H}. \tag{4.22}$$

Variables	Physical quantity	Units
Q	volumetric flow rate	L^3T^{-1}
ϕ	porosity of the porous media	dimensionless
k	permeability of the porous media	L^2
μ	viscosity	$ML^{-1}T^{-1}$
D	diameter of the pores	L
D_e	pore entry diameter	L
H	height of the sample media	L
n	number of pores	dimensionless
ΔP	pressure gradient	$ML^{-1}T^{-2}$
$\alpha_p(D)$	pore size density of capillary tubes in parallel	L^{-3}
$\alpha_s(D)$	pore size density of capillary tubes in series	L^{-3}
$\beta_{p,s}(D_e, D)$	bivariate density function	L^{-3}

Table 35: Variables and constants in bundles of capillary tubes models

This is known as the Hagen-Poiseuille equation. Also by Darcy's law [2], [9]

$$Q = \frac{k}{\mu} H^2 \frac{\Delta P}{H} \tag{4.23}$$

where k is the permeability (L^2) of the media. Combination of (4.21) to (4.23) gives the following expression for the permeability, k,

$$k = \phi \frac{D^2}{32}. \tag{4.24}$$

A pseudo three-dimensional model would arrange the n capillaries in such a way that $\frac{n}{3}$ capillaries would be parallel to x-axis, $\frac{n}{3}$ capillaries would be parallel to y-axis and $\frac{n}{3}$ capillaries would be parallel to z-axis. In this more realistic isotropic model the permeability k for the same porosity ϕ is one third of the permeability k of the one-dimensional model, that is,

$$k = \phi \frac{D^2}{96}. \tag{4.25}$$

Bundle of Capillaries of Different Diameter in Parallel Now let our bundle of capillaries consist of different diameters as in Figure 45. Then each capillary is

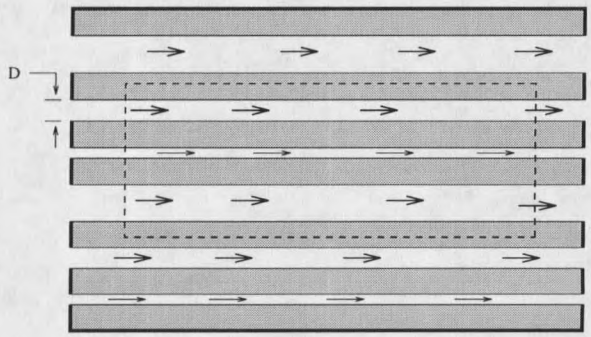

Figure 45: Bundle of parallel capillaries of different diameters representing a porous medium

assumed to have uniform cross-section and the frequency of each diameter D is given by a volume-based pore size density $\alpha_p(D)$ (L^{-3}). There is flow in $\frac{1}{3}$ of the capillaries lying in the direction of the macroscopic flow in this model. The permeability of this type of capillary model is, [9]

$$k = \frac{\phi}{96} \int_0^\infty D^2 \alpha_p(D) dD \tag{4.26}$$

where the subscript p refers to capillaries of different diameters in parallel.

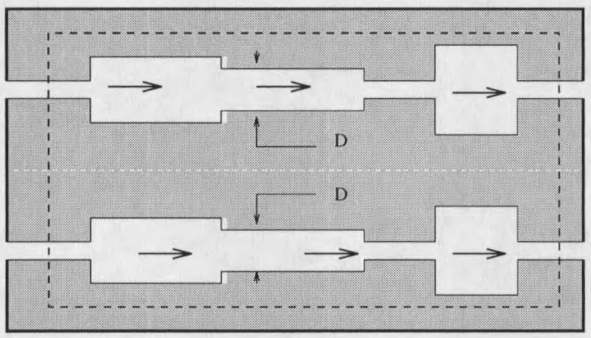

Figure 46: Illustration of the physical basis of the capillaric model of permeability expressed by (4.27)

Bundle of Identical Periodically Constricted Tubes In this capillaric model each channel is assumed to consist of segments of different diameters distributed

according to some volume-based pore size distribution density $\alpha_s(D)$ (L^{-3}), where the subscript s refers to tube segments of different diameter in series (see Figure 46). The permeability of this kind of model is, [9],

$$k = \frac{\phi}{96} \frac{\left[\int_0^\infty \frac{\alpha_s(D)}{D^2} dD\right]^2}{\int_0^\infty \frac{\alpha_s(D)}{D^6} dD} \tag{4.27}$$

The factor 96 was again introduced on the grounds that $\frac{1}{3}$ of the capillaries are pointing in each spatial direction.

Bundle of Different Periodically Constricted Tubes Both the model consisting of bundles of capillaries of different diameters in parallel and the model consisting of bundles of identical periodically constricted tubes are not very accurate for calculating the permeability of most porous media. The physical reason for this is that in most porous media both types of spatial variations in pore size are present. In other words, (1) progressing through the medium inside any pore channel the fluid particle will pass through an alternating sequence of pores and pore throats, and (2) along certain pore channels the pore throats are bigger than along others. Therefore a realistic permeability model must incorporate both the serial type and the parallel type of spatial nonuniformities of the pore size. Such a model has been introduced by Dullien, [8]. The unit cell of the model, in one-dimension, is shown in Figure 47, where it is apparent that the model consists of periodically repeating tube sections of different kinds. Two of these are shown in Figure 47 made of tube segments of different diameters. Of special importance are the throats of diameter D_{e1} and D_{e2} in Figure 47.

For each subset of capillaries of the model, characterized by a certain range of throat diameters between D_e and $D_e + dD_e$, an expression analogous to (4.27) is obtained, giving the contribution to the total permeability k by those tubes controlled

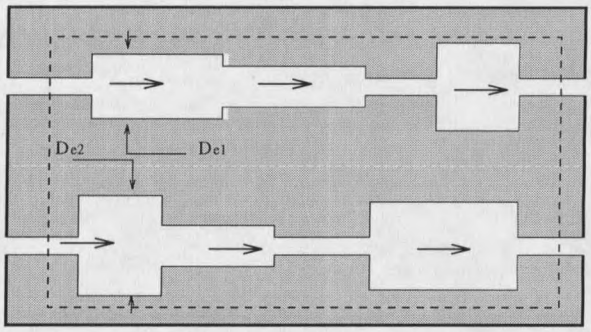

Figure 47: Illustration of the physical basis of the capillaric model of permeability expressed by (4.28) and (4.29)

by throat diameters lying in this range, that is,

$$k(D_e)dD_e = \frac{\phi(D_e)}{96} \frac{\left[\int_{D_e}^{\infty} \frac{\beta_{p,s}(D_e,D)}{D^2} dD\right]^2}{\int_{D_e}^{\infty} \frac{\beta_{p,s}(D_e,D)}{D^6} dD} dD_e \tag{4.28}$$

where $\beta_{p,s}(D_e, D)\ dD_e\ dD$ is the volume-based bivariate distribution of capillary diameters, giving the pore volume fractions consisting of pores in the diameter range D to $D + dD$, the passage through which is controlled by throats in the diameter range D_e to $D_e + dD_e$. Hence all the pores of different diameters D, characterized by the same different values of D_e, are in series. The pores characterized by different values of D_e, however, are in parallel. $\phi(D_e)dD_e$ is the contribution to the model porosity by capillaries characterized by throats in the diameter range D_e to $D_e + dD_e$.

The permeability k of this model is obtained, finally, by integrating (4.28) over all values of D_e. Which gives

$$k = \int_0^{\infty} k(D_e)dD_e. \tag{4.29}$$

A detailed description and derivation of this formula is given in [8].

Permeability in Bed of Identical Spheres Models

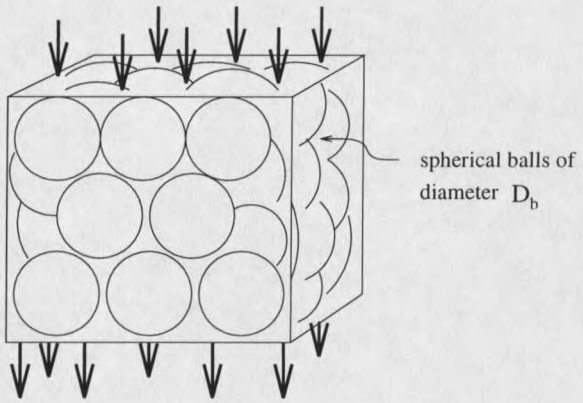

Figure 48: Bed of identical spherical balls modeling a porous medium

The relation between porosity, ϕ, and permeability, k, in a porous medium made of identical spherical balls of diameter D_b, as shown in Figure 48, is given by Brinkman's formula, [9]

$$k = \frac{D_b^2}{72}\left(3 + \frac{4}{1-\phi} - 3\left(\frac{8}{1-\phi} - 3\right)^{\frac{1}{2}}\right). \tag{4.30}$$

Lundgren, [17], later suggested that the effective viscosity of the fluid flowing through the media must be taken into account and he modified Brinkman's formula. The modified version of this formula is

$$k = \frac{D_b^2}{72M(\phi)}\left(3 + \frac{4}{1-\phi} - 3\left(\frac{8}{1-\phi} - 3\right)^{\frac{1}{2}}\right) \tag{4.31}$$

where $M(\phi)$ is the effective viscosity which may be given by the formula, [17]

$$M(\phi) = \frac{1}{1-\phi} \tag{4.32}$$

or the Einstein result

$$M(\phi) = (1 + 2.5\phi). \tag{4.33}$$

Another formula for $M(\phi)$ given by Lundgren, [17], is

$$M(\phi) = \frac{4\pi}{3}\frac{(\alpha R)^2}{(1-\phi)F((\alpha R)^2, \alpha R)} \tag{4.34}$$

Variables	Physical quantity	Units
k	permeability of the porous media	L^2
D_b	diameter of the balls	L
ϕ	porosity of the porous media	dimensionless
$M(\phi)$	effective viscosity	dimensionless
α	a parameter	L^{-1}
R	radius of the balls	L

Table 36: Variables and constants in the bed of spherical particles model

where R is the radius of the balls and αR is given by

$$\alpha R = \frac{3}{4} - \frac{3 - \left(\frac{8}{1-\phi} - 3\right)^{\frac{1}{2}}}{\left(\frac{1}{1-\phi} - \frac{3}{2}\right)}. \tag{4.35}$$

The function $F((\alpha R)^2, \alpha R)$ in (4.34) is a complicated expression involving Bessel functions and Legendre polynomials, [17]. All the variables used in this model are identified in Table 36.

Modelling Biofilm Accumulation in Porous Media

The mathematical model we are going to discuss here describes the growth of the biofilm, the corresponding changes in the porosity and permeability, and their effect on the flow through an artificial cylindrical porous medium described in the experiment below.

Experiment: Consider a cylinder both of whose ends are open. The middle part of the cylinder (l units in length) is filled with uniform sand such that the sand particles are immobile inside the cylinder. The cylinder is kept vertical as shown in Figure 49. A fluid of density $\rho_f(\mathbf{z}, t)$ flows through the cylindrical porous bed of length l. During the entire experiment, the height h of the fluid column above the bottom of the sand bed is constant. Further we assume that a constant thin layer of biofilm on the pore surface of the medium has been introduced and the fluid flowing through the medium

has nutrient for the bacteria. The bacteria will grow and will affect the porosity and the permeability and hence the flow of the fluid through the medium. Here we give a mathematical model that describes the change in the flow rate of the fluid in this experiment. Assume that:

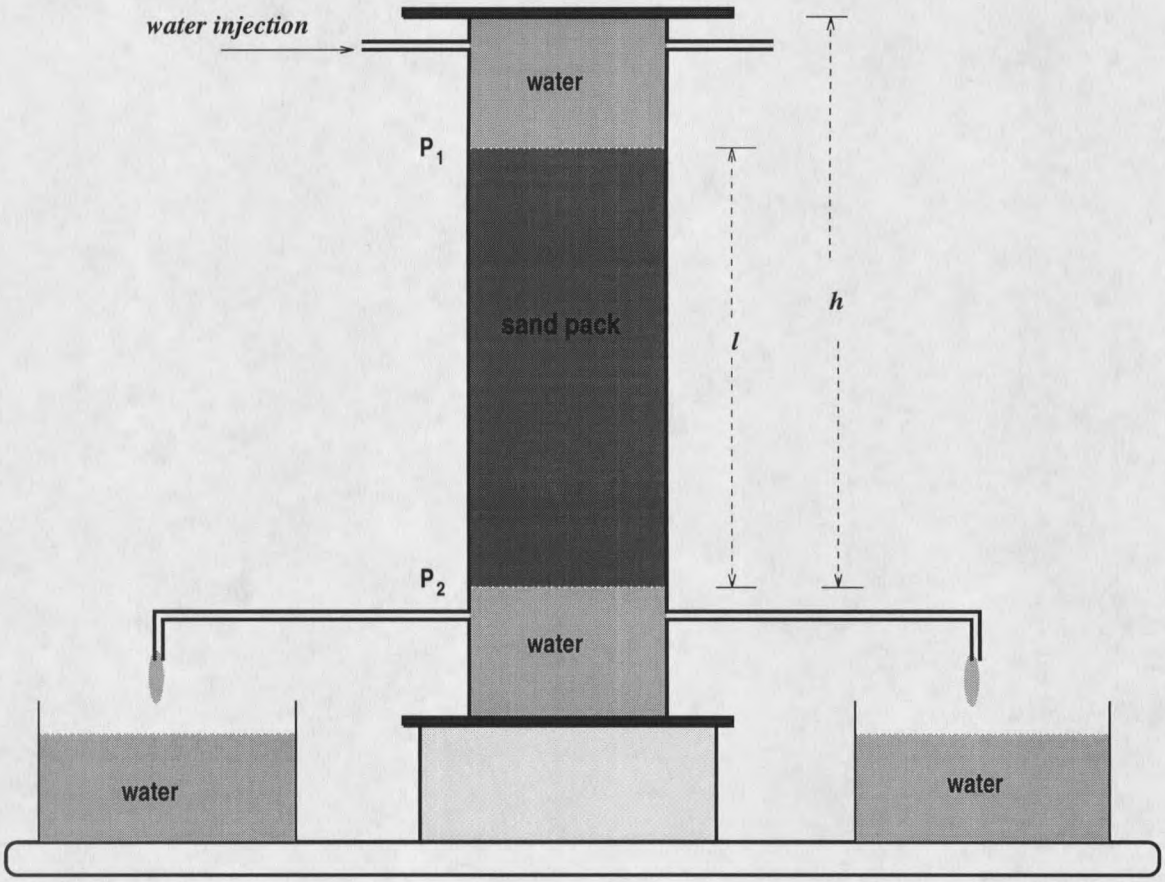

Figure 49: Biofilm growth in porous media and fluid flow

- The cylinder is kept vertical and the fluid is flowing only under the gravitational force.
- The medium, without biofilm in it, is homogeneous and the porosity is constant.
- After introducing the initial thin biofilm, the medium is still homogeneous and porosity is still constant (but different).

- The bacteria in the biofilm get the substrate from the bulk fluid flowing through the pores.

Biofilm Accumulation and Incompressible Fluid Flow

Based on both the model for incompressible fluid flow in porous media and the model for biofilm growth, here are the systems of model equations that describe the change in one-dimensional and two-dimensional flow of the incompressible fluid through the porous media as porosity and permeability of the media change. These changes are due to the biofilm growth that occurs.

Biofilm Accumulation and One-dimensional Incompressible Flow

The biofilm accumulation based on the zero-dimensional Biofilm Growth Model (BGM) is (see (2.122) - (2.126))

$$\frac{\partial}{\partial t}\Big(f(z,t)\Big) = -\frac{f(z,t)}{L(z,t)}\frac{\partial}{\partial t}\Big(L(z,t)\Big) + \left(\frac{YV_rS(z,t)}{(K+S(z,t))} - b + \frac{\delta(z,t)}{L(z,t)}\right) f(z,t), \quad (4.36)$$

$$\frac{\partial}{\partial t}\Big(L(z,t)\Big) = \frac{1}{1-\epsilon_l}\frac{YV_rL(z,t)S(z,t)f(z,t)}{K+S(z,t)} + \delta(z,t), \quad (4.37)$$

$$\begin{aligned}\frac{\partial}{\partial t}\Big(S(z,t)\Big) &= -\frac{S(z,t)}{L(z,t)}\frac{\partial}{\partial t}\Big(L(z,t)\Big) + \frac{D}{L_lL(z,t)}\Big(S_b(z,t)-S(z,t)\Big) \\ &\quad -\frac{V_rS(z,t)\ \rho\ f(z,t)}{K+S(z,t)},\end{aligned} \quad (4.38)$$

$$\frac{\partial}{\partial t}\Big(S_b(z,t)\Big) = \frac{1}{V_L(z,t)}\left(Q(z,t)(S_0-S_b(z,t)) - \frac{\sigma D}{L_l}(S_b(z,t)-S(z,t))\right), \quad (4.39)$$

and

$$\frac{\partial}{\partial t}\Big(V_L(z,t)\Big) = -\sigma\ \frac{\partial}{\partial t}\Big(L(z,t)\Big). \quad (4.40)$$

These terms are all identified in Tables 7 and 8 where it is noted that the variable z represents the vertical direction in Figure 44, (positive downward) and by using

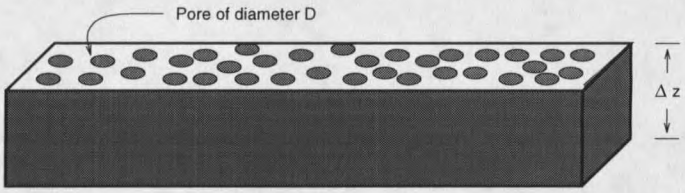

Figure 50: A sample porous medium of bulk volume V_{bulk} and height Δz with n, initially uniform, capillaries of diameter D_p

the zero-dimensional model there is no spatial dependence within the biofilm (no y dependence in Table 7).

The expression for porosity is [2], [9], [23]

$$\phi(z,t) = \frac{V_L(z,t)}{V_{bulk}} \tag{4.41}$$

where $V_L(z,t)$ is the pore volume and V_{bulk} is the bulk volume of the porous media (L^3).

If we assume that the sample porous media consists of n capillaries of uniform diameter $D_p(z,t)$ as in Figure 50, then, using (4.21), (4.41) can be written as

$$\phi(z,t) = \frac{n\pi(\frac{D_p(z,t)}{2})^2\Delta z}{V_{bulk}} \tag{4.42}$$

and the initial porosity $\phi(z,0)$ is given by,

$$\phi(z,0) = \frac{n\pi(\frac{D_p(z,0)}{2})^2\Delta z}{V_{bulk}}. \tag{4.43}$$

Dividing (4.42) by (4.43) and solving for $D_p(z,t)$ gives

$$D_p(z,t) = D_p(z,0)\sqrt{\frac{\phi(z,t)}{\phi(z,0)}}. \tag{4.44}$$

Using (4.25) the permeability can be calculated with the formula

$$k(z,t) = \phi(z,t)\frac{(D_p(z,t))^2}{96}. \tag{4.45}$$

If we assume that the porous media is a bed of identical spheres of initial diameter, $D_b(0,t)$, as shown in Figure 48, then the initial pore volume, $V_L(z,0)$ will be

$$V_L(z,0) = V_{bulk} - m\frac{4}{3}\pi\left(\frac{D_b(z,0)}{2}\right)^3 \tag{4.46}$$

where m is the number of balls in the bed. The initial porosity, $\phi(z,0)$, is given by,

$$\phi(z,0) = \frac{V_{bulk} - m\frac{4}{3}\pi\left(\frac{D_b(z,0)}{2}\right)^3}{V_{bulk}} \tag{4.47}$$

and the porosity of the medium after time t, $\phi(z,t)$, is given by

$$\phi(z,t) = \frac{V_{bulk} - m\frac{4}{3}\pi\left(\frac{D_b(z,t)}{2}\right)^3}{V_{bulk}} \tag{4.48}$$

where $D_b(z,t)$ is the diameter of the balls modeling the same porous media at time t. Dividing (4.47) by (4.48) yields

$$\frac{\phi(z,0)}{\phi(z,t)} = \frac{6V_{bulk} - m\pi(D_b(z,0))^3}{6V_{bulk} - m\pi(D_b(z,t))^3}. \tag{4.49}$$

Solving for $D_b(z,t)$ in (4.49) gives

$$D_b(z,t) = \left[\frac{6V_{bulk}}{m\pi}\left(1 - \frac{\phi(z,t)}{\phi(z,0)}\right) + \frac{\phi(z,t)}{\phi(z,0)}(D_b(z,0))^3\right]^{\frac{1}{3}} \tag{4.50}$$

Now, the permeability of the medium is given by (see (4.31) and (4.32))

$$k(z,t) = \frac{(D_b(z,t))^2(1-\phi(z,t))}{72}\left[3 + \frac{4}{1-\phi(z,t)} - 3\left(\frac{8}{1-\phi(z,t)} - 3\right)^{\frac{1}{2}}\right]. \tag{4.51}$$

The model equations governing the fluid velocity and the pressure distribution come from (4.6) and (4.7). These equations are

$$\frac{\partial}{\partial t}\Big(w(z,t)\Big) + w(z,t)\frac{\partial}{\partial z}\Big(w(z,t)\Big) + \frac{1}{\rho_f(z,t)\phi(z,t)}\frac{\partial}{\partial z}\Big(P(z,t)\Big) + \frac{g}{\phi(z,t)} = -\frac{\mu(z,t)}{k(z,t)\rho_f(z,t)}w(z,t) \tag{4.52}$$

and

$$\frac{\partial}{\partial t}\Big(\phi(z,t)\Big) + w(z,t)\frac{\partial}{\partial z}\Big(\phi(z,t)\Big) + \phi(z,t)\frac{\partial}{\partial z}\Big(w(z,t)\Big) = 0. \tag{4.53}$$

If we assume that the inertia has negligible effect on the flow, which means that $\frac{\partial}{\partial t}\Big(w(z,t)\Big) + w(z,t)\frac{\partial}{\partial z}\Big(w(z,t)\Big) = 0$, then (4.52) and (4.53) can be written in the form (see (4.11) and (4.14))

$$w(z,t) = -\frac{k(z,t)}{\mu(z,t)\phi(z,t)}\left(\frac{\partial}{\partial z}\Big(P(z,t)\Big) + \rho_f(z,t)g\right) \tag{4.54}$$

$$\begin{aligned}\frac{\partial^2}{\partial z^2}\Big(P(z,t)\Big) \;+\; & \frac{\frac{\partial}{\partial z}\Big(k(z,t)\Big)}{k(z,t)}\frac{\partial}{\partial z}\Big(P(z,t)\Big) \\ = \; & -\frac{1}{k(z,t)}\left(\phi(z,t)\omega(z,t)\frac{\partial}{\partial z}\Big(\mu(z,t)\Big) - \mu(z,t)\frac{\partial}{\partial t}\Big(\phi(z,t)\Big)\right) \\ & -\frac{\frac{\partial}{\partial z}\Big(k(z,t)\Big)}{k(z,t)}\rho_f(z,t)g - \frac{\partial}{\partial z}\Big(\rho_f(z,t)g\Big).\end{aligned} \tag{4.55}$$

Finally, if the horizontal cross-sectional area of the porous bed at a height z is $A(z,t)$, then the volumetric flow rate, $Q(z,t)$, can be computed by, [21],

$$Q(z,t) = \phi(z,t)A(z,t)w(z,t). \tag{4.56}$$

Biofilm Accumulation and Two-dimensional Incompressible Flow

The biofilm accumulation model based on the zero-dimensional BGM is (see (2.122) - (2.126))

$$\begin{aligned}\frac{\partial}{\partial t}\Big(f(x,z,t)\Big) \;=\; & -\frac{f(x,z,t)}{L(x,z,t)}\frac{\partial}{\partial t}\Big(L(x,z,t)\Big) \\ & +\left(\frac{YV_rS(x,z,t)}{(K+S(x,z,t))} - b + \frac{\delta(x,z,t)}{L(x,z,t)}\right)f(x,z,t),\end{aligned} \tag{4.57}$$

$$\frac{\partial}{\partial t}\Big(L(x,z,t)\Big) = \frac{1}{1-\epsilon_l}\frac{YV_rL(x,z,t)S(x,z,t)f(x,z,t)}{K+S(x,z,t)} + \delta(x,z,t), \tag{4.58}$$

$$\begin{aligned}\frac{\partial}{\partial t}\Big(S(x,z,t)\Big) \;=\; & -\frac{S(x,z,t)}{L(x,z,t)}\frac{\partial}{\partial t}\Big(L(x,z,t)\Big) + \frac{D}{L_lL(x,z,t)}\Big(S_b(x,z,t) - S(x,z,t)\Big) \\ & -\frac{V_rS(x,z,t)\;\rho\; f(x,z,t)}{K+S(x,z,t)},\end{aligned} \tag{4.59}$$

$$\frac{\partial}{\partial t}\Big(S_b(x,z,t)\Big) = \frac{1}{V_L(x,z,t)}\Big(Q(x,z,t)(S_0 - S_b(x,z,t)) - \frac{\sigma D}{L_l}(S_b(x,z,t) - S(x,z,t))\Big), \tag{4.60}$$

and

$$\frac{\partial}{\partial t}\Big(V_L(x,z,t)\Big) = -\sigma\,\frac{\partial}{\partial t}\Big(L(x,z,t)\Big). \tag{4.61}$$

Here the variables x and z represent the two dimensions in the porous media sample. The porosity, $\phi(x,z,t)$ can be calculated by the two-dimensional version of (4.41) given by

$$\phi(x,z,t) = \frac{V_L(x,z,t)}{V_{bulk}}. \tag{4.62}$$

If a bundle of identical capillaries is used to model the porous media then the diameter, $D(x,z,t)$ of the pores will be given by the two-dimensional version of (4.44) which is

$$D(x,z,t) = D(x,z,0)\sqrt{\frac{\phi(x,z,t)}{\phi(x,z,0)}}. \tag{4.63}$$

Using (4.25) the permeability can be calculated with the formula (see (4.45))

$$k(x,z,t) = \phi(x,z,t)\frac{(D(x,z,t))^2}{96}. \tag{4.64}$$

If a bed of identical spheres is used to model the porous media then the diameter $D_b(x,z,t)$ of the balls will be calculated by the two-dimensional version of (4.50) given by

$$D_b(x,z,t) = \left[\frac{6V_{bulk}}{m\pi}\left(1 - \frac{\phi(x,z,t)}{\phi(x,z,0)}\right) + \frac{\phi(x,z,t)}{\phi(x,z,0)}(D_b(x,z,0))^3\right]^{\frac{1}{3}} \tag{4.65}$$

and the permeability of the medium is given by the two-dimensional version of (4.51)

$$k(x,z,t) = \frac{(D_b(x,z,t))^2(1-\phi(x,z,t))}{72}\left[3 + \frac{4}{1-\phi(x,z,t)} - 3\left(\frac{8}{1-\phi(x,z,t)} - 3\right)^{\frac{1}{2}}\right]. \tag{4.66}$$

The model equations governing the fluid velocity and the pressure distribution come from (4.8), (4.9), and (4.10). These equations are

$$\frac{\partial}{\partial t}\Big(u(x,z,t)\Big)+\Big(u(x,z,t)\frac{\partial}{\partial x}\Big(u(x,z,t)\Big)+w(x,z,t)\frac{\partial}{\partial z}\Big(u(x,z,t)\Big)\Big)$$
$$+\frac{1}{\rho_f(x,z,t)\phi(x,z,t)}\frac{\partial}{\partial x}\Big(P(x,z,t)\Big)=-\frac{\mu(x,z,t)}{k(x,z,t)\rho_f(x,z,t)}u(x,z,t), \quad (4.67)$$

$$\frac{\partial}{\partial t}\Big(w(x,z,t)\Big)+\Big(u(x,z,t)\frac{\partial}{\partial x}\Big(w(x,z,t)\Big)+w(x,z,t)\frac{\partial}{\partial z}\Big(w(x,z,t)\Big)\Big)$$
$$+\frac{1}{\rho_f(x,z,t)\phi(x,z,t)}\frac{\partial}{\partial z}\Big(P(x,z,t)\Big)+\frac{g}{\phi(x,z,t)}$$
$$=-\frac{\mu(x,z,t)}{k(x,z,t)\rho_f(x,z,t)}w(x,z,t), \quad (4.68)$$

and

$$\frac{\partial}{\partial t}\Big(\phi(x,z,t)\Big)+u(x,z,t)\frac{\partial}{\partial x}\Big(\phi(x,z,t)\Big)+w(x,z,t)\frac{\partial}{\partial z}\Big(\phi(x,z,t)\Big)$$
$$+\phi(x,z,t)\frac{\partial}{\partial x}\Big(u(x,z,t)\Big)+\phi(x,z,t)\frac{\partial}{\partial z}\Big(w(x,z,t)\Big)=0. \quad (4.69)$$

Again if we assume that the inertia has negligible effect on the flow the first three terms of (4.67) and (4.68) become zero. Now (4.67), (4.68), and (4.69) can be written in the form (see (4.11) and (4.14))

$$u(x,z,t)=-\frac{k(x,z,t)}{\mu(x,z,t)\phi(x,z,t)}\frac{\partial}{\partial x}\Big(P(x,z,t)\Big), \quad (4.70)$$

$$w(x,z,t)=-\frac{k(x,z,t)}{\mu(x,z,t)\phi(x,z,t)}\left(\frac{\partial}{\partial z}\Big(P(x,z,t)\Big)+\rho_f(x,z,t)g\right), \quad (4.71)$$

and

$$\frac{\partial^2}{\partial x^2}\Big(P(x,z,t)\Big)+\frac{\partial^2}{\partial z^2}\Big(P(x,z,t)\Big)+\frac{\frac{\partial}{\partial x}\Big(k(x,z,t)\Big)}{k(x,z,t)}\frac{\partial}{\partial x}\Big(P(x,z,t)\Big)$$
$$+\quad\frac{\frac{\partial}{\partial z}\Big(k(x,z,t)\Big)}{k(x,z,t)}\frac{\partial}{\partial z}\Big(P(x,z,t)\Big)$$
$$=\quad\frac{1}{k(x,z,t)}\Big(\phi(x,z,t)u(x,z,t)\frac{\partial}{\partial x}\Big(\mu(x,z,t)\Big)$$

$$+ \phi(x,z,t)w(x,z,t)\frac{\partial}{\partial z}\Big(\mu(x,z,t)\Big) - \mu(x,z,t)\frac{\partial}{\partial t}\Big(\phi(x,z,t)\Big)\Big)$$
$$-\frac{\frac{\partial}{\partial z}\Big(k(x,z,t)\Big)}{k(x,z,t)}\rho_f(x,z,t)g. \tag{4.72}$$

Finally, if the horizontal cross-sectional area of the porous bed at a height z is $A(z,t)$, then the volumetric flow rate, $Q(x,z,t)$, can be computed by, [21],

$$Q(x,z,t) = \phi(x,z,t)A(z,t)w(x,z,t). \tag{4.73}$$

CHAPTER 5

Numerical Results

Introduction

The complete mathematical model describing biofilm growth in a homogeneous porous medium and the incompressible fluid flow through that porous medium is recorded in the next section and then is numerically solved. The numerical results for a short bed (5 cm long) of spherical balls is first presented and then compared with the experimental data, [5], [6], in the third section. In a short bed of spherical balls, the flow rate is high and the bacteria at each height receive sufficient substrate which causes a constant growth of biofilm throughout the length of the bed. Thus the one-dimensional results in the short bed show no variation along the length of the bed. However, in a longer bed of spherical balls, the flow rate is comparatively low which provides less substrate at the lower end of the bed. These numerical results of the simulation in a longer bed (60 cm long) are presented in the fourth section. A difference of 1.9 μm (.0000019 m) in the steady state biofilm thickness near the top and the bottom of the bed was predicted, however the lack of experimental data precludes the possibility of verification.

Biofilm Growth in a Porous Medium

The mathematical model for biofilm accumulation in a porous medium of length l and cross-sectional area $A(z,t) = A$ consists of three parts: (i) a system

of partial differential equations modeling biofilm growth, (*ii*) a system of partial differential equations describing the hydrodynamic flow through a porous medium, and (*iii*) a system of intermediate equations combining (coupling) systems (*i*) and (*ii*). It is assumed that the density and the viscosity of the liquid flowing through the porous bed are constant ($\rho_f(z,t) \equiv \rho_f$, $\mu(z,t) \equiv \mu$) and that inertial effects are negligible ($\frac{D\omega(z,t)}{Dt} = 0$). If the porous media is assumed to be a bundle of capillaries then the model equations we solve are (see (4.36) - (4.56) and the detachment rate given in (3.11))

$$\frac{\partial}{\partial t}\Big(f(z,t)\Big) = -\frac{f(z,t)}{L(z,t)}\frac{\partial}{\partial t}\Big(L(z,t)\Big) + \left(\frac{YV_rS(z,t)}{(K+S(z,t))} - b + \frac{\delta(z,t)}{L(z,t)}\right) f(z,t), \quad (5.1)$$

$$\frac{\partial}{\partial t}\Big(L(z,t)\Big) = \frac{1}{1-\epsilon_l}\frac{YV_rL(z,t)S(z,t)f(z,t)}{K+S(z,t)} + \delta(z,t), \quad (5.2)$$

$$\begin{aligned}\frac{\partial}{\partial t}\Big(S(z,t)\Big) &= -\frac{S(z,t)}{L(z,t)}\frac{\partial}{\partial t}\Big(L(z,t)\Big) + \frac{D}{L_lL(z,t)}\Big(S_b(z,t) - S(z,t)\Big) \\ &\quad -\frac{V_rS(z,t)\ \rho\ f(z,t)}{K+S(z,t)},\end{aligned} \quad (5.3)$$

$$\frac{\partial}{\partial t}\Big(S_b(z,t)\Big) = \frac{1}{V_L(z,t)}\left(Q(z,t)(S_0 - S_b(z,t)) - \frac{\sigma D}{L_l}(S_b(z,t) - S(z,t))\right), \quad (5.4)$$

$$\frac{\partial}{\partial t}\Big(V_L(z,t)\Big) = -\sigma\ \frac{\partial}{\partial t}\Big(L(z,t)\Big), \quad (5.5)$$

$$\delta(z,t) = -\lambda(L(z,t))^2, \quad (5.6)$$

$$\phi(z,t) = \frac{V_L(z,t)}{V_{bulk}}, \quad (5.7)$$

$$D_p(z,t) = D_p(z,0)\sqrt{\frac{\phi(z,t)}{\phi(z,0)}}, \tag{5.8}$$

$$k(z,t) = \phi(z,t)\frac{(D_p(z,t))^2}{96}, \tag{5.9}$$

$$w(z,t) = -\frac{k(z,t)}{\mu\phi(z,t)}\left(\frac{\partial}{\partial z}\Big(P(z,t)\Big) + \rho_f g\right), \tag{5.10}$$

$$\begin{aligned}&\frac{\partial^2}{\partial z^2}\Big(P(z,t)\Big) + \frac{1}{k(z,t)}\frac{\partial}{\partial z}\Big(k(z,t)\Big)\frac{\partial}{\partial z}\Big(P(z,t)\Big)\\ &= \frac{\mu}{k(z,t)}\frac{\partial}{\partial t}\Big(\phi(z,t)\Big) - \frac{\rho_f g}{k(z,t)}\frac{\partial}{\partial z}\Big(k(z,t)\Big),\end{aligned} \tag{5.11}$$

and

$$Q(z,t) = \phi(z,t)A(z,t)w(z,t) \tag{5.12}$$

with the boundary conditions

$$P(0,t) \equiv P_1,\ P(l,t) \equiv P_2,\ k(0,t) \equiv k_1,\ \text{and } k(l,t) \equiv k_2 \quad \forall t. \tag{5.13}$$

In this model, (5.1) - (5.6) are the zero-dimensional Biofilm Growth Model (BGM) equations, (5.10) - (5.13) are the porous media flow equations and (5.7) - (5.9) are the coupling equations. If we assume that the porous media is a bed of identical spheres then (5.8) and (5.9) in this system are replaced with

$$D_b(z,t) = \left[\frac{6V_{bulk}}{m\pi}\left(1 - \frac{\phi(z,t)}{\phi(z,0)}\right) + \frac{\phi(z,t)}{\phi(z,0)}(D_b(z,0))^3\right]^{\frac{1}{3}} \tag{5.14}$$

and

$$k(z,t) = \frac{(D_b(z,t))^2(1-\phi(z,t))}{72}\left[3 + \frac{4}{1-\phi(z,t)} - 3\left(\frac{8}{1-\phi(z,t)} - 3\right)^{\frac{1}{2}}\right]. \tag{5.15}$$

All the variables and constants used in this model are identified in Table 37 and Table 38, respectively. The model equations are solved numerically for the unknown variables given in Table 37 using the following algorithm.

Variables	Physical quantity	Units
$L(z,t)$	biofilm thickness	L
$V_L(z,t)$	volume of the bulk liquid-pore volume	L^3
$S_b(z,t)$	bulk substrate concentration	$M_s L^{-3}$
$S(z,t)$	substrate concentration in the biofilm	$M_s L^{-3}$
$f(z,t)$	volume fraction of active biomass in the biofilm	dimensionless
$w(z,t)$	velocity of the fluid particle	LT^{-1}
$Q(z,t)$	volumetric flow rate	L^3T^{-1}
$P(z,t)$	pressure	$ML^{-1}T^{-2}$
$\phi(z,t)$	porosity	dimensionless
$k(z,t)$	permeability	L^2

Table 37: Unknown dependent variables and their fundamental units in the one-dimensional incompressible fluid flow model with biofilm growth

Parameters	Physical quantity	Units
S_0	substrate concentration in the influent fluid	$M_s L^{-3}$
D	diffusivity coefficient of the substrate through the laminar diffusional sublayer	L^2T^{-1}
$D_p(z,t)$	diameter of the capillary tube	L
$D_b(z,t)$	diameter of the spherical ball	L
$A(z,t)$	horizontal cross-sectional area of the porous bed	L^2
L_l	thickness of laminar diffusional sublayer	L
V_r	maximum specific growth rate	$M_s M_x^{-1} T^{-1}$
K	Monod constant	$M_s L^{-3}$
ρ	biomass density	$M_x L^{-3}$
ρ_f	density of the fluid	ML^{-3}
μ	viscosity of the fluid	$ML^{-1}T^{-1}$
σ	area of the pore surface	L^2
ϵ_l	volume fraction of liquid in the biofilm	dimensionless
b	inactivation coefficient	T^{-1}
Y	yield coefficient	$M_x M_s^{-1}$
λ	detachment coefficient	$L^{-1}T^{-1}$
V_{bulk}	total volume of the porous medium	L^3
m	number of 1 mm spheres in the porous bed	dimensionless
g	gravitational acceleration	LT^{-2}
$\delta(z,t)$	detachment function	LT^{-1}

Table 38: Parameters and their fundamental units used in the one-dimensional incompressible porous media flow model with biofilm growth

Algorithm

The following steps have been taken to approximate the solution of these equations.

1. Divide the vertical domain into n equal subintervals of length $\Delta z = \frac{l}{n} (= 0.01)$.

2. At each interior spatial grid point $z_1, \cdots, z_{n-1}$, (5.1) - (5.6) are solved using the MATLAB package 'ODE23s' for a small time step Δt (= 0.01 day).

3. Using the new pore volume, $V_L(z, t + \Delta t)$, from step 2, at each interior spatial grid point $z_1, \cdots, z_{n-1}$, the new porosity, $\phi(z, t + \Delta t)$, is computed using (5.7) and the new permeability, $k(z, t + \Delta t)$, is computed using (5.8) and (5.9) (if the porous media is assumed to be a bundle of capillary tubes) or (5.14) and (5.15) (if the porous media is assumed to be a bed of identical spheres).

4. Using $\phi(z, t + \Delta t)$ and $k(z, t + \Delta t)$, (5.10), (5.11), and (5.13) are solved at each interior point $z_1, \cdots, z_{n-1}$ for the new pressure distribution, $P(z, t + \Delta t)$, and the new velocity, $w(z, t + \Delta t)$.

5. The new volumetric flow rate, $Q(z, t + \Delta t)$, is then computed at each interior spatial grid point $z_1, \cdots, z_{n-1}$ using (5.12).

Steps one through five are repeated for each time step. A computer code which solves this system is given in Appendix G.

Biofilm Growth in a Short Bed

The numerical results begin with a discussion concerning the validation of the relation between porosity and permeability for a short bed which is 5 cm long. We check the appropriateness of the relations between $k(z, t)$ and $\phi(z, t)$ given by (5.9) (for the bundle of capillary tubes) and (5.15) (for a bed of identical spheres). The

specific values for the parameters and the initial and boundary conditions for the variables are given in Table 39. All simulations are run for a porous media bed of length $l = 5$ cm made up of identical spheres so only $D_b(z,t)$ is specified ($D_p(z,t)$ is not needed).

Validation of the Relation between Porosity and Permeability

The validity of the relations between porosity, $\phi(z,t)$, and permeability, $k(z,t)$, given by (5.9) and (5.15) has been checked in this subsection. Taken from [6], the graphs of experimental normalized porosity data, $\hat{\phi}_e(z,t)$ $(\hat{\phi}_e(z,t) = \frac{\phi_e(z,t)}{\phi_e(z,0)})$ and the corresponding normalized permeability data, $\hat{k}_e(z,t)$, $(\hat{k}_e(z,t) = \frac{k_e(z,t)}{k_e(z,0)})$, both over an eight day time period, are displayed in Figure 51. This experiment involved only a bed of identical spheres. The computed normalized permeability in a bundle of capillary tubes (dashed line) and in a bed of identical spheres (dash-dot line), corresponding to the experimental porosity, are denoted by $\hat{k}_1(z,t)$ and $\hat{k}_2(z,t)$ are compared with experimental normalized permeability, $\hat{k}_e(z,t)$, in Figure 52. $\hat{k}_1(z,t)$ is computed using (5.9) while $\hat{k}_2(z,t)$ is computed using (5.15) and in each case $\phi_e(z,t)$ is used. The numerical values of these variables are given in Table 40. The computed normalized permeability for the bed of identical spheres is quantitatively and qualitatively closer to the experimental normalized permeability than the computed normalized permeability for the bundle of capillaries. This is due to the fact that the porous medium used in all the experiments in [6] is a bed of identical spheres of diameter 1 mm. This validates the use of (5.15) to compute the permeability in the next two subsections. Had experimental data been gathered for a bundle of capillary tubes, one would expect the experimental permeability to be closer to the permeability computed by (5.9).

Parameters	Values	Units
K	0.0001	mg/cm^3
V_r	4.7	mg/(mg day)
Y	.2	mg/mg
b	.35	day^{-1}
D	1.3	cm^2 /day
σ	8.25	cm^2
A	1	cm^2
L_l	.8	cm
ϵ_l	.8	dimensionless
ρ	12.2	mg /cm^3
μ	1.0	mg/(cm day)
S_0	.02	mg /cm^3
λ	800	cm^{-1}day^{-1}
ρ_f	1.1	mg/cm^3
V_{bulk}	5.0	cm^3
m	5252	dimensionless
g	981	cm/sec^2
Variables	Values	Units
$S_b(z,0)\ \ \forall z$	.04	mg /cm^3
$L(z,0)\ \ \forall z$	.00005	cm
$S(z,0)\ \ \forall z$	.00004	mg /cm^3
$f(z,0)\ \ \forall z$	.15	dimensionless
$V_L(z,0)\ \ \forall z$	2.25	cm^3
$D_b(z,0)\ \ \forall z$	.1	cm
$w(z,0)\ \ \forall z$	.1667	cm/sec
$Q(z,0)\ \ \forall z$	.075	cm^3/sec
$\phi(z,0)\ \ \forall z$	.45	dimensionless
$k(z,0)\ \ \forall z$	.000275	cm^2
$P(z,0)\ \ \forall z$	3.0	mg/(cm sec^2)
$k_1 \equiv k(0,t)\ \ \forall t$	.000275	cm^2
$k_2 \equiv k(l,t)\ \ \forall t$	.000275	cm^2
$P_1 \equiv P(0,t)\ \ \forall t$	2.5	mg/(cm sec^2)
$P_2 \equiv P(l,t)\ \ \forall t$	5.0	mg/(cm sec^2)

Table 39: The values of the parameters and the initial and boundary values of the unknown dependent variables used in the one-dimensional incompressible porous media flow model (short bed model) with biofilm growth and their units

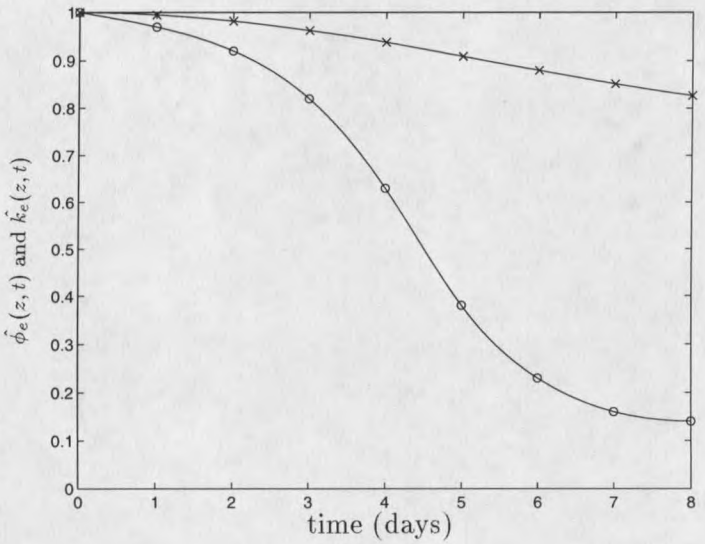

Figure 51: Experimental normalized permeability, $\hat{k}_e(z,t)$ and porosity, $\hat{\phi}_e(z,t)$, from Cunningham's experimental model, [6]. Porosity is represented by 'x' and the corresponding permeability is represented by 'o'. The solid lines passing through the data points are cubic splines through the data points.

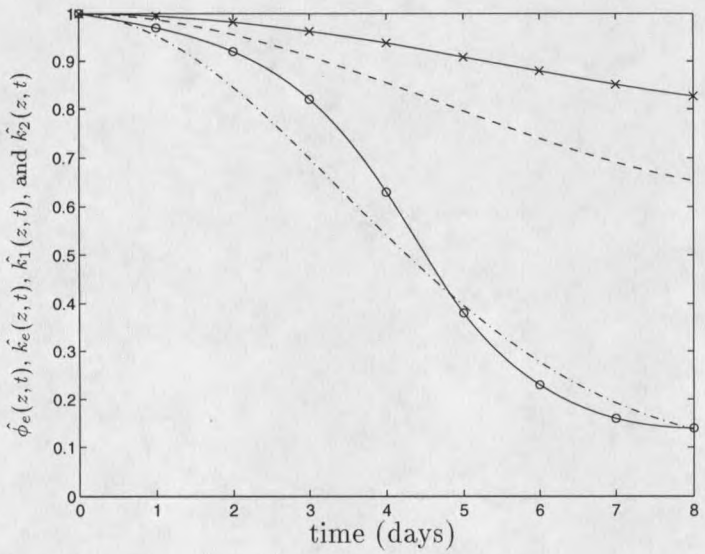

Figure 52: Experimental normalized permeability, $\hat{k}_e(z,t)$, (o) and porosity, $\hat{\phi}_e(z,t)$, (x) from Cunningham's experimental model, [6]. The computed normalized permeability, $\hat{k}_1(z,t)$, in a bundle of capillary tubes (dashed line) and the computed normalized permeability, $\hat{k}_2(z,t)$, in a bed of spheres (dash-dot line) are shown.

t(days)	$\hat{\phi}_e(z,t)$	$\hat{k}_e(z,t)$	$\hat{k}_1(z,t)$	$\hat{k}_2(z,t)$
0.0	1.00000000	1.00000000	1.00000000	1.00000000
1.0	0.99334290	0.96468116	0.98368533	0.94114069
2.0	0.98349468	0.92632674	0.95959411	0.85758126
3.0	0.96162713	0.81322249	0.90768529	0.69106693
4.0	0.93281434	0.58241123	0.84385187	0.51144611
5.0	0.90983853	0.39038718	0.79904581	0.40179484
6.0	0.87667112	0.22069692	0.73484730	0.26809669
7.0	0.85531404	0.16652762	0.69728218	0.20255801
8.0	0.82667503	0.14000000	0.65307503	0.13734191

Table 40: Comparison of the normalized experimental permeability, $\hat{k}_e(z,t)$, the computed normalized permeabilities $\hat{k}_1(z,t)$ (using capillaric model) and $\hat{k}_2(z,t)$ (using the bed of spherical balls model) for the experimental porosity data from Cunningham's experimental model, [6].

Presentation of Numerical Results

The model equations for a bed of spheres are solved numerically for the variables given in Table 38. The values of the parameters and initial values of the unknown variables are given in Table 39. The change in each variable is discussed separately.

Substrate Concentration in the Bulk Liquid It has been assumed that the porous medium is initially saturated with a liquid of substrate concentration, $S_b(z,0) = .04$ mg/cm^3. As the experiment begins, a liquid of constant substrate concentration $S_0 = .02$ mg/cm^3 is made to flow through the porous medium under a constant piezometric head gradient of 2.5 mg/(cm sec^2). As the flow begins, the bulk liquid in the pores gets replaced by influent liquid and hence the substrate concentration in the bulk liquid drops very quickly (within .1 days) to .02 mg/cm^3. This can be seen in Figure 53. The consumption of the substrate in the biofilm causes a concentration gradient across the film-liquid interface and the substrate diffuses from the region of high concentration (bulk liquid in the pore channels) to the region of low

concentration (biofilm on the spheres). The substrate concentration in the bulk liquid slowly begins to decrease and after 14 days it reaches a steady state value of .015974 mg/cm^3, which can be seen in Figure 54. The numerical values are given in Table 41.

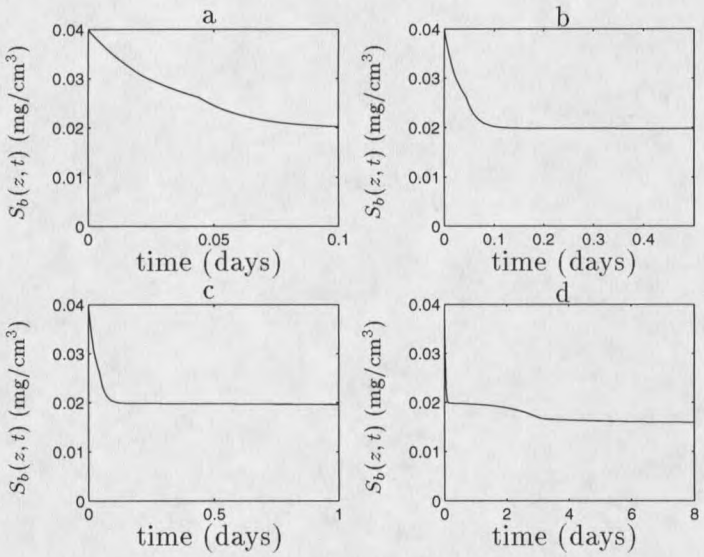

Figure 53: Substrate concentration, $S_b(z,t)$, in the bulk liquid in the pore channels over .1 days (a), .5 days (b), 1 day (c), and 8 days (d)

Substrate Concentration in the Biofilm Initially, when the concentration difference across the film-liquid interface is very high, the substrate concentration in the biofilm on the spheres, $S(z,t)$, increases very rapidly (within .01 days) from its initial value .00004 mg/cm^3 to .038985 mg/cm^3. Soon after that, as the substrate concentration in the bulk liquid in the pore channels decreases, $S(z,t)$ also decreases. After 2 days, when the biofilm thickness becomes significant, the substrate in the biofilm on the spheres gets consumed faster than it diffuses from the bulk liquid. Hence we observe a rapid decrease in $S(z,t)$. These early profiles can be seen in Figure 55. Figure 56 and Table 42 show that after 14 days $S(z,t)$ reaches a steady state value of .000053 mg/cm^3. The numerical values of $S(z,t)$ over 20 days are displayed in Table

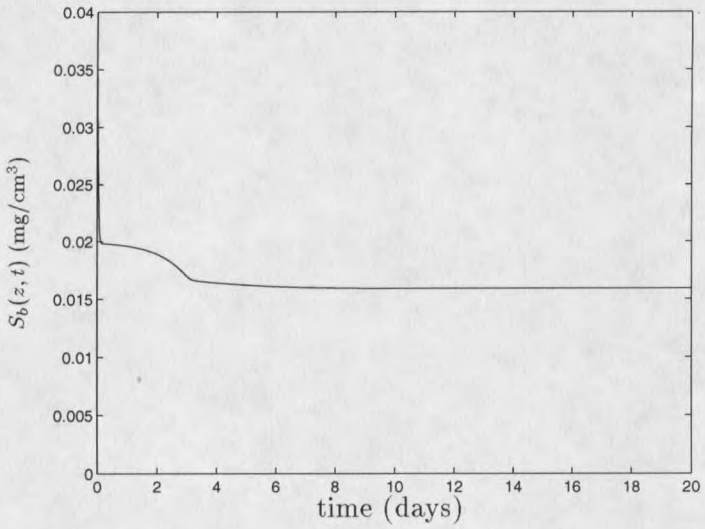

Figure 54: Substrate concentration, $S_b(z,t)$, in the bulk liquid in the pore channels over 20 days

t (days)	$S_b(z,t)$ (mg/cm^3)	t (days)	$S_b(z,t)$ (mg/cm^3)	t (days)	$S_b(z,t)$ (mg/cm^3)
0.00	0.04000000	0.00	0.04000000	0.00	0.04000000
0.01	0.03271481	0.10	0.02033862	2.00	0.01902326
0.02	0.03025999	0.20	0.01992567	4.00	0.01647789
0.03	0.02803103	0.30	0.01989961	6.00	0.01614456
0.04	0.02628012	0.40	0.01988507	8.00	0.01601429
0.05	0.02455989	0.50	0.01985697	10.00	0.01598213
0.06	0.02259885	0.60	0.01984391	12.00	0.01597554
0.07	0.02182027	0.70	0.01981015	14.00	0.01597434
0.08	0.02102188	0.80	0.01977265	16.00	0.01597416
0.09	0.02063480	0.90	0.01972946	18.00	0.01597415
0.10	0.02033862	1.00	0.01968148	20.00	0.01597415

Table 41: Substrate concentration, $S_b(z,t)$, of the bulk liquid flowing through the pore channels of the porous medium over 20 days

42 and the profiles of the substrate concentration in the biofilm on the spheres are given in Figure 55 and Figure 56.

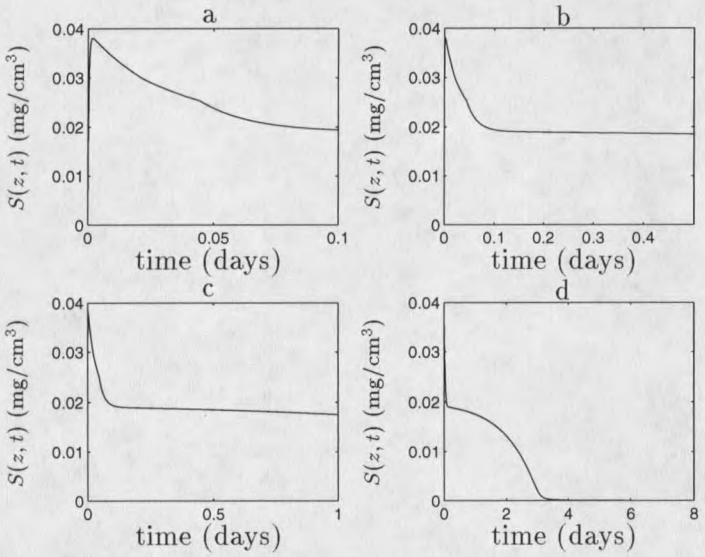

Figure 55: Substrate concentration, $S(z,t)$, in the biofilm over (a) .1 days, (b) .5 days, (c) 1 day, and (d) 8 days

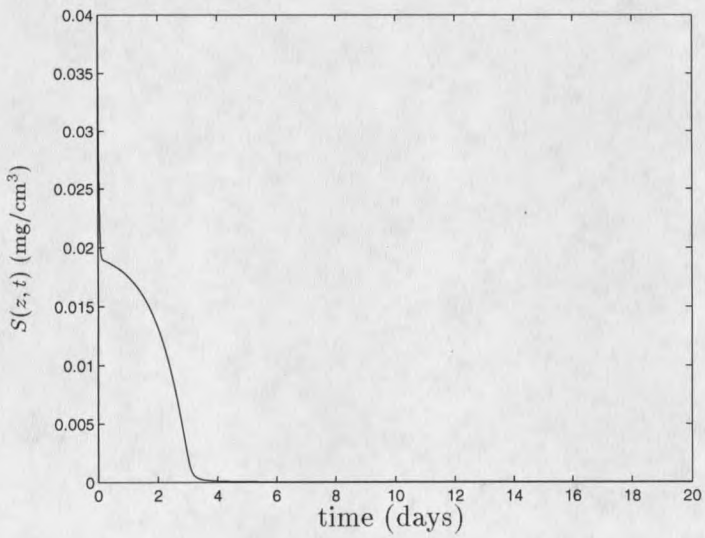

Figure 56: Substrate concentration, $S(z,t)$, in the biofilm on the spheres over 20 days

t (days)	$S(z,t)$ (mg/cm^3)	t (days)	$S(z,t))$ (mg/cm^3)	t (days)	$S(z,t)$ (mg/cm^3)
0.0000	0.00004000	0.00	0.00004000	0.00	0.00004000
0.0010	0.02359247	0.10	0.01978974	2.00	0.01377079
0.0100	0.03898468	0.20	0.01937522	4.00	0.00012536
0.0250	0.03357184	0.30	0.01922501	6.00	0.00005692
0.0400	0.02924032	0.40	0.01914167	8.00	0.00005563
0.0500	0.02604190	0.50	0.01896587	10.00	0.00005449
0.0600	0.02295709	0.60	0.01876704	12.00	0.00005365
0.0700	0.02125185	0.70	0.01866066	14.00	0.00005342
0.0800	0.02021093	0.80	0.01842466	16.00	0.00005320
0.0900	0.01989405	0.90	0.01815312	18.00	0.00005309
0.1000	0.01978974	1.00	0.01785199	20.00	0.00005309

Table 42: Substrate concentration, $S(z,t)$, in the porous media biofilm on the spheres over 20 days

Volume Fraction of Active and Inactive Biomass It has been assumed that 80% of the biofilm is liquid ($\epsilon_l = .8$). The active and inactive biomass volume fraction sum to the remaining 20% of the total biomass. Initially, when the biofilm on the spheres is thin, the substrate rapidly diffuses into the biofilm hence the substrate concentration in the biofilm rises. In the presence of high substrate concentration, the active bacteria multiply faster than they inactivate, hence the volume fraction of active bacteria increases and the volume fraction of inactive bacteria decreases (see Figure 57 and Table 43). After 3.2 days, when the substrate concentration in the biofilm is relatively low, the growth rate of active bacteria becomes less than the inactivation rate causing a decrease in the volume fraction of active bacteria. Figure 58 and Table 43 show that after 18 days the volume fractions of active and inactive bacteria reach a steady state. The active biomass volume fraction stabilizes at 0.117711 and the inactive biomass volume fraction stabilizes at .082289. The numerical values of active and inactive biomass over 20 days are given in Table 43 and the graphs are displayed in Figures 57 and 58.

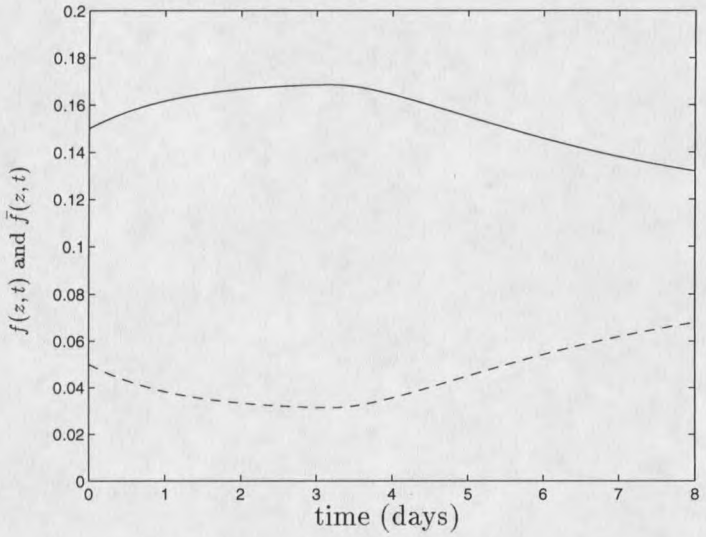

Figure 57: Active biomass volume fraction, $f(z,t)$, (solid line) and inactive biomass volume fraction, $\bar{f}(z,t)$, (dashed line) over 8 days

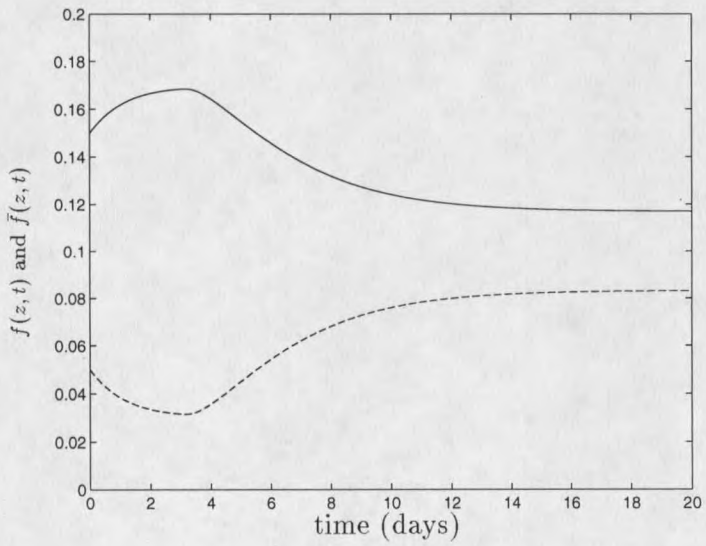

Figure 58: Active biomass volume fraction, $f(z,t)$, (solid line) and inactive biomass volume fraction, $\bar{f}(z,t)$, (dashed line) over 20 days

t(days)	$f(z,t)$	$\bar{f}(z,t)$
0.0	0.15000000	0.05000000
2.0	0.16728567	0.03271433
4.0	0.16545739	0.03454261
6.0	0.14681440	0.05318560
8.0	0.13275812	0.06724188
10.0	0.12477587	0.07522413
12.0	0.12079200	0.07920800
14.0	0.11892714	0.08107286
16.0	0.11808551	0.08191449
18.0	0.11771134	0.08228866
20.0	0.11771134	0.08228866

Table 43: Active biomass volume fraction, $f(z,t)$, and inactive biomass volume fraction, $\bar{f}(z,t)$, over 20 days

Biofilm Thickness The graphs of average biofilm thickness on the spheres, $L(z,t)$, over 8 days and 20 days are given in Figure 59 and Figure 60, respectively. Also, the numerical values of $L(z,t)$ over 20 days are displayed in Table 44. The average biofilm thickness initially increases slowly but after 2 days the growth rate becomes higher which causes a rapid decrease in the substrate concentration in the biofilm. After 6 days, when the substrate concentration becomes relatively small, the growth rate of the biofilm on the spheres slowly decreases and after 16 days the average biofilm thickness reaches its steady state value of 37.6 μm (.003760 cm).

Pore Volume Because of the biofilm accumulation on the spheres, the average pore volume, $V_L(z,t)$, decreases. This is shown in Figure 61 and Figure 62. Initially (for 2 days) the average pore volume decreases very slowly but as the biofilm thickness on the spheres increases, the decay in the average pore volume is more rapid. The graphs of $V_L(z,t)$ over 8 days and 20 days are given in Figure 61 and Figure 62, respectively, and the numerical values are displayed in Table 45. The average pore volume reaches a steady state at 1.919 cm^3 after 14 days.

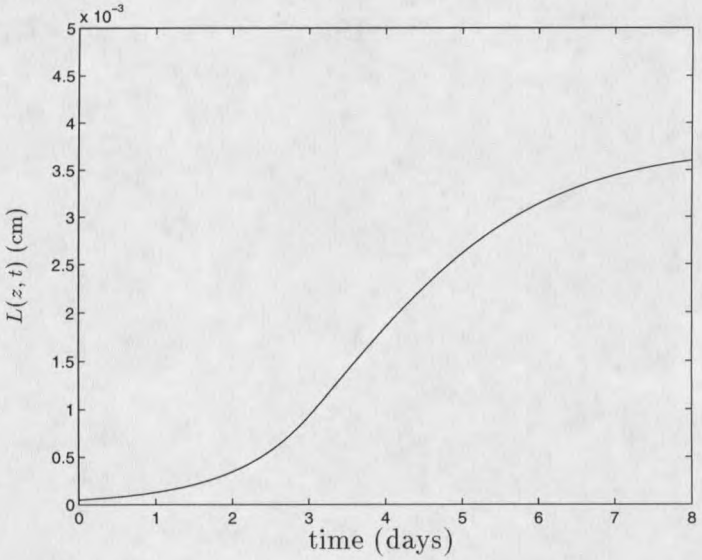

Figure 59: Average biofilm thickness on the spheres, $L(z,t)$, over 8 days

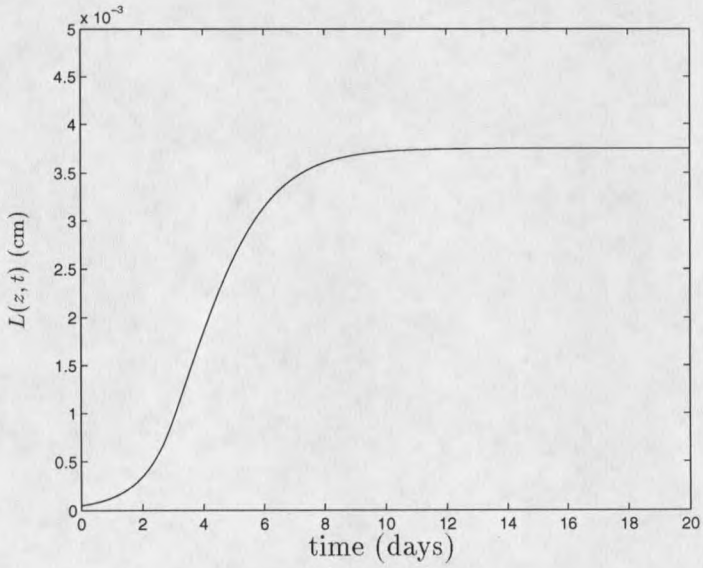

Figure 60: Average biofilm thickness on the spheres, $L(z,t)$, over 20 days

t(days)	$L(z,t)$ (cm)
0.0	0.00005000
2.0	0.00034109
4.0	0.00186939
6.0	0.00321783
8.0	0.00370719
10.0	0.00372726
12.0	0.00375316
14.0	0.00375854
16.0	0.00375964
18.0	0.00375985
20.0	0.00375989

Table 44: Average biofilm thickness on the spheres, $L(z,t)$, over 20 days

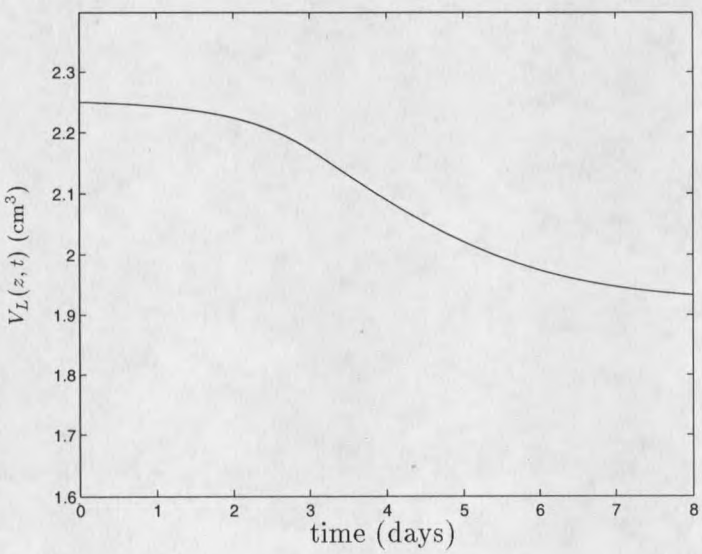

Figure 61: Average pore volume, $V_L(z,t)$, over 8 days

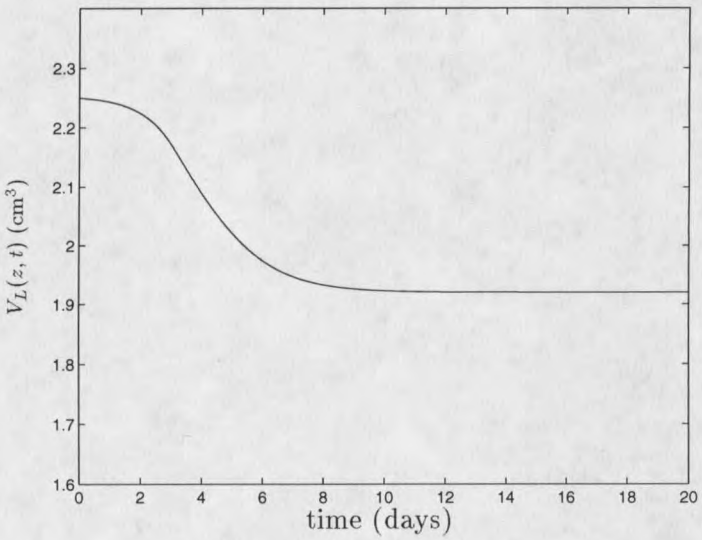

Figure 62: Average pore volume, $V_L(z,t)$, over 20 days

t(days)	$V_L(z,t)$ (cm^3)
0.0	2.25000000
2.0	2.22378819
4.0	2.09140106
6.0	1.97459479
8.0	1.93220436
10.0	1.92180359
12.0	1.91956040
14.0	1.91899994
16.0	1.91899978
18.0	1.91899969
20.0	1.91899966

Table 45: Average pore volume, $V_L(z,t)$, over 20 days

Porosity and Permeability The porosity of the porous medium is determined by the pore volume of the medium. As biofilm thickness on the pore surface (on the spheres) increases, the pore volume decreases and so does the porosity. The relation between porosity and the permeability of the medium, given by (5.14) and (5.15) has been used to determine the permeability. The profiles of the numerical porosity, $\phi_n(z,t)$, and the numerical permeability, $k_n(z,t)$, over 20 days are given in Figure 63 and Figure 64, respectively. The normalized numerical porosity, $\hat{\phi_n}(z,t) = \frac{\phi_n(z,t)}{\phi_n(z,0)}$, and normalized numerical permeability, $\hat{k_n}(z,t) = \frac{k_n(z,t)}{k_n(z,0)}$, over 20 days are displayed in Figure 65. The numerical values of the normalized porosity, $\hat{\phi_n}(z,t)$, and the normalized permeability, $\hat{k_n}(z,t)$, over 20 days are displayed in Table 46.

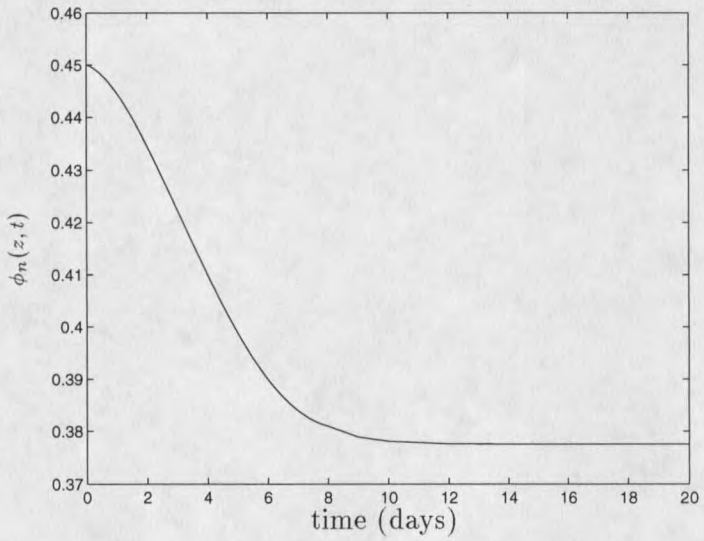

Figure 63: Numerical porosity, $\phi_n(z,t)$, of the porous medium over 20 days

Volumetric Flow Rate The volumetric flow rate through a porous bed depends on porosity, permeability, length of the bed, and the pressure gradient across the bed. The length of the porous bed (l = 5 cm) and the pressure gradient (P_2 - P_1 = 2.5 mg/(cm sec^2)) are constant here. The accumulation of the biofilm in the porous

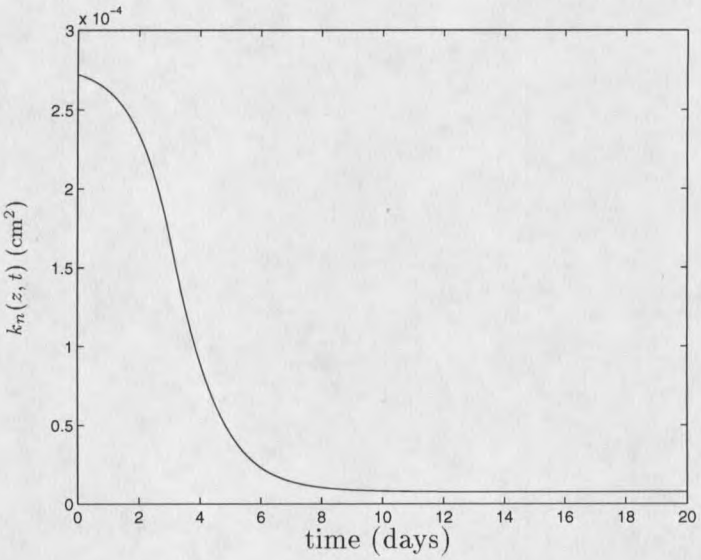

Figure 64: Numerical permeability, $k_n(z,t)$, of the porous medium over 20 days

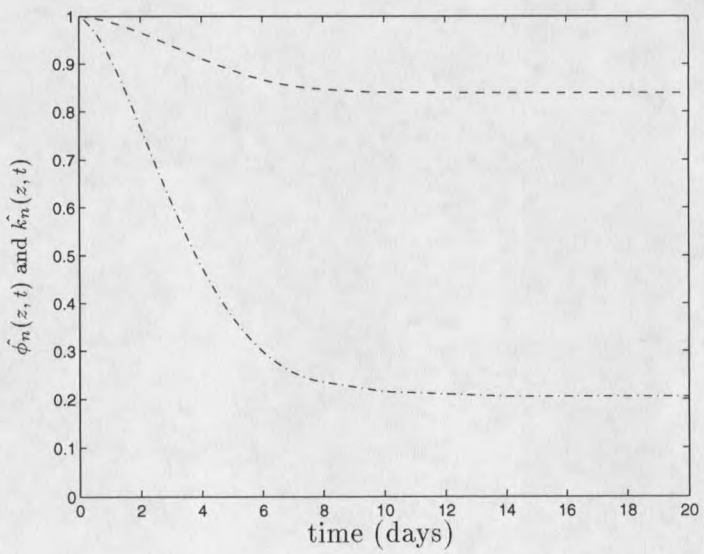

Figure 65: Normalized numerical porosity, $\hat{\phi}_n(z,t)$, (dashed line) and numerical permeability, $\hat{k}_n(z,t)$, (dash-dot line) over 20 days

t(days)	$\hat{\phi}_n(z,t)$	$\hat{k}_n(z,t)$ (cm^2)
0.0	1.00000000	1.00000000
2.0	0.96523228	0.76735758
4.0	0.91055905	0.47514109
6.0	0.86611521	0.47514109
8.0	0.84621526	0.23503012
10.0	0.83981846	0.21504012
12.0	0.83870902	0.21004262
12.0	0.83866048	0.20990973
14.0	0.83860046	0.20490009
16.0	0.83860024	0.20489985
20.0	0.83860008	0.20489984

Table 46: Normalized numerical porosity, $\hat{\phi}_n(z,t)$, and normalized numerical permeability, $\hat{k}_n(z,t)$, over 20 days

medium on the spheres causes a decrease in the porosity and the permeability which causes a decay in the volumetric flow rate. The graph of the numerical volumetric flow rate, $Q_n(z,t)$, is given in Figure 66 (over 8 days) and Figure 67 (over 20 days). The numerical values displayed in Table 47 show that $Q_n(z,t)$ attains a steady state of 0.019476 cm^3/sec after sixteen days.

t(days)	$Q_n(z,t)$ (cm^3/sec)
0.0	0.07500000
2.0	0.05948581
4.0	0.03904468
6.0	0.02578314
8.0	0.02078212
10.0	0.01966035
12.0	0.01948198
14.0	0.01947704
16.0	0.01947630
18.0	0.01947622
20.0	0.01947619

Table 47: Numerical volumetric flow rate, $Q_n(z,t)$, over 20 days

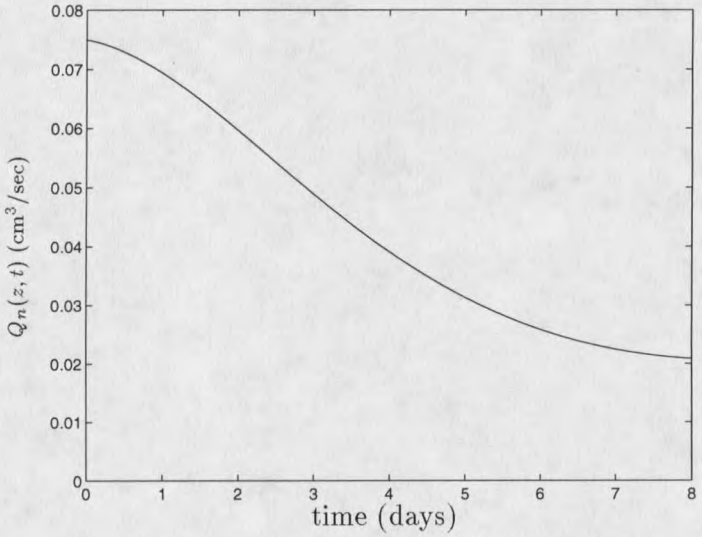

Figure 66: Numerical volumetric flow rate, $Q_n(z,t)$, over 8 days

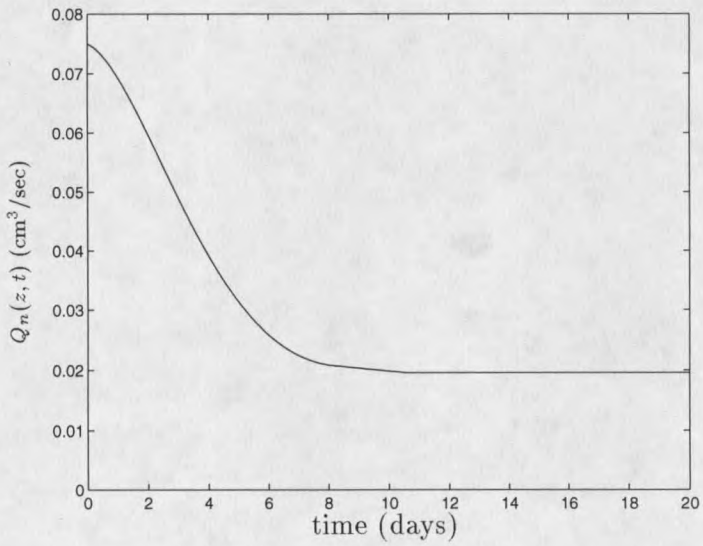

Figure 67: Numerical volumetric flow rate, $Q_n(z,t)$, over 20 days

Comparison of Numerical Results with Experimental Data

In the experimental model, [5], [6], the artificial porous medium (5 cm. long) is a bed of spherical balls of diameter .1 cm. During the eight days of the experiment, a constant pressure gradient (piezometric gradient) of 2.5 mg/(cm sec^2) across the bed is maintained and the change in the volumetric flow rate, porosity and the permeability due to biofilm accumulation are measured. A detailed description of the experiment may be found in [5], [6]. The mathematical model developed here (which describes in general the accumulation of biofilm in a porous medium), with the values of parameters and the initial and boundary values of unknown dependent variables given in Table 39 is supposed to simulate this experiment. The numerically approximated values of porosity, permeability, and the volumetric flow rate ($\phi_n(z,t)$, $k_n(z,t)$, and $Q_n(z,t)$), respectively) are compared below with the experimental results ($\phi_e(z,t)$, $k_e(z,t)$, and $Q_e(z,t)$, respectively).

Porosity and Permeability The experimental normalized porosity, $\hat{\phi}_e(z,t)$, given in Figure 51 shows a 17% decrease over 8 days of biofilm accumulation. Since the porosity of the medium is the ratio of the pore volume to the constant bulk volume ($\phi(z,t) = \frac{V_L(z,t)}{V_{bulk}}$), the parameters (detachment coefficient, λ, the yield coefficient, Y, and the maximum growth rate, V_r) in the model equations are adjusted so that the decay in the numerical pore volume is close to 17%. The best match between normalized experimental porosity, $\hat{\phi}_e(z,t)$, and numerical normalized porosity, $\hat{\phi}_n(z,t)$, (the maximum difference between the two porosity curves is minimum) is shown in Figure 68 and the numerical values are given in Table 48. The corresponding normalized experimental permeability, $\hat{k}_e(z,t)$, and the normalized numerical permeability, $\hat{k}_n(z,t)$, are compared in Figure 68 and the numerical values are compared in Table 49. $\hat{k}_e(z,t)$ and $\hat{k}_n(z,t)$ both are qualitatively and quantitatively close to each other.

Initially, since the numerical porosity decreases faster than experimental porosity, the numerical permeability also decreases faster than the experimental permeability. The steady state values of the experimental porosity and permeability are not known, however the numerical porosity and permeability reach steady state after 14 days (see Table 46). The steady state values of the normalized numerical porosity and normalized numerical permeability are 0.8386 and 0.2049, respectively.

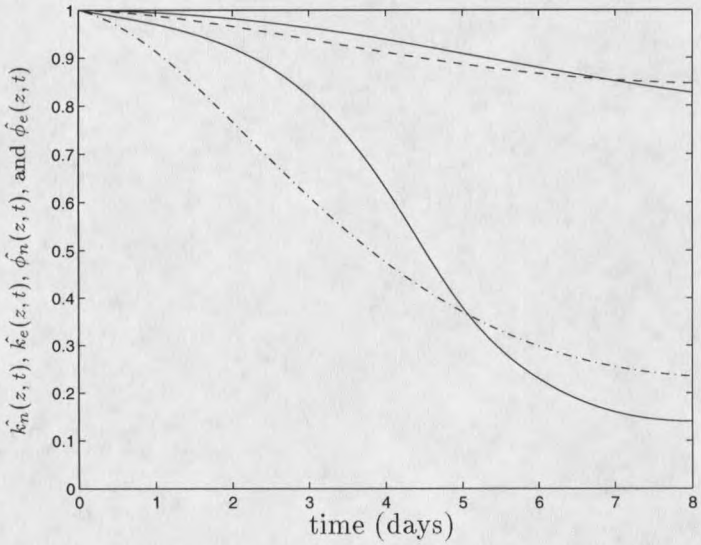

Figure 68: Normalized numerical porosity, $\hat{\phi}_n(z,t)$ (dashed line), normalized experimental porosity, $\hat{\phi}_e(z,t)$ (solid line), normalized numerical permeability, $\hat{k}_n(z,t)$ (dash-dot line), and normalized experimental permeability, $\hat{k}_e(z,t)$ (solid line)

Volumetric Flow Rate The experimental and numerical results show that the volumetric flow rate decreases with time which is caused by the decay in permeability and porosity due to biofilm accumulation on the pore surface (on the spheres). The graphs of experimental volumetric flow rate, $Q_e(z,t)$, and the numerical volumetric flow rate, $Q_n(z,t)$, over 8 days are displayed in Figure 69 and the numerical values are given in Table 50. The numerical volumetric flow rate decreases more rapidly than the experimental volumatric flow rate for the first 3 days then it slows down.

t (days)	$\hat{\phi}_e(z,t)$	$\hat{\phi}_n(z,t)$
0.0	1.00000000	1.00000000
1.0	0.99334290	0.98368465
2.0	0.98349468	0.96523228
3.0	0.96162713	0.93254502
4.0	0.93281434	0.91055905
5.0	0.90983853	0.88138736
6.0	0.87667112	0.86611521
7.0	0.85531404	0.85098562
8.0	0.82667503	0.84621526

Table 48: Normalized experimental porosity, $\hat{\phi}_e(z,t)$, and normalized numerical porosity, $\hat{\phi}_n(z,t)$, over 8 days

t (days)	$\hat{k}_e(z,t)$	$\hat{k}_n(z,t)$
0.0	1.00000000	1.00000000
1.0	0.96468116	0.88680268
2.0	0.92632674	0.76735758
3.0	0.81322249	0.58208155
4.0	0.58241123	0.47514109
5.0	0.39038718	0.35350206
6.0	0.22069692	0.47514109
7.0	0.16652762	0.24940026
8.0	0.14000000	0.23503012

Table 49: Normalized experimental permeability, $\hat{k}_e(z,t)$ and normalized numerical permeability, $\hat{k}_n(z,t)$, over 8 days

It is observed that the numerical volumetric flow rate decreases fastest between day one and day three whereas the experimental volumetric flow rate decreases fastest between day three and day five. The two flow rates are qualitatively similar over the 8 days, however on the 8th day of simulation, the numerical volumetric flow rate is .01 cm^3/sec higher than the experimental volumetric flow rate.

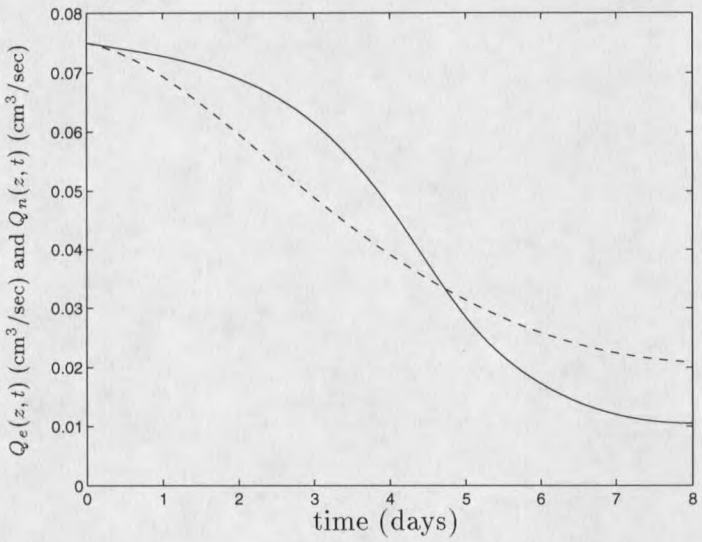

Figure 69: Experimental (solid line) volumetric flow rate, $Q_e(z,t)$, and numerical (dashed line) volumetric flow rate, $Q_n(z,t)$, over 8 days

Another Verification

For a given set of parameters, if the numerical porosity is close to the experimental porosity then it is reasonable to assume that the numerical permeability and the volumetric flow rate would also be close to the experimental data. If not, then the model would not be considered reliable. The equation

$$\hat{k}_e^*(z,t) = a_0 + a_1\hat{\phi}_e(z,t) + a_2(\hat{\phi}_e(z,t))^2 + a_3(\hat{\phi}_e(z,t))^3 + a_4(\hat{\phi}_e(z,t))^4 \qquad (5.16)$$

where $a_0 = -1.1255$, $a_1 = 5.2231$, $a_2 = -9.0477$, $a_3 = 6.9312$, and $a_4 = -1.9801$ is a fourth-degree least-squares polynomial fit between the normalized experimental

t(days)	$Q_e(z,t)$ (cm^3/sec)	$Q_n(z,t)$ (cm^3/sec)
0.0	0.07500000	0.07500000
1.0	0.07235108	0.06745568
2.0	0.06947450	0.05948581
3.0	0.06099168	0.04670479
4.0	0.04368084	0.03904468
5.0	0.02927903	0.03001045
6.0	0.01655226	0.02578314
7.0	0.01248957	0.02192916
8.0	0.01050000	0.02078212

Table 50: Experimental volumetric flow rate, $Q_e(z,t)$, and the numerical volumetric flow rate, $Q_n(z,t)$, over 8 days

porosity ($\hat{\phi}_e(z,t) = \frac{\phi_e(z,t)}{\phi_e(0,t)}$) and the normalized experimental permeability ($\hat{k}_e(z,t) = \frac{k_e(z,t)}{k_e(0,t)}$). The graph of this computed normalized experimental permeability, $\hat{k}_e^*(z,t)$, as a function of the normalized experimental porosity, $\hat{\phi}_e(z,t)$, from (5.15), is given in Figure 70. The graph of $\hat{k}_e(z,t)$ is also included. Next, $\hat{k}_c(z,t)$ (permeability given by (5.14) and (5.15), as a function of normalized experimental porosity, $\hat{\phi}_e(z,t)$) is also included. The model equations are solved using the parameter values given in Table 39 and (5.16) (instead of (5.14) and (5.15)) to calculate $k_n^*(z,t)$. The graphs of this new normalized numerical porosity ($\hat{\phi}_n^*(z,t)$) and normalized numerical permeability ($\hat{k}_n^*(z,t)$) computed here, using (5.15), are superimposed on the graphs given in Figure 68 and are shown in Figure 71. Also the graph of numerical volumetric flow rate ($Q_n^*(z,t)$) computed here, using the result of (5.15), is superimposed on the graphs given in Figure 69 and is shown in Figure 72. The numerical values of the normalized experimental porosity, $\hat{\phi}_e(z,t)$, normalized numerical porosity, $\hat{\phi}_n(z,t)$, computed from the original model, and normalized numerical porosity, $\hat{\phi}_n^*(z,t)$, computed using (5.16) are displayed in Table 51. The numerical values of the normalized experimental permeability, $\hat{k}_e(z,t)$, normalized numerical permeability, $\hat{k}_n(z,t)$, computed from the original model, and the normalized numerical porosity, $\hat{k}_n^*(z,t)$, computed using

(5.16) are displayed in Table 52. Also the numerical values of the experimental volumetric flow rate, $Q_e(z,t)$, numerical volumetric flow rate, $Q_n(z,t)$, computed from the original model, and numerical volumetric flow rate, $Q_n^*(z,t)$, computed using (5.16) are displayed in Table 53. It is clear that $\hat{\phi}_n^*(z,t)$ and $\hat{k}_n^*(z,t)$ are closer to $\hat{\phi}_e(z,t)$ and $\hat{k}_e(z,t)$, respectively, than $\hat{\phi}_n(z,t)$ and $\hat{k}_n(z,t)$ (see Figure 71). Also $Q_e^*(z,t)$ is closer to $Q_e(z,t)$ than $Q_n(z,t)$ (see Figure 72). This is because of the relation (5.15) between the porosity and the permeability used to solve the model equation. As the numerical simulation begins, step 3 of the algorithm computes the porosity ($\phi_n(z,\Delta t)$ or $\phi_n^*(z,\Delta t)$) of the medium after a small time Δt. These two porosities $\phi_n(z,\Delta t)$ and $\phi_n^*(z,\Delta t)$ are the same after the first time step, and they stay close to the experimental porosity due to the choice of the parameter values. But after the first time step the permeability computed by (5.15) ($k_n^*(z,\Delta t)$) remains closer to the experimental permeability ($k_e(z,\Delta t)$) than the permeability computed by (5.14) ($k_n(z,\Delta t)$) because (5.15) gives a better approximation of permeability as a function of porosity than (5.15). Hence the volumetric flow rate ($Q_n^*(z,\Delta t)$) computed after the first time step stays closer to $Q_e(z,\Delta t)$ than $Q_n(z,\Delta t)$. As long as $\phi_n^*(z,t)$ is close to the experimental porosity, $k_n^*(z,t)$ and $Q_n^*(z,t)$ remain close to the experimental data.

Prediction for a Long Bed Experiment

Similar to the simulation done in the last section in a short bed of length, l, = 5 cm, a simulation in a long bed (l = 60 cm) is done in this section and the results are presented. No experimental data is available to verify these predictions but parameters similar to those used in the 5 cm bed simulations (which were experimentally validated) are used. These are given in Table 54. To show the dependence of the dependent variables on the spatial variable, z, each dependent variable at three

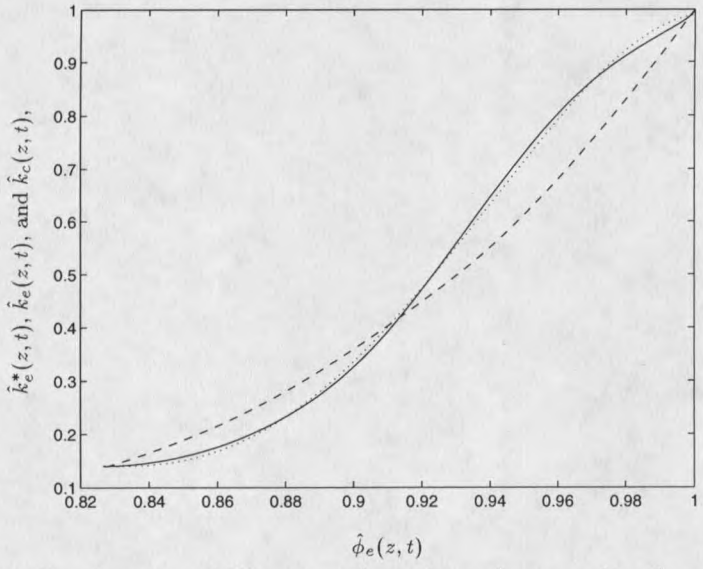

Figure 70: Normalized permeability as a function of normalized experimental porosity. Solid line represents the normalized experimental permeability, dashed line represents the computed normalized permeability, $\hat{k}_c(z,t)$, using (5.15), and dotted line represents the computed normalized permeability, $\hat{k}_e^*(z,t)$, using (5.16)

t (days)	$\hat{\phi}_e(z,t)$	$\hat{\phi}_n(z,t)$	$\hat{\phi}_n^*(z,t)$
0.0	1.00000000	1.00000000	1.00000000
1.0	0.99334290	0.98368465	0.99253558
2.0	0.98349468	0.96523228	0.97712844
3.0	0.96162713	0.93254502	0.95549521
4.0	0.93281434	0.91055905	0.93105746
5.0	0.90983853	0.88138736	0.90215000
6.0	0.87667112	0.86611521	0.87339623
7.0	0.85531404	0.85098562	0.85061513
8.0	0.82667503	0.84621526	0.83134996

Table 51: Normalized experimental porosity, $\hat{\phi}_e(z,t)$, normalized numerical porosity, $\hat{\phi}_n(z,t)$, (using (5.14) and (5.15)), and the normalized numerical porosity, $\hat{\phi}_n^*(z,t)$, (using (5.16)) over 8 days

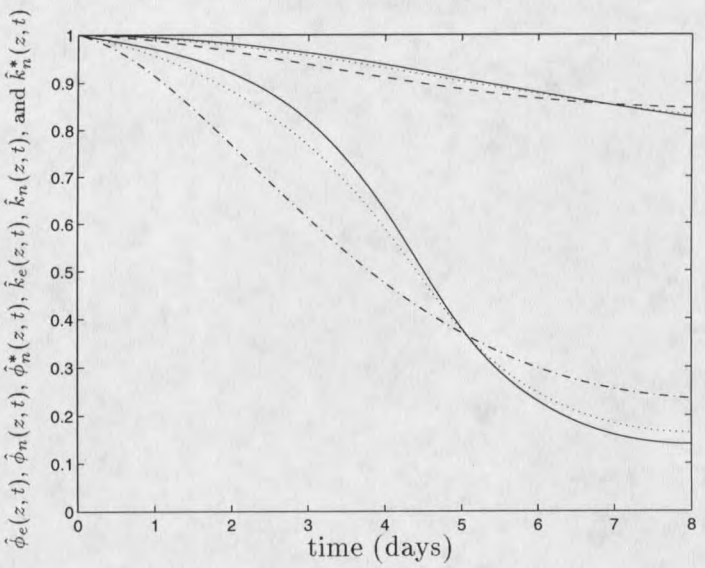

Figure 71: Upper three curves represent porosities and the lower three curves represent permeabilities. Solid curves represent experimental data ($\hat{\phi}_e(z,t)$ and $\hat{k}_e(z,t)$). The dotted curves represent the computed normalized numerical porosity ($\hat{\phi}_n(z,t)$) and computed normalized numerical permeability ($\hat{k}_n(z,t)$) using (5.15). The dashed and dash-dot curves represent the computed normalized numerical porosity ($\hat{\phi}_n^*(z,t)$) and computed normalized numerical permeability ($\hat{k}_n^*(z,t)$), respectively, using (5.14).

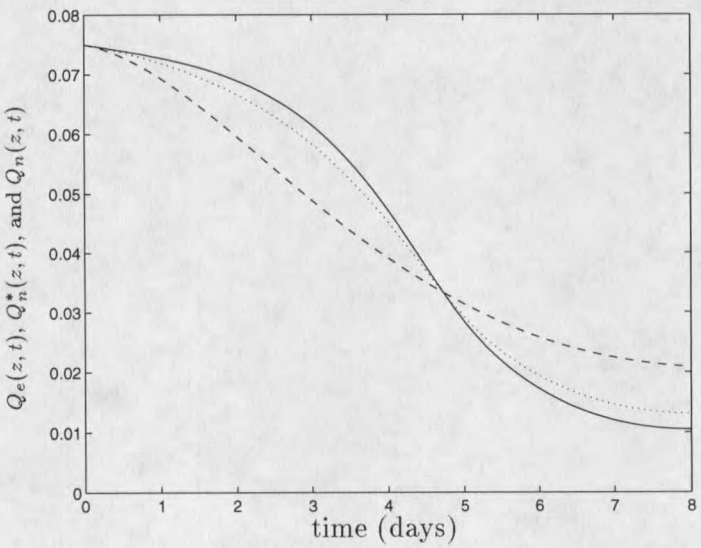

Figure 72: Experimental volumetric flow rate, $Q_e(z,t)$, (solid line), numerical volumetric flow rate, $Q_n^*(z,t)$, (dotted line) computed using (5.15), and numerical volumetric flow rate, $Q_n(z,t)$, (dashed line), computed using (5.14)

t (days)	$\hat{k}_e(z,t)$	$\hat{k}_n(z,t)$	$\hat{k}_n^*(z,t)$
0.0	1.00000000	1.00000000	1.00000000
1.0	0.96468116	0.88680268	0.95506324
2.0	0.92632674	0.76735758	0.87994501
3.0	0.81322249	0.58208155	0.76259188
4.0	0.58241123	0.47514109	0.59114891
5.0	0.39038718	0.35350206	0.37502810
6.0	0.22069692	0.47514109	0.23876711
7.0	0.16652762	0.24940026	0.18235706
8.0	0.14000000	0.23503012	0.16380496

Table 52: Normalized experimental permeability, $\hat{k}_e(z,t)$, normalized numerical permeability, $\hat{k}_n(z,t)$, (using (5.14) and (5.15)), and the normalized numerical permeability (using (5.16)), $\hat{k}_n^*(z,t)$, over 8 days

t(days)	$Q_e(z,t)$ (cm^3/sec)	$Q_n(z,t)$ (cm^3/sec)	$Q_n^*(z,t)$ (cm^3/sec)
0.0	0.07500000	0.07500000	0.07500000
1.0	0.07235108	0.06745568	0.07178876
2.0	0.06947450	0.05948581	0.06646821
3.0	0.06099168	0.04670479	0.05792254
4.0	0.04368084	0.03904468	0.04520971
5.0	0.02927903	0.03001045	0.02905421
6.0	0.01655226	0.02578314	0.01927287
7.0	0.01248957	0.02192916	0.01456354
8.0	0.01050000	0.02078212	0.01315056

Table 53: Experimental volumetric flow rate, $Q_e(z,t)$, the numerical volumetric flow rates, $Q_n(z,t)$, (using (5.14) and (5.15)), and $Q_n^*(z,t)$, (using (5.16)) over 8 days

different points z_1^*, z_2^*, and z_3^* has been computed and compared. z_1^* is a point which is one cm below the top of the bed ($z = 1$ cm), z_2^* is the midpoint of the bed ($z = 30$ cm), and z_3^* is one cm above the bottom of the bed ($z = 59$ cm).

Substrate Concentration in the Bulk Liquid As the simulation begins, the average substrate concentration in the bulk liquid, $S_b(z,t)$, begins to decrease from its initial value, .04 mg/cm^3, because an influent liquid of constant substrate concentration, $S_0 = .02$ mg/cm^3, continuously flows into the medium. Also, the substrate concentration in the bulk liquid in the pore channels decreases because of a continuous diffusion of the substrate from the bulk liquid into the biofilm on the spheres. This diffusion occurs due to the concentration gradient across the film-liquid interface caused by the consumption of the substrate by the active bacteria in the biofilm. The graphs of $S_b(z,t)$ at z_1^*, z_2^*, and z_3^* are given in Figure 73 (over 20 days) and Figure 74 (over the last 18 days). The variable $S_b(z,t)$ at z_1^*, z_2^*, and z_3^* are denoted by $S_{b1}(t)$, $S_{b2}(t)$, and $S_{b3}(t)$, respectively, and their numerical values are displayed in Table 55. The value of $S_b(z,t)$ decreases rapidly for the first two days. Table 55 and Figure 74, which is a blown up view of the steady state of $S_b(z,t)$, show that $S_b(z,t)$ at all three points reaches its steady state after 4 days. The predicted steady state values of $S_{b1}(t)$, $S_{b2}(t)$, and $S_{b3}(t)$ are .002012 mg/cm^3, .000405 mg/cm^3, and .0000026 mg/cm^3, respectively (see Table 55).

Substrate Concentration in the Biofilm The average substrate concentrations at z_1^*, z_2^*, and z_3^* are denoted by $S_1(t)$, $S_2(t)$, and $S_3(t)$, respectively, and their numerical values are given in Table 56 (over .001 days), Table 57 (over 1 day), and Table 58 (over 20 days). The graphs of these variables are displayed in Figure 75 (over .001 days, .01 days, .1 days, and 1 day), Figure 76 (over 20 days), and Figure 77 (over the last 18 days), respectively. The solid line, dotted line, and dashed line

Parameters	Values	Units
K	0.0001	mg/cm^3
V_r	4.7	mg/(mg day)
Y	.2	mg/mg
b	.35	day^{-1}
D	1.3	cm^2 /day
σ	99	cm^2
A	1	cm^2
L_l	.8	cm
ϵ_l	.8	dimensionless
ρ	12.2	mg /cm^3
μ	1.0	mg/(cm day)
S_0	.02	mg /cm^3
λ	800	cm^{-1}day^{-1}
ρ_f	1.1	mg/cm^3
V_{bulk}	5.0	cm^3
m	63024	dimensionless
g	981	cm/sec^2

Variables	Values	Units
$S_b(z,0)\ \forall z$	.04	mg /cm^3
$L(z,0)\ \forall z$	.00005	cm
$S(z,0)\ \forall z$	.00004	mg /cm^3
$f(z,0)\ \forall z$	.15	dimensionless
$V_L(z,0)\ \forall z$	27.00	cm^3
$D_b(z,0)\ \forall z$	.1	cm
$w(z,0)\ \forall z$	.0139	cm/sec
$Q(z,0)\ \forall z$	.00625	cm^3/sec
$\phi(z,0)\ \forall z$	.45	dimensionless
$k(z,0)\ \forall z$	.000275	cm^2
$P(z,0)\ \forall z$	3.0	mg/(cm sec^2)
$k_1 \equiv k(0,t)\ \forall t$	.000275	cm^2
$k_2 \equiv k(l,t)\ \forall t$	.000275	cm^2
$P_1 \equiv P(0,t)\ \forall t$	2.5	mg/(cm sec^2)
$P_2 \equiv P(l,t)\ \forall t$	5.0	mg/(cm sec^2)

Table 54: The values of the parameters and the initial and boundary values of the unknown dependent variables used in the one-dimensional incompressible porous media flow model (long bed model) with biofilm growth and their units

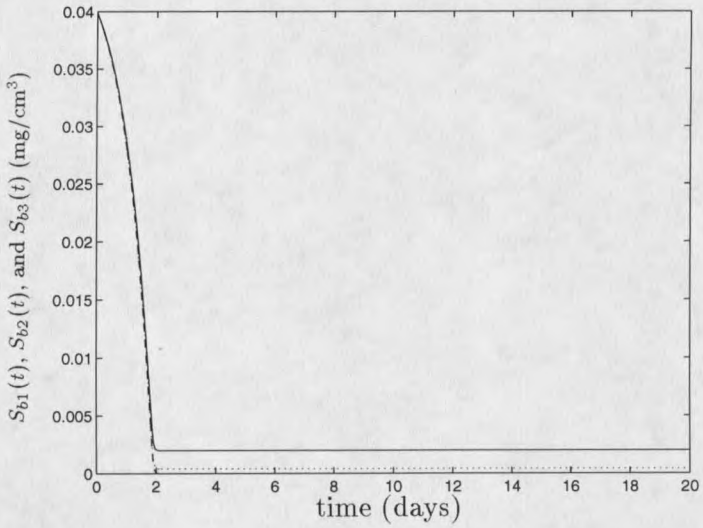

Figure 73: Substrate concentration in the bulk liquid, $S_b(z,t)$, at the points z_1^* $(S_{b1}(t))$, z_2^* $(S_{b2}(t))$, and z_3^* $(S_{b3}(t))$ over 20 days. Solid line represents $S_{b1}(t)$, dotted line represents $S_{b2}(t)$ and the dashed line represents $S_{b3}(t)$.

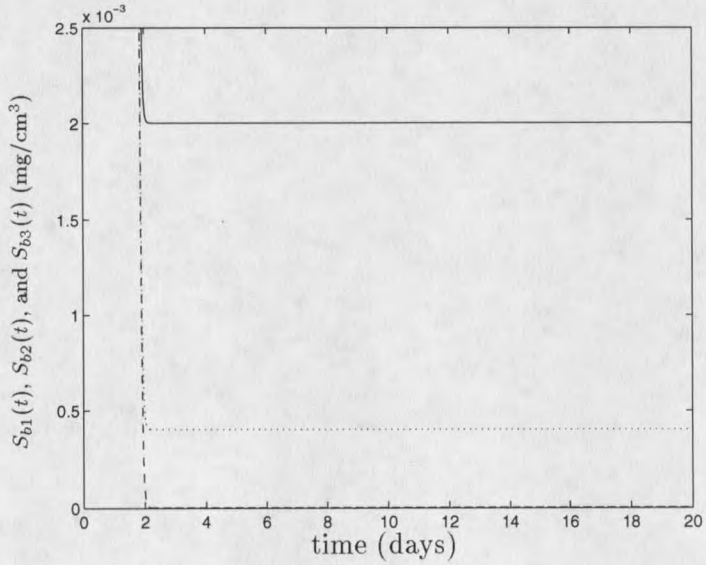

Figure 74: Steady state (last 18 days) of the substrate concentration, $S_b(z,t)$ in the bulk liquid at z_1^* $(S_{b1}(t))$, z_2^* $(S_{b2}(t))$, and z_3^* $(S_{b3}(t))$. Solid line represents $S_{b1}(t)$, dotted line represents $S_{b2}(t)$ and the dashed line represents $S_{b3}(t)$.

t(days)	$S_{b1}(t)$(mg/cm^3)	$S_{b2}(t)$(mg/cm^3)	$S_{b3}(t)$(mg/cm^3)
0.0	0.040000000	0.04000000	0.04000000
2.0	0.00208731	0.00048269	0.00008132
4.0	0.00201234	0.00040446	0.00000249
6.0	0.00201234	0.00040446	0.00000250
8.0	0.00201235	0.00040447	0.00000251
10.0	0.00201236	0.00040448	0.00000251
12.0	0.00201236	0.00040448	0.00000252
14.0	0.00201237	0.00040449	0.00000253
16.0	0.00201238	0.00040450	0.00000253
18.0	0.00201239	0.00040451	0.00000254
20.0	0.00201239	0.00040452	0.00000255

Table 55: Substrate concentration in the bulk liquid, $S_b(z,t)$, at the points z_1^* ($S_{b1}(t)$), z_2^* ($S_{b2}(t)$), and z_3^* ($S_{b3}(t)$) over 20 days.

represent the substrate concentrations at the points z_1^*, z_2^*, and z_3^*, respectively, in these figures. Initially the substrate concentration in the biofilm is $S(z,0) = .00004$ mg/cm^3 and the substrate concentration in the bulk liquid is $S_b(z,0) = .04$ mg/cm^3. Due to a high substrate concentration gradient, the substrate from the bulk liquid in the pore channels very rapidly diffuses into the biofilm on the spheres causing a rapid increase in the substrate concentration, $S(z,t)$, in the biofilm. This is shown in Figure 75 and Table 56. Figure 75a shows that initially (over .001 day), the substrate concentration at z_1^* remains slightly lower than the substrate concentrations at z_2^* and z_3^* because of the influent fluid which, in such a short time, affects the substrate concentration of the bulk liquid only near the top of the bed. As the substrate consumption becomes significant and the influent fluid of less concentration flows into the medium, the substrate concentration in the bulk liquid, $S_b(z,t)$, decreases, which causes a decrease in $S(z,t)$. Figure 76 shows that $S(z,t)$ decreases rapidly for the first two days. The substrate concentration in the biofilm reaches a steady state after 4 days of simulation. The predicted steady state values of $S(z,t)$ at z_1^*, z_2^*, and z_3^* are

.000019 mg/cm^3, .0000048 mg/cm^3, and .00000019 mg/cm^3, respectively (see Table 58).

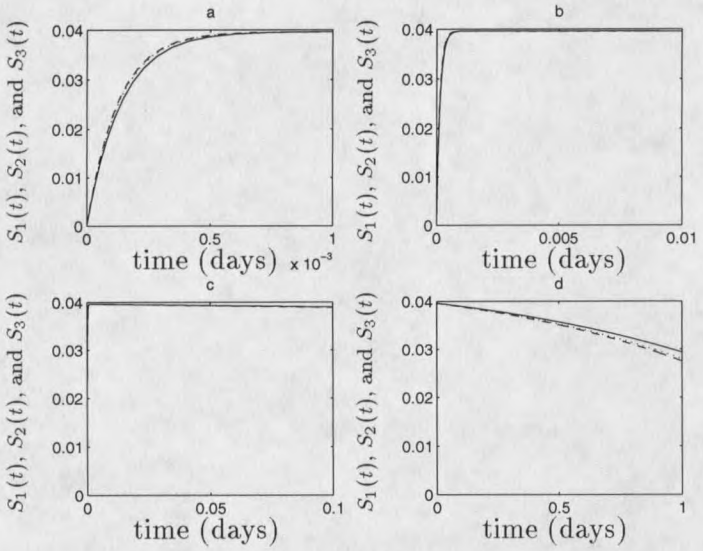

Figure 75: Substrate concentration in the biofilm, $S(z,t)$, at the points z_1^* ($S_1(t)$), z_2^* ($S_2(t)$), and z_3^* ($S_3(t)$) over (a) .001 days (b) .01 days (c) .1 days and (d) 1 day. The solid line represents $S_1(t)$, the dotted line represents $S_2(t)$, and the dashed line represents $S_3(t)$.

t(days)	$S_1(t)$(mg/cm^3)	$S_2(t)$(mg/cm^3)	$S_3(t)$(mg/cm^3)
0.0000	0.00004000	0.00004000	0.00004000
0.0001	0.02234611	0.02232669	0.02626069
0.0002	0.03114036	0.03255812	0.03256279
0.0003	0.03577866	0.03664762	0.03665229
0.0004	0.03795938	0.03837853	0.03838321
0.0005	0.03883657	0.03908828	0.03909297
0.0006	0.03937888	0.03950555	0.03951026
0.0007	0.03967115	0.03965169	0.03957301
0.0008	0.03973391	0.03977719	0.03958989
0.0009	0.03979667	0.03978844	0.03973603
0.0010	0.03981354	0.03981094	0.03981566

Table 56: Substrate concentration in the biofilm, $S(z,t)$, at the points z_1^* ($S_1(t)$), z_2^* ($S_2(t)$), and z_3^* ($S_3(t)$) over .001 days

t(days)	$S_1(t)$(mg/cm^3)	$S_2(t)$(mg/cm^3)	$S_3(t)$(mg/cm^3)
0.0	0.00004000	0.00004000	0.00004000
0.1	0.03915768	0.03908124	0.03907199
0.2	0.03845046	0.03830007	0.03825658
0.3	0.03763917	0.03739979	0.03735258
0.4	0.03678769	0.03644362	0.03635033
0.5	0.03585526	0.03538785	0.03523913
0.6	0.03478553	0.03417099	0.03400711
0.7	0.03360924	0.03287850	0.03264113
0.8	0.03237461	0.03145143	0.03112668
0.9	0.03095822	0.02980673	0.02944771
1.0	0.02947171	0.02806006	0.02758650

Table 57: Substrate concentration in the biofilm, $S(z,t)$, at the points z_1^* ($S_1(t)$), z_2^* ($S_2(t)$), and z_3^* ($S_3(t)$) over 1 day

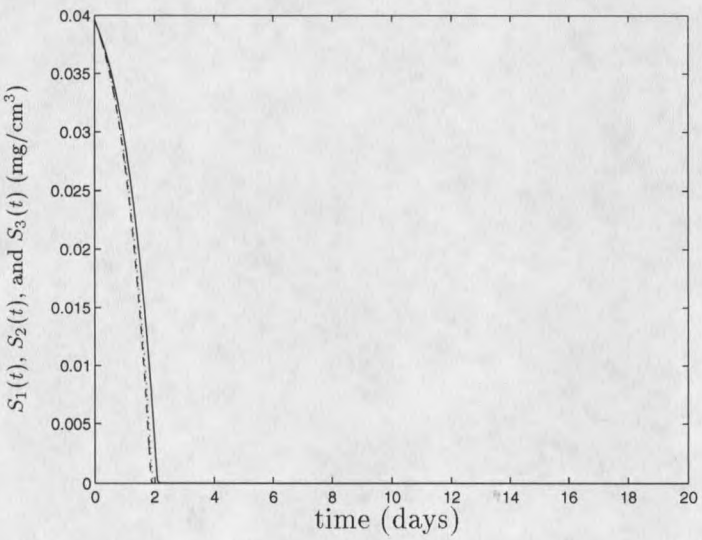

Figure 76: Substrate concentration in the biofilm, $S(z,t)$, at the points z_1^* ($S_1(t)$), z_2^* ($S_2(t)$), and z_3^* ($S_3(t)$) over 20 days. The solid line represents $S_1(t)$, the dotted line represents $S_2(t)$ and the dashed line represents $S_3(t)$.

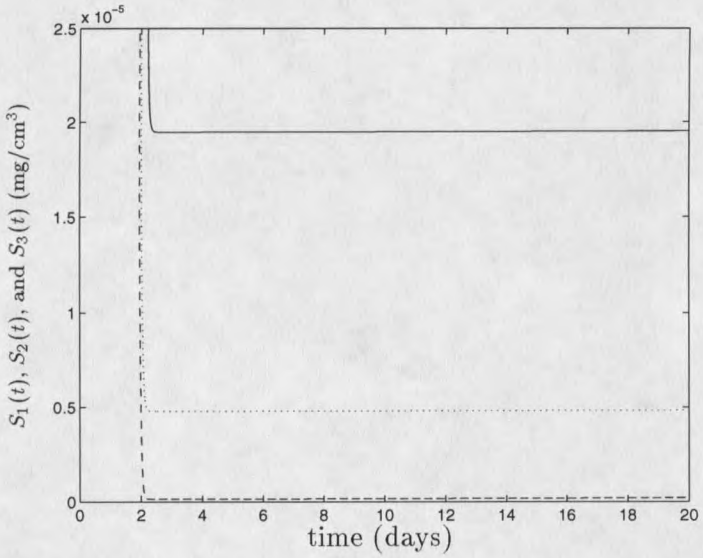

Figure 77: Steady state (last 18 days) of the substrate concentration in the biofilm at the points z_1^* ($S_1(t)$), z_2^* ($S_2(t)$), and z_3^* ($S_3(t)$). The solid line represents $S_1(t)$, the dotted line represents $S_2(t)$ and the dashed line represents $S_3(t)$.

t(days)	$S_1(t)$(mg/cm^3)	$S_2(t)$(mg/cm^3)	$S_3(t)$(mg/cm^3)
0.0	0.00004000	0.00004000	0.00004000
2.0	0.00345476	0.00002190	0.00000453
4.0	0.00001925	0.00000479	0.00000013
6.0	0.00001926	0.00000480	0.00000014
8.0	0.00001926	0.00000481	0.00000015
10.0	0.00001927	0.00000481	0.00000016
12.0	0.00001928	0.00000482	0.00000016
14.0	0.00001928	0.00000483	0.00000017
16.0	0.00001929	0.00000484	0.00000018
18.0	0.00001930	0.00000484	0.00000019
20.0	0.00001930	0.00000484	0.00000019

Table 58: Substrate concentration in the biofilm, $S(z,t)$, at the points z_1^* ($S_1(t)$), z_2^* ($S_2(t)$), and z_3^* ($S_3(t)$) over 20 days

Volume Fraction of Active and Inactive Bacteria The average active biomass volume fraction, $f(z,t)$, at the points z_1^*, z_2^*, and z_3^* are denoted by $f_1(t)$, $f_2(t)$, and $f_3(t)$, respectively. The average inactive biomass volume fraction, $\bar{f}(z,t)$ at the points z_1^*, z_2^*, and z_3^* are denoted by $\bar{f}_1(t)$, $\bar{f}_2(t)$, and $\bar{f}_3(t)$, respectively. The numerical values of the average active biomass volume fraction are given in Table 59 (over 1 day) and Table 60 (over 20 days) and the numerical values of average inactive biomass volume fraction are given in Table 61 (over 1 day) and Table 62 (over 20 days). The graphs of these variables over 20 days are displayed in Figure 78. The solid lines represent the graphs of the active and inactive biomass at the point z_1^*, the dotted lines represent the graphs of the active and inactive biomass at the point z_2^*, and the dashed lines represent the graphs of the active and inactive biomass at the point z_3^*. Initially (.6 days), due to the presence of sufficient substrate, $f(z,t)$ at all three points increases (see Table 59) and $\bar{f}(z,t)$ at all three points decreases (see Table 61). As the substrate concentration in the biofilm begins to decrease, $f(z,t)$ at all three points decreases (see Table 59 again) and $\bar{f}(z,t)$ increases (see Table 61 again). This can also be seen in Figure 78. The steady state values of $f(z,t)$ at z_1^*, z_2^*, and z_3^* are predicted to be .059099, .047417, and .045957, respectively, after 16 days and the steady state values of $\bar{f}(z,t)$ at z_1^*, z_2^*, and z_3^* are predicted to be .140901, .152583, and .154043, respectively, after 16 days. Note that the steady state inactive biomass volume fraction is higher than the active biomass volume fraction. This is caused by the limited substrate in the bulk liquid due to a relatively low volumetric flow rate through the medium. In the 5 cm bed, as we saw in the last section, the relatively high volumetric flow rate keeps the substrate concentration of the bulk liquid close to the constant influent substrate concentration ($S_0 = .02$ mg/cm^3). In this case, the active bacteria gets sufficient substrate and multiplies faster than it inactivates. In the 60 cm bed, due to a relatively low substrate concentration of the bulk liquid,

the active bacteria does not get sufficient substrate. In this case, the inactivation rate becomes higher than the growth rate of the bacteria causing a lower steady state for the active biomass volume fraction (hence a higher steady state for the inactive biomass volume fraction).

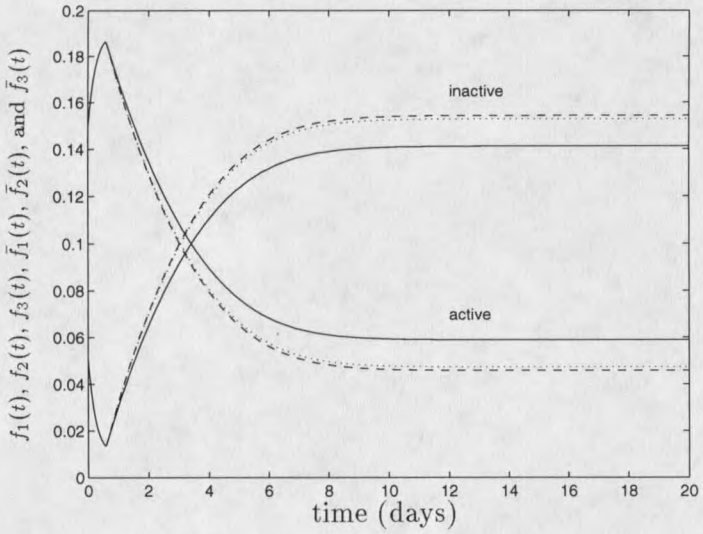

Figure 78: Average active biomass volume fraction, $f(z,t)$, at the points z_1^* ($f_1(t)$), z_2^* ($f_2(t)$), and z_3^* ($f_3(t)$) and the average inactive biomass volume fraction, $\bar{f}(z,t)$, at the points z_1^* ($\bar{f}_1(t)$), z_2^* ($\bar{f}_2(t)$), and z_3^* ($\bar{f}_3(t)$) over 20 days. The solid lines represent $f_1(t)$ and $\bar{f}_1(t)$, the dotted lines represent $f_2(t)$ and $\bar{f}_2(t)$, and the dashed lines represent $f_3(t)$ and $\bar{f}_3(t)$.

Biofilm Thickness The average biofilm thickness, $L(z,t)$, at the points z_1^*, z_2^*, and z_3^* is denoted by $L_1(t)$, $L_2(t)$, and $L_3(t)$, respectively, and their computed numerical values are given in Table 63 (over 5 days) and Table 64 (over 20 days). The graphs of $L_1(t)$ (solid line), $L_2(t)$ (dotted line), and $L_3(t)$ (dashed line) over 20 days are displayed in Figure 79. Initially, when the biofilm is thin, the active bacteria at each point in the porous bed gets sufficient substrate causing a constant growth all across the bed. The rapid growth in the biofilm thickness causes a quick decay in the substrate concentration in the biofilm which, in turn, slows down the growth

t(days)	$f_1(t)$	$f_2(t)$	$f_3(t)$
0.0	0.15000000	0.15000000	0.15000000
0.1	0.16510289	0.16510288	0.16510288
0.2	0.17517467	0.17517467	0.17517467
0.3	0.18003740	0.18003740	0.18003740
0.4	0.18349734	0.18349731	0.18349730
0.5	0.18620110	0.18620082	0.18620079
0.6	0.18667156	0.18657601	0.18656407
0.7	0.18226869	0.18172601	0.18165817
0.8	0.17807400	0.17715498	0.17704010
0.9	0.17434732	0.17308614	0.17292850
1.0	0.17046555	0.16883243	0.16862830

Table 59: Average active biomass volume fraction, $f(z,t)$, at the points z_1^* $(f_1(t))$, z_2^* $(f_2(t))$, and z_3^* $(f_3(t))$ over 1 day

t(days)	$f_1(t)$	$f_2(t)$	$f_3(t)$
0.0	0.15000000	0.15000000	0.15000000
2.0	0.13304441	0.12793049	0.12729125
4.0	0.08999428	0.08103745	0.07991784
6.0	0.06694537	0.05594758	0.05457286
8.0	0.06137105	0.04988543	0.04844972
10.0	0.05940877	0.04775336	0.04629644
12.0	0.05919377	0.04751992	0.04606069
14.0	0.05910692	0.04742568	0.04596552
16.0	0.05909902	0.04741712	0.04595688
18.0	0.05909868	0.04741675	0.04595651
20.0	0.05909869	0.04741676	0.04595652

Table 60: Average active biomass volume fraction, $f(z,t)$, at the points z_1^* $(f_1(t))$, z_2^* $(f_2(t))$, and z_3^* $(f_3(t))$ over 20 days

t(days)	$\bar{f}_1(t)$	$\bar{f}_2(t)$	$\bar{f}_3(t)$
0.0	0.05000000	0.05000000	0.05000000
0.1	0.03489710	0.03489711	0.03489711
0.2	0.02482532	0.02482532	0.02482532
0.3	0.01996259	0.01996259	0.01996259
0.4	0.01650265	0.01650268	0.01650269
0.5	0.01379889	0.01379917	0.01379920
0.6	0.01332843	0.01342398	0.01343592
0.7	0.01773130	0.01827398	0.01834182
0.8	0.02192599	0.02284501	0.02295989
0.9	0.02565267	0.02691385	0.02707149
1.0	0.02953444	0.03116756	0.03137169

Table 61: Average inactive biomass volume fraction, $\bar{f}(z,t)$, at the points z_1^* $(\bar{f}_1(t))$, z_2^* $(\bar{f}_2(t))$, and z_3^* $(\bar{f}_3(t))$ over 1 day

t(days)	$\bar{f}_1(t)$	$\bar{f}_2(t)$	$\bar{f}_3(t)$
0.0	0.05000000	0.05000000	0.05000000
2.0	0.06695558	0.07206950	0.07270874
4.0	0.11000571	0.11896254	0.12008215
6.0	0.13305462	0.14405241	0.14542713
8.0	0.13862894	0.15011456	0.15155027
10.0	0.14059122	0.15224663	0.15370355
12.0	0.14080622	0.15248007	0.15393930
14.0	0.14089307	0.15257431	0.15403447
16.0	0.14090097	0.15258287	0.15404311
18.0	0.14090131	0.15258324	0.15404348
20.0	0.14090130	0.15258323	0.15404347

Table 62: Average inactive biomass volume fraction, $\bar{f}(z,t)$, at the points z_1^* $(\bar{f}_1(t))$, z_2^* $(\bar{f}_2(t))$, and z_3^* $(\bar{f}_3(t))$ over 20 days

rate. As the substrate concentration in the biofilm reaches a steady state with a higher substrate concentration near the top of the bed and relatively lower substrate concentration near the bottom of the bed, $L(z,t)$ also reaches a steady state at a relatively higher average thickness near the top of the bed as compared to the average biofilm thickness near the bottom of the bed. The thickness reaches a steady state after 8 days at z_1^*, after 12 days at z_2^* and after 16 days at z_3^* (see Table 64 and Figure 79). The steady state values of $L_1(t)$, $L_2(t)$, and $L_3(t)$ are .001996 cm, .001736 cm, and .001707 cm, respectively (see Table 64).

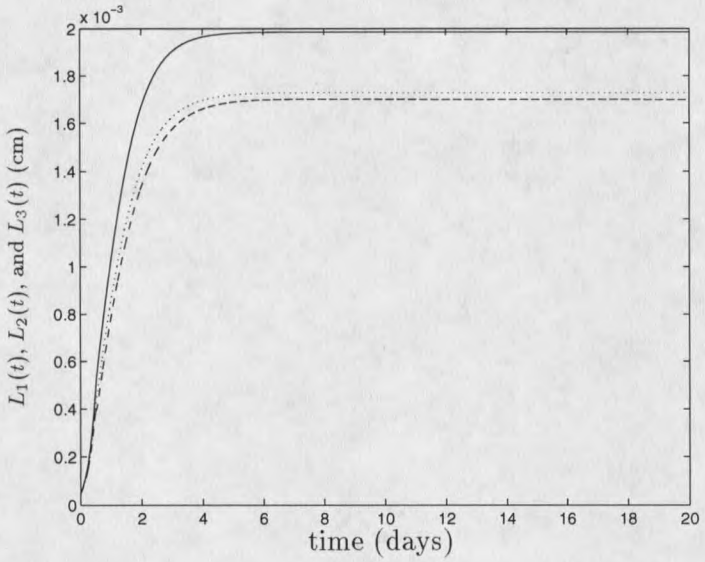

Figure 79: Biofilm thickness, $L(z,t)$, at the points z_1^* ($L_1(t)$), z_2^* ($L_2(t)$), and z_3^* ($L_3(t)$). Solid line represents $L_1(t)$, the dotted line represents $L_2(t)$ and dashed line represents $L_3(t)$ over 20 days.

Pore Volume The accumulation of biofilm on the pore surface causes a decay in the free pore space in the porous medium. The computed values of the average pore volume, $V_L(z,t)$, at z_1^* ($V_{L1}(t)$), z_2^* ($V_{L2}(t)$), and z_3^* ($V_{L3}(t)$) are given in Table 65 (over 5 days) and Table 66 (over 20 days). The graphs of $V_{L1}(t)$ (solid line), $V_{L2}(t)$ (dotted line), and $V_{L3}(t)$ (dashed line) are given in Figure 80. As the average biofilm

t(days)	$L_1(t)$ (cm)	$L_2(t)$ (cm)	$L_3(t)$ (cm)
0.0	0.00005000	0.00005000	0.00005000
0.5	0.00050227	0.00042913	0.00039540
1.0	0.00103056	0.00086207	0.00078961
1.5	0.00142067	0.00119071	0.00111418
2.0	0.00167839	0.00141350	0.00134229
2.5	0.00182973	0.00155153	0.00149027
3.0	0.00191168	0.00163242	0.00158127
3.5	0.00195399	0.00167852	0.00163558
4.0	0.00197527	0.00170451	0.00166750
4.5	0.00198583	0.00171913	0.00168609
5.0	0.00199104	0.00172734	0.00169680

Table 63: Biofilm thickness $L(z,t)$, at the points z_1^* $(L_1(t))$, z_2^* $(L_2(t))$, and z_3^* $(L_3(t))$ over 5 days

t(days)	$L_1(t)$ (cm)	$L_2(t)$ (cm)	$L_3(t)$ (cm)
0.0	0.00005000	0.00005000	0.00005000
2.0	0.00167839	0.00141350	0.00134229
4.0	0.00197527	0.00170451	0.00166750
6.0	0.00199487	0.00173443	0.00170621
8.0	0.00199601	0.00173689	0.00170921
10.0	0.00199609	0.00173669	0.00170856
12.0	0.00199609	0.00173640	0.00170794
14.0	0.00199610	0.00173623	0.00170758
16.0	0.00199610	0.00173613	0.00170737
18.0	0.00199610	0.00173608	0.00170726
20.0	0.00199610	0.00173605	0.00170719

Table 64: Biofilm thickness $L(z,t)$, at the points z_1^* $(L_1(t))$, z_2^* $(L_2(t))$, and z_3^* $(L_3(t))$ over 20 days

thickness approaches its steady state, the pore volume also approaches a steady state. The predicted steady state value for $V_{L1}(t)$ is 25.082525 cm^3, for $V_{L2}(t)$ is 25.256658 cm^3, and for $V_{L3}(t)$ is 25.273822 cm^3, all attained after 16 days.

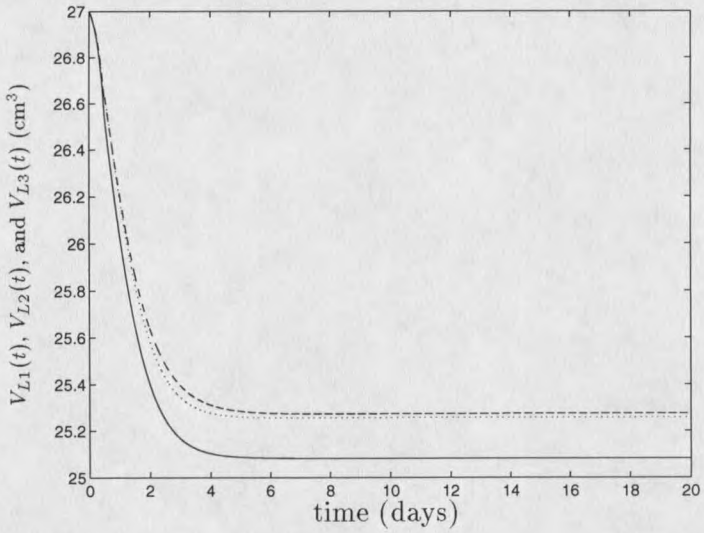

Figure 80: Pore volume, $V_L(z,t)$, at the points z_1^* ($V_{L1}(t)$), z_2^* ($V_{L2}(t)$), and z_3^* ($V_{L3}(t)$). Solid line represents $V_{L1}(t)$, dotted line represents $V_{L2}(t)$ and dashed line represents $V_{L3}(t)$ over 20 days.

Porosity and Permeability As the pore volume decreases, the porosity and the permeability of the medium also decrease. The values of the porosity, $\phi(z,t)$, at z_1^* ($\phi_1(t)$), z_2^* ($\phi_2(t)$), and z_3^* ($\phi_3(t)$) are given in Table 67 (over 5 days) and Table 68 (over 20 days). The graphs of $\phi_1(t)$ (solid line), $\phi_2(t)$ (dotted line), and $\phi_3(t)$ (dashed line) are displayed in Figure 81. Figure 82 shows a blown up view of the steady state (last 18 days) of $\phi_1(t)$, $\phi_2(t)$, and $\phi_3(t)$. The values of the permeability, $k(z,t)$, at z_1^* ($k_1(t)$), z_2^* ($k_2(t)$), and z_3^* ($k_3(t)$) are given in Table 69 (over 5 days) and Table 70 (over 20 days). The graphs of $k_1(t)$ (solid line), $k_2(t)$ (dotted line), and $k_3(t)$ (dashed line) are displayed in Figure 83. Figure 84 shows the blown up view of the steady state (last 18 days) of $k_1(t)$, $k_2(t)$, and $k_3(t)$. The normalized porosity, ($\hat{\phi}(z,t) = \frac{\phi(z,t)}{\phi(z,0)}$)

t(days)	$V_{L1}(t)$ (cm^3)	$V_{L2}(t)$ (cm^3)	$V_{L3}(t)$ (cm^3)
0.0	27.00000000	27.00000000	27.00000000
0.5	26.55495076	26.63489772	26.63179964
1.0	26.03581027	26.19516735	26.20995513
1.5	25.65170114	25.83054495	25.87042885
2.0	25.39762672	25.58006828	25.63466938
2.5	25.24812277	25.42784301	25.48448145
3.0	25.16691176	25.34320888	25.39405436
3.5	25.12482270	25.29872430	25.34123546
4.0	25.10354757	25.27613218	25.31081472
4.5	25.09292519	25.26493162	25.29342157
5.0	25.08731711	25.25917556	25.28287708

Table 65: Pore volume $V_L(z,t)$, at the points z_1^* ($V_{L1}(t)$), z_2^* ($V_{L2}(t)$), and z_3^* ($V_{L3}(t)$) over 5 days

t(days)	$V_{L1}(t)$ (cm^3)	$V_{L2}(t)$ (cm^3)	$V_{L3}(t)$ (cm^3)
0.0	27.00000000	27.00000000	27.00000000
2.0	25.39762672	25.58006828	25.63466938
4.0	25.10354757	25.27613218	25.31081472
6.0	25.08374698	25.25586429	25.27500292
8.0	25.08256665	25.25553377	25.27229886
10.0	25.08250995	25.25604488	25.27282230
12.0	25.08251613	25.25637245	25.27333969
14.0	25.08252193	25.25655632	25.27364915
16.0	25.08252525	25.25665843	25.27382232
18.0	25.08252508	25.25665820	25.27382213
20.0	25.08252504	25.25665819	25.27382207

Table 66: Pore volume $V_L(z,t)$, at the points z_1^* ($V_{L1}(t)$), z_2^* ($V_{L2}(t)$), and z_3^* ($V_{L3}(t)$) over 20 days

and the normalized permeability, ($\hat{k}(z,t) = \frac{k(z,t)}{k(z,0)}$) at z_1^*, z_2^*, and z_3^* are graphed in Figure 85. The numerical values of the normalized porosity, $\hat{\phi}(z,t)$, at the points z_1^* ($\hat{\phi}_1(t)$), z_2^* ($\hat{\phi}_2(t)$), and z_3^* ($\hat{\phi}_3(t)$) are given in Table 71. Also, the numerical values of the normalized permeability, $\hat{k}(z,t)$, at the points z_1^* ($\hat{k}_1(t)$), z_2^* ($\hat{k}_2(t)$), and z_3^* ($\hat{k}_3(t)$) are given in Table 72. The model predicts that the porosity at z_1^* reaches a steady state after ten days time and the porosity at z_2^* and z_3^* reaches a steady state after 16 days. The predicted steady state porosities at z_1^* (after 10 days), z_2^* (after 16 days), and z_3^* (after 16 days) are .418042, 0.420944 and 0.421230, respectively (see Table 68). The model also predicts that the permeability at z_1^*, z_2^* and z_3^* reaches a steady state after six days time. The predicted steady state permeabilities at z_1^*, z_2^*, and z_3^* are .000131 cm^2, .000141 cm^2, and .000142 cm^2, respectively (see Table 70).

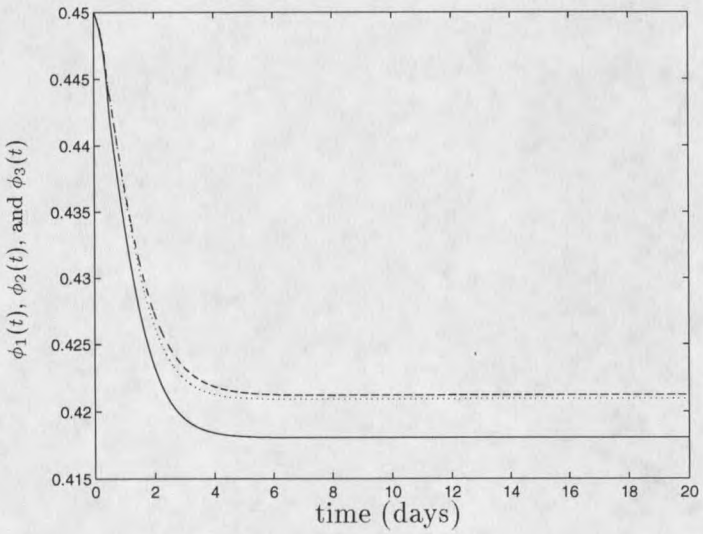

Figure 81: Porosity $\phi(z,t)$, at the points z_1^* ($\phi_1(t)$), z_2^* ($\phi_2(t)$), and z_3^* ($\phi_3(t)$). Solid line represents $\phi_1(t)$, dotted line represents $\phi_2(t)$ and dashed line represents $\phi_3(t)$ over 20 days.

Volumetric Flow Rate The computed volumetric flow rate, $Q(z,t)$, at the points z_1^*, z_2^*, and z_3^*, is denoted by $Q_1(t)$, $Q_2(t)$, and $Q_3(t)$, respectively, and the numerical

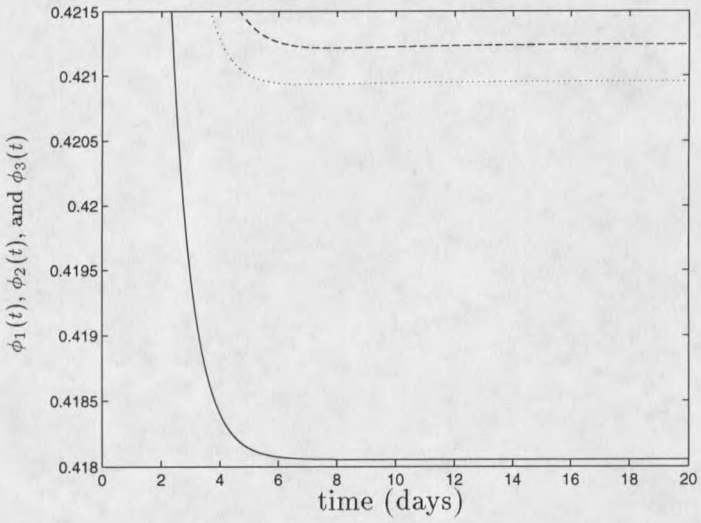

Figure 82: Steady state (last 18 days) of the porosity at the points z_1^* ($\phi_1(t)$), z_2^* ($\phi_2(t)$), and z_3^* ($\phi_3(t)$). Solid line represents $\phi_1(t)$, dotted line represents $\phi_2(t)$ and dashed line represents $\phi_3(t)$.

t(days)	$\phi_1(t)$	$\phi_2(t)$	$\phi_3(t)$
0.0	0.45000000	0.45000000	0.45000000
0.5	0.44258250	0.44391496	0.44386332
1.0	0.43393016	0.43658611	0.43683257
1.5	0.42752835	0.43050907	0.43117381
2.0	0.42329377	0.42633447	0.42724448
2.5	0.42080203	0.42379737	0.42474135
3.0	0.41944852	0.42238680	0.42323423
3.5	0.41874704	0.42164539	0.42235392
4.0	0.41839244	0.42126886	0.42184690
4.5	0.41821541	0.42108219	0.42155702
5.0	0.41812194	0.42098625	0.42138127

Table 67: Porosity $\phi(z,t)$, at the points z_1^* ($\phi_1(t)$), z_2^* ($\phi_2(t)$), and z_3^* ($\phi_3(t)$) over 5 days

t(days)	$\phi_1(t)$	$\phi_2(t)$	$\phi_3(t)$
0.0	0.45000000	0.45000000	0.45000000
2.0	0.42329377	0.42633447	0.42724448
4.0	0.41839244	0.42126886	0.42184690
6.0	0.41806244	0.42093106	0.42125004
8.0	0.41804276	0.42092555	0.42120497
10.0	0.41804182	0.42093407	0.42121369
12.0	0.41804192	0.42093953	0.42122231
14.0	0.41804202	0.42094259	0.42122747
16.0	0.41804207	0.42094429	0.42123036
18.0	0.41804210	0.42094423	0.42123036
20.0	0.41804212	0.42094414	0.42123034

Table 68: Porosity $\phi(z,t)$, at the points z_1^* $(\phi_1(t))$, z_2^* $(\phi_2(t))$, and z_3^* $(\phi_3(t))$ over 20 days

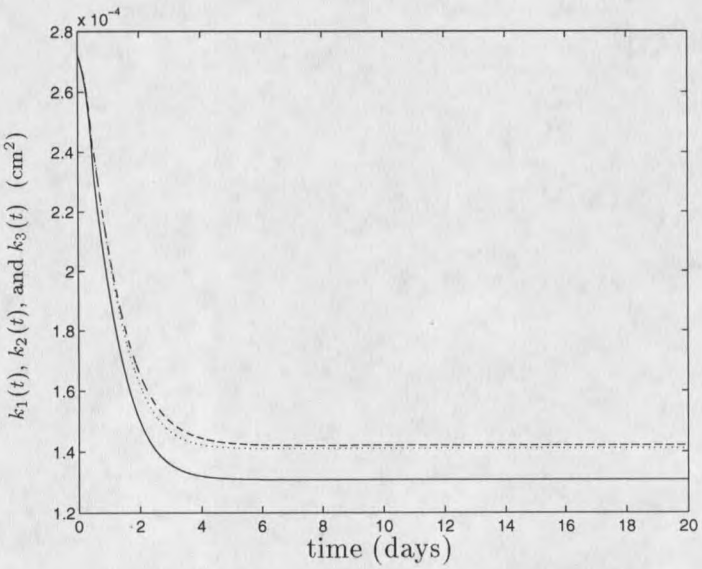

Figure 83: Permeability $k(z,t)$, at the points z_1^* $(k_1(t))$, z_2^* $(k_2(t))$, and z_3^* $(k_3(t))$. Solid line represents $k_1(t)$, dotted line represents $k_2(t)$ and dashed line represents $k_3(t)$ over 20 days.

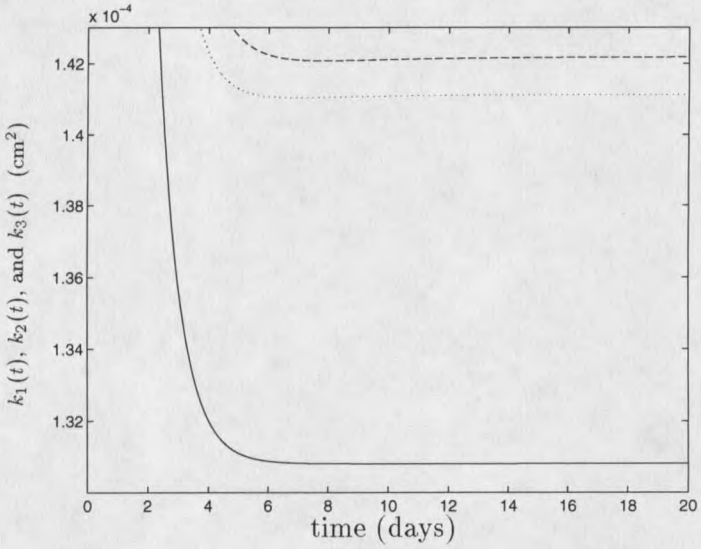

Figure 84: Steady state of the permeability $k(z,t)$, at the points z_1^* $(k_1(t))$, z_2^* $(k_2(t))$, and z_3^* $(k_3(t))$. Solid line represents $k_1(t)$, dotted line represents $k_2(t)$ and dashed line represents $k_3(t)$.

t(days)	$k_1(t)$ (cm^2)	$k_2(t)$ (cm^2)	$k_3(t)$ (cm^2)
0.0	0.00027500	0.00027500	0.00027500
0.5	0.00023364	0.00024028	0.00024002
1.0	0.00019324	0.00020514	0.00020627
1.5	0.00016630	0.00017854	0.00018134
2.0	0.00014982	0.00016155	0.00016516
2.5	0.00014060	0.00015172	0.00015534
3.0	0.00013574	0.00014642	0.00014959
3.5	0.00013326	0.00014368	0.00014630
4.0	0.00013201	0.00014230	0.00014442
4.5	0.00013140	0.00014162	0.00014335
5.0	0.00013107	0.00014127	0.00014271

Table 69: Permeability $k(z,t)$, at the points z_1^* $(k_1(t))$, z_2^* $(k_2(t))$, and z_3^* $(k_3(t))$ over 5 days

t(days)	$k_1(t)$ (cm^2)	$k_2(t)$ (cm^2)	$k_3(t)$ (cm^2)
0.0	0.00027500	0.00027500	0.00027500
2.0	0.00014982	0.00016155	0.00016516
4.0	0.00013201	0.00014230	0.00014442
6.0	0.00013086	0.00014107	0.00014223
8.0	0.00013080	0.00014105	0.00014206
10.0	0.00013079	0.00014108	0.00014210
12.0	0.00013079	0.00014110	0.00014213
14.0	0.00013079	0.00014111	0.00014215
16.0	0.00013079	0.00014111	0.00014216
18.0	0.00013079	0.00014112	0.00014216
20.0	0.00013079	0.00014112	0.00014217

Table 70: Permeability $k(z,t)$, at the points z_1^* ($k_1(t)$), z_2^* ($k_2(t)$), and z_3^* ($k_3(t)$) over 20 days

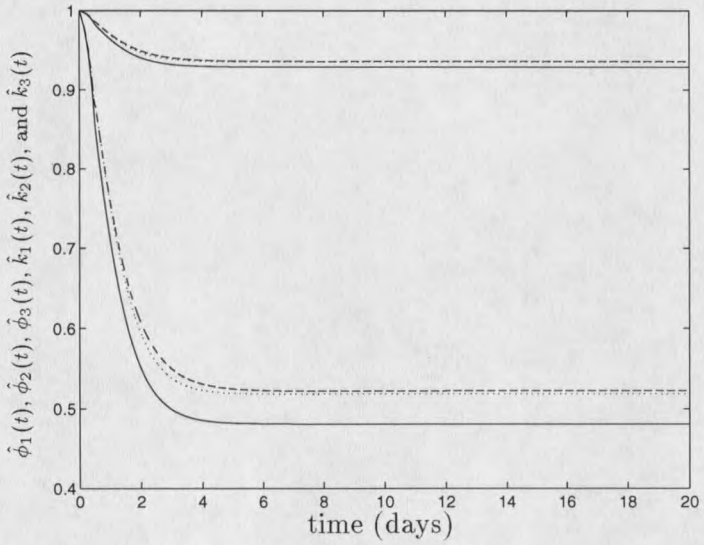

Figure 85: The upper set of curves represents the normalized porosity, $\hat{\phi}(z,t)$, and the lower set of curves represents the normalized permeability, $\hat{k}(z,t)$, at z_1^*, z_2^*, and z_3^*. In the upper set of curves, the solid line represents normalized porosity at z_1^* ($\hat{\phi}_1(t)$), the dotted line represents normalized porosity at z_2^* ($\hat{\phi}_2(t)$), and the dashed line represents the normalized porosity at z_3^* ($\hat{\phi}_3(t)$). In the lower set of curves, the solid line represents the normalized permeability at z_1^* ($\hat{k}_1(t)$), dotted line represents the normalized permeability at z_2^* ($\hat{k}_2(t)$), and the dashed line represents the normalized permeability at z_3^* ($\hat{k}_3(t)$).

t(days)	$\hat{\phi}_1(t)$	$\hat{\phi}_2(t)$	$\hat{\phi}_3(t)$
0.0	1.00000000	1.00000000	1.00000000
2.0	0.93832171	0.94506206	0.94707931
4.0	0.92745688	0.93383306	0.93511442
6.0	0.92672535	0.93308426	0.93379135
8.0	0.92668174	0.93307205	0.93369145
10.0	0.92667964	0.93309093	0.93371078
12.0	0.92667987	0.93310303	0.93372990
14.0	0.92668008	0.93310983	0.93374133
16.0	0.92668021	0.93311359	0.93374773
18.0	0.92668028	0.93311566	0.93375127
20.0	0.92668031	0.93311681	0.93375322

Table 71: Normalized porosity, $\hat{\phi}(z,t)$, at the points z_1^* ($\hat{\phi}_1(t)$), z_2^* ($\hat{\phi}_2(t)$), and z_3^* ($\hat{\phi}_3(t)$) over 20 days

t(days)	$\hat{k}_1(t)$	$\hat{k}_2(t)$	$\hat{k}_3(t)$
0.0	1.00000000	1.00000000	1.00000000
2.0	0.54934021	0.59235576	0.60561205
4.0	0.48406801	0.52177234	0.52955500
6.0	0.47985025	0.51725632	0.52152011
8.0	0.47959953	0.51718287	0.52091641
10.0	0.47958749	0.51729645	0.52103324
12.0	0.47958880	0.51736926	0.52114873
14.0	0.47959003	0.51741013	0.52121781
16.0	0.47959074	0.51743273	0.52125648
18.0	0.47959113	0.51744522	0.52127787
20.0	0.47959134	0.51745211	0.52128969

Table 72: Normalized permeability, $\hat{k}(z,t)$, at the points z_1^* ($\hat{k}_1(t)$), z_2^* ($\hat{k}_2(t)$), and z_3^* ($\hat{k}_3(t)$) over 20 days

values are displayed in Table 73 (over 5 days) and Table 74 (over 20 days). The graphs of $Q_1(t)$, $Q_2(t)$, and $Q_3(t)$ are given in Figure 86. Figure 87 shows the blown up view of the steady state (last 18 days) of $Q_1(t)$, $Q_2(t)$, and $Q_3(t)$. As the porosity and the permeability of the medium approach their steady states, the volumetric flow rate also decreases and approaches a steady state. The model predicts a rapid decrease in $Q(z,t)$ at all three points for the first three days. The volumetric flow rate through z_1^*, $Q_1(t)$, attains a steady state at .003235 cm^3/sec after 8 days time. Similarly the volumetric flow rate through z_2^*, $Q_2(t)$, attains a steady state at .003465 cm^3/sec after 10 days time and the volumetric flow rate through z_3^*, $Q_3(t)$, attains a steady state at .003488 cm^3/sec after 10 days time (see Table 74).

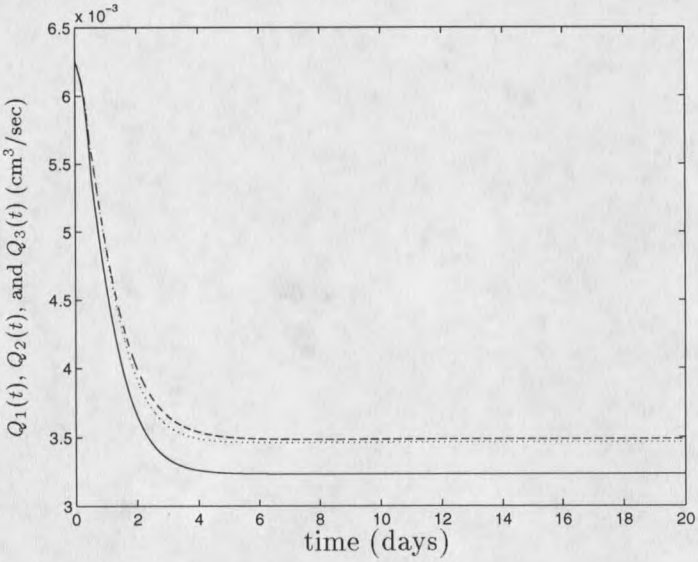

Figure 86: Volumetric flow rate $Q(z,t)$, at the points z_1^* $(Q_1(t))$, z_2^* $(Q_2(t))$, and z_3^* $(Q_3(t))$. Solid line represents $Q_1(t)$, dotted line represents $Q_2(t)$ and dashed line represents $Q_3(t)$ over 20 days.

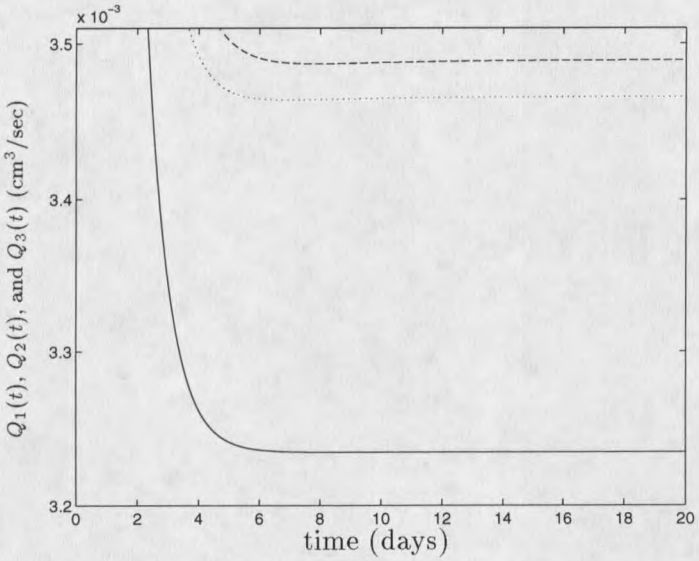

Figure 87: Steady state of the volumetric flow rate, $Q(z,t)$, at the points z_1^* $(Q_1(t))$, z_2^* $(Q_2(t))$, and z_3^* $(Q_3(t))$. Solid line represents $Q_1(t)$, dotted line represents $Q_2(t)$ and dashed line represents $Q_3(t)$

t(days)	$Q_1(t)$ (cm^3/sec)	$Q_2(t)$ (cm^3/sec)	$Q_3(t)$ (cm^3/sec)
0.0	0.00625000	0.00625000	0.00625000
0.5	0.00544361	0.00558162	0.00557624
1.0	0.00459206	0.00484527	0.00486914
1.5	0.00401125	0.00427651	0.00433690
2.0	0.00364980	0.00390752	0.00398646
2.5	0.00344550	0.00369184	0.00377133
3.0	0.00333711	0.00357471	0.00364484
3.5	0.00328165	0.00351396	0.00357201
4.0	0.00325380	0.00348330	0.00353042
4.5	0.00323994	0.00346815	0.00350674
5.0	0.00323264	0.00346039	0.00349244

Table 73: Volumetric flow rate $Q(z,t)$, at the points z_1^* $(Q_1(t))$, z_2^* $(Q_2(t))$, and z_3^* $(Q_3(t))$ over 5 days

t(days)	$Q_1(t)$ (cm^3/sec)	$Q_2(t)$ (cm^3/sec)	$Q_3(t)$ (cm^3/sec)
0.0	0.00625000	0.00625000	0.00625000
2.0	0.00365896	0.00391733	0.00399647
4.0	0.00326197	0.00349205	0.00353928
6.0	0.00323610	0.00346460	0.00349051
8.0	0.00323456	0.00346415	0.00348685
10.0	0.00323449	0.00346484	0.00348756
12.0	0.00323450	0.00346529	0.00348826
14.0	0.00323450	0.00346530	0.00348828
16.0	0.00323451	0.00346531	0.00348830
18.0	0.00323451	0.00346532	0.00348830
20.0	0.00323451	0.00346532	0.00348830

Table 74: Volumetric flow rate $Q(z,t)$, at the points z_1^* ($Q_1(t)$), z_2^* ($Q_2(t)$), and z_3^* ($Q_3(t)$) over 20 days

Conclusion

The complete mathematical model describing biofilm growth in a homogeneous porous medium and its effect on one-dimensional incompressible fluid flow through the medium has been solved and the numerical results have been presented. The comparison of the numerical results for a short bed with the experimental results (presented in the third section) and the discussion of the results (predictions) for a long bed experiment (presented in the fourth section) lead to the following conclusions.

- The mathematical model predicts the change with respect to time of the average substrate concentration of the bulk liquid, the average substrate concentration in the biofilm, the average volume fraction of active and inactive biomass, the average biofilm thickness, the average pore volume, the porosity of the medium, the permeability of the medium, and the volumetric flow rate through the medium.

- Biofilm accumulation on the pore surface of a porous medium causes a significant decrease in the porosity and the permeability of the medium which decreases

the volumetric flow rate through the medium.

- Numerically computed porosity, permeability and volumetric flow rate in a short bed are found to be qualitatively and quantitatively close to the experimental results in [5], [6], which validates the reliability of the model developed in this dissertation.

- In the short bed, the volumetric flow rate is relatively high which keeps the bulk liquid substrate concentration close to the constant influent substrate concentration of 0.02 mg/cm^3. In this case, the active bacteria at each position gets sufficient substrate causing a constant biofilm thickness all across the bed. No variation along the spatial direction was observed.

- The volumetric flow rate in a long bed is significantly lower than the volumetric flow rate in the short bed due to the same pressure drop assumed across the bed. The simulation for a long bed experiment shows that the low volumetric flow rate through the medium causes relatively lower steady state average bulk substrate concentration. Because of this, the average steady state substrate concentration in the biofilm and the steady state average biofilm thickness are relatively low. Also, the simulation for the long bed experiment predicts a higher average substrate concentration near the top of the bed than the bottom of the bed causing a higher steady state average biofilm thickness near the top of the bed. This in turn leads to a spatially varying porosity and permeability along the length of the bed, with lower porosity and permeability near the top.

These simulations and others like them, should allow one to study the influence of biofilm accumulation in a porous media. Whether the application is the introduction of a biobarrier for contaminant or the elimination of plugging due to bacteria,

the capabilities of this model should provide a powerful tool for the study of such system.

REFERENCES CITED

[1] M.B. Allen, I. Herrera, and G. Pinder. *Numerical Modelling in Science and Engineering.* A Wiley-Interscience Publication, 1988.

[2] Jacob Bear. *Dynamics of Fluids in Porous Media.* Dover Publications, Inc. New York, 1972.

[3] R. L. Burden and J. D. Faires. *Numerical Analysis.* Prindle, Weber & Schmidt, Boston, 3rd edition, 1985.

[4] W. G. Characklis, K. C. Marshall, and A. Cunningham. *Biofilms.* John Wiley and Sons Inc, New York, 1st edition, 1990.

[5] David Jay Crawford. Hydraulic effect of biofilm accumulation in simulated porous media flow systems. Master's thesis, Department of Civil Engineering, Montana State University, 1987.

[6] Alfred B. Cunningham, William G. Characklis, Feisal Abedeen, and David Crawford. Influence of biofilm accumulation on porous media hydrodynamics. *Environ. Sci. Technol.*, 25:1305 – 1311, 1991.

[7] Henry Darcy. *La Fountaina Publiques de Ville de Dijon.* Dalmont, Paris, 1856.

[8] F.A.L. Dullien. New network permeability model of porous media. *AIChE J.*, 21:299 – 307, 1975.

[9] F.A.L. Dullien. *Porous Media Fluid Transport and Pore Structure.* Academic Press, Inc., New York, 2nd edition, 1992.

[10] Leah Edelstein-Keshet. *Mathematical Models in Biology.* The Random House/Birkhauser Mathematics Series, 1987.

[11] H. R. Ehrlich and D. S. Holms. *Workshop on Biotechnology for the Mining, Metal-Refining and Fossil Fuel Processing Industries.* Rensselaer Polytechnic Institute, Troy, NY, 1985.

[12] V. Gadani, P. Villon, J. Manem, and B. Rittman. A new method to solve a non-steady-state multispecies biofilm model. *Bulletin of Mathematical Biology*, 55:1039–1061, 1993.

[13] C. W. Gear. *Numerical Initial Value Problems in Ordinary Differential Equations.* Prentice-Hall, Englewood, NJ, 1st edition, 1971.

[14] Brian Goldstein. Program description for biofilm accumulation model. *Center For Biofilm Engineering, Montana State University*, 1992.

[15] A. Hall and T. A. Porsching. *Numerical Analysis of Partial Differential Equations.* Prentice-Hall, New Jersey, 1st edition, 1990.

[16] H. M. Lappin-Scott, F. Cusack, and J. W. Costerton. Nutrient resuscitation and growth of starved cells in sand stone core: a novel approach to enhance oil recovery. *Appl. Environ. Microbiol.*, 54:1373 – 1382, 1986.

[17] T. S. Lundgren. Slow flow through stationary random beds and suspensions of spheres. *J. Fluid Mech.*, 51:273 – 287, 1972.

[18] Ross Wade Lundman. Transport of substrate and biomass in a packed bed bioreactor. Master's thesis, Department of Chemical Engineering, Montana State University, 1992.

[19] F. A. MacLeod, H. M. Lappin-Scott, and J. W. Costerton. Plugging of a model rock system by using starved bacteria. *Appl. Environ. Microbiol.*, 54:1365 – 1372, 1986.

[20] Morris Muskat. *The Flow of Homogeneous Fluids Through Porous Media.* J. E. Edwards, Ann Arbor, Michigan, 3rd edition, 1946.

[21] D. W. Peaceman. *Fundamentals of Numerical Reservoir Simulation.* New York: Elsevier Scientific Publishing Company, 1955.

[22] Polubarinova-Kochina. *Theory of ground water movement.* Princeton University Press, Princeton, N.J., 1962.

[23] Adrian E. Scheidegger. *The Physics of Flow Through Porous Media.* The McMillan Company, New York, 2nd edition, 1958.

[24] Lawrence F. Shampine and Mark W. Reichelt. The MATLAB suite. *MathWorks, Inc., MATLAB 4.2*, 1992.

[25] O. Wanner and W. Gujar. Multispecies biofilm model. *Biotechnology and Bioengineering*, XXVIII:314–328, 1986.

[26] B. H. Wilson, G. B. Smith, and J. F. Rees. Biotransformation of selected alkylbenzenes and halogenated alphatic hydrocarbons in mathanogenic aquifer material: a microcosm study. *Environ. Sci. Technol.*, 20:997 – 1002, 1986.

[27] H. Zedan. A variable order/variable-stepzise rosenbrock-type algorithm for solving stiff systems of ode's. *Tech. report YCS114, Dept. Comp. Sci., Univ. of York*, 1989.

APPENDICES

APPENDIX A

Computer Code for Subroutine ODE23s

```
function [tout,yout,stats] = ode23s(ydot,tspan,y0,options)
%ODE23S Solve stiff differential equations, low order method.
%  [T,Y] = ODE23S('ydot',TSPAN,Y0) with TSPAN = [T0 TFINAL]
%  integratesthe system of first order differential
%  equations y' = ydot(t,y) from time T0 to TFINAL with
%  initial conditions Y0.  Function ydot(t,y) must return a
%  column vector.  Each row in solution matrix Y corresponds
%  to a time returned in column vector T.  To obtain solutions
%  at the specific times T0, T1, ..., TFINAL (all increasing
%  or all decreasing), use TSPAN = [T0 T1 ... TFINAL].
%
%  [T,Y] = ODE23S('ydot',TSPAN,Y0,OPTIONS) solves as above with
%  default integration parameters replaced by values in OPTIONS,
%  an argument created with the ODESET function.  See ODESET
%  for details.  Commonly used options are scalar relative error
%  tolerance 'rtol' (1e-3 by default) and vector of absolute
%  error tolerances 'atol' (all components 1e-6 by default).
%
%  It is possible to specify tspan, y0 and options in ydot. If
%  TSPAN or Y0 is empty, or if ODE23S is invoked as
%  ODE23S('ydot'), ODE23S calls [tspan,y0,options] = ydot([],[])
%  to obtain any values not supplied at the command line.  TYPE
%  CHM6EX to see how this is coded. The Jacobian matrix J(t,y)
%  is critical to the reliability and efficiency of the
%  integration.  If J(t,y) is constant and/or sparse, use the
%  'constantJ' and/or 'sparseJ' options (see B5EX, BRUSSEX).
%  If ydot is coded so that ydot([t1 t2 ...],[y1 y2 ...]) returns
%  [ydot(t1,y1) ydot(t2,y2) ...], setting 'vectorized' true may
%  speed up the computation of J (see VDPEX). If an M-file
%  function that evaluates analytically J(t,y) is available, use
%  the 'analyticJ' option (see VDPJAC, BRUSSJAC).
%
%  As an example, the command
%
%           ode23s('vdpex',[0 3000],[2 0]);
%
%  solves the system y' = vdpex(t,y) with the default relative
```

```
%  error tolerance 1e-3 and the default absolute tolerance of
%  1e-6 for each component.  When called with no output
%  arguments, as in this example, ODE23S calls the default
%  output function ODEPLOT to plot the solution as it is computed.
%
%  ODE23S also solves problems M*y' = ydot(t,y) with a constant
%  mass matrix M that is nonsingular and (usually) sparse.  Use
%  the 'mass' option to supply either M or the name of a function
%  that returns M (see FEM2EX).  See ODE15S if M is time-dependent.
%
%  See also
%          other ODE solvers:   ODE15S, ODE45, ODE23, ODE113
%          options handling:    ODESET, ODEGET
%          output functions:    ODEPLOT, ODEPHAS2, ODEPHAS3
%          ydot examples:       VDPEX, BRUSSEX, B5EX, CHM6EX
%          ydot Jacobians:      VDPJAC, BRUSSJAC
%          Jacobian functions:  NUMJAC, COLGROUP
%          mass matrices:       FEM2EX, FEM2MASS
%
%  ODE23S is an implementation of a new modified Rosenbrock
%  (2,3) pair with a "free" interpolant.  Local extrapolation
%  is not done.  By default, Jacobians are generated numerically.
%  Details are to be found in The MATLAB ODE Suite, L. F.
%  Shampine and M. W.  Reichelt, Rept. 94-6, Math. Dept., SMU,
%  Dallas, TX, 1994.
%
%  Mark W. Reichelt and Lawrence F. Shampine, 3-22-94
%  Copyright (c) 1984-95 by The MathWorks, Inc.
%
false = 0;
true = ~false;

nsteps = 0;                              % stats
nfailed = 0;                             % stats
nfevals = 0;                             % stats
npds = 0;                                % stats
ndecomps = 0;                            % stats
nsolves = 0;                             % stats

if nargin == 1
  tspan = []; y0 = []; options = [];
elseif nargin == 2
  y0 = []; options = [];
```

```
elseif nargin == 3
  options = [];
end

% Get default tspan and y0 from ydot if none are specified.
if (length(tspan) == 0) | (length(y0) == 0)
  [ydot_tspan,ydot_y0,ydot_options] = feval(ydot,[],[]);
  if length(tspan) == 0
    tspan = ydot_tspan;
  end
  if length(y0) == 0
    y0 = ydot_y0;
  end
  if length(options) == 0
    options = ydot_options;
  else
    options = odeset(ydot_options,options);
  end
end

% Test that tspan is internally consistent.
tspan = tspan(:);
ntspan = length(tspan);
if ntspan == 1
  t = 0;
  next = 1;
else
  t = tspan(1);
  next = 2;
end
tfinal = tspan(ntspan);
if t == tfinal
  error('The last entry in tspan must be different...
         from the first entry.');
end
tdir = sign(tfinal - t);
if any(tdir * (tspan(2:ntspan) - tspan(1:ntspan-1)) <= 0)
  error('The entries in tspan must strictly increase or decrease.');
end

y = y0(:);
neq = length(y);
```

```
% Get options, and set defaults.
rtol = odeget(options,'rtol',1e-3);
atol = odeget(options,'atol',1e-6);
atol = atol(:);
if (rtol <= 0) | any(atol <= 0)
  error('Tolerance rtol and all entries of atol must be positive.');
end
if rtol < 100 * eps
  rtol = 100 * eps;
  fprintf('Warning: rtol has been increased to %e\n',rtol);
end
if length(atol) == 1
  atol = atol + zeros(neq,1);
elseif length(atol) ~= neq
  error(['Vector atol must be same length as y0 vector...
  (' num2str(neq) ').']);
end
threshold = atol ./ rtol;

userhmax = abs(odeget(options,'hmax',0.1*abs(tfinal-t)));
hmax = min(userhmax, abs(tfinal-t));

hmin = 8 * eps * abs(t);
userhmin = abs(odeget(options,'hmin',hmin));
hmin = min(max(hmin, userhmin), hmax);

if nargout ~= 0
  outfun = odeget(options,'outfun');
else
  outfun = odeget(options,'outfun','odeplot');
end

refine = odeget(options,'refine',1);

printstats = odeget(options,'printstats',false);

vectorized = odeget(options,'vectorized',false);
constantJ = odeget(options,'constantJ',false);
Js = odeget(options,'sparseJ');
analyticJ = odeget(options,'analyticJ');
if length(analyticJ) == 0
  notanalyticJ = true;
else
```

```
  notanalyticJ = false;
end

mass = odeget(options,'mass');
if length(mass) ~= 0
  if isstr(mass)
    M = feval(mass);
  else
    M = mass;
  end
  constantM = odeget(options,'constantM',true);
  if ~constantM
    error('For a non-constant mass matrix, M(t)*y'', use ODE15S.');
  end
  [L,U] = lu(M);
else
  M = sparse((1:neq)',(1:neq)',1,neq,neq);
  L = M;
  U = M;
  constantM = true;
end

% Initialize the output function.
if length(outfun) == 0
  haveoutfun = false;
else
  haveoutfun = true;
  feval(outfun,[t tfinal],y,'init');
end

% Allocate memory if we're generating output.
if nargout ~= 0
  if (ntspan == 1) & (refine == 0)  % only 1 output at tfinal
    nout = 0;
  else
    if ntspan > 2                   % output only at tspan points
      tout = zeros(ntspan,1);
      yout = zeros(ntspan,neq);
    else                            % alloc in chunks
      chunk = max(ceil(128 / neq),refine);
      tout = zeros(chunk,1);
      yout = zeros(chunk,neq);
    end
```

```
    nout = 1;
    tout(nout) = t;
    yout(nout,:) = y.';
  end
end

% Initialize method parameters.
pow = 1/3;
d = 1 / (2 + sqrt(2));
e32 = 6 + sqrt(2);

% Set the output flag.
if (ntspan > 2) | (refine == 0)
  outflag = 1;                      % output only at tspan points
elseif refine == 1
  outflag = 2;                      % computed points, no refinement
else
  outflag = 3;                      % computed points, with refinement
  ones1r = ones(1,refine-1);
  S = (1:refine-1) / refine;
  p1 = (S .* (1 - S)) ./ (1 - 2*d);
  p2 = (S .* (S - 2*d)) ./ (1 - 2*d);
end

% Compute an initial step size h using y'(t).
f0 = feval(ydot,t,y);
[m,n] = size(f0);
if n > 1
  error(['Function ' ydot '(t,y) must return a column vector.'])
elseif m ~= neq
  error(['Vector ' ydot '(t,y) must be same length as initial...
         conditions.']);
end
F0 = U \ (L \ f0);
wt = abs(y) + threshold;
absh = min(hmax, abs(tspan(next) - t));
rh = norm(F0 ./ wt,inf) / (0.8 * rtol^pow);
if absh * rh > 1
  absh = 1 / rh;
end
absh = max(absh, hmin);
h = tdir * absh;
```

```
% Using h, compute partial derivatives at (t,y) for use now and in
% the first step.  Compute y''(t) and a better initial step size.
sqrteps = sqrt(eps);
tdel = (t + tdir*min(sqrteps*max(abs(t),abs(t+h)),absh)) - t;
f1 = feval(ydot,t+tdel,y);
nfevals = nfevals + 2;                    % stats
dfdt = (f1 - f0) ./ tdel;

if notanalyticJ
  [dfdy,fac,g,nF] = numjac(ydot,t,y,f0,atol,[],vectorized,Js,[]);
  nfevals = nfevals + nF;                 % stats
else
  dfdy = feval(analyticJ,t,y);
end
npds = npds + 1;                          % stats

absh = min(hmax, abs(tspan(next) - t));
rh = sqrt(0.5*norm((U \ (L \ (dfdt + dfdy*F0))) ./ wt,inf))/(0.8...
     * rtol^pow);
if absh * rh > 1
  absh = 1 / rh;
end
absh = max(absh, hmin);
h = tdir * absh;

% THE MAIN LOOP

done = false;
while ~done

  hmin = max(userhmin, 8 * eps * abs(t));
  if 1.1*absh >= abs(tfinal - t)
    h = tfinal - t;
    absh = abs(h);
    done = true;
  end

  if ~constantJ
    if notanalyticJ
      [dfdy,fac,g,nF] = numjac(ydot,t,y,f0,atol,fac,vectorized,...
      Js,g);
      nfevals = nfevals + nF;             % stats
    else
```

```
    dfdy = feval(analyticJ,t,y);
  end
  npds = npds + 1;                          % stats
end
tdel = (t + tdir*min(sqrteps*max(abs(t),abs(t+h)),absh)) - t;
f1 = feval(ydot,t+tdel,y);
dfdt = (f1 - f0) ./ tdel;
nfevals = nfevals + 1;                      % stats

% LOOP FOR ADVANCING ONE STEP.
nofailed = true;                            % no failed attempts
while true

  [L,U] = lu(M - (h*d)*dfdy);               % sparse if dfdy is sparse
  k1 = U \ (L \ (f0 + (h*d)*dfdt));
  f1 = feval(ydot, t + 0.5*h, y + 0.5*h*k1);
  Mk1 = M * k1;
  k2 = (U \ (L \ (f1 - Mk1))) + k1;
  tnew = t + h;
  ynew = y + h*k2;
  f2 = feval(ydot, tnew, ynew);
  k3 = U \ (L \ (f2 - e32*(M*k2 - f1) - 2*(Mk1-f0)+(h*d)*dfdt));
  ndecomps = ndecomps + 1;                  % stats
  nfevals = nfevals + 2;                    % stats
  nsolves = nsolves + 3;                    % stats

  % Estimate the error.
  err = norm(((absh/6)*(k1-2*k2+k3))./(max(abs(y),...
  abs(ynew))+threshold),inf);

  % Accept the solution only if the weighted error is no more
  % than the tolerance rtol.  Estimate an h that will yield an
  % error of rtol on the next step or the next try at taking
  % this step, as the case may be, and use 0.8 of this value to
  % avoid failures.
  if err > rtol                             % Failed step
    nfailed = nfailed + 1;                  % stats
    if absh <= hmin
      fprintf('Step failure at %e with a minimum step size of...
      %e\n', t, h);
      if nargout ~= 0
        tout = tout(1:nout);
        yout = yout(1:nout,:);
```

```
        stats = [nsteps; nfailed; nfevals; npds; ndecomps;...
        nsolves];
      end
      return;
    end

    nofailed = false;
    absh = max(hmin, absh * max(0.1, 0.8*(rtol/err)^pow));
    h = tdir * absh;
    done = false;

  else                                % Successful step
    break;

  end
end

if nargout ~= 0
  oldnout = nout;
  if outflag == 2              % computed points, no refinement
    nout = nout + 1;
    if nout > length(tout)
      tout = [tout; zeros(chunk,1)];
      yout = [yout; zeros(chunk,neq)];
    end
    tout(nout) = tnew;
    yout(nout,:) = ynew.';
  elseif outflag == 3          % computed points, with refinement
    nout = nout + refine;
    if nout > length(tout)
      tout = [tout; zeros(chunk,1)];% requires chunk >= refine
      yout = [yout; zeros(chunk,neq)];
    end
    i = oldnout+1:nout-1;
    tout(i) = t + h*S';
    yout(i,:) = (y(:,ones1r) + k1*(h*p1) + k2*(h*p2)).';
    tout(nout) = tnew;
    yout(nout,:) = ynew.';
  elseif outflag == 1              % output only at tspan points
    while true
      if next > ntspan
        break;
      elseif tdir * (tnew - tspan(next)) < 0
```

```
        break;
      end
      nout = nout + 1;   % tout and yout are already allocated
      tout(nout) = tspan(next);
      s = (tspan(next) - t) / h;
      p1 = h * s * (1 - s) / (1 - 2*d);
      p2 = h * s * (s - 2*d) / (1 - 2*d);
      yout(nout,:) = (y + p1*k1 + p2*k2).';
      next = next + 1;
    end
  end

  if haveoutfun
    for i = oldnout+1:nout
      if feval(outfun,tout(i),yout(i,:).') == 1
        tout = tout(1:nout);
        yout = yout(1:nout,:);
        stats = [nsteps; nfailed; nfevals; npds; ndecomps;...
        nsolves];
        return;
      end
    end
  end

elseif haveoutfun
  if outflag == 2
    if feval(outfun,tnew,ynew) == 1
      return;
    end
  elseif outflag == 3    % computed points, with refinement
    for i = 1:refine-1
      yinterp = y + k1*(h*p1(i)) + k2*(h*p2(i));
      if feval(outfun,t + h*S(i),yinterp) == 1
        return;
      end
    end
    if feval(outfun,tnew,ynew) == 1
      return;
    end
  elseif outflag == 1              % output only at tspan points
    while true
      if next > ntspan
        break;
```

```
        elseif tdir * (tnew - tspan(next)) < 0
          break;
        end
        s = (tspan(next) - t) / h;
        p1 = h * s * (1 - s) / (1 - 2*d);
        p2 = h * s * (s - 2*d) / (1 - 2*d);
        yinterp = y + p1*k1 + p2*k2;
        if feval(outfun,tspan(next),yinterp) == 1
          return;
        end
        next = next + 1;
      end
    end
  end

  % If there were no failures compute a new h.
  if nofailed                % note h may shrink by 0.8
    absh = min(hmax, absh / max(0.2, 1.25*...
    (err/rtol)^pow)); % err may be 0
    h = tdir * absh;
  end

  % Advance the integration one step.
  t = tnew;
  y = ynew;
  nsteps = nsteps + 1;              % stats
  f0 = f2;                          % because formula is FSAL

end

if printstats                       % print cost statistics
  fprintf('%g successful steps\n', nsteps);
  fprintf('%g failed attempts\n', nfailed);
  fprintf('%g calls to ydot\n', nfevals);
  fprintf('%g partial derivatives\n', npds);
  fprintf('%g LU decompositions\n', ndecomps);
  fprintf('%g solutions of linear systems\n', nsolves);
end

if nargout ~= 0
  tout = tout(1:nout);
  yout = yout(1:nout,:);
  stats = [nsteps; nfailed; nfevals; npds; ndecomps; nsolves];
```

```
end
```

APPENDIX B

Computer Code for One-dimensional BGM

```
%
% This program solves one-dimensional BGM. It calls the function
% program odsys.m and uses ODE23s to solve the model equations.
% The output of this program is a matrix y = [f fbar Sf L Vl Sb].
% f represents the volume fraction of active bacteria.
% fbar represents the volume fraction of inactive bacteria.
% Sf represents the substrate concentration in the biofilm.
% L represents the biofilm thickness.
% Sb represents the substrate concentration in the bulk liqid
%
clear;
flops(0);        % Set the flops to zero before run stars.
t0 = 0;          % Set the time to zero before run starts.
tt = clock;      % tt is the actual clock time before run starts.
knowns;          % Get the parameter values from 'knowns.m'.
tfinal = input('Enter tfinal :');   % Enter the final time, T
%
% y0 = [f(0) fbar(0) Sf(0) L(0) Vl(0) Sb(0)]'
%
% Initial biofilm thickness
Lint = .00005;
% number of spatial grids
nz  = 5;
% step-size
delz = Lint/(nz-1);
% Initial biofilm thickness
L0(1:nz) = 0:delz:Lint;
% volume fraction of active
f0(1:nz) = .15*ones(nz,1);
% volume fraction of inactive bacteria
fbar0(1:nz) = .05*ones(nz,1);
% Substrate concentration in the biofilm
Si(1:nz) = .00004*ones(nz,1);
% Substrate concentration of the bulk liquid
Sb0 = .04;
% volume of the bulk liquid
Vl0 = .03;
```

```
% Initial values of unknown variables in a matrix form
y0 = [L0 f0 fbar0 Si Sb0 Vl0]';
% Call the function program 'FF.m' and use 'ODE23s' to solve
% the system.
[t,y] = ode23s('odsys',[t0 tfinal],y0);
%********* Plot the solution *********** %
% Graph of influent substrate concentration
figure(1);
plot(t,S0*ones(length(t),1)),
aa=0;
bb=2*S0;
ax=axis;
axis([0 tfinal aa bb]);
title ('S0'), xlabel('ox'), ylabel('oy'), drawnow;
%************************************************************
% Graph of the substrate concentration in the biofilm
figure(2);
plot(t,y(:,3*nz+1),'--',t,y(:,nz*4)),
aa = 0;
bb = .04;
ax=axis;
axis([0 tfinal aa-.0001 bb+.0001]);
title ('S'), xlabel('ox'), ylabel('oy'), drawnow;
text(1.5,.0125,'s1');
text(1.5,.0020,'s2');
%************************************************************
% Graph of the substrate concentration in the bulk liquid
figure(3);
plot(t,y(:,4*nz+1)),
title('Sb'), xlabel('ox'), ylabel('oy'), drawnow;
aa = 0;
bb = .05;
ax=axis;
axis([0 tfinal aa-.0001 bb+.0001]);
text(1.5,.0225,'sub');
%************************************************************
% Graph of volume fraction of active and inactive bacteria
figure(4);
plot(t,y(:,nz+1),'--',t,y(:,nz*2),t,y(:,2*nz+1),'--',...
t,y(:,3*nz))
title ('ffbar'), xlabel('ox'), ylabel('oy'), drawnow;
text(1.5,.19,'vfr1');
text(1.5,.145,'vfr2');
```

```
text(1.5,.055,'bvfr1');
text(1.5,.01,'bvfr2');
aa = 0;
bb = .2;
ax=axis;
axis([0 tfinal aa-.0001 bb+.0001]);
%************************************************************
% Graph of the biofilm thickness.
figure(5);
plot(t,y(:,nz)),
ax=axis;
axis([0 tfinal 0 .014]);
title('L'), xlabel('ox'), ylabel('oy'), drawnow;
text(1.5,.0095,'thick');
%************************************************************
% Graph the Volume of the bulk liquid
figure(6);
plot(t,y(:,4*nz+2)),
title('Vl'), xlabel('ox'), ylabel('oy'), drawnow;
aa = 0;
bb = .03;
ax=axis;
axis([0 tfinal aa-.0001 bb+.0001]);
text(1.5,.013,'vol');
%****************** plotting ends  ************************
flop = flops                    % Number of flops this run took.
elapsedtime = etime(clock,tt)% etime gives (current time  - tt)
                                % tt is the time when the run started.

%
%       Known parameter values needed for the system in odsys.m
%
K  = 0.0001;     % <--- Monod constant.
Vr = 4.3;        % <--- Maximum growth rate.
Y  = .5;         % <--- Yield coefficient.
b  = 0.35;       % <--- Death rate.
D  = 1.3;        % <--- Diffusivity coefficient in the bulk liquid.
d  = .8*D;       % <--- Diffusivity coefficient in the film.
Q0 = 1100.0;     % <--- Volumetric flow rate.
sigma  = 1.0;    % <--- Surface area of the interface.
Li = 0.8;        % <--- Thickness of the laminar sublayer.
S0 = 0.02;       % <--- Influent substrate concentration.
el = 0.8;        % <--- Volume fraction of the liquid in the biofilm.
lambda = 500;    % <--- Detachment coefficient
```

```
ro = 12.2;       % <--- Biomass density
function yp = odsys(t,y)
knowns;     %  <----  Get the known parameters from 'knowns.m'.
nz = 5;
delz = y(nz)/(nz-1);
L(1:nz) = y(1:nz);
f(1:nz) = y(nz+1:2*nz);
fbar(1:nz) = y(2*nz+1:3*nz);
S(1:nz) = y(3*nz+1:4*nz);
Sb = y(4*nz+1);
Vl = y(4*nz+2);
L = y(nz);
%********* Calculate rhs of dL/dt velocities ******************
U(1) = 0;                                  % velocity at the substratum
for i = 2:nz-1                             %
  U(i) = U(i-1) + Y*Vr*delz/(1-el)*...     % velocities at the different
       .5*(S(i+1)*f(i+1)/(K+S(i+1))+...    % grid points.
       S(i-1)*f(i-1)/(K+S(i-1)));          %
end                                        %
U(nz) = U(nz-1)+Vr*delz^2/(1-el)*.5*...    % velocity of the interface.
    (S(nz)*f(nz)/(K+S(nz))+(S(nz-1)*...    %
    f(nz-1)/(K+S(nz-1))))-lambda*L^2;      %
%******************* Calculate rhs of df/dt ***********************
F(1) = Y*Vr*S(1)*f(1)*fbar(1)/((K+S(1))*(1-el))-b*f(1);
for i = 2:nz-1
  if U(i) < 0;
    r1 = (f(i+1)-f(i))/delz;
  else
    r1 = (f(i)-f(i-1))/delz;
  end
  F(i) = -U(i)*r1+Y*Vr*S(i)*f(i)*fbar(i)/((K+S(i))*(1-el))-b*f(i);
end
F(nz) = -U(nz)*(f(nz)-f(nz-1))/delz+Y*Vr*S(nz)*f(nz)*fbar(nz)/...
    ((K+S(nz))*(1-el))-b*f(nz);
%****************** Calculate the rhs of dfbar/dt ****************
Fb(1) = -Y*Vr*S(1)*f(1)*fbar(1)/((K+S(1))*(1-el))+b*f(1);
for i = 2:nz-1
  if U(i) < 0;
    r2 = (fbar(i+1)-fbar(i))/delz;
  else
    r2 = (fbar(i)-fbar(i-1))/delz;
  end
  Fb(i) = -U(i)*r2-Y*Vr*S(i)*f(i)*fbar(i)/((K+S(i))*(1-el))+b*f(i);
```

```
end
Fb(nz) = -U(nz)*(fbar(nz)-fbar(nz-1))/delz-Y*Vr*S(nz)*f(nz)*...
         fbar(nz)/((K+S(nz))*(1-el))+b*f(nz);
%***************** Calculate the rhs of dS/dt *********************
DS(1) = -Vr*S(1)*f(1)*(Y*S(1)/(1-el)+ro)/(K+S(1))+2*d*...
        (S(2)-S(1))/delz^2;
for i = 2:nz-1
  if U(i) < 0
    r3 = S(i+1)-S(i);
  else
    r3 = S(i)-S(i-1);
    DS(i) = -U(i)*r3/delz - Vr*S(i)*f(i)/(K+S(i))*...
        (Y*S(i)/(1-el)+ro)+D*(S(i+1)-2*S(i)+S(i-1))/delz^2;
  end
end
if U(nz) < 0
    r4 = S(nz)-Sb;
  else
    r4 = Sb-S(nz);
    end
DS(nz) = -Vr*S(nz)*f(nz)/(K+S(nz))*...
        (Y*S(1)/(1-el)+ro)+d*(Sb-2*S(nz)+S(nz-1))/delz^2;
%*************** Calculate the rhs of dSb/dt **********************
DSb = 1/Vl*(Q0*(S0-Sb)-sigma*D*(Sb-S(nz))/Li);
%******************** Calculate the rhs of dVl/dt ****************
DVl = -U(nz)*sigma;
%*************************************************************************
yp = [ U F Fb DS DSb DVl]';
```

APPENDIX C

Computer Code for Zero-dimensional BGM-A

```
%
% This program solves zero-dimensional BGM. This program calls the
% function zdbgmssys1.m and uses ODE23s to solve the model equations.
%
clear
flops(0);
tt = clock; % time when run started
t0 = 0;
                                        %
tfinal = input('Enter tfinal :');  % Enter the final time, T
                                        %
%
% initially, y0 = [Sb L Sf f V]' is given below.
%
% Initial values of the unknown variables:
% Bulk substrate concentration = .04
% Biofilm thickness = .00005
% Biofilm substrate concentration = .00004
% Biomass volume fraction = .15
% Bulk volume = 2.0
%
y0 = [.04 .00005 .00004 .15 0.03]';
%
% Call the system of equations from the function program "jnbgms.m"
% and use ODE23s to solve it.
%
[t,y] = ode23s('zdbgmsys1',[t0 tfinal],y0);
%
% This program returns the matrix y whose first column, y(:,1),
% represents the bulk substrate concentration, second column, y(:,2),
% represents the biofilm thickness, third column, y(:,3), represents
% the biofilm substrate concentration, fourth column, y(:,4),
% represents the biomass volume fraction, and the fifth column,
% y(:,5), represents the bulk volume over the time interval [0,T].
%
figure(1);
plot(t,y(:,1)),
```

```
 ax=axis;
 axis([0 tfinal 0 .05]);
title ('Sb(BGM)'),drawnow;
figure(2);
plot(t,y(:,2)),
title L
 aa = 0;
 bb = .01;
 ax=axis;
 axis([0 tfinal ax(3:4)]);
figure(3);
plot(t,y(:,3)),
aa = 0;
bb = .04;
 ax=axis;
 axis([0 tfinal aa-.0001 bb+.0001]);
title ('Sf')
%subplot(224),
figure(4);
plot(t,y(:,4),t, .2-y(:,4)),
title ' f and fbar '
 aa = 0;
 bb = .2;
 ax=axis;
 axis([0 tfinal aa-.0001 bb+.0001]);
 figure(5);
plot(t,y(:,5)),
title V
 aa = 0;
 bb = .035;
 ax=axis;
axis([0 tfinal aa-.0001 bb+.0001]);
flop = flops
elapsedtime = etime(clock,tt)
%
% Function program (zdbgmsys1.m) for the zero-dimensinal BGM
%
function yp = jbgms(t,y)
%
% The parameter values
%
K       = 0.0001;% <----- Monod constant.
mu      = 4.3;   % <----- Maximum growth rate.
```

```
Y      = 0.5;   % <----- Yield coefficient.
b      = 0.35;  % <----- Death rate.
D      = 1.3;   % <----- Diffusivity coefficient.
Q0     = 1100.0;% <----- Volumetric flow rate.
sigma  = 1.0;   % <----- Surface area of the interface.
Li     = 0.8;   % <----- Thickness of the laminar sublayer.
S0     = 0.02;  % <----- Influent substrate concentration.
el     = 0.8;   % <----- Volume fraction of the liquid in the
                %        biofilm.
lamda  = 500;   % <----- Detachment coefficient
ro     = 12.2;  % <----- Biomass density
yp = [(Q0*(S0-y(1))-sigma*D*(y(1)-y(3))/Li)/y(5)
    Y*mu*y(3)*y(4)*y(2)/((K+y(3))*(1-el))-lamda*y(2)^2
    D*(y(1)-y(3))/(Li*y(2))-mu*y(3)*y(4)/(K+y(3))*(ro+y(3)*Y/...
    (1-el)) + lamda*y(3)*y(2)
    Y*mu*y(3)*y(4)/(K+y(3))*(1-y(4)/(1-el))-b*y(4)
    -sigma*(Y*mu*y(4)*y(3)*y(2)/((1-el)*(K+y(3)))-lamda*y(2)^2)];
% y = [Sb L Sf f V]'
```

APPENDIX D

Computer Code for Zero-dimensional Rittman's Model

```
%
% This program solves Zero-dimensional Rittman's Model. This program
% calls the function zdritsys.m and uses ODE23s to solve the model
% equations.
clear
flops(0);
tt = clock; % time when run started
t0 = 0;
                                        %
tfinal = input('Enter tfinal :');  % Enter the final time, T
                                        %
%
% initially, y0 = [Sb L Sf f V]' is given below.
%
% Initial values of the unknown variables:
% Bulk substrate concentration = .04
% Biofilm thickness = .00005
% Biofilm substrate concentration = .00004
% Biomass volume fraction = .2
%
y0 = [.04 .00005 .00004 .2]';
%
% Call the system of equations from the function program jrits.m
% and use ODE23s to solve it.
%
[t,y] = ode23s('zdritsys',[t0 tfinal],y0);
%
% This program returns the matrix y whose first column, y(:,1),
% represents the bulk substrate concentration, second column, y(:,2),
% represents the biofilm thickness, third column, y(:,3), represents
% the biofilm substrate concentration, fourth column, y(:,4), and
% represents the biomass volume fraction over the time interval [0,T].
%
figure(1);
subplot(221),plot(t,y(:,1)),
ax=axis;
axis([0 tfinal ax(3:4)]);
```

```
title ('Sb(RIT)'),drawnow;
subplot(222),plot(t,y(:,2)),
title L
 aa=min(y(:,2));
 bb=max(y(:,2));
 ax=axis;
 axis([0 tfinal aa-.0001 bb+.0001]);
subplot(223),plot(t,y(:,3)),
 ax=axis;
 axis([0 tfinal ax(3:4)]);
title Sf
subplot(224),plot(t,y(:,4));
title f
 aa = 0;
 bb = 1;
 ax=axis;
 axis([0 tfinal aa-.0001 bb+.0001]);
flop = flops
elapsedtime = etime(clock,tt)
%
% Function program (zdritsys.m) for the zero-dimensinal
% Rittman's model
function yp = zdritsys(t,y)
%
% The parameter values
%
K      = 0.0001;% <----- Monod constant.
Vr     = 4.3;   % <----- Maximum growth rate.
Y      = 0.2;   % <----- Yield coefficient.
b      = 0.35;  % <----- Death rate.
D      = 1.3;   % <----- Diffusivity coefficient.
Q0     = 1100.0;% <----- Volumetric flow rate.
sigma  = 1.0;   % <----- Surface area of the interface.
Li     = 0.8;   % <----- Thickness of the laminar sublayer.
S0     = 0.02;  % <----- Influent substrate concentration.
fd     = 0.0;   % <----- Biodegradable fraction of the biomass.
V      = 2.0;   % <----- Volume of the bulk liquid
Bprime = 0.31;  % <----- Detachment coefficient
X      = 12.2;  % <----- Biomass density
yp = [Q0*S0/V-(Q0/V + sigma*D/(V*Li))*y(1)+sigma*D/(V*Li)*y(3)
      ((Y*Vr*y(3)/(K+y(3))-b*fd)*y(4)-Bprime)*y(2)
      b*fd*y(3)*y(4)+Bprime*y(3)-Vr*y(3)*y(4)*(Y*y(3)+X)/...
      (K+y(3))+D/(Li*y(2))*(y(1)-y(3))
```

```
      Y*Vr*y(3)*(1-y(4))*y(4)/(K+y(3))-b*y(4)+b*fd*y(4)^2];
% yp = [ sb L S f]
```

APPENDIX E

Computer Code for Zero-dimensional BAM

```
%
% This program solves zero-dimensional BAM. This program calls the
% function zdbamsys.m and uses ODE23s to solve the model equations.
%
clear
flops(0);
tt = clock; % time when run started
t0 = 0;
                                        %
tfinal = input('Enter tfinal :');  % Enter the final time, T
                                        %
%
% initially, y0 = [Sb L Sf f V]' is given below.
%
% Initial values of the unknown variables:
% Bulk substrate concentration = .04
% Biofilm thickness = .00005
% Biofilm substrate concentration = .00004
% Biomass volume fraction = .2
%
y0 = [.04 .00005 .00004 .2]';
%
% Call the system of equations from the function program jnbs.m
% and use ODE23s to solve it.
%
[t,y] = ode23s('zdbamsys',[t0 tfinal],y0);
%
% This program returns the matrix y whose first column, y(:,1),
% represents the bulk substrate concentration, second column, y(:,2),
% represents the biofilm thickness, third column, y(:,3), represents
% the biofilm substrate concentration, fourth column, y(:,4), and
% represents the biomass volume fraction over the time interval [0,T].
%
figure(2);
subplot(221),plot(t,y(:,1)),
ax=axis;
axis([0 tfinal ax(3:4)]);
```

```
title ('Sb'),drawnow;
subplot(222),plot(t,y(:,2)),
title L
 aa=min(y(:,2));
 bb=max(y(:,2));
 ax=axis;
 axis([0 tfinal aa-.0001 bb+.0001]);
subplot(223),plot(t,y(:,3)),
 ax=axis;
 axis([0 tfinal ax(3:4)]);
title Sf
subplot(224),plot(t,y(:,4)),
title f
 aa = 0;
 bb = 1;
 ax=axis;
 axis([0 tfinal aa-.0001 bb+.0001]);
flop = flops
elapsedtime = etime(clock,tt)
%
% Function program (zdbamsys.m) for the zero-dimensinal BAM.
%
function yp = zdbamsys(t,y)
%
% The parameter values
%
K       = 0.0001;% <----- Monod constant.
Vr      = 4.3;   % <----- Maximum growth rate.
Y       = 0.2;   % <----- Yield coefficient.
b       = 0.35;  % <----- Death rate.
D       = 1.3;   % <----- Diffusivity coefficient.
Q0      = 1100.0;% <----- Volumetric flow rate.
sigma   = 1.0;   % <----- Surface area of the interface.
Li      = 0.8;   % <----- Thickness of the laminar sublayer.
S0      = 0.02;  % <----- Influent substrate concentration.
el      = 0.0;   % <----- Volume fraction of the liquid in the
                 %        biofilm.
V       = 2.0;   % <----- Volume of the bulk liquid
lamda   = 500;   % <----- Detachment coefficient
ro      = 12.2;  % <----- Biomass density
yp = [Q0*(S0-y(1))/V-sigma*D*(y(1)-y(3))/(V*Li)+sigma*(y(1)-y(3))*...
      (Y*mu*y(3)*y(2)*y(4)/((1-el)*(K+y(3)))-lamda*y(2)^2)/V
      mu*y(3)*y(2)*y(4)*Y/((1-el)*(K+y(3)))-lamda*y(2)^2
```

```
      D*(y(1)-y(3))/(Li*y(2))-mu*y(3)*y(4)/(K+y(3))*(ro+Y*y(3)/...
      (1-el))+lamda*y(2)*y(3)
      (1-y(4)/(1-el))*mu*Y*y(3)*y(4)/(K+y(3))-b*y(4)];
% yp = [ sb L S f]
```

APPENDIX F

Computer Code for One-dimensional BGM-B

```
%
% This program solves Zero-dimensional BGM. This program calls the
% function "zdbgmsys2.m" and uses ODE23s to solve the model equations.
%
clear
flops(0);
tt = clock; % time when run started
t0 = 0;
                                        %
tfinal = input('Enter tfinal :');  % Enter the final time, T
                                        %
%
% initially, y0 = [Sb L Sf f V]' is given below.
%
% Initial values of the unknown variables:
% Bulk substrate concentration = .04
% Biofilm thickness = .00005
% Biofilm substrate concentration = .00004
% Biomass volume fraction = .2
% Bulk volume = 2.0
%
y0 = [.04 .00005 .00004 .2 2.0]';
%
% Call the system of equations from the function program "zdbgmsys2.m"
% and use ODE23s to solve it.
%
[t,y] = ode23s('zdbgmsys2',[t0 tfinal],y0);
%
% This program returns the matrix y whose first column, y(:,1),
% represents the bulk substrate concentration, second column, y(:,2),
% represents the biofilm thickness, third column, y(:,3), represents
% the biofilm substrate concentration, fourth column, y(:,4),
% represents the biomass volume fraction, and the fifth column,
% y(:,5), represents the bulk volume over the time interval [0,T].
%
figure(3);
subplot(221),plot(t,y(:,1)),
```

```
ax=axis;
axis([0 tfinal ax(3:4)]);
title ('Sb(BGM)'),drawnow;
subplot(222),plot(t,y(:,2)),
title L
aa=min(y(:,2));
bb=max(y(:,2));
ax=axis;
axis([0 tfinal aa-.0001 bb+.0001]);
subplot(223),plot(t,y(:,3)),
ax=axis;
axis([0 tfinal ax(3:4)]);
title ('Sf')
subplot(224),plot(t,y(:,4)),
title f
aa = 0;
bb = 1;
ax=axis;
axis([0 tfinal aa-.0001 bb+.0001]);
flop = flops
elapsedtime = etime(clock,tt)
%
% Function program (zdbgmsys2.m) for the zero-dimensinal BGM
%
function yp = zdbgmsys2(t,y)
%
% The parameter values
%
K       = 0.0001;% <----- Monod constant.
mu      = 4.3;   % <----- Maximum growth rate.
Y       = 0.2;   % <----- Yield coefficient.
b       = 0.35;  % <----- Death rate.
D       = 1.3;   % <----- Diffusivity coefficient.
Q0      = 1100.0;% <----- Volumetric flow rate.
sigma   = 1.0;   % <----- Surface area of the interface.
Li      = 0.8;   % <----- Thickness of the laminar sublayer.
S0      = 0.02;  % <----- Influent substrate concentration.
el      = 0.0;   % <----- Volume fraction of the liquid in the
                 %        biofilm.
lamda   = 500;   % <----- Detachment coefficient
ro      = 12.2;  % <----- Biomass density
yp = [(Q0*(S0-y(1))-sigma*D*(y(1)-y(3))/Li)/y(5)
    Y*mu*y(3)*y(4)*y(2)/((K+y(3))*(1-el))-lamda*y(2)^2
```

```
    D*(y(1)-y(3))/(Li*y(2))-mu*y(3)*y(4)/(K+y(3))*(ro+y(3)*Y/...
    (1-el)) + lamda*y(3)*y(2)
    Y*mu*y(3)*y(4)/(K+y(3))*(1-y(4)/(1-el))-b*y(4)
    -sigma*(Y*mu*y(4)*y(3)*y(2)/((1-el)*(K+y(3)))-lamda*y(2)^2)];
% y = [Sb L Sf f V]'
```

APPENDIX G

Computer Code for Porous Media Flow and BGM

```
%
% This program uses function program zdbgmsys3.m and
% ODE23s to solve the biofilm growth model equations
% combines with porous media flow model equations
%
clear;
flops(0);
t0 = 0;
tt = clock; % time when run started
T = input('Final Time = ');
nt =  input('Number of Time-Steps = ');
delt = T/nt;
lbed = input('Bed-length = ');
n = input('Number of Nodes = ');
delz = lbed/n-1;
save fi1 delt delz n;
rr = (delz)^2/delt;
mu = 1;
rof = 1.1;
Vbulk = 5;
g = 981;
m = 5252;
%  Initially we have
phi0 = .45 * ones(n,1)';
per0 = .000275 * ones(n,1)';
perf = .000275;
perlast = .000275;
Db = .1 * ones(n,1);
Q0 = .075 * ones(n,1)';
save fi2 Q0;
A = 1;
u0 = .1667 * ones(n,1)';
u = u0;
%Boundary Condition:
p0 = 5;
plast = 2.5;
p = 3*ones(n,1);
```

```
pnew = p;
v = ones(n-1,1);
M = diag(v,-1) + diag(v,1) - 2*eye(n,n);

%***************************
  y10 = .04*ones(1:n);
  y20 = .00005*ones(1:n);
  y30 = .00004*ones(1:n);
  y40 = .15*ones(1:n);
  y50 = 2.25*ones(1:n);
  y0 = reshape([y10' y20' y30' y40' y50']',5*n,1);
%***************************

for k = 1 : nt

  %******* Solve for biofilm growth ***************
  t0 = (k-1)*delt;
  tfinal = k*delt;
  [t,y] = ode23s('zdbgmsys3',[t0 tfinal],y0);
  % Change in porosity and permeability due to
  % biofilm growth
  vol0 = y0(5:5:5*n);
  phi = vol0/Vbulk;
  y0 = y(length(t),1:n*5)';
  vol = y0(5:5:5*n);
  phinew = vol/Vbulk;
  Db = (6*Vbulk/m/pi*(1-phinew./phi)+phinew./...
phi.*Db.^3).^(1/3);
  per = Db.^2.*(1-phinew)/72.*(3+4./(1-phinew)-3*...
(8./(1-phinew)-3).^.5);
  %*********** Solve for new flow rate ************
  for i = 2:n-1
    R(i) = (per(i+1)-per(i-1))/(4*per(i));
    S(i) = rr*mu*(phinew(i)-phi(i))/per(i)-(per(i+1)-...
per(i-1))*rof*g*delz/(2*per(i));
  end
  R(1) = (per(2)-perf)/(4*per(1))
  R(n) = (perlast-per(n-1))/(4*per(n));
  S(1) = rr*mu*(phinew(1)-phi(1))/per(1)-(per(2)-...
perf)*rof*g*delz/(2*per(1));
  S(n) = rr*mu*(phinew(n)-phi(n))/per(n)-(perlast-...
per(n-1))*delz*rof*g/(2*per(n));
  MM = diag(v-R(2:n)',-1) + diag(v-R(1:n-1)',1) -...
```

```
 2*eye(n,n);
  G = S - [(1-R(1))*p0 zeros(1,n-2) (1+R(n))*plast];
  pnew = inv(MM)*G';
  for j = 2:n-1
    u(j) = -per(j)/(mu*phi(j))*((pnew(j+1)-pnew(j-1))/...
(2*delz)+rof*g);
  end
  u(1) = -per(1)/(mu*phi(1))*((pnew(2) - p0)/(2*delz)+...
rof*g);
  u(n) = -per(n)/(mu*phi(n))*((plast - pnew(n-1))/...
(2*delz)+rof*g);
  Q0 = (A*phinew.*u')';
  save fi2 Q0;
  k
  Data = [ y0(1:5:5*n) y0(2:5:5*n) y0(3:5:5*n)...
 y0(4:5:5*n)  y0(5:5:5*n)]
end


%
% This is the function program for the biofilm growth model.
%
%
function yp = zdbgmsys3(t,y)
K  = 0.0001;
mu = 4.7;
Y1  = .2;
D  = 1.3;
load fi1;
load fi2;
sigma  = 1;
Li = .8;
ro = 12.2;
S0 = 0.02;
b = .2;
el = .8;
lamda = 800;
for i = 1:n
  y1(i) = (Q0(i)*(S0-y((i-1)*5+1))-sigma*D*(y((i-1)*...
      5+1)-y((i-1)*5+3))/Li)/y((i-1)*5+5);
  y2(i) =  mu*y((i-1)*5+3)*y((i-1)*5+4)*y((i-1)*...
      5+2)/((K+y((i-1)*5+3))*(1-el))-lamda*y((i-1)*...
      5+2)^2;
  y3(i) =  D*(y((i-1)*5+1)-y((i-1)*5+3))/(ro*Li*...
```

```
        y((i-1)*5+2))-Y1*mu*y((i-1)*5+3)*y((i-1)*...
        5+4)/(K+y((i-1)*5+3))*(1+y((i-1)*5+3)/...
        (1-el))+lamda*y((i-1)*5+3)*y((i-1)*5+2)^2;
    y4(i) =  mu*y((i-1)*5+3)*y((i-1)*5+4)/(K+y((i-1)*...
        5+3))*(1-y((i-1)*5+4)/(1-el))-b*y((i-1)*5+4);
    y5(i) =  -sigma*(mu*y((i-1)*5+4)*y((i-1)*5+3)*...
        y((i-1)*5+2)/((1-el)*(K+y((i-1)*5+3)))-lamda*...
        y((i-1)*5+2)^3);
end

yp = reshape([y1' y2' y3' y4' y5']',5*n,1);
```